University of Nottingham
UK | CHINA | MALAYSIA

Tissue resident CD8 T cells subsets: prognostic significance in colorectal cancer

By Shahd Talhouni, M.Sc.

Thesis submitted to the University of Nottingham
For the degree of
Doctor of Philosophy
August 2021

University of Nottingham
Faculty of Medicine and Health Sciences
School of Medicine
Academic Unit of Clinical Oncology

Abstract:

The past few years have seen remarkable success in the field of oncology with the advent of cancer immunotherapies and checkpoint inhibitors. The effectiveness of immunomodulatory strategies has been shown to depend on natural intra-tumoral T cell infiltration and on reactivation of pre-existing immunity via inhibition of inhibitory checkpoints on T cells. T-cell membrane microdomains are enriched with proteins and glycolipids collectively involved in cell activation and signal transduction. Tetraspanin-enriched microdomains are an example of such microdomains that have been shown to play a pivotal role in T-cell regulation. One such tetraspanin protein is TSPAN32 that has not been widely studied. For the purpose of further studying the immuno-regulatory role of TSPAN32, especially in its ability to inhibit T cell proliferation, we developed an innovative immunisation method using plasma membrane glycolipid extraction of TSPAN32 transfected cells to produce an anti-TSPAN32 antibody. Developing a fully function TSPAN32 monoclonal antibody could help further understand its immune function and could also potentially help in the development of novel immunotherapies that improve immune response in cancers.

Among different tumour infiltrating T cells, high levels of CD8 T cell infiltration – a hallmark of immunologically “hot” tumours - are a favourable indicator for patient survival and immunotherapy responsiveness. In colorectal cancer (CRC), the Immunoscore index developed based on the density of CD3+ and CD8+ TILs infiltrating the centre and invasive margin of the tumour, was found to be a better predictor of patient survival than the current histopathological methods. . In our study, we aimed to investigate the predictive role of intraepithelial and stromal CD3+ and CD8+ T cells in three different regions of the tumour luminal side (LS), the centre of the tumour (CT), the invasive margin (IM) and the adjacent normal tissue in CRCs. The results showed high infiltration of CD3+ and CD8+ T cells in tumour regions (LS,

CT and IM), but not in the adjacent normal tissue was significantly associated with better survival in patients with CRC.

CRC patients are classified based on the occurrence of left or right colon tumours which have been shown to have different phenotypic characteristics and tumour micro-environment (TME). To define the differences in the immune infiltrates between RCRCs and LCRCs, we compared the distribution of CD8+ TILs and tissue-resident T cells (CD103+ TILs) between RCRCs and LCRCs. We found that RCRCs were associated with significantly higher infiltration of intraepithelial CD8 TILs and CD103 TILs compared to LCRCs. Furthermore, we have shown that high infiltration of intraepithelial CD103 TILs was an independent predictor of patient survival in RCRCs. Tumour infiltrating CD8 T cells represent a heterogeneous cell population comprising tumour-specific T cells and bystander T cells. In solid tumours, co-expression of CD39 and CD103 on CD8 T cells has been shown to identify tumour reactive tissue resident memory T cells (TRM). Our study presents the largest study (n=1000) yet to compare the landscape and prognostic significance of recently activated tumour specific TRM cells and other CD8+ TILs phenotypes within the TME of colorectal tumours. Using multiplex immunohistochemistry staining, followed by training using advanced image-analysis software, CD8+ TILs, co-expressing CD103 and/or CD39 on their surface, were detected and quantified within tumour epithelium and stroma of each TMA core. CD8 TRM T-cells were shown to be an independent predictor of survival in CRC. We further investigated the prognostic role of this unique population between different CRC tumour sidedness and showed that in LCRCs, the only CD8 phenotype that predicted survival was the recently activated TRM CD8-T cells. In contrast, RCRCs with heavily infiltrated tumours regardless of the presence of this TRM subset, still had good survival.

Acknowledgement:

I would like to express my gratitude to my supervisor Dr. Judith Ramage. She has been an incredible mentor who patiently guided, encouraged and supported me through the course of my PhD. It has been a great honour to work with her and learn from her valuable scientific insights and research experiences. I would also like to thank Dr. Ian Spendlove and Dr. Andrew Jackson for their kind help and valuable advice, which motivated me to improve my work. Special thanks to Professor Mohammad Ilyas and Wakkas Fadhil who kindly provided us with CRC TMA cohort for our study. I would also like to thank Kelly Hunter for his help in optimising the multiplex staining and analysing R reports.

I would also like to thank the Antibody Group members, Professor Lindy Durrant, Dr. Richard McIntosh and Chua Jia Xin for the insightful discussions, guidance and support in many aspects of my PhD. I want to specially thank my colleagues who became my best friends and supporters throughout my PhD journey- Dr Aanchal Preet Kaur and Dr Tajkia Mussarat. I thank all the members of the Academic Unit of Clinical Oncology who have kindly donated blood to support our research work. Importantly, I am grateful to Al-Zaytoonah University for sponsoring my PhD course.

Last but not the least, I want to thank my mother (Sahar abusham), who have been my pillar of strength, my most fierce supporter and my inspiration in not only during my Ph.D., but in every step of my life. I am also grateful for the love and support I received from my husband Nabil Sakkihja, and my sisters Shuker and Baraa talhouni, which helped me to continue this challenging journey.

Contents:

Table of Contents

List of figures:

List of tables:

Abbreviations

A

APC.	Antigen presenting cell.
αGalCer	Alpha galactosylceramide.
ATM	Ataxia telangiectasia mutated.
APC	Adenomatous polyposis coli.

B

BSA	Bovine serum albumin.
BRAF	v-raf murine sarcoma viral oncogene homolog B1.

C

CMV	Cytomegalovirus.
CD	Cluster of differentiation.
CTL	Cytotoxic T lymphocyte.
CTLA-4	Cytotoxic T lymphocyte-associated protein 4.
CRC	Colorectal cancer.
CTLs.	Cytotoxic CD8+ T-cell lymphocytes.
cSMAC	central supramolecular activation cluster

D

DC	Dendritic cell.
DHP	Dihexadecyl phosphate.
DOPC	1,2-dioleoyl-sn-glycero-3-phosphocholine.
dMMR	Mismatch repair deficient.
DMSO	Dimethyl sulfoxide.
DFS	Disease-free survival.
DAB	3,3’-diaminobenzidine.
DP TIL	Double positive tumour infiltrating lymphocytes.

E

EGFR	Epidermal growth factor receptor.

G

GFP	Green Fluorescent Protein.

H

HER2	Human epidermal growth factor receptor 2.

I

IRES	Internal ribosome entry site.
IHC	Immuno-histochemistry.
ICOS	Inducible T-cell costimulator.
IL-	Interleukin.
iNKT	Invariant natural killer.
ITAM	Immunoreceptor tyrosine-based activation motif.
IP	Immunised intraperitoneally.

K

KRAS	Kirsten rat sarcoma viral oncogene homolog.

L

LAG-3	Lymphocyte activation gene – 3.
LCRC	Left-sided colorectal cancer.

M

mAb	Monoclonal antibody.
MHC	Major histocompatibility complex.
MO	Monocytes.
MSI	Microsatellite instability.
MSS	Microsatellite stable.
MFI	Median fluorescence intensity.
mIHC/IF	Multiplex immunohistochemistry/immunofluorescence.
MLH1	MutL homolog 1.
MSH2	MutS homolog 2.
MSH6	MutS homolog 6.

N

NIH 3T3	Mouse embryonic fibroblast.
NRAS	Neuroblastoma RAS viral [v-ras] oncogene homolog.

O

ORF	Open reading frame.

P

PBMC	Peripheral blood mononuclear cell.
PBS	Phosphate-buffered saline.
PD-1	Programmed death 1.
PDL1	Programmed death 1 ligand.
PM	Plasma membrane.
Poly-A	A- Polyadenylation.
PTL	Primary Tumour Location.
PBS	Phosphate buffered saline.
PIK3CA	Phosphatidylinositol-4,5-bisphosphate 3-kinase, catalytic alpha.
POLE	Polymerase epsilon.
POLD1	Polymerase delta 1.
PTEN	Phosphatase and TENsin homolog deleted on chromosome 10.
PAMP	Pathogen-associated molecular patterns

R

RCRC	Right-sided colorectal cancer.
RAS	Rat sarcoma.

S

SDS-PAGE	Sodium dodecyl sulfate polyacrylamide gel electrophoresis.
SP TIL	Single positive tumour infiltrating lymphocytes.
SLEC	Short-lived effector cells

T

TLR	Toll-like receptor.
Tregs	T-regulatory cells.
TCR.	T-cell receptor.
TEM	Tetraspanin-enriched microdomain.
TIL	Tumour infiltrating lymphocytes.
TLR	Toll-like receptor.
Tregs	T-regulatory cells.
TRM	Tissue-resident memory T cells.
TGF-β	Transforming growth factor beta.
TMA	Tissue microarray.
TME	Tumour microenvironment.
TIM3	T cell immunoglobulin and mucin domain-containing protein 3.
TP53	Tumor protein p53 gene.
TP TIL	Triple positive tumour infiltrating lymphocytes.

V

VEGF	Vascular endothelial growth factor.

Chapter 1: Introduction

The immune system is a host defence system that helps organisms to protect themselves from potentially harmful substances and to combat infections caused by pathogenic micro-organisms [1, 2]. This complex network of cells, tissues, organs and proteins has a multi-faceted role and is even competent in systematically eliminating endogenous challenges that arise from genetic and somatic mutations.

The adaptive immunity is the acquired ability to eliminate infection by proliferation, differentiation and coordinated function of antigen-specific B-cells and T-cells that demonstrate unique specificity and memory in order to generate faster response upon reencounter to the same pathogen[1, 3]. This process entails recognition of antigen following processing and presentation by specialised antigen-presenting cells. B cells produce antibodies and regulate the humoral response against the antigen. T cells mediate cytotoxicity to eliminate virus-infected cells, assist B-cell differentiation and maturation and support the activity of macrophages in eliminating intracellular pathogens.[2]

1.1 T- cells development

Thymus-derived lymphocytes (T-cells) were discovered in the 1960s by Graham Mitchell and Jacques Miller as the cell population which could proliferate in response to antigen and even though they did not produce antibody, they enabled bone-marrow derived B-cells to develop into antibody forming cells. [4, 5] T-cells have been studied extensively in the last few decades leading to the identification of multiple T-cell subsets with distinct functions.

T-cells originate from bone-marrow derived multipotent Haemopoietic Stem Cells (HSC) through a stringently regulated process [6]. The earliest T-cell specific precursor derived from HSC is known as the Early Thymic Progenitor or Early T-cell Precursor (ETP). This represents a small cell population in the thymus where the TCR genes were maintained in the germline state but differed in HSC as they expressed low level of CD-4 which was down-regulated in subsequent developmental stages [7]. Recent fate-mapping studies indicate that potentially there could be an intermediate state between HSC and ETP, termed Thymic Seeding Progenitor (TSP) which migrate from bone marrow to thymus and serve as a precursor for ETP. Interestingly, ETP has the potential to differentiate into only T-cells in thymus but could give rise to both B-cells and T-cells if transferred intravenously into recipient mice[8]. However, further studies supported the observation that ETPs do not retain the potential to develop into myeloid lymphocytes under physiological conditions[9, 10, 11, 12]. With each gradual step in the generation of functional T-cells from HSC, the precursor potential to develop into multiple progenitor becomes restricted. This is due to intra-thymic environment and establishes ETP as the earliest precursor committed to both αβ and γδ T-cell generation.[8, 11, 13]

ETP progresses to Double Negative cells (DN, CD4- CD8-), which can be further divided into multiple subgroups of progenitor cells. The DN subsets are determined on the basis of sequential expression CD44 and CD25 where CD44+CD25-, CD44+CD25+, CD44-CD25+ and CD44-CD25- are termed as DN1, DN2, DN3 and DN4, respectively. At the DN1 stage, Notch1 signalling ensures the lineage commitment to T-cell generation by preventing conversion to dendritic cells[14, 15]. The interaction between Notch1 receptor on DN1 with its ligand Delta-like 4 (DLL4) on Thymic Epithelial Cells (TEC) in the corticomedullary junction of the thymus [16, 17] serves as one of the checkpoints in T-cell development from ETP.

DN1 cells differentiate to DN2 cells following migration deeper into the cortex, where the cells prepare for the TCR gene rearrangement, mediated by RAG1 and RAG2 in DN3 cells [18, 19]. The extensive gene rearrangement in the β, γ and δ loci to determines the fate of the progenitor cells, emerging as either αβ, following β-selection or γδ T-cells occur in the DN3 stage[20]. Signalling through the pre-TCR and Notch1 pathways are essential to progress from DN3 and DN4 to the Double Positive state (DP) [21]. Here the gene rearrangement in the α-loci leads to the production of correctly assembled αβ TCR[22].

The binding of both CD4 and CD8 on cells that bind to the invariant region of MHC class-II and MHC class-I respectively, ensures that useful MHC-restricted TCR expressing cells are rescued from death. This occurs as the co-receptors bring Lck into physical proximity with cytosolic domains of the engaged TCR to initiate signalling that potentially assists with RAG gene repression, long-term survival, migration into the medulla, and differentiation into mature T cells in a process called positive selection.[23, 24, 25] In the last stage, cells go through a negative selection process which results in the deletion of self-reactive T-cells before the single positive CD4+ and CD8+ T-cells emerge from the thymus and circulate in the periphery.

1.2 Different T cell subsets

1.2.1 CD8 T cells

The cytotoxic activity of thymus-derived lymphocytes was noted in several early studies focusing on allogeneic, MHC-mismatched tissue, tumour transplantation models and allogeneic mixed lymphocyte cultures.[26, 27, 28] However, it was the depletion of Ly-2 (CD8a) and Ly-3 (CD8b) bearing lymphocytes[29, 30, 31] as well as studies with virus infected animal models which confirmed that specific T-cell

receptor-bearing CD8 T-cells recognise fragments of antigen in context of MHC class-I and mediated the killing of the target cells. [27, 32 33, 34] Naïve CD8 T-cells (or CTLs) interact with antigen-presenting DCs in the lymph node [35, 36, 37] and differentiate into short-lived effector cells (SLEC), which die after the infection is eliminated. Some become memory precursor effector cells (MPEC) which contribute to secondary immune response upon encounter with the same antigen [38 39, 40].

CD8 T-cells not only develop robust immune responses against intracellular pathogens [41 42] but they are also capable of responding to exogenous antigenic targets by cross presentation. [43 44, 45 46] CD8 T-cells confer their cytotoxicity by two direct cell-cell contact dependent mechanism – i) interaction between Fas-Fas ligand , ii) granzyme and perforin mediated cytolysis; and indirectly affect target cells by producing pro-inflammatory cytokines including IFN-γ, TNF-α.[47] Fas-Fas ligand interaction between target cell and CD8 T-cells results in classical apoptosis of the target cell[48]. Granzyme and perforin mediated cytotoxicity to eliminate target cell without killing the bystander cells by caspase-dependent and -independent manner.[49, 50] It has also been reported that CD8 T-cells can kill 2-16 virus-infected cells per day[51] and cooperate to increase this rate while demonstrating dual polarity in their ability to kill multiple targets simultaneously.[51, 52, 53] CD8 T-cells play important role in cancer and auto-immune diseases [54 55 56 57]. CD8 T-cells specific for neo-antigens expressed by tumour cells are critical for anti-tumour immunity. However, chronic antigenic exposure might impair activity rendering them ineffective in providing anti-tumour immunity.[58, 59, 60, 61] On the other hand, self-antigen specific CD8 T-cells are also associated with the auto-immune disease initiation in diabetes [62 63] and early-stage Multiple sclerosis (MS) [64, 65] It was demonstrated that Myelin basic protein specific auto-reactive CD8 induce MS. [66] Depleting CD8 T-cells ameliorated the severity of disease by reducing the number of lesions and relapses.[67] An altered gene prolife of CD8 T-cells were also found to correlate with poor prognosis in systemic lupus

erythematosus (SLE) patients. [68] These findings suggest a multifaceted role of CD8 T-cells in immune system.

1.2.2 CD4 T cells

T-cells were initially identified as supporting cells which were necessary to develop antibody responses by B-cells.[69, 70, 71, 72, 73] Later it was discovered that a specific subset of T-cells, termed CD4 T-cells, produced soluble factor such as IL-4 and provided co-stimulation by CD40-CD40L which promoted antibody production against foreign antigens by B-cells.[74, 75, 76, 77, 78] These CD4 helper T-cells bind to the antigen in context of MHC class-II on antigen-presenting cells.[79, 80] B cells, when acting as antigen-presenting cells, promote the activation of helper cells that in response produce cytokines that support B cell development. During activation of CD8 T cells by Dendritic cells, the CD4 cells promote the licencing of DCs and support the development of memory CD8 responses. [81, 82, 83, 84, 85] In some animal studies, even in the absence of CD4 T-cells, primary CD8 T-cell responses were observed against viruses, but they failed to mount effective response upon secondary challenge.[85, 86, 87, 88] CD4 T-cells constitutes a major part of PBMCs (25-30%)[89] and CD4 Tcell population consists of several distinct subpopulations which are: T Helper 1 (Th1) cells, T Helper 2 (Th2) cells, Th3 cells, Th9 cells, Th17 cells, Th22 cells, Follicular helper T-cells (TFH) and Regulatory T-cells.

1.2.3 γδ T cells

γδ T-cells represent an unconventional T-cells subset which constitute 1-5% of total population[90] TCR of γδ T-cells are composed of γ and δ TCR chain instead of a and b TCR chain like most of the CD3+ T-cells. γδ T-cells emerge earlier than ab T-cells in the thymus during T-cell development [91, 92] γδ T-cells distributed throughout the

lymphoid system and they are enriched as part of interepithelial lymphocytes (IEL) which are located within the epithelial layer of mucosal and barrier tissues [93, 94, 95] γδ T-cells recognising antigens such as phosphoantigens, i.e., phosphorylated microbial non-peptide molecules that are metabolic intermediates of the isoprenoid biosynthesis[96, 97, 98, 99] Vd1+ γδ T-cells also recognise glycolipid antigens as well as sulfatides in complex with CD1d [100, 101] that accumulate in lesions in MS patients[101] Interestingly, γδ T-cells were also termed the "innate adapter of immune system" [102] as they coordinate with neutrophil by releasing chemokines such as CXCL8. [103, 104] MCP-2[105] and promote the differentiation into antigen-presenting cells which in turn activate conventional CD4 and CD8 T-cells [104, 105, 106] They also secrete IFN-g and IL-17 to provide a powerful pro-inflammatory environment thought to be important in the development of autoimmune disease[107, 108, 109, 110]

1.2.4 Natural Killer T-cells (NKT cells)

Natural Killer T-cells (NKT) cells (only ~0.5% of total T-cell population) were first identified in 1987 as a distinct CD4-CD8- (Double negative, DN) T-cell population which expressed intermediate level of αβ TCR as well as NK cell marker NK1.1.[107, 111, 112, 113, 114, 115] NKT cells are defined by expression of CD1d-restricted αβ TCR, NK1.1 and recognition of hydrophobic ligand including various lipids and glycolipids (e.g. α-Galactosylceramide, glycosylphosphatidylinositol etc.). [108, 109, 110, 116] The TCR of NKT cells predominantly express an invariant α-chain consisting of Va14 Ja281 (now known as Ja18) [117, 118] required for the development of NKT Cells.[118] NKT cells population consists of a heterogeneous population of cells with varied functions. CD4+ NKT cells produce both Th1 (IFN-γ, TNF-α , IL-17) and Th2 (IL-4, IL-13) cytokines while the CD4-, NKG2D+ NKT cells secrete only Th1 cytokines upon activation.[119, 120, 121] It was also reported that CD8α+ NKT cells produce higher amount of IFN-γ and have more cytotoxic potential in comparison to CD4+ or CD4−CD8−

subsets. Moreover, all NKT subsets upregulate CD40L upon activation with antigen and promote IL-12 as well as IL-10 production by dendritic cells.[121]

1.2.5 Mucosal associated invariant T-cells (MAIT)

Mucosal associated invariant T-cells (MAIT) are non-classical innate-like T-cell population which are restricted by highly conserved MHC class-I related molecule MR1 and is abundant in intestinal lamina propria (LP) of humans and mice.[122, 123] They are CD4-CD8- (double negative, DN) T-cells with invariant a-chain - Va7.2-Ja33/20/12 in humans and Va19- Ja33 in mice, in conjunction with oligoclonal TCRβ chain.[122, 123] Further research revealed the existence of CD4+ and CD8+ MAIT cells [123] The selection and development of MAIT cells require B-cells as B-cells deficiency results in absence of MAIT. [124, 125] In human, most of the MAIT cells are dependent on the transcription factor Promyelocytic Leukaemia Zinc Finger (PLZF) for development. [123] MAIT cells recognise various microbial Vitamin B2 metabolites (Riboflavin) and Vitamin B9 (folic acid). [126, 127, 128] However, MAIT can also be activated in TCR-independent way by IL-18 in synergy with IL-12, IL-15 and/or interferon-a/β.[128, 129, 130] Following activation, MAIT cells produce high level of IL-17 [131] [132] and IFN-γ, IL-4, IL-10, GM-CSF etc.[128] MAIT produce granzyme-B (GzB) and perforin upon bacterial antigen recognition and mediate the cytotoxic killing of the infected cells [133] and have been associated with brain lesions in MS patients.[134, 135]

1.2.6 Natural regulatory T-cells (nTreg)

Thymus derived natural regulatory T-cells (nTreg), defined as CD4+CD25HighCD127LowFoxP3+, are important regulator of immuneresponses and they are essential to maintain tolerance and prevent autoimmunity. [136, 137] nTreg constitutes up to 10% of peripheral CD4 T-cells [138, 139] CD4 nTregs have been studied

extensively in the last few decades and only recently several studies have also reported the important role CD8+CD25+FoxP3+ nTreg in immune-regulation.[140, 141, 142, 143]

nTreg cells are currently defined as CD4+FoxP3+CD25HighCD127Low [144, 145, 146, 147]. These cells also express LAG-3, 4-1BB, GITR, CTLA-4,OX-40, CD73, CD39 and neuropilin-1.[137, 148, 149, 150] However, none of these markers are exclusively expressed by nTreg and a combination of markers are still required to identify these cells. Interestingly, nTreg cells could also be divided into two groups based on CD45RA and CD45RO expression.[151, 152, 153, 154] The CD45RA+ nTreg and CD45RO+ nTreg cells are termed naïve and memory nTreg, respectively. CD45RA+ nTreg differ from CD45RO+ nTreg in their reduced potential for proliferation and migration.[151] It was also reported that CD45RA+ nTreg were preferentially located in the bone marrow and cord blood whereas CD45RO+ nTreg were predominant in the skin and peripheral blood. Moreover, it was also demonstrated that naïve nTreg cells are less susceptible to CD95-CD95L (FAS-FASL) mediated apoptosis compared to memory nTreg.[153] Interestingly, FoxP3+CD25+ regulatory cells with similar suppressive potential as nTreg can also develop from naïve CD4+CD25- T-cells in the peripheral immune system. These non-thymic FoxP3+CD25+ cells are known as peripheral Treg (pTreg) and the induction of pTreg is dependent IL-2 as well as TGF-b.[155, 156, 157] Comparative studies to determine their functional potential also demonstrated that pTreg cells were more immune-suppressive compared to nTreg with the same TCR specificity.[158] It has also been suggested that neuropilin-1 (Nrp-1) could be used as a surrogate marker to distinguish nTreg, which express Nrp-1, from pTreg in order to further investigate the role of these immune cells in mediating tolerance[148, 159, 160].

1.3 T cells activation and differentiation

Inactive naïve T-cells migrate to the periphery and continuously recirculate between secondary lymphoid organs and blood via the lymphatic system until they encounter cognate antigen. Under the appropriate circumstances, with the help of co-stimulatory signals and supporting cytokine milieu, naïve T-cell become activated which results in proliferation and differentiation into various kind of effector and memory cells.

1.3.1 Naïve T-cells

Thymus derived antigen-inexperienced and inactive cells are usually considered naïve T-cells. Until recently, these were perceived to be part of a developmentally synchronised and homogeneous T-cell population. However, several studies have demonstrated heterogeneity, as they differ on the basis of phenotype, dynamics, location and function[161]. Human naïve T-cells have a considerably longer lifespan of 6-9 years compared to (6-11 weeks) in mice, where thymic output exclusively sustains the naïve T-cell pool throughout their life without any peripheral proliferation[162]. The human naïve T-cell pool is maintained by homeostatic peripheral proliferation of thymic emigrant T cells. This maintains naïve T cell numbers later in life due to reduced thymic output and atrophy of thymus with age [162, 163]. Naïve human T-cells can be defined by combinations of different markers. However, this usually includes; CD45RA+CD45RO-CD62L+CCR7+. Expression of the homing receptor such CD62L and CCR7 assist the trafficking of naïve T-cells to secondary lymphoid organs after exiting the thymus. They also express the intermediate level of CD28 and CD27 co-stimulatory markers[164, 165]. Human CD4 and CD8 naïve T-cells can also be divided into distinct subpopulations based on the expression of CD31 and CD103, respectively.[161]

1.3.2 Effector T-cells

Naïve cells can differentiate to effector cells following antigen recognition and obtain the effector phenotype defined as CD45RA+/-CD45RO+CCR7– CD62L–. These effector T-cells upregulate several activation markers such as CD69, CD71, CD25 and HLA-DR. Effector cells might also dynamically express proliferation markers, such as Ki67[166]. Effector cells expand rapidly during an immune response, and at the end of the immune response, ~90% of effectors die during the contraction phase[167].

1.3.3 Central Memory T-cells (TCM cells)

After activation, some effector T-cells develop into Effector memory or Central memory T-cells which are capable to responding to secondary antigenic challenge. Central memory (TCM) are identified by expression of CD45RA-CD45RO+CCR7+CD62L+CD27+ CD28+CD127+. The re-expression of homing receptor provides them with the potential to relocate to secondary lymphoid organs. It has been suggested that TCM might serve as a precursor for effector memory T-cells (TEM) as TCM have longer telomere and TCM can generate TEM in vitro[168, 169].

1.3.4 Effector memory T-cells

Effector T cells can also develop into effector memory (TEM) T-cells which are defined as CD45RA-CD45RO+CCR7-CD62L-CD27+/-CD28+/- CD127+. The lack of homing receptor CCR7 and CD62L restricts these cells to the peripheral non-lymphoid tissue [170]. TEM cells also express chemokine receptors such as CXCR3, CCR4 which allows them to be retained in the inflamed tissue[168, 171, 172] and have a more rapid response following antigenic restimulation[167].

1.3.5 Terminally differentiated effector memory cells re-expressing CD45RA (TEMRA) T cells

In the recent years, another subset of activated T-cells has been identified which is characterised by the apparent re expression of the naïve marker CD45RA+. They are CD45RA+CD45RO+/-CCR7-CD27-CD28−PD-1+KLRG1+. TEMRA cells demonstrate relatively lower effector function, and it has been suggested that TEMRA cells might derive from TCM cells in the absence of antigen and in the presence of low Interleukin-2 and high interferon-gamma secretion [173]. Although CD8+ TEMRA cells have been studied more, CD4+ TEMRA cells have also been identified in peripheral blood. These cells have been associated with protective immunity against Dengue virus and Cytomegalovirus (CMV) infection [174, 175, 176, 177] . TEMRA cells can be further divided into two subsets depending on the expression of CD57 along with GPR56+ [178].

1.3.6 Tissue-resident memory T cells (TRM)

In recent years, studies in viral models have discovered a distinct subset of memory T cells that retain in peripheral tissues and can provide much greater protection compared to their TCM cell counterparts.[179] This non-recirculating memory T cell subset is defined as Resident Memory T cells (TRM). TRM cells can be either CD4+ or CD8+, and they reside in epithelial, connective tissues, muscle and the sinusoids of the liver, neuronal tissue, and some were found in secondary lymphoid organs. [180, 181, 182, 183]

The development of TRM cells is summarised in a two-step model (figure 1.1).

TRM cells development is initiated in the lymph nodes by a specific type of DC (BATF3+ DCs in mice). This DC subset directs the generation of a putative TRM cell precursor (pTRM) but is not necessary to induce other T cell subsets (TCM cells, TE cells or TEM cells).[184] After reactivation, TCM cells maintain the ability to develop into

TRM cells, presumably by the same subset of DCs. A crucial second step in the development of TRM cells is recruitment into the tissue. This process is prompted by tissue inflammation and IFN-γ produced by CD4+ T cells[185], which elicit chemokines production and the expression of adhesion molecules on the endothelium.[186 187] Once inside the tissue (parenchyma), precursors of TRM cells further mature under the influence of inflammatory signals like type I interferons and acquire markers such as CD69. Although TEM cells and TE cells can also enter the tissue, they would not develop into TRM cells. TRM cell precursors that enter the epithelial layer upregulate CD103 under the influence of local TGF-β[188, 189].

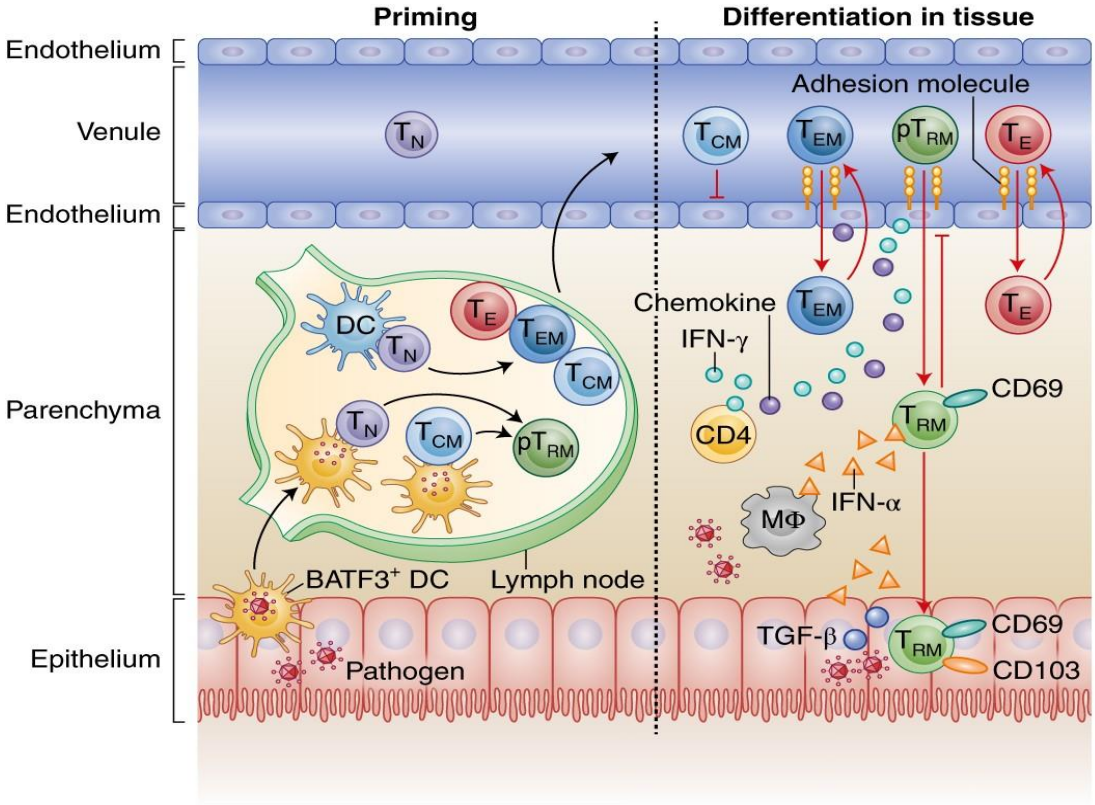

Figure 1. 1 TRM cells development in two-step model.

The first step is the initiation of TRM cells development by a specific type of DCs in the lymph node [left]. This DC subset induces the production of a putative TRM cell precursor (pTRM) but is not necessary for the induction of other T cell lineages (TE cells, TEM cells or TCM cells). The second step of TRM cells development is recruitment into the tissue (right). This process is elicited by IFN-γ produced by CD4+ T cells and tissue inflammation, which enable the production of chemokines and the expression of adhesion molecules on the endothelium. Inside the parenchyma, TRM cell precursors further mature

under the influence of inflammatory signals (such as type I interferons) and acquire markers such as CD69. TE and TEM cells can also enter the tissue, but they do not develop into TRM cells. Under the influence of local TGF-β, TRM cell precursors that enter the epithelial layer upregulate CD103. MΦ , macrophage. TN, naive T cell. **(taken from Amsen et al., Nature Immunology, 2018[187])**

The defining characteristic of all TRM cells is the commitment to their tissue of residence. This distinguishes them from naive T cells, TE cells, TEM cells and TCM cells, all of which recirculate between lymphoid organs and the blood and/or lymphatics (figure 1.1). The two major mechanisms used to ensure TRM cells retention within the peripheral tissues are the resistance to signals that promote homing into the blood or lymphoid tissue and adhesion to their home tissue. TRM cells have a low-level expression of receptors for sphingosine-1-phosphate (S1P), a chemoattractant produced by endothelial cells.[190] Unresponsiveness to S1P is amplified by CD69 (C-type lectin), which hinders the surface expression of the S1P receptor. [190 191] Although CD69 is commonly known as a marker of recently activated T cells, most TRM cells constitutively express this molecule. It is often used to identify these cells within the organs.[181, 190, 191] Moreover, TRM cells lack the expression of CD62L, an adhesion molecule needed for the entry into lymph nodes, and CCR7, which is a chemokines receptor produced in lymphoid tissue.[183]

The adhesion of TRM cells to the tissue is actively promoted by the expression of adhesion molecules. The most important among these is the integrin CD49a (α 1β 1; VLA-1). This integrin binds to the extracellular matrix components laminin and collagen. [192, 193, 194] Similar to effector and memory T cells, TRM cells express the activation and memory marker CD44, which might allow binding to hyaluronic acid (another matrix component).[183, 195] Localisation of TRM cells mainly depends on tissue-specific retention molecules. For example, the most-studied TRM cells reside in epithelial tissue and express CD103 maker. [187]

CD103 (integrin αE), present on intraepithelial or peripheral T cells, some peripheral Treg cells and gut mucosal dendritic cells (DC), is a human integrin protein coded by ITGAE gene. CD103 is considered to be responsible for better recognition, homing and retention of antigen-specific CD8+ T cells in the epithelial tissue and cancer tissue. It is usually found on the surface of TILs, and it binds to E-Cadherin on epithelial cells. TGF-β has been recognised to be responsible for regulating the expression of CD103/β7 on the surface of T lymphocytes.[196] TGF-β is a highly pleiotropic cytokine expressed in many tissue types and is often overexpressed in most cancers. However, TGF-β alone cannot regulate CD103/ β7 expression; concurrent signalling through TCR in combination with high levels of TGF-β can cause rapid CD103/ β7 expression on T lymphocytes.[187, 196] The role of this immune maker is further discussed in 1.9.

1.4 T cell activation and inhibition

The development of productive and protective T cell responses requires proper T cells activation. T cells polarisation and expansion responses rely on three signals provided by DC (figure1.2): antigen presentation in the context of MHC-peptide complexes (signal 1); co-stimulatory signals provided by CD80 and CD86 (signal 2); and signal 3 provided by inflammatory cytokines. [197, 198, 199] Some studies have proposed a role for chemokines in providing a fourth signal (signal 0) in driving the chemotaxis of T cells.[197, 198] Signals 0, 2 and 3 are generated by DC on the binding of PAMPs (Pathogen associated molecular patterns) or DAMPs (danger-associated molecular patterns) to TLRs on DC.[199]

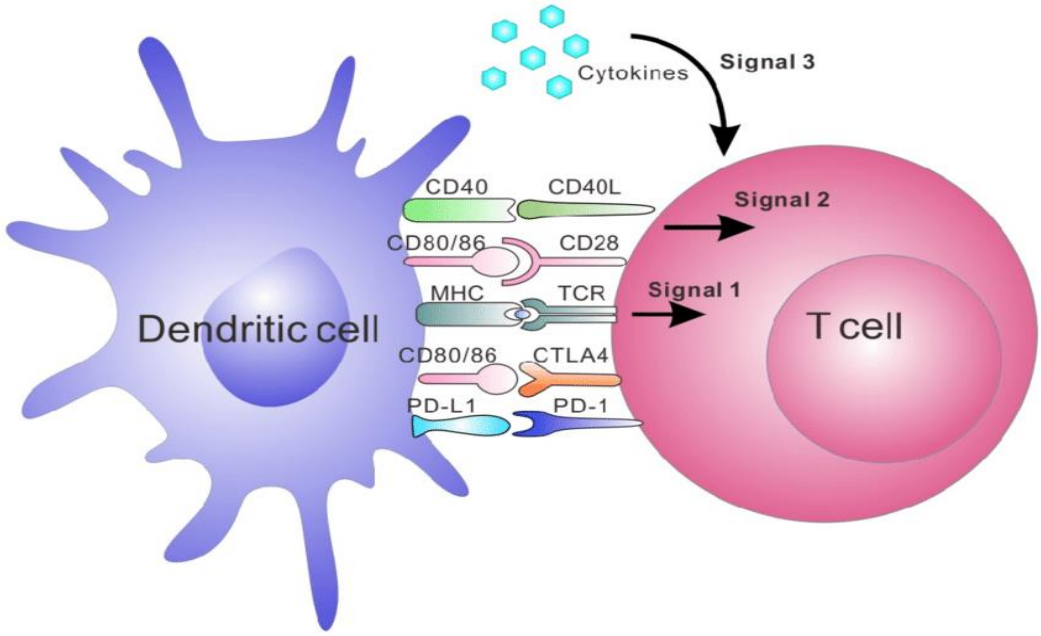

Figure 1. 2 Three signal activation model for T cells.

Signal 1 comprises the presentation of antigen peptides, in the context of MHC class II molecules, which is recognised by the antigen-specific TCR. Signal 2 involves the stabilisation of the synapse through adhesion molecules and the generation of signals via co-stimulatory molecules present on the surface of APCs and T cells. CD80/CD86 on APCs interact with their receptor, CD28, on T cells to generate activatory signals, while interaction with cytotoxic T lymphocyte-associated protein 4 (CTLA4) generates inhibitory signals. Signal 3 is produced by the secretion of cytokines by APCs, which signal via cytokine receptors on T cells in order to polarise them toward an effector phenotype. (taken from Wang et al. , Theranostics, 2017[200])

1.4.1 Signal 1 - T-cell receptor activation

Signal 1 is initiated by binding of TCR complex to MHC peptide complex presented by APCs. The TCR signalling is mediated by co-receptors CD4 and CD8. Upon engagement of TCR, the extracellular domains of these co-receptors act as an auxiliary anchor to stabilise binding between TCR and MHC peptide complex[201, 202]. In contrast, the cytoplasmic domain of CD4 and CD8 interacts with Lymphocyte tyrosine kinase (Lck), mediating recruitment of Lck close to the TCR complex once it

engages antigen presented by the MHC molecules[201, 203, 204]. Then Lck phosphorylates immunoreceptor tyrosine-based activation motifs (ITAMs) on CD3γ chain, CD3δ chain, CD3ε chains, and CD3ζ-chains[205]. Phosphorylation of these ITAMs leads to the recruitment of Zap70 protein (zeta-chain associated protein of 70 kDa) to the TCR and its phosphorylation and activation by Lck.

Activated Zap70 in turn phosphorylates linker of activation of T-cell protein (LAT) at four key tyrosine residues. Activated LAT recruits multiple proteins involved in signalling to form a multiprotein complex termed as LAT signalosome[205, 206]. The key signalling proteins within this complex include phospholipase Cγ1 (PLCγ1), growth factor receptor-bound protein 2 (GRB2), GRB2-related adaptor protein GADS, SLP76 (SH2 domain-containing leukocyte protein of 76 kDa), adhesion- and degranulation-promoting adaptor protein (ADAP), interleukin-2-inducible T cell kinase (Itk), NCK1 and VAV1[205].

The LAT signalosome transduces signals to several signalling pathways involved in T-cell growth and differentiation, for example, the MAPK kinase pathway, the Ca2+ pathway and NF-κB pathway[205, 206] . Activation of these signalling pathways leads to mobilisation of transcription factors into the nucleus, resulting in the expression of genes involved in T-cell effector function, growth, differentiation and survival [206, 207]. The proteins within the LAT signalosome are also involved in actin cytoskeletal reorganisation and activation of integrin inside-out signalling. These two major events are important for facilitating T-cell and APC cell surface contact and adhesion and immune synapse formation [205, 206].

LAT plays a pivotal role as loss of its expression leads to complete loss of TCR signalling [206]. In vivo, thymocytes development in LAT-/- mice halted at the double negative CD25+ CD44- stage and no mature αβ T-cells were found in the mice

secondary lymphoid organs[208]. Studies in LAT-deficient Jurkat T-cells showed that several TCR signalling events were defective, including Ca2+ mobilisation, Ras activation, CD69 expression, and Erk activation [209]. The role of LAT as a nucleating site for other adaptor proteins involved in TCR signalling has made it indispensable in TCR signalling.

1.4.2 Signal 2- Co-stimulation/Co-inhibition

TCR stimulation alone without signal 2 and 3 on TCR-MHC-peptide complex binding renders T cell anergic or cause apoptosis due to inadequate activation. This is considered a peripheral T cell tolerance mechanism against self-antigens. Mature DC upregulate the expression of co-stimulatory molecules, which provide signal 2 on ligation[210, 211, 212]. The most prominent T-cell co-stimulatory molecule is CD28[213]. It is constitutively expressed on naive T-cells and binds to B7-1 (CD80) and B7-2 (CD86) expressed on the cell surface of APCs. The B7-CD28 co-stimulatory pathway is the best characterised to date and is the most commonly used pathway in T cell studies. The B7-CD28 interaction on DC and T cells yields the strongest co-stimulatory signal for amplifying T cell activation[214]. Nearly all human CD4+ T cells express CD28, while only half the CD8+ T cell express CD28. It has been suggested that the rest of the CD8+ T cells do not express CD28 due to exhaustion by chronic activation and they become regulatory in nature. CD28 ligation leads to the production of cytokines like IL-4, IL-5, IL-13, IFN-γ and TNF-α, as well as chemokines like IL-8 and RANTES[215, 216].

In order to balance T-cell responses, there is a negative secondary signal exerted by inhibitory molecules expressed on T-cells. The most prominent example of a T cell co-inhibitory molecule is CTLA-4. Expression of CTLA-4 is induced 24-48 hours after TCR triggering on naive conventional T-cells. However, it is also constitutively

expressed on CD4+CD25+FOXP3+ Treg cells[217, 218]. In naive conventional T-cells, CTLA-4 is found mainly in the intracellular vesicles by interacting with the μ2 subunit of clathrin adaptor protein complex AP-2[218]. T-cell activation induced trafficking of CTLA-4 to the cell surface; however, it is constitutively endocytosed from the plasma membrane and is either recycled back to the cell surface or subject to degradation in the lysosomes[218].

CTLA-4 shares the same ligands as CD28: B7-1 (CD80) and B7-2 (CD86). However, CTLA-4 binds to both ligands with higher affinity and avidity than CD28 does[218]. It is thought that this is one of the CTLA-4 mechanisms of action, which is to outcompete CD28 for binding to the ligands, thus attenuating T-cell responses[217]. T-cells of CTLA-4-deficient mice exhibited hyperproliferation and multiorgan infiltration, and the mice died within 3-4 weeks after birth[218], suggesting its negative regulatory role in T-cells. Autoimmune pathology observed in CTLA-4-deficient mice has been shown to be CD28-dependent, with specific CD28 binding motifs in the CD28 cytoplasmic tail responsible for disease development has now been identified [219]. This shows that CTLA-4 functions by opposing CD28 effects on T-cell signalling.

Previous studies using CTLA-4 specific antibodies have shown that crosslinking of CTLA-4 caused inhibition of T cell activation and proliferation, thus proving CTLA-4 involvement in transducing negative signals to T cells[218]. Tregs are the major CTLA-4-expressing cell type [220]. It has been shown that CTLA-4 is required in mediating Tregs functions of suppression, hyposignalling and anergy [221]. Mice lacking CTLA-4 on their Tregs have been shown to develop autoimmunity, further supporting the role of CTLA-4 in Tregs suppressive function[218].

Multiple co-stimulatory and co-inhibition molecules have since been described and used as targets for immunotherapy in disease and cancer (figure 1.3). The PD-1

(Programmed cell death receptor-1) is another co-inhibitory molecule expressed on T cells that shares homology with CD28. The Interaction of PD-1 with its ligands PD-L1 and PD-L2 induce immunosuppression of T cell responses, and hence this pathway is being targeted to reverse immunosuppression in cancer. DC constitutively express CD40, which is further upregulated on maturation and binds to CD40L on CD4+ T cells. CD40 ligation to CD40L (CD154) further upregulates MHC Class II expression on DC and increases cytokine and chemokine production by DC by process of reverse co-stimulation.[215, 216]

The co-stimulatory pathways either fall into the immunoglobulin (Ig) superfamily, T cell immunoglobulin and mucin (TIM) domain family or the tumour necrosis factor TNF/TNFR superfamily. So far, seven members of the B7 family have been identified (B7.1, B7.2, ICOS-L (B7-H2), PD-L1, PD-L2, B7-H3 and B7-H4). Whereas six co-stimulatory molecules belonging to the TNF/TNFR family have been described so far, namely, HVEM, BTLA, CD70, CD30, 4-1BB-L (also called CD137) and OX-40L. The interaction of co-stimulatory molecules with their ligands triggers expression and transcription of cytokine genes, stabilises cytokine mRNA, increases glucose uptake and utilisation (also necessary for CCR7 oligomerisation), promotes T cell viability and promotes memory responses by ensuring that T cells remain responsive upon re-stimulation[215, 216, 222]

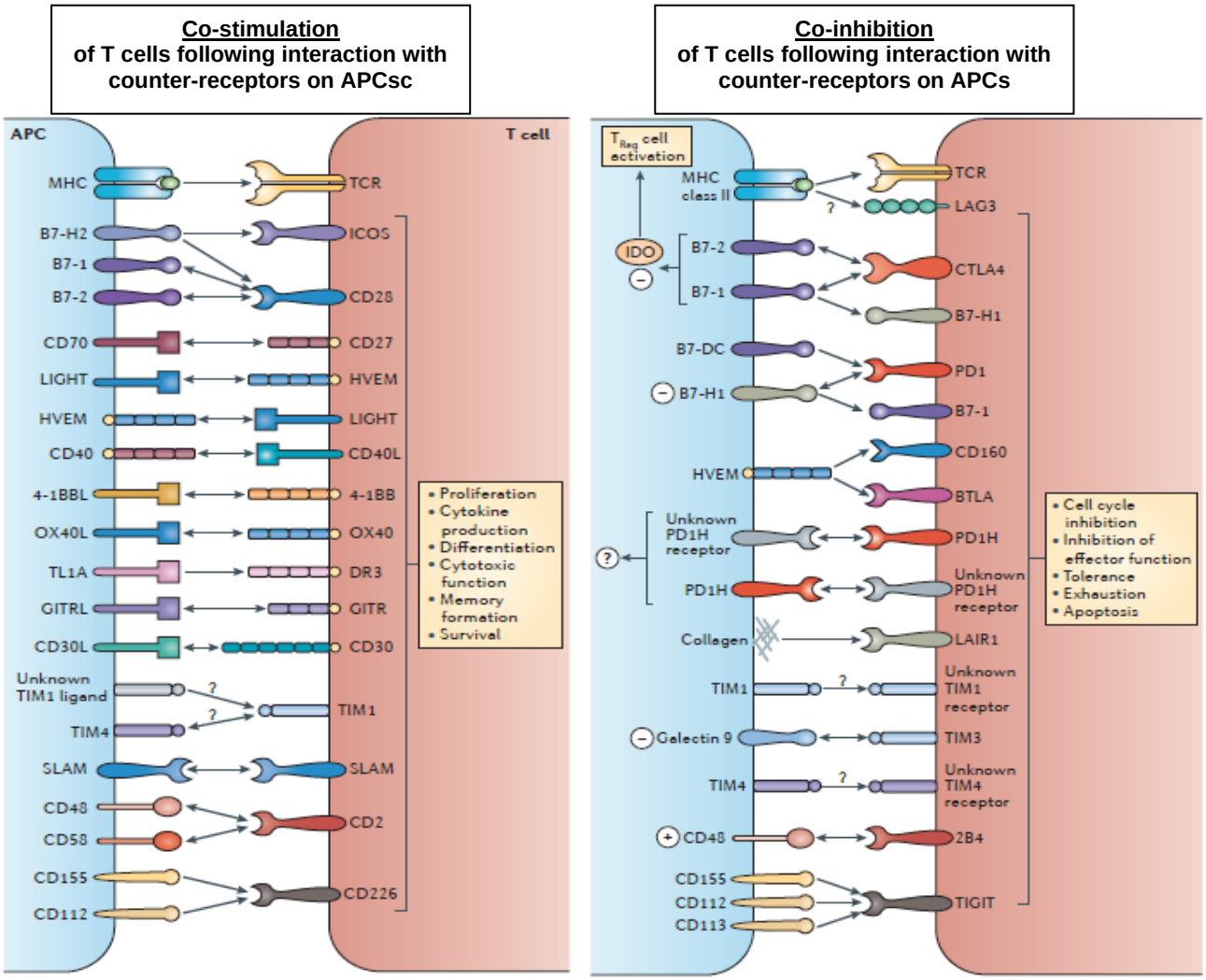

Figure 1. 3 Costimulatory and co-inhibitory molecules expressed on the surface of T-cells and their ligands/counter receptors expressed on APCs.

(taken from Chen et al., Molecular mechanisms of T cell co-stimulation and co-inhibition. Reviews, 2013[223])

The balance between co-stimulation and co-inhibition is required to provide immunity while avoiding undesirable autoimmunity. This can be achieved in several ways. Regulation of cell surface expression is the primary mode of achieving balance[223]. Most co-stimulatory and co-inhibitory molecules are induced following activation, and their expression might be overlapping during the course of T-cell activation and differentiation.[214, 223]

1.4.3 Signal 3

The absence of signal 3 cytokines on the binding of TCR-MHC-peptide complex and co-stimulation leads to impaired T cell effector functions, poor survival and the cells do not develop or differentiate into a responsive memory subset. Signal 3 cytokines, type I IFN and IL-12, have been described as critical factors required for CD8+ T cell survival and expansion. They also promote cytolytic activity and IFN-γ production by CD8+ T cells[210, 211, 212, 224]. Similarly, signal 3 in the form of inflammatory cytokines is also required for optimum CD4+ T cell activation and this has been proposed to be mediated by IL-1 cytokine[211, 225]. IL-12 can provide an early signal necessary for the development of the effector and central memory T cell population. However, prolonged signalling by antigen and IL-12 can lead to the development of short-lived effector cells (SLEC) instead[211]. This concept has been challenged by Pham et al.[210] who demonstrate that signal 3 cytokines are needed for clonal expansion of CD8+ T cells but not for differentiation into effector/memory T cells.

Signal 3 cytokines govern the polarisation and differentiation of T cell subsets into different effector and memory T cell populations. The pattern of cytokine expression and the nature of the immune function of T cells induced depends on the cytokine milieu generated by DC on exposure to microbial PAMPs[211]. For example, IL-12 produced by DC exposed to intracellular bacteria induces Th1 differentiation, while parasites drive DC to produce cytokines that induce Th2 differentiation. Once a Th1 or Th2 response develops, it inhibits the differentiation of naïve T cells into the other type of T helper cell. IFN-γ produced by Th1 cells inhibits the development of Th2 cells, while IL-4 and IL-10 produced by Th2 cells inhibit the development of Th1 cells[198, 227].

1.5 Tumours

Tumours are defined by the uncontrolled growth of cells, the invasion of surrounding tissue and metastasis. Tumours are considered one of the leading causes of death in the modern world, with 367,000 new cases of cancer diagnosed in the UK between (2015- 2017). Breast, bowel, lung and prostate cancers accounted for over half (53%) of all new cancer cases in the UK in 2017. There were 166,000 deaths from cancer in the UK in 2018. Breast, bowel, lung and prostate cancers account for 45% of all cancer deaths in the UK in 2018.

1.6 Overview of Immune system in the tumour microenvironment

The tumour microenvironment contains different soluble factors like chemokines and cytokines, lymph and blood vessels, immune cells and diverse cell types, such as fibroblasts. The metastatic capacity, survival and growth rate of tumours are controlled by these components. [228]

The expression of neoantigens or cancer-testis antigens or overexpressed antigens can be a result of the genetic alterations associated with cancer cells, which will enable the immune system to distinguish between normal and cancer tissue via the interactions of the different antigens and major histocompatibility class I (MHCI) molecules on the surface of tumour cells.[229] This process of immune system participation in cancer cells recognition and elimination is defined as tumour immunosurveillance.[228]

Protecting the host against cancer development can be accomplished by the innate and adaptive immune systems via mechanisms of immunosurveillance.[230] NK cells attack the first few transformed cells by detecting specific ligands on the surface of

the tumour cells. Then the destruction of the transformed cells due to that interaction will facilitate dendritic cells (DC) and macrophages uptake of the fragments and process it. Simultaneously, when dendritic cells and macrophages are activated, different inflammatory cytokines will be secreted, and cancer cell-derived molecules will be presented on DC and macrophages to interact with T cells. Additional cytokines are produced due to T- and B cells activation, which will further enhance innate immunity activation and promote the expansion of tumour-specific T cells and antibodies production. Therefore, remaining tumour cells will be eliminated and destroyed by the adaptive immune system through the generation of immune memory to certain cancer components, which may prevent the recurrence of that tumour in the future. [231] Although several publications illustrated, using mouse models, that tumours growth and militancy were associated with immune deficiencies. Tumour-infiltrating T cell association with favourable prognosis in various human cancers is the most convincing proof of tumour immunosurveillance.[232, 233]

1.7 Role of T cells in the antitumour immune response

Tumour -infiltrating T cells are part of the cancer immunity cycle. The cytotoxic T cell infiltration into cancer tissue from the bloodstream recognise and kill cancer cells by the interaction between cancer cells MHCI and T cell receptor (TCR) (figure.1.4). [234] Antigen expressing target cells can be destroyed directly and indirectly by different types of T cells. CD4 T helper, which differentiates into different subsets: Th1, Th2, Th22, Th17, Th9, and Treg (regulatory T cells), indirectly participate in cancer immunity through increasing cytotoxic anti-tumour response mediated by CD8 T cells.

Cytotoxic CD8 T cells are known as the critical effector cells, which are responsible for the direct removal of target cells. Several studies investigated the prognostic significance of CD8+ T cells in different types of cancers.[235, 236, 237]. For instance, some studies conducted on patients with colorectal, liver and oesophageal cancers showed significant disease-free survival with intratumoral CD8+ T cells compared to stromal areas within the tumour. [238]

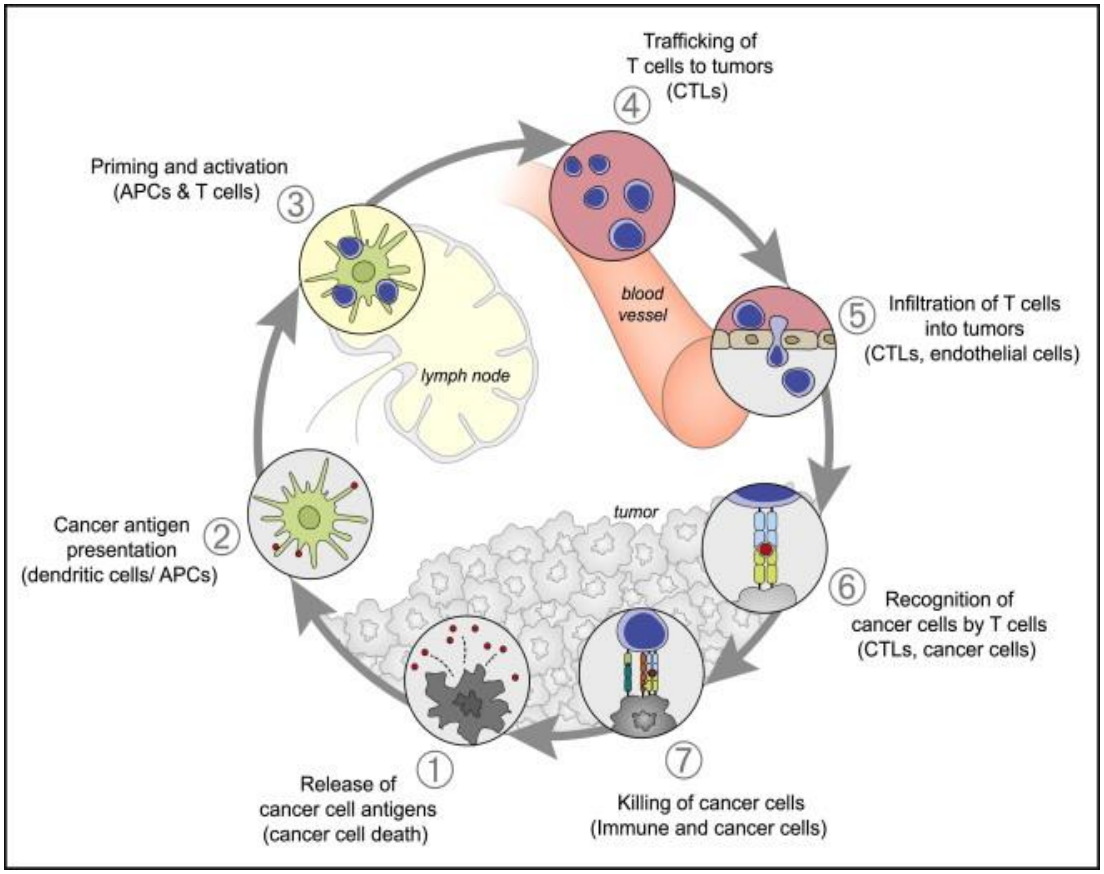

Figure 1. 4 The seven main steps Cancer-Immunity cycle.

The cycle starts with cancer cells releasing specific antigens and ends by killing them. Each step is described in the figure, with the location and primary cell types involved in each step. CTLs: cytotoxic T lymphocytes, APCs: antigen-presenting cells. [Taken from Mellman et al. *Oncology Meets Immunology: The Cancer-Immunity Cycle. Immunity*. 2013[234]]

1.8 Immunoscore: Hot tumours vs cold tumours

Galon et al. studies[239, 240, 241, 242] on the immune cell infiltration in tumour in-situ and the ability of T cells to predict prognosis lead to the development of the system called 'Immunoscore'. Immunoscore is a system that quantifies the number of lymphocytes, particularly CD3 TILs and CD8 TILs, in both centre of the tumour (CT) and invasive margin (IM). The Immunoscore provides a scoring system ranging from low CD3 and CD8 TILs densities found at both the CT and the IM, Immunoscore 0 (I0) to high immune cell densities stratified as Immunoscore 4 (I4), with increasing score correlating with better disease prognosis. This system has been approved for colorectal cancer patients and is used to provide important prognostic information [243, 244]

According to Galon et al., tumours can also be classified based on their immunological data into four categories: hot (highly infiltrated, Immunoscore I4), excluded, immunosuppressed, and cold (non- infiltrated, Immunoscore I0) tumours (Figure 1.5). The 'excluded' phenotype is characterised by high T cell density at the edge of tumour sites without infiltrating them within the tumour nest. This reflects the intrinsic ability of the host immune system to mount a T cell effectively- mediated immune response and the ability of the tumour to escape such response by physically hindering T cell infiltration. In contrast, tumour sites are associated with a low degree of immune infiltration, are identified as 'immunosuppressed' phenotype. Immunosuppressed tumours are characterised by the absence of physical barriers and the presence of an immunosuppressive environment that limits further recruitment and expansion.[245] Depending on the pre-existing immunity of the tumour microenvironment, different therapeutical approaches were recommended to treat such tumours with combination immunotherapies, including checkpoint inhibitors. Regarding combination immunotherapy, it is critical to understand the mechanisms

responsible for hot, altered or cold immune tumours in order to effectively treat patients with weak antitumour immunity.

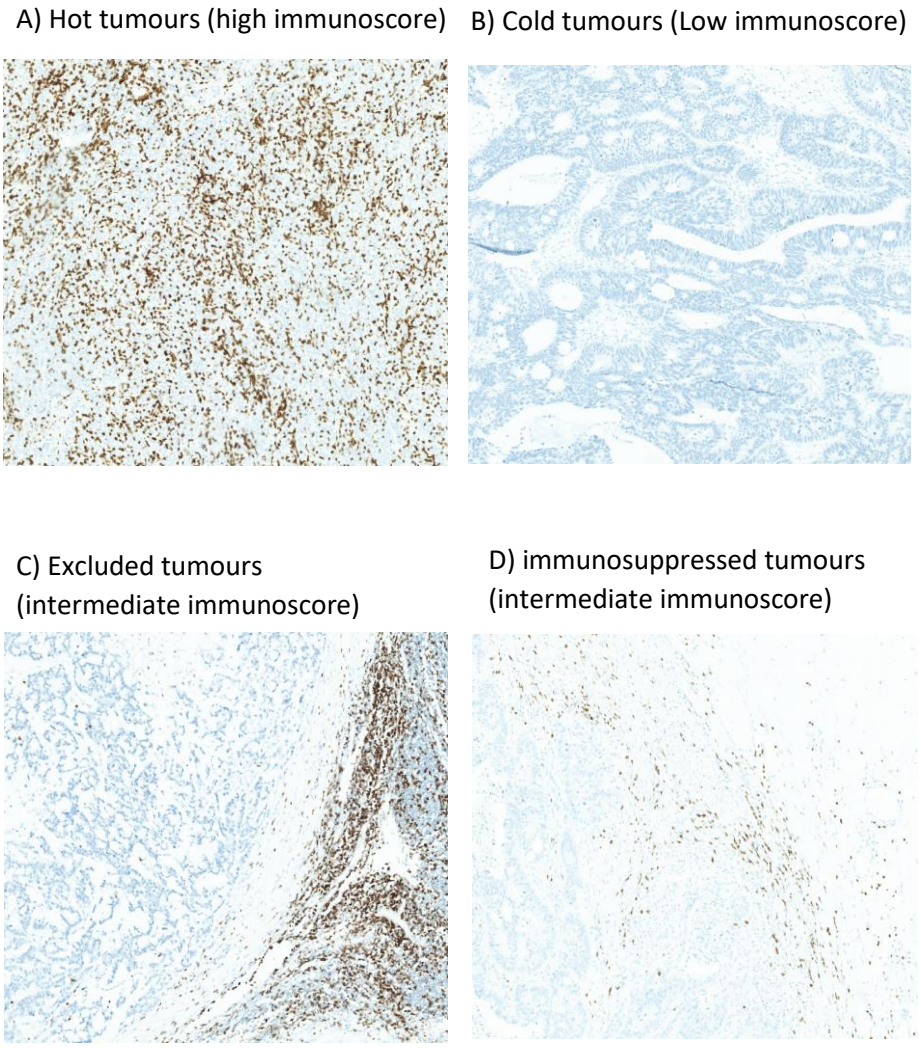

Figure 1. 5 Illustrative examples of 'hot', 'altered' and 'cold' immune tumours

Immunoscore as a new approach for the classification of cancer. A, B, C and D represent hot, cold, excluded, and immunosuppressed tumours, respectively**.** [taken from Galon et al., *Approaches to treat immune hot, altered and cold tumours with combination immunotherapies*. Nature reviews Drug discovery, 2019 [245]]

1.9 The role of CD103+ TRM cells as a positive prognostic factor in solid tumours

Solid tumours, most of which are of epithelial origin, often show enrichment for epithelial TRM cells, which are marked by the expression of the integrin CD103 (α Eβ 7).[246] Among tumours with similar degrees of T cell infiltration, those with the greatest proportion of CD103+ TRM cells have the best prognosis.[247, 248, 249, 250] In a state of viral infection, CD103+ TRM play an essential role in providing protection to human epithelial tissues by the expression of CTLA-4 and PD-1 inhibitory receptors and maintain peripheral tolerance[251]. In a cancerous setting, the adhesive interaction between CD103 and E-Cadherin allows the CTL to release their cytotoxic granules, causing lysis of the tumorigenic epithelial cell. Thus, CD103 interaction with E-Cadherin promotes CTL effector function by promoting the formation of an immunological synapse, subsequent polarisation and release of cytotoxic granules. [187]In addition to this, the interaction is also responsible for intracellular signalling: E-Cadherin interacts with β-catenin, which further interacts with actin cytoskeleton, which can change the motility and shape of the lymphocyte. Cross-linking of surface CD103 also affects the shape and motility of lymphocytes, leading to increased T cell proliferation and lysis of target cells.[132]

In high-grade serous ovarian cancer (HGSC) patients, CD103+ TILs are usually activated CD8+ T cells and NK cells. These TILs are strongly associated with patient survival. Tumours that contained CD8+CD103- TILs showed a poor prognosis compared to CD103+ CD8+ TILs.[252] In patients with NSCLC, CD103+ TIL density is associated with patient survival in an early stage of the disease. These TILs also expressed high levels of PD-1, a biomarker of tumor-specific T cells.[246, 247] CD103 TILs were reported to be present in all breast cancer types, but the highest numbers were seen in ER-negative tumours. These TILs were indicative of a good prognosis

in basal like breast cancer.[250] In endometrial cancer, CD103 is a good marker to differentiate between intraepithelial and stromal T cell populations. The total number of CD103+ TILs in high risk endometrial adenocarcinoma patients was an independent predictor of improved survival.[249] CD8 TILs enriched with high densities of CD103 showed higher cytotoxicity and proliferation, suggesting that in patients with high CD103 density, there was a more robust immune response to the tumour and this can affect the clinical outcome. Lung cancer patients with higher densities of cells with the CD103 marker had better survival.[246] CD103+ T cells are also a prognostic factor for survival in patients with cervical cancer. Cervical cancer patients who had undergone chemotherapy or radiotherapy had fewer numbers of CD103+ TILs. This number decreased further with higher stages of the disease.[248] Several studies have reported that CD8 TILs in CD103hi tumours produce higher quantities of granzyme B when compared to CD103low tumours. This suggested that in tumours rich with TRM cells, there is more robust anti-tumour immunity - the tumour harboured actively proliferating CD8+ T cells, and there is higher production of cytotoxic granules.[252]

1.10 The role of CD39 marker within the tumour microenvironment.

CD39 is a cell surface enzyme encoded by the ENTPD1 gene, responsible for the conversion of pro-inflammatory extracellular adenosine triphosphate (eATP) to adenosine monophosphate (AMP).[253] CD73 further hydrolyses AMP into adenosine. This whole conversion cycle plays a very important role in regulating immune responses. Adenosine is a very potent immune-suppressor of cells that express A2 and A3 receptors. It binds to the A2A receptors present on lymphocytes and thus

prevents effector responses. According to *van Duijn et al* , adenosine accumulation resulting from CD39 upregulation inhibits cytokine responses in CD39+CD8+ TILs and CD39-CD8TILs. (figure 1.6). [254]

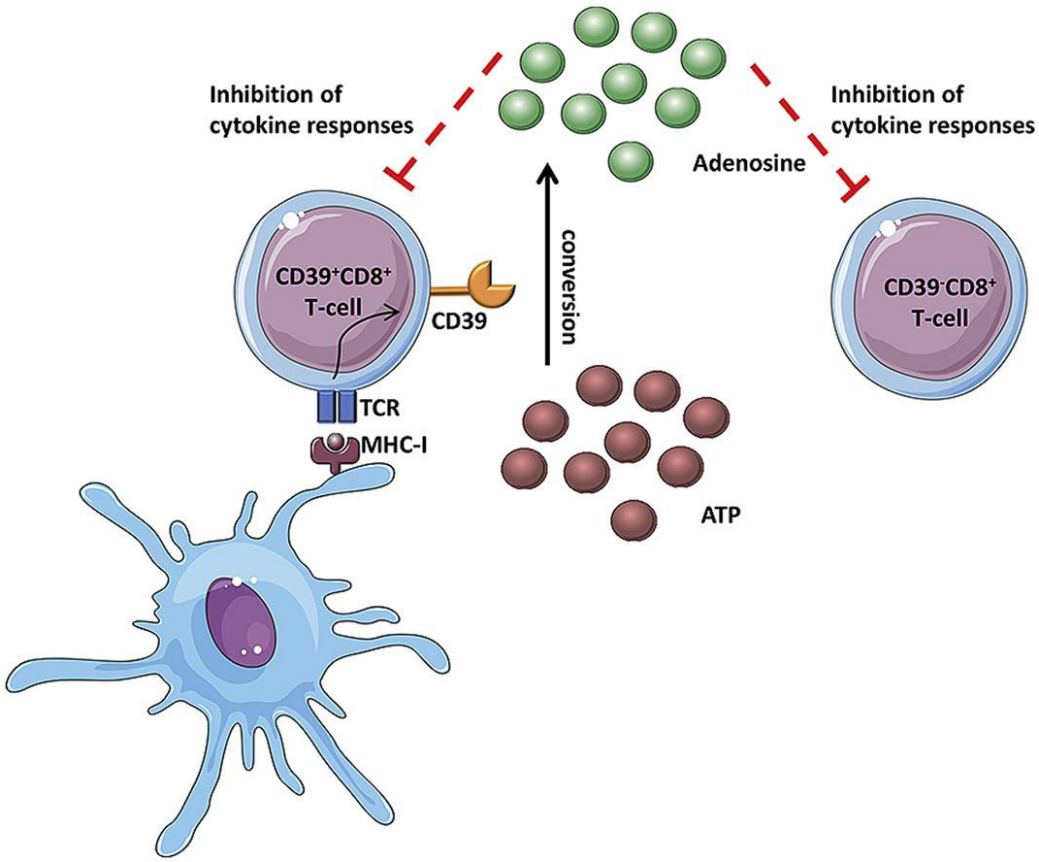

Figure 1. 6 Upregulation of CD39 marker on the surface of CD8TILs due to chronic TCR stimulation.

Adenosine molecules, which result from the conversion of ATP via CD39, inhibit cytokine responses. Therefore, these molecules are considered immunosuppressive molecules. [taken from van Duijn et al., *CD39 identifies a microenvironment-specific anti-inflammatory CD8+ T-cell population in atherosclerotic lesions.* Nature Communications. 2019[254]]

CD39, the rate-limiting enzyme in this cycle, plays a very important role in tumour progression. It is considered a marker for exhausted T cells. CD8+ T cells expressing high levels of CD39 on their surface are considered to be terminally exhausted in chronic viral infections and also in cancer. CD39hiCD8+ TILs express higher levels of effector and exhaustion-associated transcription factors such as Blimp-1, Eomes and Tbet when compared to CD39-CD8+ TILs.[255] CD39+CD8+ T cells have been reported in both- tumours and metastatic lymph nodes in patients with melanoma and breast cancer. These cells are predominantly present in the tumour and metastatic lymph nodes and are usually absent in peripheral tissue, but if present, their frequencies are low. This cell type also showed impaired IL-2 and IFN-γ production in the patient cohort.[256]

Expression of CD39 marker in CD8+ TILs defines a population as highly exhausted and absence of the CD39 marker defines a population of TILs that have undergone chronic antigen stimulation at the site of the tumour. Previous studies have shown that CD8+ TILs show highly heterogenous frequencies of CD39 expression in colorectal and lung cancer.[255]

CD39 is constitutively expressed by Foxp3+ Treg cells and suppression of Th1 and Th17 responses in an adenosine-dependent manner have been well documented for CD39+ Treg cells. Moreover, CD39+ Treg cells also express CD25, activation markers, co-inhibitory molecules, and suppressive cytokines but lower levels of CD127 compared with CD39- Treg cells[125]. According to Zhao et al. CD39hi CD25low Tregs, exhibit sustained Foxp3 levels and functional abilities, indicating it could represent a new specific marker of Tregs. This indicates that CD39 would be a novel checkpoint inhibitor target in preventing adenosine-triggered immune-suppressive effect. [257]

1.11 Recently activated Tumour specific memory resident CD8 T-cells.

Intratumoral CD8+ T cell population can be divided into two types based on their antigen specificities - tumour-reactive T cells and bystander T cells. Within the population of CD8+ TILs, CD103+CD39+ cells are considered tumour-reactive T cells, and bystander cells are absent in CD39, indicating the role of CD39 as a tumour specific marker. [255] A study in human lung cancer patients has shown that CD103+CD8+ TILs express much higher levels of CD39 protein than CD103-CD8+ TILs. [246] As discussed earlier, concurrent signalling through TCR in combination with high levels of TGF-β can cause rapid CD103 expression on T lymphocytes.

The co-expression of markers CD103 and CD39 identify a unique T cell population with an exhausted TRM signature. Although there is limited information in the literature regarding this specific cell type, a study conducted by Duhen et al. has shown that these cells have a very high expression of exhaustion markers such as Tim-3, TIGIT, CTLA-4, PD-1. Also, it was reported that Triple positive (TP) TILs, CD103+CD39+CD8+ TILs, are frequently found in high frequencies in primary tumour nests and tumour-infiltrating lymph nodes, suggesting that CD103+CD39+ expression on CD8 T cells identifies a population of cells found predominantly in the tumour microenvironment with a distinct T-cell receptor (TCR) repertoire. It was reported that TP clones expanded in the tumour but were present at low frequencies in the periphery (Figure 1.7). In the same study, TP TILs had an increased cytotoxic potential as demonstrated by a significantly higher frequency of granzyme B positive cells. In head and neck cancer patients, higher infiltration of CD103+CD39+ CD8 TILs was associated with better overall survival.[258] Based on the aforementioned findings, the markers CD103 and CD39 can be used to identify recently activated

tumour-specific TRM cells in solid tumours, suggesting that CD39+CD103+ TRM could be a suitable biomarker for immunotherapy.

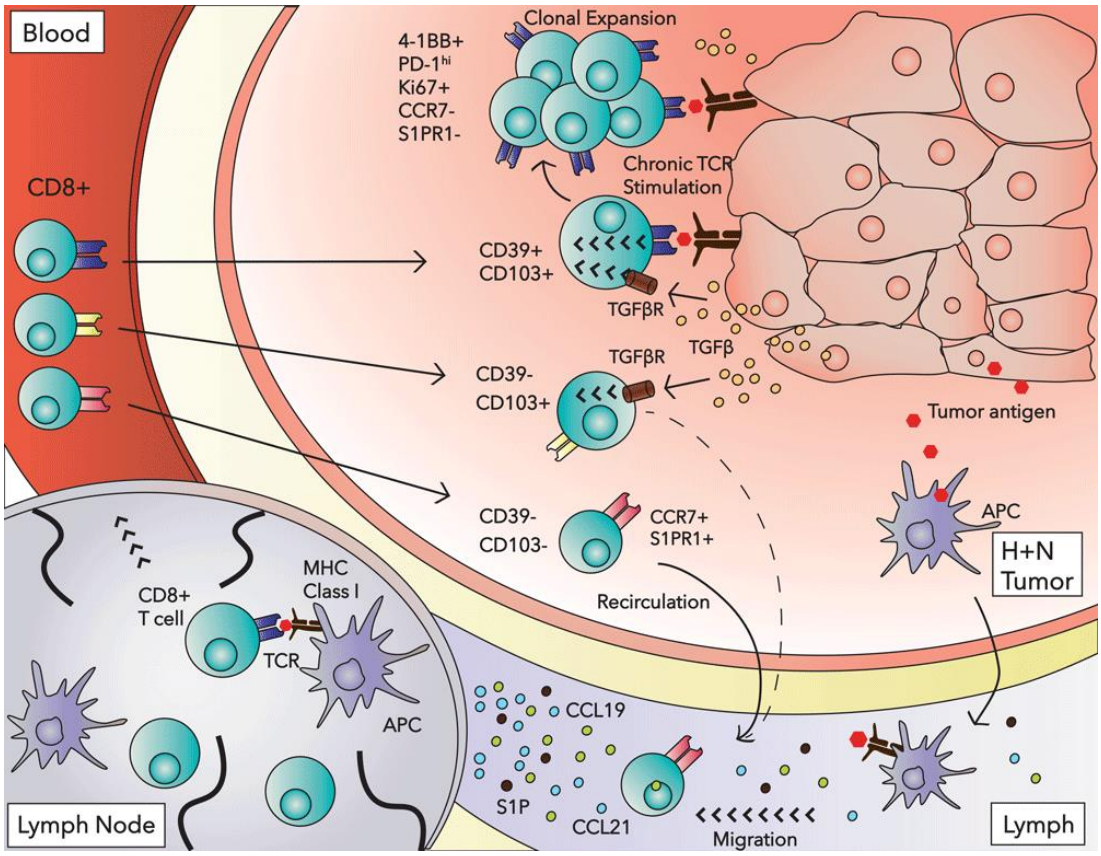

Figure 1. 7 Co-expression of CD39 and CD103 on CD8+ T cells in human solid tumours.

The upregulation of CD39 and CD103 on CD8TILs is governed by the presence of TGF-β and chronic TCR stimulation. The upregulation of CD39 and CD103 on CD8 TILs resulted in clonal expansion of TP TILs (CD8+CD103+CD39+). TP TILs are tissue-resident cells. Therefore, these cells will not recirculate into the blood compared to other CD8 TILs subsets. [taken from Duhen et al., *Co-expression of CD39 and CD103 identifies tumour-reactive CD8 T cells in human solid tumors.* Nature Communications. 2018 [258]]

1.12 Colorectal cancers.

Colorectal cancer (CRC) is the second leading cause of cancer-related deaths and the third most commonly diagnosed cancer worldwide.[259] In 2017, CRC was reported as the 4th most common cancer in the UK, accounting for 11% of all new cancer cases (CRUK, 2017). Colorectal adenocarcinoma occurs when glandular epithelial cells in the large intestine acquire several genetic or/and epigenetic mutations, giving rise to abnormally hyperproliferating cells. There is evidence that CRC is not only caused if one has a genetic predisposition for the disease but also because of strong risk factors including a western diet, smoking and alcohol consumption, therefore, CRC is most often seen in individuals from developed nations. Also, unbalanced gut microbiome, acromegaly, inflammatory bowel disease (IBD), and hamartomatous polyposis syndrome are considered high-risk factors for developing CRC. Hereditary CRC syndromes are bowel-related genetic disorders that increase the risk of developing CRC. The most common familial colon cancer syndromes include Lynch Syndrome (also known as hereditary nonpolyposis colorectal cancer) and familial adenomatous polyposis (FAP). Together, these two syndromes account for about 5% of all CRC cases. Totally, 75% of CRC tumours are sporadic (no family history for CRC).[259]

Surgery, chemotherapy, radiotherapy and targeted therapies are currently the four approaches used for colorectal cancer treatments. For stage I colorectal cancer, surgical excision is usually the only treatment, as the recurrence rate for node-negative T1 colorectal cancer is rare.[260] For stage II and III colorectal patients, adjuvant therapy is the standard treatment. Stage IV patients require chemotherapy or targeted therapies combined with surgery, where appropriate.

Better understanding of the molecular pathology of cancer has helped to develop a number of targeted agents which have demonstrated improved outcomes in metastatic colorectal cancer patients, with combination chemotherapy. Among the first of these drugs to be developed and approved for use by the food and drug administration (FDA) in metastatic colorectal cancer is Bevacizumab [261], Cetuximab [262] and Panitumumab.[263]

Bevacizumab is a humanised IgG1 mAb that specifically targets vascular endothelial growth factor (VEGF). Bevacizumab competes with VEGF from interacting VEGF receptors in vascular endothelial cells. As a result, cell signalling pathways that enhance angiogenesis, and thus the blood supply for tumours, are diminished. In 2004, Bevacizumab was approved by FDA as a first line treatment for patients with metastatic colorectal cancer. Bevacizumab is commonly used in combination with standard chemotherapeutic agents such as 5-FU as the first treatment for patients with metastatic colorectal cancer and improves the overall survival of these patients by approximately five months. [264, 265]

Cetuximab is a chimeric IgG1 mAb and panitumumab is a human IgG2 mAb that specifically recognises epidermal growth factor receptor (EGFR). EGFR is a 170kDa glycoprotein located in chromosome 7[266] and it is known to be overexpressed in tumours of epithelial origin, including colorectal cancer. EGFR activation is triggered by the binding of EGF to the extracellular domain of the EGFR and subsequently initiates both the RAS/RAF/MAPK and the phosphatidylinositol 3-kinase (PI3K) signalling pathways. As a result, EGFR is directly involved in cell proliferation and survival and therefore contributes to metastatic progression. Cetuximab and Panitumumab act as competitive antagonists of EGF and induce tumour cell death

via antibody dependent cell-mediated cytotoxicity (ADCC) and complement dependent cytotoxicity (CDC). [267]

1.13 Microsatellite Instability in colorectal cancers.

Mismatch repair (MMR) system plays a crucial role in correcting DNA sequence mismatches that may arise during DNA replication. This repair system is principally composed of four proteins (MLH1, MSH2, MSH6 and PMS2). These proteins interact to identify mismatches and excise them, permitting the resynthesis and religation of DNA strands by DNA ligase and DNA polymerase δ [268]. Microsatellites are short-tandem DNA repeat sequences of 1–6 bases distributed throughout the genome. Microsatellites were found to be prone to replication errors because of their repeated structure, which is typically repaired by the MMR system.[269] Therefore, Microsatellite instability (MSI) is due to a DNA mismatch repair (MMR) system deficiency. This deficiency can be caused by two possible mutations - epigenetic silencing of a DNA mismatch repair associated gene, MLH1, or a germline mutation of a DNA repair gene along with somatic inactivation of the second allele of the same gene (Lynch syndrome). This leads to errors in DNA replication which cause insertion or deletion of DNA sequences at random at the microsatellite region. These gene mutations result in frameshift mutations (mutations that change the reading frame of subsequent codons), considered a potential source of immunogenic neo-antigens recognised by the immune system.[270] MSI is reported in sporadic colon, sporadic endometrial, gastric and the majority of other cancers.[271] Approximately, 15-20 % of colorectal cancers display MSI. In CRC, determining the MSI status of the tumour has prognostic and therapeutic implications. [272] The most common method for MSI detection is via PCR-based amplification of specific microsatellite repeats. Also, an

indirect method to detect MSI status is by the analysis of MMR protein expression using Immunohistochemical (IHC) staining. [273]

In MSI tumours, the cancerous cells undergo constant immuno-editing. Thus a very high number of tumour specific antigens are produced. This gives MSI tumours a higher neoantigen mutational burden (highly immunogenic) when compared to microsatellite stable (MSS) tumours as MSS tumours arise in a less immunologically stimulating environment. Several studies have shown that MSI tumours have higher number of TILs infiltrating the tumour when compared to MSS tumours and this is attributed to the fact that there a higher neoantigen burden in MSI tumours, thus attracting more TILs. Galon and colleagues have confirmed in their study that there is significantly higher intratumoral CD8 T cell density in the tumour glands, both - in the CT and IM of the tumour, in MSI patients compared to MSS tumours.[274] Moreover, Galon et al. showed in the same study that MSI tumours had a higher number of proliferating T cells and increased cytokine expression in the IM and lymphoid islets (Lls) and total density in the CT compared to MSS tumours. [274]

1.14 Different characteristics and treatment approaches between Right-sided colon, left-sided colon and rectal cancers.

Tumours arising from the colon and rectum are often grouped together and generally categorised as colorectal cancer (CRC). However, growing evidence suggests that CRC should be considered a heterogeneous disease due to the distinctly different clinical behaviours and management requirements needed for patients with different primary tumour sidedness. Therefore, CRCs are composed of two different types based on the anatomical positioning of the tumor– right sided CRC tumors (RCRC)

and left sided CRC tumors (LCRC)[275]. Considering the differences in origin, RCRC tumours arise from the ascending colon and proximal two-thirds of the transverse colon. In contrast, the LCRC tumors arise from the descending colon, sigmoid colon and distal one third of the transverse colon. RCRC tumours have a different blood supply and embryological origin from LCRC tumours. Midgut structures from the mid-duodenum to the mid-transverse colon is supplied by the superior mesenteric artery, while hindgut structures from the mid-transverse colon to the rectum is supplied by the inferior mesenteric artery. [276]

Tumours in the right colon and left colon exhibit different characteristics on a molecular level and also have different histology (figure 1.8). RCRC tumours often have high numbers of mutations in the DNA mismatch repair pathway/genes and are associated with BRAF mutations, CpG island hypermethylation and microsatellite instability (MSI), with flat histology and poorly differentiated cells in most of the cases, whereas LCRC tend to have mutations related to chromosomal instability (CIN) pathways – KRAS, APC, p53, PIK3CA mutations - giving these tumours a more polypoid-like morphology, which makes it is easier to detect them with colonoscopy in the early stages of carcinogenesis.[277, 278]

Therapy responses are different between these tumour entities. LCRC patients often respond to adjuvant chemotherapies such as 5-fluorouracil (5-FU)-based regimes and targeted therapies such as anti-epidermal growth factor receptor (EGFR) therapy. In contrast, RCRC patients do not respond well to conventional chemotherapies. However, RCRC patients do show promising results in response to immunotherapy due to the high mutational burden and MSI tumours within right-sided colon. [275, 279] The efficiency of pembrolizumab (Anti-PD-1 inhibitor) was evaluated with multi-centered KEYNOTE study that demonstrated promising results in MSI-high tumours[280, 281]. Moreover, the effectiveness of anti-PD-1 antibody (nivolumab) had been investigated in a large cohort of CRC patients. Nivolumab has shown promising

results in MSI-high tumours [282]. The combination of two immunotherapies, Ipilimumab and Nivolumab was also evaluated among the CRC population that showed a better survival benefit and was found to be well-tolerated by patients[283].

The immune landscape differences between RCRC and LCRC tumour microenvironment was demonstrated by Zhang et al. [284] They found that RCRC tumours were associated with enhanced CD8+ T cell infiltration, higher cytotoxic activity and higher IFN-γ signature compared to their LCRC counterparts. In contrast, higher $CD56^{bright}$ natural killer cell infiltration and active 4-1BB/IFN-α signalling were associated with LCRC tumours (figure 1.8).

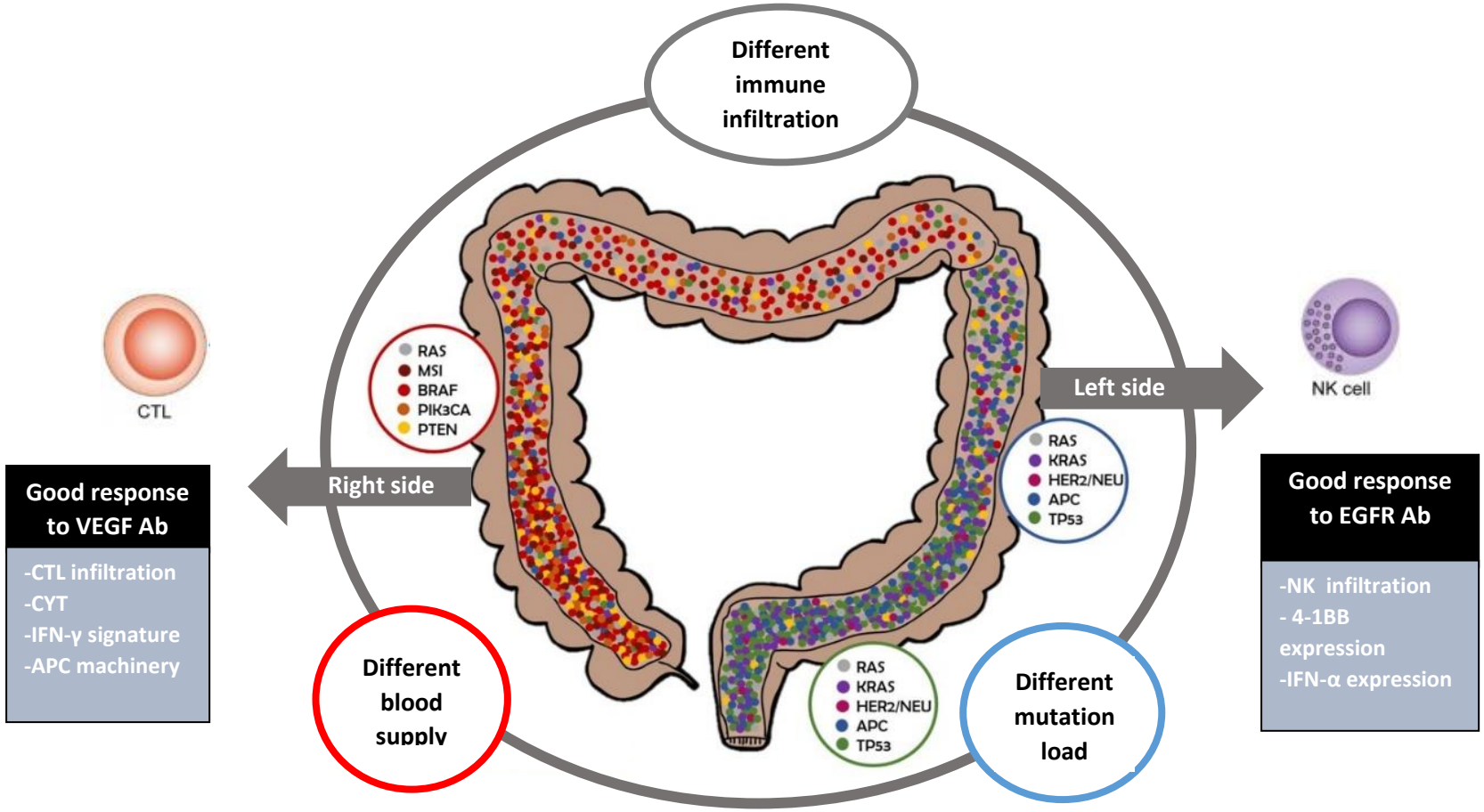

Figure 1. 8 CRCs tumour sidedness mutational alterations, immune landscape and implications for immunotherapy.

Right-side colon (cecum to transverse colon) cancer and left colorectal (splenic flexure to rectum) cancer have different blood supplies, mutation loads and immune infiltration; Moreover, different signalling pathways, immune cell infiltration profiles and effector molecule in left-side CRC and right-side colon cancer might lead to different treatment responses. [Adapted from salem et al.[275] and Zhang et al.[284]]

1.15 Immunotherapy (Checkpoint inhibitors).

As discussed earlier in (1.4.2), checkpoint signalling is used to reduce the activation of T cell responses. Many signalling pathways with immune regulatory functions such as T cell membrane protein 3 (TIM3), B7-related protein 1 (B7RP1), inducible T cell co-stimulatory (ICOS), B and T lymphocyte attenuator (BTLA), herpesvirus entry mediator (HVEM) and galectin 9 (GAL9) were identified. Immune checkpoint is a term used to describe these signalling pathways, and they are considered to be a potential target for cancer immunotherapy.[285] So far, one of the most well-known immune checkpoints is CTLA4, which competes with CD28 for CD80/86 in order to cause inhibition instead of co-stimulation response in order to prevent prolonged or inappropriate T-cell activation[286].

According to CTLA-4 function as a negative regulator of adaptive immune responses, it was thought that blocking CTLA-4 using a monoclonal antibody "Checkpoint inhibitor" might facilitate CD28 interaction with CD80/86 and lead to increased T-cell activation and proliferation. However, few studies demonstrated that anti-CTLA-4 antibodies may increase intratumoral effector/regulatory T-cell ratios via Fcγ-receptor-dependent intratumoral depletion of Treg cells.[286] Ipilimumab and Tremelimumab are two commercial checkpoint inhibitors for CTLA-4. Although Tremelimumab had no significant impact on the survival rate of advanced melanoma patients. A randomised double blind Phase III study demonstrated that when ipilimumab was given as an adjuvant therapy in high-risk stage III melanoma, recurrence free survival rates were significantly improved (25%) comparing to patients who only had the conventional therapy. [287]

In addition to CTLA-4, PD-1 is another example of immune checkpoints. The cell-surface receptor PD-1 is expressed by T cells on activation during priming or

expansion and binds to one of two ligands, PD-L1 and PD-L2. Many types of cells can express PD-L1, including tumour cells and immune cells after exposure to cytokines such as interferon (IFN)-γ; however, PD-L2 is expressed mainly on dendritic cells in normal tissues. The binding of PD-L1 or PD-L2 to PD-1 generates an inhibitory signal that attenuates the activity of T cells. Overactivation of tumours and poor patient prognosis is associated with a high frequency of PD-1/PD-L1 axis[288]. PD-1 monoclonal antibodies such as Nivolumab and Pembrolizumab target epitopes on the PD-1 molecule with high specificity and affinity. Blocking the interaction between PD-L1 and PD-1 can promote T-cell responses.[289]

The therapeutic efficacy of PD-1 mAbs was observed in different studies and different types of cancers. For instance, a randomised, double-blind, phase 3 trial was conducted on patients with complete resection of stage IIIB, IIIC, or IV melanoma treated with either Nivolumab or Ipilimumab as adjuvant therapy. The findings showed that better recurrence-free survival was with Nivolumab group (70.5%) in comparison to Ipilimumab group (60.8%, P<0.001). While treatment-related grade 3 or 4 adverse events of Nivolumab and Ipilimumab were reported as 14.4% and 45.9%, respectively.[290] However, in more advanced trials, the combination of Nivolumab and Ipilimumab had even better clinical outcomes than each regimen separately because both inhibitors activate the immune system in different pathways, which may produce a synergistic antitumor effect.[285]

Table 1. 1 Comparison of anti-CTLA-4 and anti-PD1 checkpoint inhibitors different pathways, targets and functions.

(Adapted from *Wei et al*.[291] and *Sharma et al*.[292])

Anti-CTLA-4	Anti-PD-1
Hard wired.	Induced resistance.
Targets CD28 pathway.	Targets TCR pathway.
Works mainly during priming.	Works mainly on exhausted T cells.
Expands clonal diversity.	Does not expand clonal diversity.
Primarily affects CD4 T cells.	Primarily affects CD8 T cells.
Can move T cells into cold tumours.	Does not move T cells into tumours.
Responses are often slow.	Responses are usually rapid.
Adverse events are relatively frequent.	Adverse events less frequent.
Disease recurrence after response is rare.	Disease recurrence after the response is significant.

1.16 Tetraspanins as a target for T-cell immunoregulatory antibodies

Apart from costimulatory and coinhibitory molecules discussed earlier, there are other potential receptors on T-cells that could be targets for therapeutic antibodies. These include tetraspanin protein family residing in their own specialised microdomains within the T-cell plasma membrane.

Tetraspanins are ubiquitously expressed across all cell types. Human genomic studies have revealed about 20 tetraspanins that can be expressed on the surface of leukocytes[293]. Some of these tetraspanins have restricted leukocytes expression for example CD37, CD53 and TSPAN32, while others are more widespread (CD9, CD63, CD81 and CD82) [294]. Table 1.2 shows the expression of various tetraspanins on

immune cells. They play roles in cellular adhesion, motility, activation and tumour invasion [293].

Table 1. 2 Expression of tetraspanins on blood cells

(adapted from *Tarrant et al*.[293])

Tetraspanin	Expression
CD9	B-cells, activated T-cells, granulocytes, MO, DCs, megakaryocytes, platelets, blood proginetors, widespread
CD37	B-cells, T-cells, MO, DCs, granulocytes
CD53	B-cells, T-cells, MO, DCs, granulocytes, NK cells
CD63	B-cells, T-cells, MO, DCs, granulocytes, platelets, widespread
CD81	B-cells, T-cells, MO, DCs, granulocytes, NK cells, blood progenitors, widespread
CD82	B-cells, T-cells, granulocytes, MO, CD34+ progenitors, widespread
CD151	B-cells, T-cells, granulocytes, megakaryocytes, platelets, erythroleukemia and T-cell lines, widespread
TM4-B	**B-cells, T-cells, erythroleukemia, myeloid cell lines, widespread**
CD231	T-cell line, Burkitt lymphoma cell lines, various tissues
Co029	Burkitt lymphoma cell lines, colon carcinoma
NAG-2	B- and T-cell, erythroleukemia, and megakaryocytes cell lines; DCs, lymphocytes, widespread
NET-2	B- and T-cell and myeloid cell lines, various tissues
NET-5	B- and T-cell and myeloid cell lines, various tissues
NET-6	B- and T-cell and myeloid cell lines, various tissues
NET-7	B- and T-cell and myeloid cell lines, various tissues
SAS	Burkitt lymphoma cell lines, sarcoma
Tspan-2	T-cell, pre-B and myeloid cell lines, various tissues
Tspan-3	B-cells, T-cells, DCs, NK cells, MO, widespread
Tspan-5	T- and pre-B-cell and myeloid cell lines, widespread
Tssc6 (Tspan-32)	B-cells, T-cells, granulocytes, MO, DCs, erythroid cells, blood progenit

1.16.1 Tetrasapnins structure

Tetraspanins are best characterised by their four-transmembrane domains. What differentiates them from other protein families consisting of four transmembrane domains is the highly conserved CCG and PXSC motifs in their major extracellular domain (EC2)[293]. Tetraspanins contain four transmembrane domains, a small extracellular domain/loop (SEL/EC1), a large extracellular domain/loop (LEL/EC2), a

very short intracellular loop and short N- and C-terminal cytoplasmic tails. The LEL/EC2 can be further divided into two regions: a constant region that is conserved among tetraspanins and a highly variable region that is a site for various protein-protein interactions, including monoclonal antibody epitope binding[295]. Cysteine residues within EC2 form between 2-4 disulphide bonds, depending on the specific tetraspanin. Membrane-proximal cysteines located near the four transmembrane domains contribute to sites for palmitoylation. This post-translational modification contributes to tetraspanin-tetraspanin interactions and assembly of tetraspanin-enriched microdomains (TEMs). Mutagenesis studies have shown that palmitoylation of CD9 mediates its interaction with CD81 and CD53 [296] while palmitoylation-deficient CD151 showed decreased association with CD81 and CD63, and also weakens the interaction of integrin α3β1 with TEMs[297] . Most tetraspanins display N-linked glycosylation sites at the extracellular domains. The functional relevance of tetraspanin glycosylation has been shown in CD82 and CD9 in which these tetraspanins could only influence motility or apoptosis when glycosylated[298, 299]. Glycosylation has also been implicated in the proper folding of tetraspanin Tspan-1 and its transition through the endoplasmic reticulum[300] . However, some tetraspanins like CD81 are not glycosylated.

Tetraspanins function by associating with themselves or with various other proteins, including integrins, immunoreceptors, signalling molecules through the large extracellular domain EC2. These associations can be via lateral, extracellular, and intracellular interactions [301]. General functions of tetraspanins include facilitating the trafficking of partner proteins to the cell surface and regulation of these partners lateral mobility and clustering within the plasma membrane[302]. Moreover, tetraspanins are thought to associates with/among themselves or partner proteins in a specialised microdomain within the cell membrane. This microdomain is termed tetraspanin-enriched microdomain (TEM). TEM serves as a platform for signal transduction, as

proteins converge together to perform a specific function. TEM constituents vary among cell type as tetraspanins associate with different partner proteins to exert different functions[303]. In B-cells for example, CD81 associates with CD19 whereas in T-cells, CD81 associates with CD4 and CD8.

1.16.2 Tetraspanins on T-cells

1.16.2.1 CD81

CD81, originally named target of anti-proliferative antibody (TAPA-1), was first identified for its anti-proliferative effect on lymphoma cells. Expression of CD81 is widespread across various normal tissues. It is also expressed by a number of immune cells, including B-cells, T-cells, MO, DCs, granulocytes and NK cells [293]. CD81 associates with several partner proteins and this association is cell-type specific. For example, CD81 interacts with CD4 and CD8 on T-cells and this association only requires the cytoplasmic domain of CD4 [304, 305]. In B-cells CD81 associates with CD19 and also indirectly with CD21, as discussed earlier.

One of the roles of CD81 in T-cell has been demonstrated in the formation and maturation of the immune synapse (IS). The immune synapse is a dynamic structure formed at the T-cell-APC contact area. TCR and other key molecules localise at the central supramolecular activation cluster (cSMAC) of the IS, while adhesion proteins and integrins localise in the peripheral activation cluster (pSMAC) [306]. In a study done by Rocha-Perugini's laboratory, CD81 was shown to colocalise with CD3 at the cSMAC shortly after contact of T-cell and B-cell (early IS)[306] . The interaction between CD81 and CD3 is maintained as the IS matures (late IS). Impaired CD3 clustering to the IS was observed in CD81-silenced cells, suggesting CD81 role in CD3 dynamics. CD81 also plays a role in the control of T-cell activation threshold as CD81-silenced

cells showed reduced surface expression of CD69, reduced IL-2 secretion, as well as reduced phosphorylation of TCR key signalling molecules, including CD3δ, Zap-70, LAT and ERK[306] .

The role of CD81 in T-cell costimulation has been shown in antibody ligation studies. It is well documented that the full activation of T-cells requires two signals, one from the engagement of TCR:MHC: peptide complex and the second from the engagement of costimulatory molecules on T-cells. Todd et al. were the first to demonstrate the ability of immobilised anti-CD81 mab (clone 5A6) to induce proliferation in human thymocytes, in combination with anti-CD3 mab[305]. No proliferative response was observed when the mab was used soluble, either alone or with anti-CD3 mab. The activation markers CD69 and CD25 expression were upregulated following a 3-day culture. CD81 costimulation was shown to be IL-2 dependent as the addition of blocking anti IL-2R inhibits cell growth. Todd et al., however did not show whether IL-2 was produced in his study. Engagement of T-cells with anti-CD81 antibody bias towards Th2 response[307] .It involves interaction between T-cell and its cognate B-cell as APC. IL-4 synthesis by T-cells was impaired in CD81 null mice.

Costimulation via CD81 is independent of CD28 as shown in murine studies in Witherdern laboratory[308]. Costimulation via both CD28 and CD81 showed additive effects, and costimulatory ability of CD81 was not altered in CD28 deficient mice, suggesting that the molecules function in different pathways. To prove this hypothesis, Witherden et al. treated cells with cyclosporine A and found that costimulation via CD81 was inhibited, but it did not affect CD28 costimulation. They also reported no IL-2 was produced during CD81 costimulation, which was strikingly different than CD28 costimulation. This further support the distinct pathways employed by these two costimulatory molecules in T-cell activation.

Although CD81 expression is widespread, its loss of expression in humans mostly affects B-cells, while T cell function was not affected. CD81-null mice had normal T-

cell development but were hyperproliferative in response to various stimuli when compared to the wild-type animals [309]. On the other hand, although B-cell development was normal, mice lacking CD81 showed a variable effect on humoral response. Stimulation of null mice with anti-CD40 antibody or LPS resulted in enhanced proliferation in comparison to wildtype mice, but the opposite was observed when cells were stimulated by BCR crosslinking[309] . This could partly be due to the effect of CD81 on CD19 expression on B-cells. As demonstrated by van Zelm and co-workers, CD81-deficient patients had an absence of CD19 expression on B-cells leading to impaired specific antibody responses[310] . These differences further support the notion that the function of CD81 is cell-type specific.

1.16.2.2 CD9

Another tetraspanin that has been shown to have a role in T cell costimulation is CD9. A CD9 mab (clone 9D3) has been demonstrated to costimulate murine T-cells in the absence of APCs [311]. Immobilised or soluble 9D3 mab alone did not exert any proliferative response. Costimulation with anti-CD9 mab is comparable to that of CD28 costimulation, and is independent of CD28 as the proliferative response was still enhanced in CD28-/- deficient mice. In another murine study done by Yashiro-Ohtani and co-workers, CD9 was shown to be localised in lipid raft, together with other non-CD28 costimulatory molecules such as CD5, CD44 and CD2[312] Coligation of CD3 and CD9 with mAbs induced CD3 association with the lipid rafts as well as enhanced LAT phosphorylation. These findings further support the role of CD9 in T-cell costimulation. However, the localisation of tetraspanins in lipid raft is still not fully understood as discussed earlier.

A study carried out by Kobayashi and colleagues seek to understand the expression and function of CD9 in human T-cells. They demonstrated using anti-5H9 mAb, developed by immunising mice with erythroleukemia cell line K562, that CD9 is

preferentially expressed on human naive T-cells (CD4+CD45RA+CD62L+) [313]. They also highlighted that engagement of CD9 with anti-5H9 mAb induced T-cell proliferation in combination with anti-CD3 mAb. However, anti-5H9 costimulation induced weaker proliferative activity on human peripheral blood T-cells compared to CD28 costimulation. This could be due to the restricted expression of CD9 as compared to CD28 expression, which is more widespread among all T-cell subsets.

The role of CD9 in T-cell activation has been elucidated by Rocha-Perugini and co-workers[314]. They demonstrated that CD9 is enriched in the cSMAC of the IS, colocalising with CD3, upon contact of primary T-lymphoblasts/J77 cell line with CMAC-labeled Staphylococcus enterotoxin E (SEE)-loaded Raji B cells (Raji/SEE). Knockdown of CD9 gene using small-interfering RNA (siRNA) resulted in reduced CD69 activation marker expression and IL-2 production, two key events following TCR stimulation. Silenced CD9 showed impaired relocalisation of integrin α4 and β1 into the IS, as well as reduced focal adhesion kinase (FAK) and extracellular signal-regulated kinase 1/2 (ERK1/2) phosphorylation, suggesting its role in mediating integrin signalling, which in turn leads to proper T-cell activation.

1.16.2.3 CD37

While many tetraspanins have broad expression across the tissues, several have more restricted expression, including CD37. CD37 expression is restricted on leukocytes- B-cells, T-cells, monocytes, macrophages, neutrophils, and DCs. It is not expressed by NK cells, platelets or erythrocytes [295, 315]. CD37 is highly expressed on mature B-cells; however its expression is absent during the early stage of B-cell development and terminally differentiated plasma cells[295] . CD37-deficient mouse showed normal lymphocyte development[316]; however, its absence suggests its regulatory role in T-cells [315]. T-cells isolated from CD37-/- mice showed enhanced T-cell proliferation and upregulation of cytokine IL-2 and IL-4

compared to the control mice upon TCR stimulation. Meanwhile, IFN-γ expression was not altered. Hyperproliferative response of CD37-/- T-cells could be due to increased Lck phosphorylation, as evidenced in vitro kinase activity assay. Van Spriel et al. demonstrated that antibody engagement of CD37 on human T-cells inhibited proliferation. This further supports the regulatory role of CD37 in T-cells [130]. Sheng and co-workers also showed that CD37 might have a regulatory role in T-cell activation by demonstrating that CD37-deficient DCs were hyperstimulatory towards T-cells. In their work, CD37 was shown to regulate DC function by mediating peptide/MHC presentation [317].

1.16.2.4 TSPAN32

TSPAN32 was first known as Phemx (Pan hematopoeitic expression) identified in mice[318]. The name was given due to the restricted expression of TSPAN32 on hematopoietic progenitors. Expression of human TSPAN32 is expressed at low levels in child thymus, blood T-cells, Jurkat cells, with higher levels of expression in bone marrow mononuclear cells, blood monocytes and cultured dendritic cells [318]. It is also found in multiple hematopoietic cell lines [319]. However, due to an absence of mAb this has only been demonstrated at the RNA level.

A previously published study on the function of TSPAN32 on T-cell was conducted by Tarrant and colleagues showed that mice deficient in TSAPN32 gene showed normal T-cell and B-cell development[320] . However, Tspan32 null mice showed an elevated T cells proliferative response compared to the wild-type animals, suggesting it's negative regulatory role on T lymphocytes. **[320]** Furthermore, double knockout mice

(Tspan32-/ CD37-) was used to determine the functional correlation between both tetraspanins. The role of these tetraspanins in cellular immunity was identified by the responses of dendritic cell stimulation and T cell proliferation in vitro, which were significantly higher with both tetraspanins absence in comparison to counterparts with a single knockout. However, the risk of inducing autoimmune adverse events is similar in both cases.[321] These observations suggest that TSPAN32 can be a potential target for novel immune checkpoint inhibitors. However, the functional role of TSPAN32 is still unclear due to the lack of functional mAb that identifies the natural structure of that protein.

1.17 Hypothesis and Aims.

The immune system can identify and eliminate tumour cells through T-cell-mediated mechanisms. Hence, various therapeutic approaches have focused on boosting and/or restoring T-cell function in cancer patients. Immunotherapies such as ICB have shown great success in treating patients with hot tumours such as melanoma. However, some patients did not respond to these checkpoint inhibitors. Therefore, a combination of ICB inhibitors or developing a novel checkpoint inhibitor is needed to improve the responsiveness to immunotherapies. Some tetraspanin proteins expressed on T cells, such as TSPAN32 have shown an immunoregulatory effect on T cells in knockout mice experiment similar to CTL-A and PD-1. The functional role of TSPAN32 on T cell activation and proliferation is still unclear due to the lack of mAb that recognises the native structure TSPAN32.

An effective immune response involves the concerted action of several different cell types, among which CD8 T cells are key players that can specifically recognise and kill cancer cells via the release of cytokines and cytotoxic molecules. However, not all Tumour infiltrating CD8 T cells recognise tumour-associated antigens or are considered tumour specific. Some CD8 TILs were identified as ‘bystanders’, which can recognise epitopes unrelated to cancer even when presented within the tumour microenvironment. These bystander CD8 TILs were found to have diverse phenotypes that overlap with tumour specific cells but lack CD39 expression indicating the role of CD39 as a tumour specificity marker. Recently, a unique CD8 TILs subset co-expressing CD103 and CD39 with enhanced cytolytic potential was identified as recently activated tumour-specific TRM cells.

In colorectal cancer, the analysis of the location, density and functional orientation of the different immune cell populations termed as ‘immune contexture’ were found to

be a better predictor of patient survival than the histopathological methods currently used to stage colorectal cancer. Nevertheless, only right-sided CRC patients demonstrate more promising results with immunotherapies because of the increased mutational burden and higher presence of TILs within these tumours compared to left colorectal tumours. In the light of these observations, this study investigates the prognostic role of TILs (CD3 and CD8) when located in the luminal side (LS), the centre of the tumour (CT), the invasive margin (IM) and the adjacent normal tissue in CRCs. We further evaluate the predictive role of different CD8+ TIL subsets between different tumour sidedness to identify a tumour-specific CD8+ subset with the best predictive impact to be a potential target for cancer immunotherapies. With these aims established for the study, we hypothesise that:

1. High infiltration of intraepithelial and stromal CD3+ and CD8+ T cells in any region within the tumour (LS, CT and IM), but not in the adjacent normal tissue, is associated with prolonged disease-free survival time in CRC patients.

2. Right-sided colon tumours, which are considered as hypermutated tumours with increased neoantigens generation, are associated with higher infiltration of intraepithelial CD103+ TILs, and that the presence of CD103+ TILs in high levels within right-sided colon tumours would show better prognostic value compared to left-side colon and rectal cancers.

3. Heavily infiltrated tumours with recently activated tissue-specific TRM cells (CD8+CD103+CD39+) uniquely predict survival in both left and right-sided colon tumours.

4. Using innovative immunisation methods such as DNA immunisation or immunising with PM glycolipid extraction of cells expressing TSPAN32 would produce a mAb against TSPAN32. The development of a functional anti-

TSPAN32 mAb would help to understand the role of TSPAN32 on T cells proliferation and might be a potential checkpoint inhibitor.

Chapter 2: Materials and Methods

2.1 Ethical Approval

Blood was collected from each donor after all donors provided written consent according to the Ethical rules of Nottingham City Hospital and University of Nottingham. Blood taken from healthy donors was covered by Nottingham Research ethics approval: 161-1711.

2.2 Cell Lines and Cell Culture

NIH 3T3 cell line was obtained and brought up from liquid nitrogen storage. NIH 3T3 cells were maintained in Dulbecco's Modified Eagle's Medium (DMEM) (Sigma) with 10% heat inactivated foetal bovine serum (Sigma), 1% penicillin/streptomycin (Sigma) and 2% HEPES Buffer 1M (Sigma). Cells were kept in a humidified incubator at 37ºC and 5% CO2.

NIH 3T3 cells were split every two days. They were placed in 1x Tyrpsin-EDTA (sigma, T4174) for 2-3 minutes. After adding the selected media, Cells were centrifuged and split by 1:10 dilutions. Every two days, cells were split in 1:3, cultured in a $75cm^2$ culture flask and topped up to 20ml of fresh media.

2.3 DNA Plasmids and Maxi Prep

A DNA plasmid with Tetraspanin 32 gene (GeneCopoeia, cat# H2264) was used to transfect NIH 3T3 cell lines. The plasmid quantities were amplified using the QIAGEN plasmid Maxi kit (see Appendix .1). Plasmid concentrations were as follows: EX-NEG-M61 (control; DNA plasmid with GFP only) = 1117.8ng/µl, EX-H2264-M61 (DNA plasmid with GFP AND Tspan32) = 1411.5ng/µl.

2.4 DNA restriction

Cutting our circular DNA plasmid in one restriction site was conducted by using ScaI-HF® (BioLabs, cat # R3122S) restriction enzyme using PCR at 37 °C for 4 hr. Agarose gel electrophoresis was used to evaluate DNA restriction procedure. In contrast, we used ethanol precipitation protocol, with 1:2 ratio of 0.3 M Sodium Acetate to 100% ethanol, to obtain the cut and uncut of both EX-NEG-M61 and EX-H2264-M61 DNA plasmid. The concentrations were as follows: EX-NEG-M61 (Uncut)= 241.8 ng/µl, EX-NEG-M61 (Uncut)= 221.8ng/µl, EX-H2264-M61 (Uncut)= 485.5ng/µl EX-H2264-M61 (cut)= 592.1ng/µl.

2.5 NIH 3T3 cells transfection with TSPAN32 :

70% confluent NIH 3T3 cells were transfected with 10µl of Lipofectamine® 2000 Transfection Reagent (Life Technologies), 2.5µg of DNA plasmid and 500µl Opti-MEM (Life Technologies) per well, in 6 well plates. The cells were maintained in the selected media of each cell line with G418 Geneticin (InvivoGen, cat# 08321-42-2) as a selective antibiotic and were incubated at 37ºC with 5% CO_2 . The optimum concentration of G418 was determined by performing a sensitivity selection by using different concentrations of G418 antibiotic in order to determine the optimum concentration of G418 to achieve a successful selection (Table. 2.1). According to the findings, the lowest concentration that gave massive NIH 3T3 cells death after four days and killed all the cells after seven days was 500µl/ml, which was used to select transfected cells and kill the non-transfected ones.

Table 2. 1 Geneticin Sensitivity Selection of Un-transfected NIH 3T3 Cells. Cell viability was compared for five concentrations at days 2,4 and 11 of adding Geneticin on 70% confluent NIH 3T3cells.

	Day 2 **Cell confluence**	**Day 4** **Cell confluence**	**Day 11** **Final cell count**
Plate #1 (0µl/ml)	100%	>100%	$6.42x10^6$
Plate #2 (0µl/ml)	100%	>100%	$5.71 x10^6$
Plate #1 **(300µl/ml)**	70-80%	75-80%	$6.6 x10^6$
Plate #2 **(300µl/ml)**	70-80%	80-85%	$6.7x10^5$
Plate #1 **(400µl/ml)**	40%	20%	$1.2 x10^5$
Plate #2 **(400µl/ml)**	20-30%	25-30%	$1.68 x10^5$
Plate #1 **(500µl/ml)**	10-20%	*10%	0
Plate #2 **(500µl/ml)**	10-20%	*10%	0
Plate #1 **(700µl/ml)**	5-10%	0%	0
Plate #2 **(700µl/ml)**	5-10%	0%	0

2.6 Single-cell cloning

After transfecting cells with the optimum transfection conditions, single cloning, which was conducted by transferring a single transfected cell into each well of a 96-well

plate was required to confirm that the cells can yield antibiotic-resistant colonies and obtain a pure transfected cell population. In order to ensure that only one cell in each well, serial dilution was conducted. 96-well plates were incubated and observed for two weeks.

2.7 Western Blot

TSAPN32 NIH 3T3 cells and other control cells were lysed using NuPAGE® LDS Sample Buffer (Life Technologies), reduced with the NuPAGE® (10x) reducing agent and diluted to desired quantity using PBS. Samples were stored at -20ºC. 25µl of the sample from each day mixed with 7µl of sample buffer and 3µl of reducing agent and heated at 100°C for 5 minutes. SDS-PAGE (ThermoFisher) placed in the running tank and inner chamber filled with running buffer and antioxidant. An equal amount (8µl) of pre-heated samples and SeeBlue™ Plus2 Pre-stained Protein (ThermoFisher- LC5925) and MagicMark XP standard loaded onto the gel and ran at 160V for an hour.

For transferring proteins from gel to nitrocellulose membrane (Sigma- GE10600002), the prepared sandwich located in the chamber filled with transfer buffer and ran at 25V for 2 hours. The membrane was blocked in blocking buffer (5% dried non-fat milk diluted in PBS-Tween) for an hour, followed by overnight incubation at 4°C with primary antibodies on two different gels: TSPAN32 polyclonal antibody [PA5-18045] from ThermoFisher (1:2500) and TSPAN32/TSSC6 antibody (2B4) [H00010077-M02] from Abnova (1:3000). We added 1/1000 diluted mouse anti-human anti-Beta tubulin antibody (Abcam). Primary antibodies were detected by donkey anti-rabbit (1/2500- 800CW) (Licor) and donkey anti-mouse (1/5000- 680CW) (Licor).

2.8 Isolation of PBMCs from fresh human blood

Whole blood from a healthy donor was collected in heparin tubes and diluted with serum-free RPMI 1640 medium. Diluted blood 25 ml of blood was overlaid onto a 15ml layer of Lymphocyte Separation Medium purchased from GE Healthcare (Little Chalfont, UK) and centrifuged at 425 g for 20 minutes with minimal accelerator and break using Jouan C3i Multifunction Centrifuge (Thermofisher, Paisley, UK). The buffy coat was collected into a fresh tube and washed with sterile PBS twice.

2.9 Isolation of PBMCs from leukocyte reduction system (LRS) cone

PBMCs were obtained from LRS cone of healthy donors. Cells were collected in a 50-ml tube, and 20 ml of Hanks Salt Balanced Solution (HBSS) purchased from Sigma was passed through the cone using a 23G needle and a syringe. Cells were washed with up to 50ml HBSS. PBMCs were isolated as previously described.

2.10 T cell activation after isolating PBMCs

175 x 10^6 cells of PBMCs were cultured in a T-175 flask purchased from Corning (Flintshire, UK) in a 37°C incubator for 1 hour. After 1 hour, medium containing non-adherent cells/lymphocytes was transferred to a new T-175 flask pre-coated with 1µg/ml anti-CD3 antibody and 5µg/ml anti-CD28 antibody in RPMI 1640 medium supplemented with 10% FBS, HEPES buffer, penicillin, streptomycin and sodium pyruvate for 48 hours at 37°C in a humidified atmosphere of 5% CO_2.

2.11 Flow Cytometry Analysis

MACS Flow Cytometry and FC 500 were used to evaluate transfection efficacy, due to the presence of green fluorescent protein (GFP) in the DNA plasmid transfected cells were detected on FITC (fluorescein) channel. For T cell activation screening, $1x10^5$ cells were stained for different markers such as CD3-FITC, CD8-PE, CD4-APC, CD69-PE and CD25-APC (Miltenyi), 2µl of each marker was added to 100ml of PBS in a U shape well for 30 min at 4°C. For antibody detection after each immunisation, mice sera were screened with goat anti-mouse IgG (Biotin) (ab97263) (1:500) at 4°C, then washed and incubated with Streptavidin, (APC) (SA1005) (1:100) at 4°C.

2.12 Immunisations

2.12.1 Gene gun immunisation (DNA immunisation)

The bullet manufacture reagents were: 2.5mg PVP, 0.5M spermidine, 1M $CaCl_2$ sdH_2O, Gold (16.6mg aliquots) and Anhydrous EtOH (100%). We weighted out 16.6mg of gold 2.5mg of PVP into a large eppendorf. The PVP stock was prepared by adding 1ml EtOH to the 2.5mg PVP and vortexed to dissolve. Then, PVP stock was diluted to 1/100 in EtOH. 2ml of PVP diluted solution was needed per batch of bullets. Spermidine was also diluted to 1/10 in sdH_2O (200µl/bullet batch). Tefzel tubing was cut to length and put on prepping station to dry With N_2. We added 200µl of diluted spermidine to gold aliquot and sonicated. Next, the DNA was added (36µg per bullet batch) dropwise to gold whilst sonicating. Then 200µl of $CaCl_2$ (1M) was also added dropwise whilst sonicating. The mixture was left at room temperature for 10 mins, after washing the pellet gold three times. Then the pellet was resuspended with 800µl diluted PVP and transferred transfer to falcon tube. The solution was made up to 2ml with diluted PVP and sonicated well. The N2 was turned off on the bullet

station. Using a syringe, the gold was removed from the tube and left to settle for 10 mins. Once gold appeared visibly dry, we turned on the rotator for approximately 5 mins. Then the bullets were cut to size.

2.12.2 Plasma membrane glycolipid extraction

TSPAN32 transfected NIH 3T3 (5×10^7 cells) or activated T cell (1×10^8 cells) pellets were resuspended in 500µl of Mannitol/HEPES buffer (50mM Mannitol; 5mM HEPES, pH7.2, both Sigma) and passed through 3 needles (23G, 25G, 27G) 30 times each. 5µl of lM $CaCl_2$ was added to the cells and passed through 3 needles 30 times each as above. Sheared cells were incubated on ice for 20 min then spun at 3,000g for 15 min at room temperature. The supernatant was collected and spun at 48,000g for 30 min at 4°C, and the supernatant was discarded. The pellet was resuspended in 1ml methanol followed by 1ml chloroform and incubated with rolling for 30 min at room temperature. The sample was then spun at 1,200g for 10 min to remove precipitated protein. The supernatant containing plasma membrane glycolipids was collected and stored at -20°C. (All work with chloroform and methanol was carried out in a fume hood).

2.12.3 Liposome preparation

TSPAN32 transfected NIH 3T3 or activated T cell plasma membrane (PM) glycolipid extract was mixed with a total concentration of 10 mg of lipids [Cholesterol, dihexadecyl phosphate (DHP), 1,2-dioleoyl-sn-glycero-3-phosphocholine (DOPC), and α-GalCer] in a round bottom flask at various ratios (Table 2.2). The lipid mixture was then dried down using a rotary evaporator at 60°C until the solvent had evaporated, leaving a uniform lipid film on the wall of the flask. The flask was allowed to cool-down to room temperature before the addition of 100µl of sterile PBS. The opening of the flask was covered with parafilm and then immersed in an ultrasonic

bath for 10 min to generate liposomes. (All work with chloroform and methanol was carried out in a fume hood). For immunisation of animals with anti-CD40 mAb, the mAb (in PBS) was added to the liposome after it was made.

Table 2. 2 Liposome constituents for the immunisation of one mouse. Four components were mixed with plasma membrane (PM) glycolipid extract was mixed with a total concentration of 10mg of lipids. [DHP: dihexadecyl phosphate, DOPC: 1,2-dioleoyl-sn-glycero-3-phosphocholine, Brij97: polyoxyethylene-(10)-oleyl-etherand, α-GalCer: α-galactosylceramide]

Liposome	Cholesterol (mg)	DHP (mg)	DOPC (mg)	Brij97 (mg)	α-GalCer (mg)	Total (mg)
TSPAN32 transfected NIH 3T3 (5 x 10^7 cell equiv.) plasma membrane lipid extract + α-GalCer	2.44	0.36	6.92	0.02	0.26	10
Activated T cells (1 x 10^8 cell equiv.) plasma membrane lipid extract + α-GalCer	2.44	0.36	6.92	0.02	0.26	10
TSPAN32 transfected NIH 3T3 (5 x 10^7 cell equiv.) plasma membrane lipid extract + anti-CD40 mAb (10μg)	2.52	0.44	7	0.02	0	10
Activated T cells (1 x 10^8 cell equiv.) plasma membrane lipid extract + anti-CD40 mAb (10μg)	2.52	0.44	7	0.02	0	10

2.12.4 Immunisation protocol

BALB/c mice were between 6 to 8 weeks old (Charles.River, UK). Prior to immunisation, normal mouse serum (NMS) was collected via tail bleed extraction and

stored at -20°c. The NMS was used in the latter experiments as negative controls. Mice were immunised intraperitoneally (IP) with either liposomes or cells at two weekly intervals using 1ml insulin syringe (BD Bioscience, Spain). Seven days after the third immunisation, and every seven days for subsequent immunisations, anti-sera was collected via tail bleed extraction and screened for lgG antibody responses. Once an animal with a high titre of lgG response was identified, it was boosted intraperitoneally (i.p.) with liposome in the presence of a-GalCer or cells and sacrificed 5 days later.

2.13 Generation of mAb

2.13.1 Isolation of splenocytes

Mice were sacrificed and sterilised using 70% ethanol. The spleen was collected using sterilised dissecting instruments (scissors and forceps) and transferred to a sterile petri dish (100mm). The spleen was washed with 5ml serum-free medium (RPMI 1640) using a 25-gauge needle and then agitated with sterile forceps gently to harvest splenocytes. 5ml of splenocytes were collected into a sterile 25ml universal tube while excess fat and connective tissues were discarded. The total fluid volume containing the splenocytes was increased to 25ml with serum-free medium (RPMI 1640) and centrifuged at 100g for 10 min. The supernatant was removed, leaving 1ml of medium and the splenocytes. The splenocytes were then resuspended in 5ml serum-free medium (RPMI 1640) and counted using a haemocytometer with trypan blue, staining for viability assessment.

2.13.2 Fusion of splenocytes with NS0 myeloma cells.

Washed splenocytes were combined with healthy NS0 myeloma cells in a ratio of 1:10 (NS0: splenocytes; 1×10^7: 1×10^8 cells) in a 25ml universal tube and centrifuged at 150g for 5 min. The supernatant was aspirated and the combined cell pellet was

resuspended in 800µl of polyethylene glycol (PEG) gently and gradually over 1 min. The cell mixture was agitated gently for 1 min prior to the addition of 1ml of serum-free medium (RPMI 1640) over 1 min while continuing to agitate. A further 20ml of serum-free medium (RPMI 1640) was added over 1 min while agitating. Then the cell mixture was centrifuged at 150g for 5 min. The supernatant was removed and the cell mixture was resuspended in 15ml of hybridoma medium

[500 ml hybridoma serum-free medium (Gibco): 10ml HT (hypoxanthine thymidine) supplement (50x Hybri-Max; Sigma): 31µl (31µg) methotrexate (1mg/ml; Sigma): 25ml of Hybridoma cloning factor (Opti-Clone II; MP): 50ml of filtered NS0 spent medium]. The cell suspension was spread evenly across a 96 well flat bottom plate and incubated at 37°C in cell culture incubator (5% CO2).

2.14 Immunohistochemistry

2.14.1 Colorectal Cancer Tissue Micro-Array (TMA)

Tissue microarrays (TMAs) represent a powerful method for undertaking large-scale tissue-based biomarker studies. In this study, a colorectal TMA was kindly provided from Queen's Medical Centre by Professor Mohammad Ilyas. This TMA was papered by taking a core of tissue from a 'donor' tissue block with a needle and transferring it to an empty 'recipient' block using TMA Guidelines by *Ilyas et al.,* Histopathology 2013. The TMA consisted of 1000 CRC patients randomly selected in chronological order with a mean follow-up period of 53.6 months (year 2008 –2012). There are three tumour cores (0.6 mm) and one core for adjacent normal epithelium from each case. All cases were adenocarcinoma, and 89% were moderate histological grade. Sixteen per cent of the patient cohort were TNM stage

I, 40% were stage II, 32% were stage III, and 12% were TNM stage IV, comparable with previously published national numbers. [368, 369]

2.14.2 Chromogenic Immunohistochemistry (IHC)

Immunohistochemistry was performed for CD3+, CD8+, and CD103+ cells detection at room temperature. This procedure was performed on 4µm thickness of formalin-fixed paraffin-embedded (FFPE) human tonsil (whole sections) and colorectal cancer tissue (TMA cores) sections embedded in paraffin. For antibodies studied, Novolink™ Polymer Detection System (RE7150-K) was used to stain the sections. To confirm adhesion of tissue sections with the slide surface, sections were placed on a hot plate (60 °C) for 10 minutes and left to cool. Slides were dewaxed and rehydrated using the Autostainer through xylene and graded alcohols, and then antigen retrieval was performed by placing the slides in EDTA (pH:9) for 35 min in a steamer. Then the slides were cooled down in TBS for 10 minutes. Endogenous peroxidase was blocked by 0.3% hydrogen peroxide in Tris-buffered saline (TBS) for 5 minutes. To block nonspecific binding of the primary antibody, all sections were treated with the protein block for 5 min, then incubated for one hour at room temperature with anti CD3, CD8 and CD103 antibodies with 1/300, 1/300 and 1/250 dilution of antibody, respectively. Anti CD3-rabbit monoclonal antibody [SP7], Abcam (ab16669)), anti- CD8 mouse monoclonal antibody, DAKO Clone (C8/144B) and Anti CD103 -rabbit monoclonal antibody [EPR4166(2)] (Abcam) were used for this study.

Primary antibody was detected by prediluted anti-rabbit poly HRP antibody in animal serum and TBS and incubated for 30 minutes. Chromogenic visualisation was performed with 3,3'-diaminobenzidine (DAB) for 5. Slides were counterstained with hematoxylin and dehydrated in xylene.

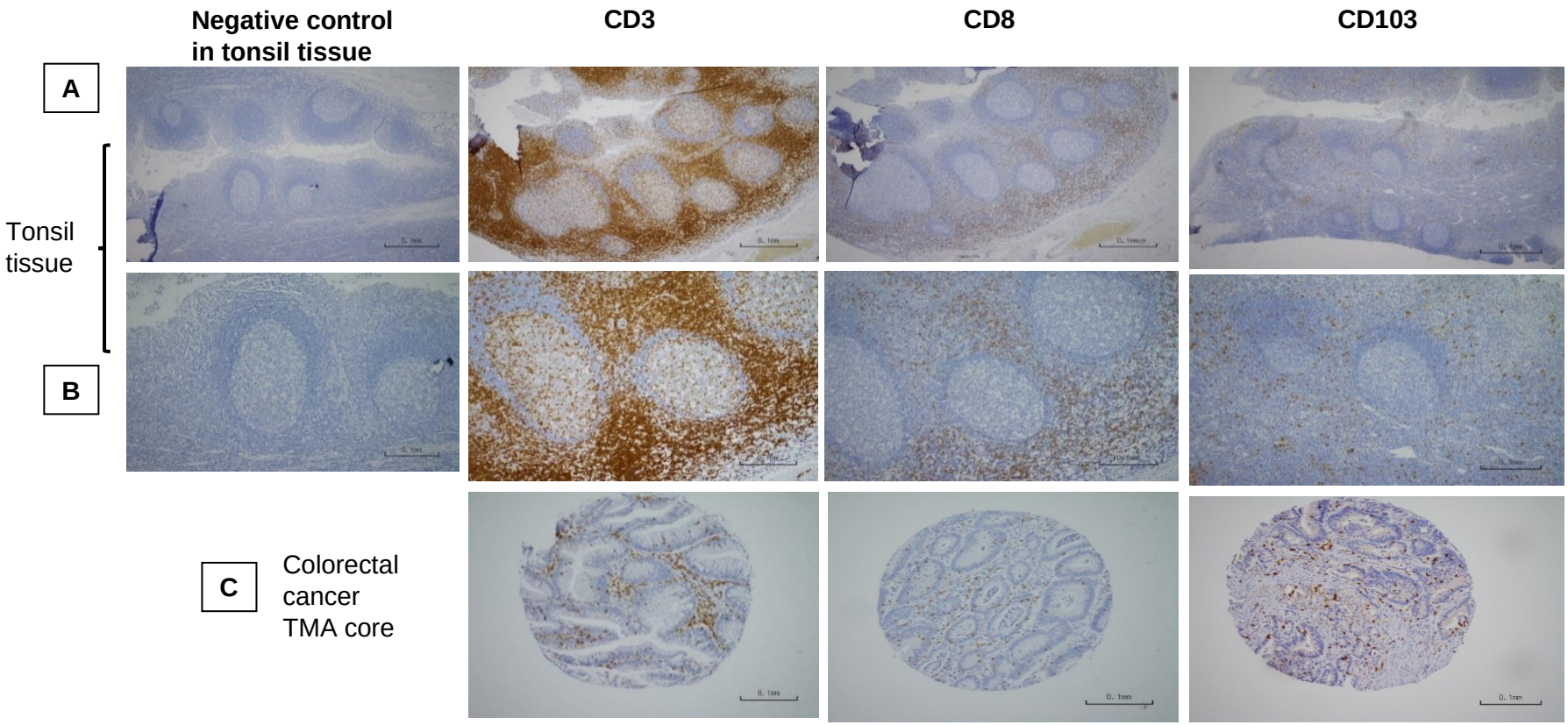

Figure 2. 1 IHC staining of CD3, CD8 and CD103 biomarkers on human tonsil and colorectal cancer tissue.

Microscopic images were obtained at **(A)** (x10) and **(B)** (x20) magnifications of the whole tonsil section stained with negative control, CD3 (1:300), CD8 (1:300) and CD103 (1:250), respectively. **(C)** Microscopic images (x10) of colorectal cancer TMA cores stained with negative control, CD3 (1:300), CD8 (1:300) and CD103 (1:250), respectively.

2.15 Scanning and scoring

TMA slides for standard IHC were captured digitally and stored as high-resolution image files and viewed by NDP viewer software (U12388-02). All markers were counted by Halo software and confirmed by two assessors who were blind to patients' data. We had 3 TMA core samples from each patient. For scoring, we determined tumour and stomal areas and counted positive cells in each part separately. For calculating density, we combined all three cores from each patient. The density of the positive cells per area of tumour or stroma is calculated by the following formula:

$$\textit{Density of positive cells} = \frac{\textit{Total number of counted cells in tumour tissue or stroma}}{\textit{Area of tumour or stroma } (mm^2)}$$

2.16 Multiplex immunohistochemistry

Multiplex immunohistochemistry/immunofluorescence (*mIHC/IF*) enables simultaneous antibody-based detection and quantification of the expression of up to six protein markers and a nuclear counterstain on a single tissue section. For this study, we used *mIHC/IF to perform a* simultaneous detection of CD8, CD103 and CD39 biomarkers on the same CRC TMA core using Opal 4-colour IHC kit (NEL810001KT). Although this method provides high sensitivity and prevents Ab crossreactivity, some challenges are associated with this technique, like the umbrella (blocking) effect. In this study, we minimised these effects to obtain reliable and reproducible data by optimising the multiplex staining procedure. Opal 690 dye has the least fluorescence intensity compared to Opal 520 and Opal 570. Therefore, it was recommended to use Opal 690 to detect targets with high density. In this study

and according to the observations of standard IHC staining, intratumoral CD103+ cells were more abundant than CD8+cells and CD39+cells. Opal fluorophores 520 (green) ,570 (yallow) and 690 (red) were paired with CD8,CD39 and CD103, respectively.

The Multiplex procedure (summarised in figure 2.2) was initiated by placing the slides on 60 °C hot plate for an hour, then deparaffinised in xylene and rehydrated in three baths of 100%, 90%, and 70% ethanol by auto-strainer machine. Next, slides were subjected to 96°C warmed Bond Epitope retrieval solution (EDTA, pH 9) for 35 minutes for antigen retrieval and cooled down in TBS for 10 minutes. Endogenous peroxidase was blocked by 0.3% hydrogen peroxide in Tris-buffered saline (TBS) for 5 minutes. To block nonspecific binding of the primary antibody, all sections were treated with the protein block for 5 min. Then, the slides were incubated with anti-CD39 (1:300) AT 4C overnight. The next day, the attached primary antibody was detected by HRP conjugated secondary antibody (slides incubated for 30 min). Then slides were washed and incubated Opal 570 (1:100) for 10 min. After the signal amplification step, antibody stripping was performed via microwave treatment with Tris-EDTA (pH9) (PerkinElmer, AR900250ML). The same steps were repeated with anti-CD103 primary antibody (1 hour, room temperature), which was detected and paired with Opal 690 and stripped. Finally, the slides were stained with anti- CD8 primary antibody (1 hour, room temperature), followed by the secondary antibody and Opal 520. Then slides were incubated for 10 min with DAPI for counterstaining.

Following the mIHC/IF staining, the CRC TMA slides were scanned by PerkinElmer Vectra microscope. To confirm the quilty of staining, the slides were viewed in singleplex and multiplex settings, as shown in figure 2.3. The scanned images were then analysed by Phenochat and InForm software (version 2.4.6). The densities of the detected phenotypes were calculated automatically and extracted from PhenoRepots. (refer to chapter 6 for more details).

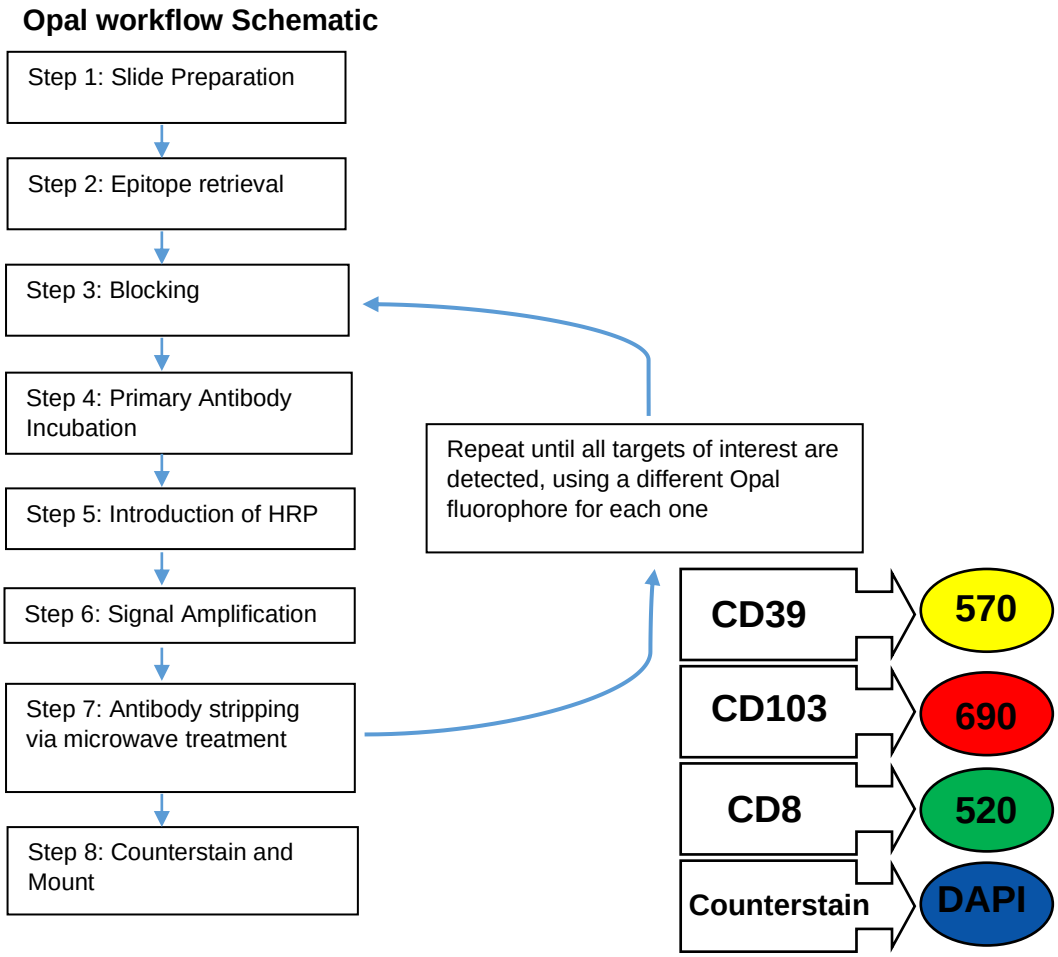

Figure 2. 2 Multiplex IHC staining for simultaneous detection of CD8, CD103 and CD39 biomarkers on the same CRC TMA core.

Opal fluorophores 520 (green) ,570 (yellow) and 690 (red) were paired with CD8, CD39 and CD103, respectively. The first staining cycle targeted CD39, the second targeted CD103 and the final cycle targeted CD8. At the end of each cycle, the primary and secondary antibodies were stripped for the addition of the next primary antibodies.

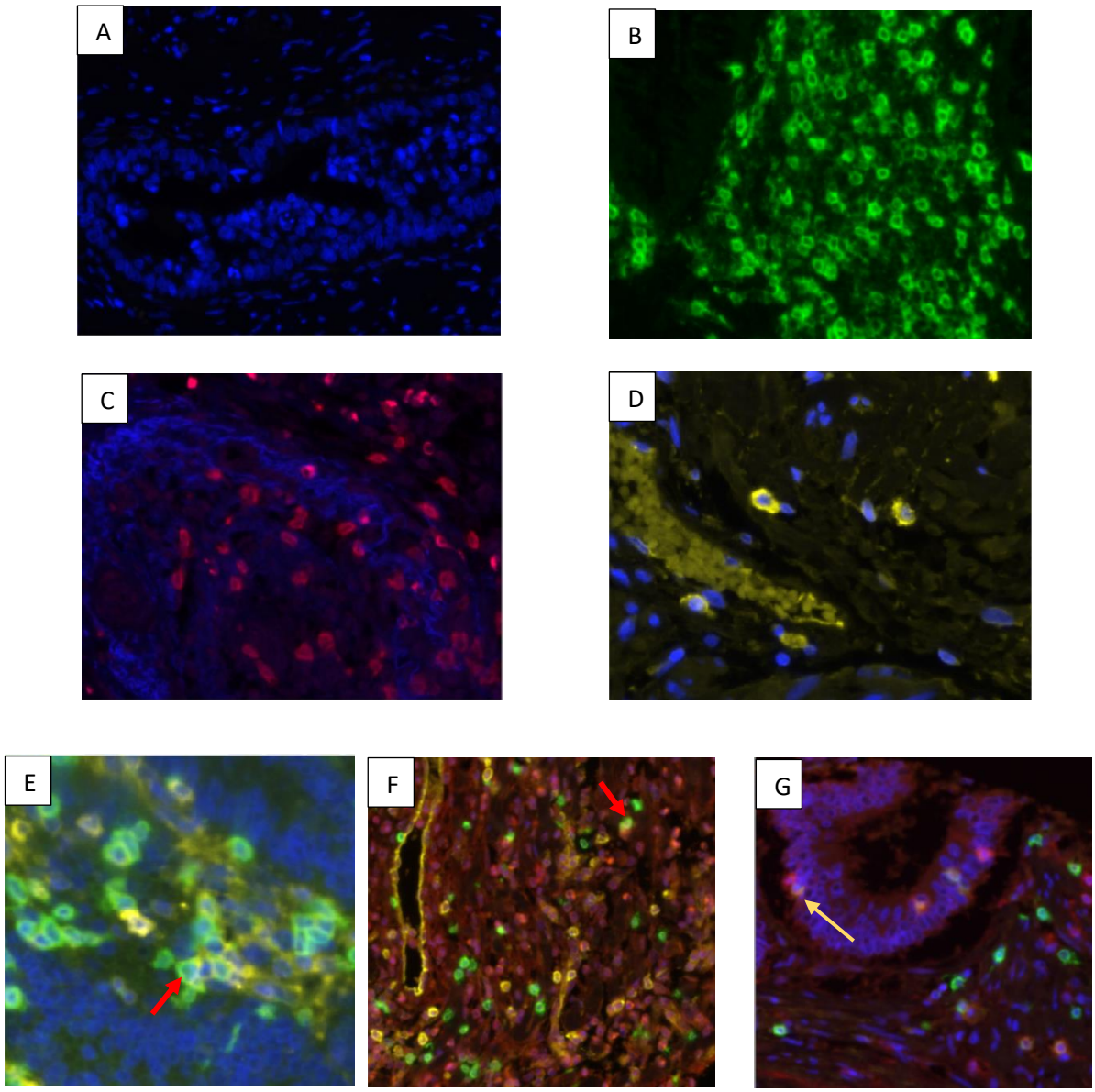

Figure 2. 3 Multiplex IHC staining of CD8, CD103 and CD39 on human tonsil and colorectal cancer tissue.

Slides stained by: **(A)** DAPI alone (CRC tissue), **(B)** Staining CD8 by Opal 520 alone (Tonsil tissue), **(C)** Staining CD103 with Opal 690 and DAPI (CRC tissue), **(D)** staining CD39 by Opal570 and DAPI (CRC tissue), **(E)** Dual staining for CD8 and CD39 (CRC tissue). Green cells are CD8+ and yellow ones are CD39+ cells. Red arrow shows a dual positive cell. **(F)** and **(G)** Detecting all 3 markers on one slide (CRC tissues). Red cells are CD103+, yellow and green cells are CD39+ and CD8+, respectively. Red arrow shows CD8+CD39+ cell. The yellow arrow shows CD103CD39+ cell.

2.17 Statistical Analysis

The optimal cut-off point for TILs density was defined using X-tile bioinformatics software (Yale University, version 3.6.1). TILs were classified into high and low infiltration depending on these cut-off points. For assessing factors influencing overall survival statistical analysis, we used Kaplan- Meier curves via SPSS software (version 24 for windows). Pearson's χ^2-tests were used to determine the significance of association between categorical variables. Disease-specific survival calculations included all patients whose death related to CRC and deaths from other causes censored at the time of death. Multivariate analysis was used to determine the relative risk and independent significance of each factor. P-values <0.05 were considered as statistically significant.

The comparations between different TILs densities was done using GraphPad PRISM version 8. Summary statistics show 25 percentile, median and 75 percentile, unless stated otherwise. Statistical difference between two groups was assessed by the two tailed paired t-test with Wilcoxon adjustments for non-parametrically distributed variables or by comparing ranks using the Mann Whitney test for unpaired and non-parametric variables. Test performed for measuring the statistical difference has been mentioned with the graphs. Also, GraphPad PRISM version 8 was used to perform Bland-Altman test to analyse the agreement between HALO and the manual counting methods.

Chapter 3: Generating a functional monoclonal antibody against TSPAN 32 to reactivate T cell proliferation

3.1 Introduction

Tetraspanins are a superfamily consisting of 33 members of small transmembrane proteins in the human species, many of which are widely expressed in human tissue (CD9, CD151, CD63, CD81, CD82). In contrast, others are restricted to hematopoietic cells (TSPAN32, TSPAN33, CD53 and CD37).[322] Tetraspanin proteins have been shown to regulate fundamental cellular processes like proliferation, fusion, survival, signalling, invasion and migration.[323] In immune cells, tetraspanins interact with crucial leucocyte proteins such as integrins and immunoreceptors [CD19, MHC molecules, CD3, CD4, CD8 and BCR complex].[310, 324, 325, 326, 327] These interactions enable the modulation of immune responses and processes like leukocyte migration and extravasation, antibody production and antigen presentation.[317, 328, 329, 330] In addition to that, tetraspanins can regulate the activation of T cells positively or negatively depending on how they will control the process of Ag- presentation on antigen-presenting cells, which has a powerful effect on anti-tumour immunity.[331]

Several members of the tetraspanin superfamily (CD53, CD37, CD9, CD151, CD82, CD81 and TSPAN32) have been implicated in T cell co-stimulation and TCR-mediated proliferation. Numerous studies investigated the association of tetraspanin knock out mice with T cell proliferation. For example, Van Spriel and co-workers have shown that CD37 knockout mice had a hyperproliferative T cell response on stimulation, suggesting a negative regulatory role of this tetraspanin in T cells.[332] Also, CD81 knockout mice showed increased T cell proliferation following T-cell antigen receptor (TCR) interaction in CD81 knockout mice compared to the control mice.

Moreover, CD151 null T cells showed a significant increase in stimulation when cross-linked with CD3 and CD28 antibodies, which indicates the regulatory role of CD151 T lymphocyte proliferation. [333] The immune-modulatory role of the previously mentioned tetraspanins on T cell co-stimulation has been studied extensively.[334] However, limited data have been published regarding the pathophysiological role of TSPAN32 (a.k.a. Tssc6) in the regulation of immune responses.

TSPAN32 is a tumour suppressor gene discovered on the same gene as CD81, human chromosome 11p15.[335] The expression of TSPAN32 is known to be restricted to hematopoietic cells, while its exact functional role is still undefined. [336] In a previous study, T cells bearing a null mutation of the TSPAN32 gene showed enhanced responses to stimulation due to increased interleukin 2 production, indicating that TSPAN32 may play a role in the negative regulation of peripheral T cell proliferation. [320] Furthermore, Gartlan and colleagues determined the functional correlation between CD37 and TSPAN32 using double knockout mice (TSPAN32-/ CD37-). They reported that the role of these tetraspanins in cellular immunity was identified by the responses of dendritic cell stimulation and T cell proliferation *in vitro*, which were significantly higher with both tetraspanins absent than in counterparts with the single knockout. However, the risk of inducing autoimmune adverse events is similar in both cases.[321]

The previous data highlights the importance of TSPAN32 in regulating immune responses and suggest that a functional anti-TSPAN32 mAb might co-stimulate T cell activation and proliferation, acting as a potential checkpoint inhibitor. However, the role of TSPAN32 is undefined yet due to the lack of mAb that recognises the tertiary structure of TSPAN32. The difficulty in raising antibodies to tetraspanins lies behind their small size and structure, protruding only 4-5nm above the membrane, as well as their associations with larger proteins, making them inaccessible for detection [294]. On

top of that, tetraspanins are highly conserved between species, making it difficult to raise the antibodies by conventional mice immunisation. For example, TSPAN9 has amino acid sequence homology of 97% for humans compared with mouse [337]. However, new immunisation approaches have managed to develop a functional mAb to CD81 (tetraspanin protein). For instance, Fofana and colleagues used genetic Immunisations to generate a functional anti-CD81 mAb that efficiently blocks Hepatitis C virus spread and dissemination during liver transplantation. [338] Moreover, a previous doctoral student in our research group has developed an in house mAb that recognises CD81 via mice immunisation with plasma membrane lipid extract from four NSCLC cell lines. (unpublished data)

In this study, we aimed to develop a functional mAb against TSPAN32 using different immunisation methods. It was hypothesised that using a novel immunisation method such as DNA immunisation or immunising with PM glycolipid extraction of cells expressing TSPAN32 would generate an anti-TSPAN32 IgG response within the immunised mice. The development of a functional anti-TSPAN32 mAb would help to confirm the regulatory role of TSPAN32 on T cells and the possibility of being a potential checkpoint inhibitor.

3.2 Results

3.2.1 Stable transfection of TSPAN32 in NIH 3T3 cells

In order to determine the efficacy of the immunisation methods used to produce IgG response to TSPAN32, it was essential to use cells expressing TSPAN32 to screen mice sera for the presence of IgG antibodies. Here, we demonstrate the optimisation steps to obtain mouse embryonic fibroblast (NIH 3T3 cells) stably transfected with TSPAN32. A successful stable transfection needs an effective DNA delivery and a

proper method to select cells that have integrated the DNA plasmid. For every 10^4 transfected cells, one cell is found to integrate DNA stably. However, the efficiency varies depending on the type of the cells and whether circular or linear DNA plasmid is used.[339] Several studies reported that DNA integration is most efficient when transfection is performed with linear DNA.[340, 341] Thus, TSPAN32 DNA construct was linearised using ScaI restriction enzyme to ensure better DNA integration (Figure 3.1). TSPAN32 DNA plasmid contained neomycin resistant gene; therefore, G418 was used as a selectable marker, which is required to select cells that stably express TSPAN32. Also, green fluorescent protein (GFP) was part of the DNA construct as a marker for gene expression and protein localisation in eukaryotic cells.[342]

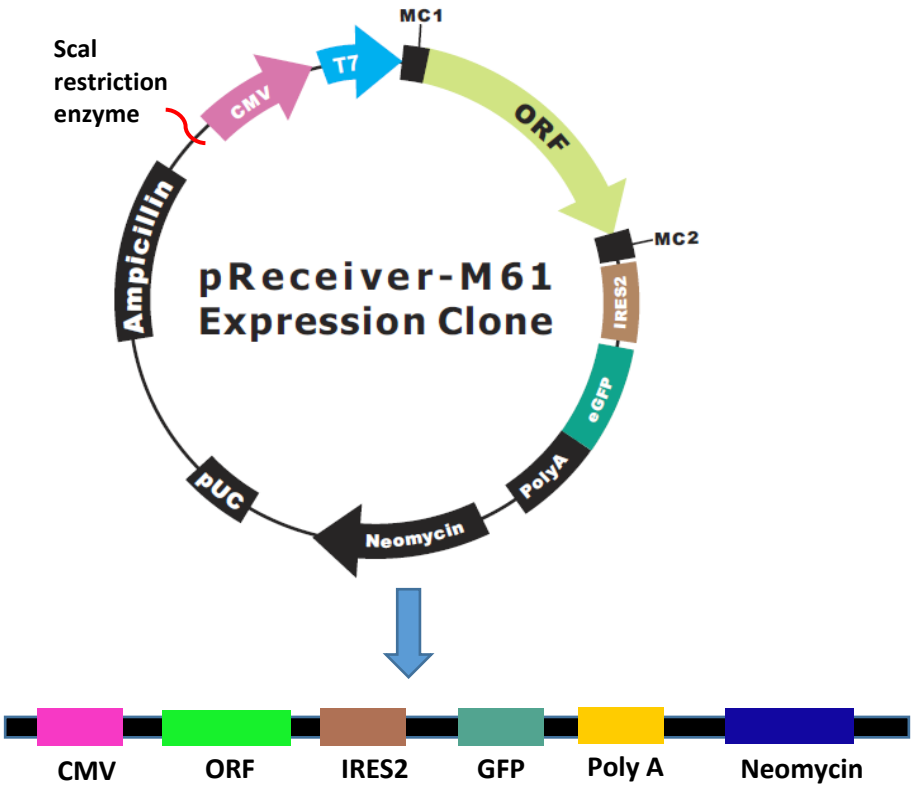

Figure 3. 1 Linearisation of TSPAN32 circular DNA vector into a linear shape DNA plasmid using ScaI restriction enzyme.

Abbreviations: ORF- open reading frame, IRES- internal ribosome entry site, CMV- Cytomegalovirus, GFP - green fluorescent protein, Poly A- Polyadenylation, Neomycin – antibiotic resistance gene

TSPAN32 DNA transfection was initiated by adding DNA-Lipofectamine® mixture to 70% confluent NIH 3T3 cells plated in a six-well plate.[339] Forty-eight hours following transfection, a selective medium containing 500 µl/ml of G418 (optimum concentration was determined using a sensitivity selection experiment (refer to chapter 2) was added to the transfected cells. To determine the transfection efficiency, the expression of GFP was analysed by flow cytometry, as shown in figure 3.2. The transfection of NIH 3T3 cells with TSPAN32 DNA gave 25.9% cells positive for GFP at day 8, and at day 12 the transfected cells were 53.6%. Although The transfection of NIH 3T3 cells with GFP only as a positive control gave a higher percentage of transfected cells than transfection with TSAPN32 at day 8, the per cent of transfected cells was similar at day 12 due to the presence of G418 in the medium, which eliminates the non-transfected cells and helps G418-resistant clones to grow faster.

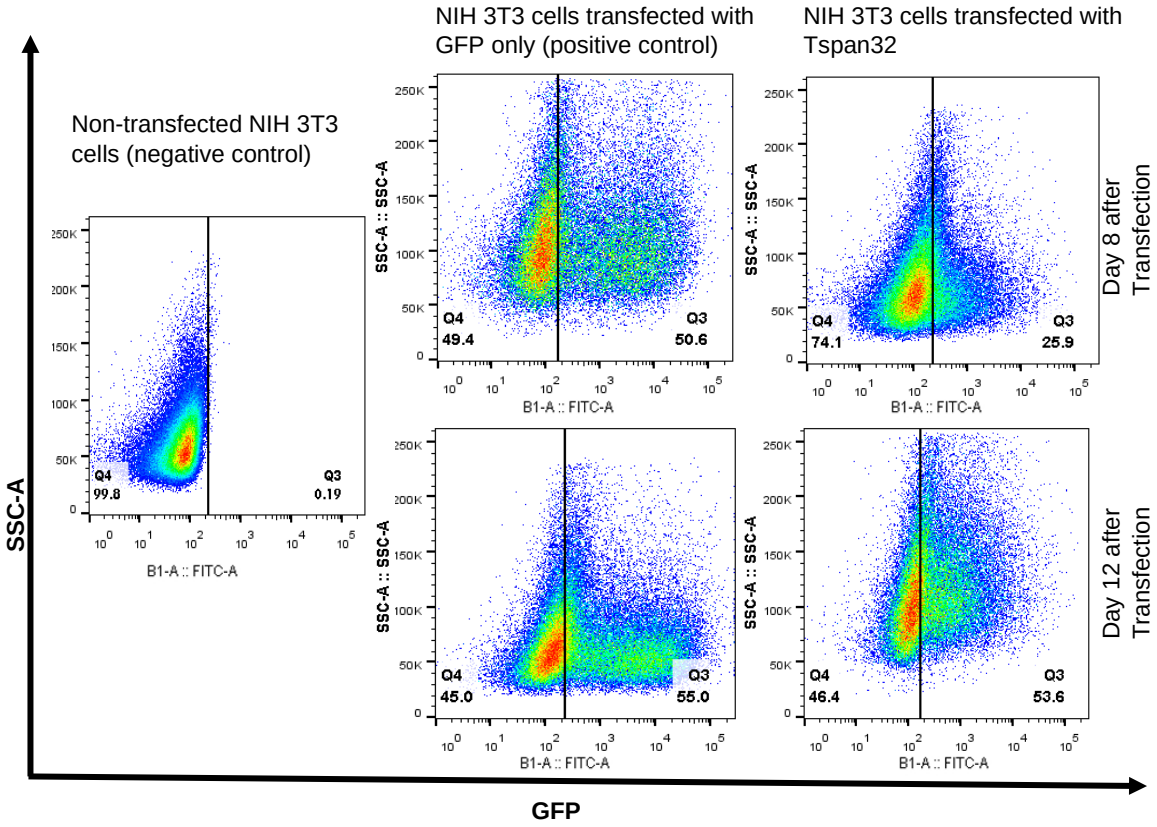

3. 2 NIH 3T3 cells transfected with TSAPN32.

Dot plots represent the GFP expression level of NIH 3T3 cells transfected with TSAPN32 compared with the non-transfected NIH 3T3 cells (negative control), and NIH 3T3 transfected with GFP only (positive control) at two-time points; day 8 and day 12 after transfection to determine transfection efficacy.

In order to obtain pure stably transfected clones, single-cell cloning from both the positive control and TSPAN32 transfected NIH 3T3 was performed on day 12 after transfection. A 96-well plate was seeded with a single cell for each well and incubated with a growing medium containing G418 for two weeks. Out of 96 wells, 25 wells showed antibiotic-resistant pure clones. The two wells which gave the highest GFP expression under the fluorescent microscopy were chosen from the positive control and TSPAN32 transfected cells (Figure 3.3 A). Using flow cytometry, these cells were confirmed to be a single population expressing high GFP levels with MFI of 27350 and 66564 for the positive control and TSPAN32 transfected cells, respectively (Figure 3.3 B and C).

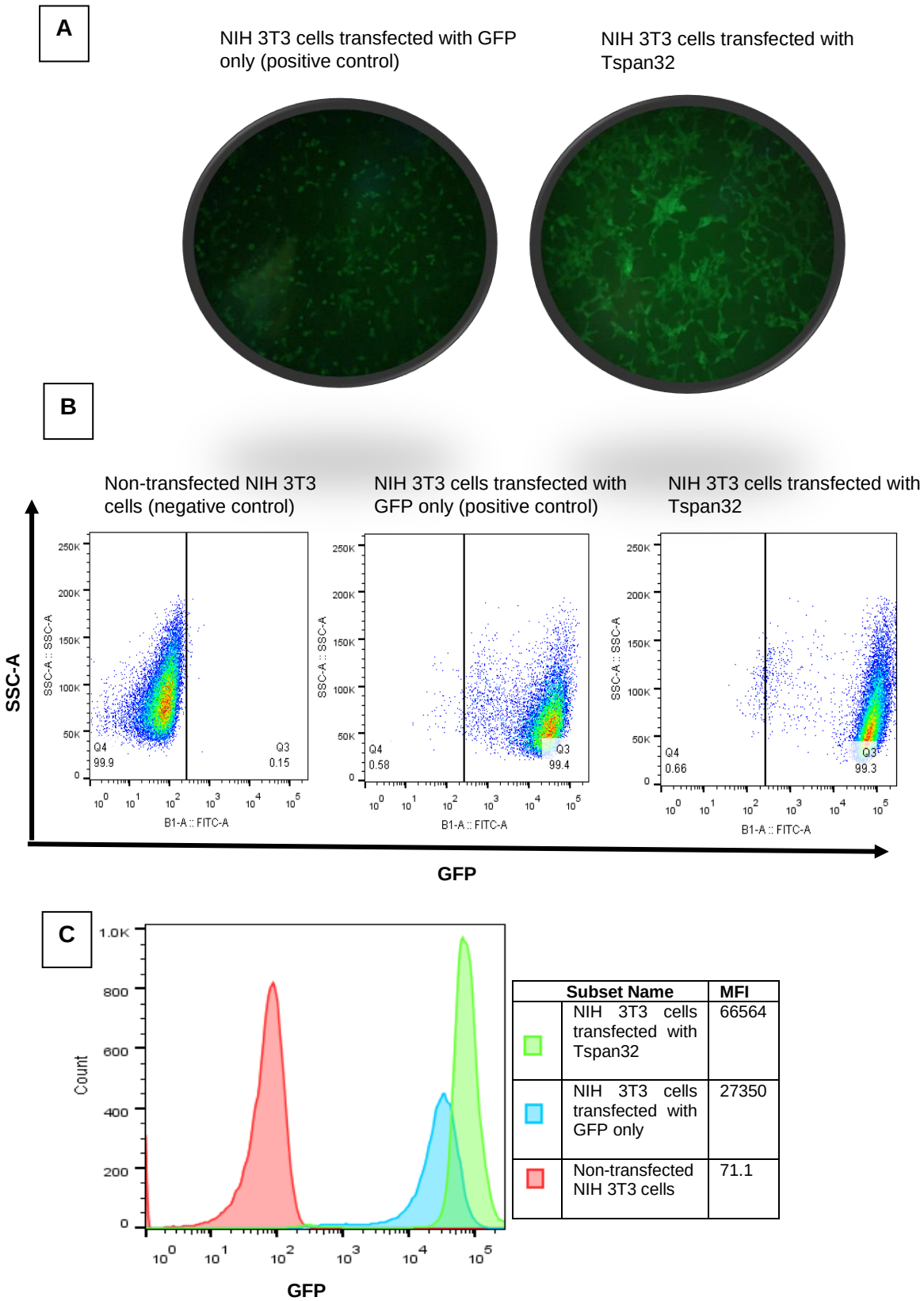

Figure 3. 3 Pure clones of TSPAN32 transfected NIH 3T3 cells were obtained using single-cell cloning.

Two clones of the positive control and TSPAN32 transfected cells with the highest GFP expression were chosen out of 25 antibiotic-resistant pure clones. **A, B** and **C** represent the

microscopic images, FACs dot plots, histograms of these pure stably transfected clones, respectively. MFI: median fluorescence intensity.

In order to confirm the expression of TSPAN32 protein on the transfected cell line, two different commercial antibodies were purchased: TSPAN32/TSSC6 antibody (2B4) [H00010077-M02] from Abnova and TSPAN32 polyclonal antibody [PA5-18045] from ThermoFisher and used to perform western blots, which are shown in figure 3.4 A and B, respectively. Both these antibodies produced a band on western blots, at approximately 34 KDa. This is the expected weight for TSPAN32. However, these bands were also present in the negative controls (Non-transfected NIH 3T3 cells and NIH 3T3 cells transfected with GFP only). As a loading control, the western blots were also probed for β-tubulin. These bands appeared around 50 KDa in figure 3.4 B. Unfortunately, these results showed that the commercially available TSPAN32 antibodies were not specific enough to confirm the expression of TSPAN32 on the transfected cell line. However, this indicates the urgent need to develop a highly specific mAb to recognise TSPAN32 using innovative immunisation approaches, which will be discussed next in this chapter.

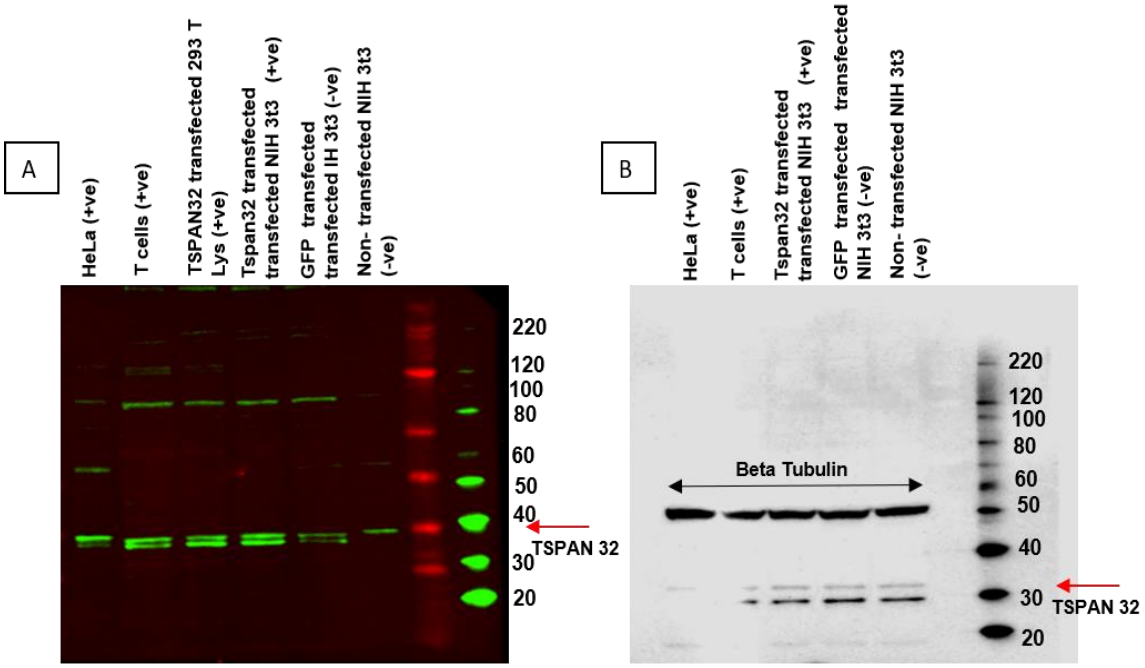

Figure 3. 4 Western blots to confirm the expression of TSPAN32 on the transfected NIH 3T3 cells at the protein level.

Two WB were performed using two different commercial antibodies: **A)** TSPAN32/TSSC6 antibody (2B4) [H00010077-M02] from Abnova; **B)** TSPAN32 polyclonal antibody [PA5-18045] from ThermoFisher. In both western blots, non-transfected NIH 3T3 cells and NIH 3T3 cells transfected with GFP were used as negative controls. In contrast, HELA cells and T cells were used as a positive control for TSPAN32 expression. Non-specific binding of both antibodies produced bands at approximately 34 KDa, the expected weight for TSPAN32, for TSPAN32 transfected cells, the negative and positive controls. β-tubulin was used as a loading control (~50 KDa).

3.2.2 TSPAN32 mice immunisation approaches: Particle-Mediated DNA Immunisation (Gene gun immunisation)

Genetic immunisation has applications in both vaccine development [343] and producing high-quality monoclonal antibodies. [344] According to *Hansen et al.,* gene gun immunisation is the obvious route to produce antibodies against membrane proteins because the membrane protein antigen is expressed, folded, and modified within a native membrane environment by the gene-immunised host. Therefore, DNA immunisation is expected to permit immune recognition of the myriad in-membrane

interactions with other macromolecules as well as of intermediate assembly states of the membrane protein. [345]

Gene gun Immunisation is a highly efficient method for biolistic delivery of DNA-gold micronanoplexes. These complexes consist of micron-sized gold particles that enable dermal penetration and nanometer-sized gold particles, which allow better DNA binding by providing a higher surface area than micron gold alone. Upon delivery, the DNA-gold complex is propelled through bullets via a high-pressure burst of helium gas. The DNA-gold particles penetrate the epidermal cells, which include dendritic cells and keratinocytes. Upon exposure to antigen, an adaptive immune response is elicited due to the migration of dendritic cells into the lymph nodes.[346] Therefore, DNA-gold micronanoplex method leads to direct DNA transfection of dendritic cells and *in vivo* expression of the protein in both the dermal tissues and the lymph nodes.[346, 347]

In this study, the gene gun immunisation method was used to produce mAb against TSPAN32 using gold bullets coated with pEF6/Myc-His (Invitrogen) plasmid cloned with TSPAN32 (figure 3.5 A). This plasmid was gifted by Dr. Michael Tomlinson from the University of Birmingham. The immunisation procedure was initiated by bleeding three female BALB/c mice (1R, 1P and 1L) to obtain the normal untreated mouse serum (NMS) as a negative control for the serum screen process. Next, 1R, 1P and 1L mice were immunised with two bullets (1 µg of TSPAN32 DNA per bullet) using a gene gun every two weeks (figure 3.5 B). Mice were immunised four times then boosted with TSPAN32 transfected NIH 3T3 cells via intraperitoneal injection (IP). The immunisation protocol is shown in Table 3.1.

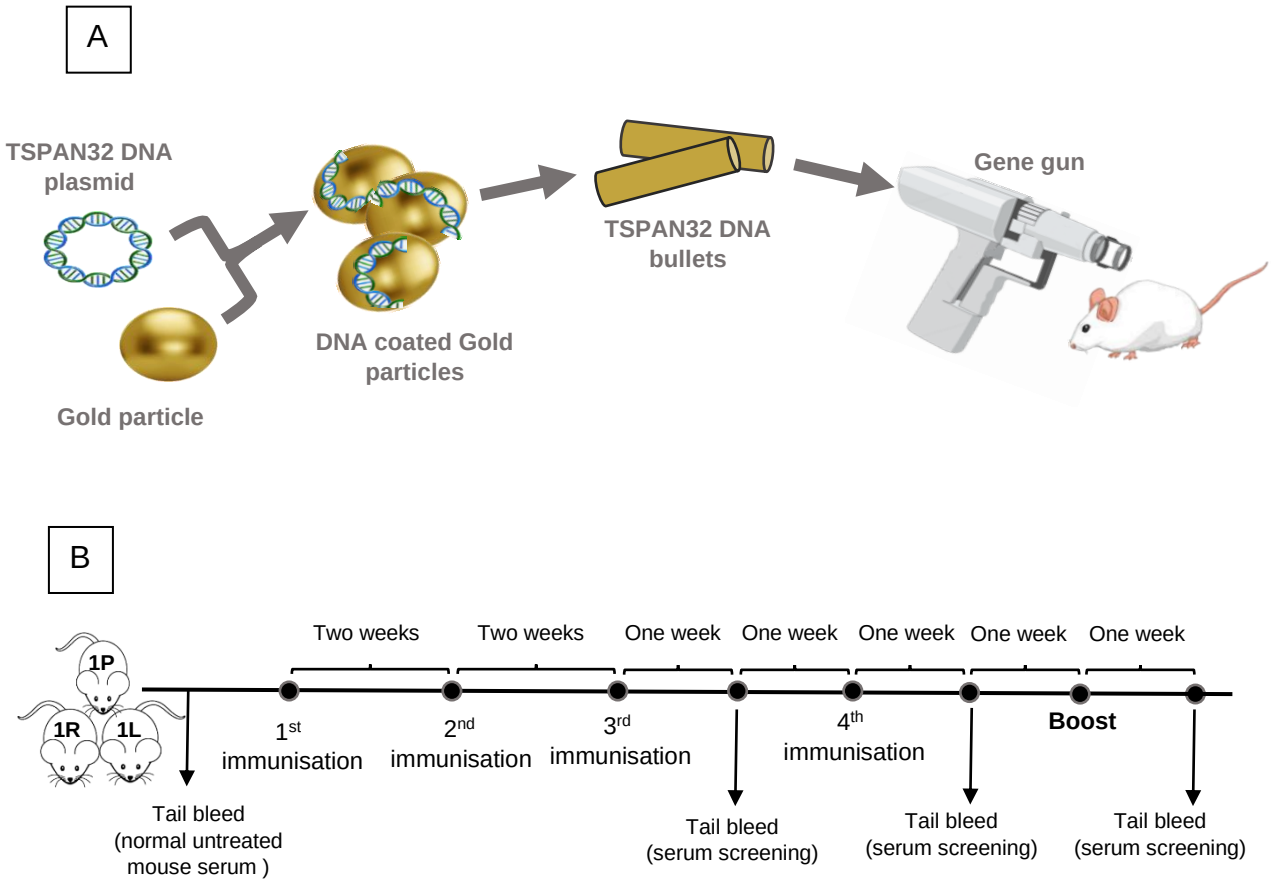

Figure 3. 5 TSPAN32 Gene Gun immunisation.

(A) represents the attachment of TSPAN32 circular plasmid to gold nanoparticles, then combined to form nanocomplexes. The nanocomplexes are then introduced into mice with a gene gun via a high-pressure burst of helium gas to inoculate the mice. **(B)** Mice immunisation scheme over a period of 9 weeks, immunisations were performed every two weeks, and serum screening (tail bleed) was conducted after a week of the 3rd, 4th immunisations and the boost.

Table 3. 1 Immunisation schedule of TSPAN 32 DNA bullets using a gene gun. Mice [1R,1P and 1L] were immunised four times with two DNA bullets each time for each mouse. The mice were boosted with TSPAN32 transfected NIH 3T3 cells via intraperitoneal injection (IP).

	Mouse 1R	**Mouse 1P**	**Mouse 1L**
1st Immunisation	2 xTspan32 DNA bullets (1µg of DNA in each bullet)	2 xTspan32 DNA bullets (1µg of DNA in each bullet)	2 xTspan32 DNA bullets (1µg of DNA in each bullet)
2nd Immunisation	2 xTspan32 DNA bullets (1µg of DNA in each bullet)	2 xTspan32 DNA bullets (1µg of DNA in each bullet)	2 xTspan32 DNA bullets (1µg of DNA in each bullet)
3rd Immunisation	2 xTspan32 DNA bullets (1µg of DNA in each bullet)	2 xTspan32 DNA bullets (1µg of DNA in each bullet)	2 xTspan32 DNA bullets (1µg of DNA in each bullet)
4th Immunisation	2 xTspan32 DNA bullets (1µg of DNA in each bullet)	2 xTspan32 DNA bullets (1µg of DNA in each bullet)	2 xTspan32 DNA bullets (1µg of DNA in each bullet)
Boost	-----	1x 10^6 of NIH 3T3 cells transfected with Tspan32 in 250ul PBS via I.P. injection	1x 10^6 of NIH 3T3 cells transfected with Tspan32 in 250ul PBS via I.P. injection

To assess whether the immunised mice (1R, 1P and 1L) generated anti-TSPAN32 antibody responses, anti-sera were screened against TSPAN 32 transfected NIH 3T3 cells after the third immunisation, fourth Immunisation and the boost and analysed using flow cytometry. Figure 3.6 represents histograms of TSPAN 32 transfected NIH 3T3 cells treated with three serum dilutions 1/100, 1/500, 1/1000 of normal mouse serum as a negative control and mouse serum after the third and fourth immunisations of 1R, 1P and 1L mice. An anti-mouse IgG Fc secondary antibody was used to detect the presence of IgG antibodies within the mice sera. According to the flow cytometric analysis, a shift in MFI was observed for all three immunised mice at 1/100 dilution but not at the 1/500 and 1/1000 serum dilutions. This indicates that a low IgG titre is generated even after four immunisations.

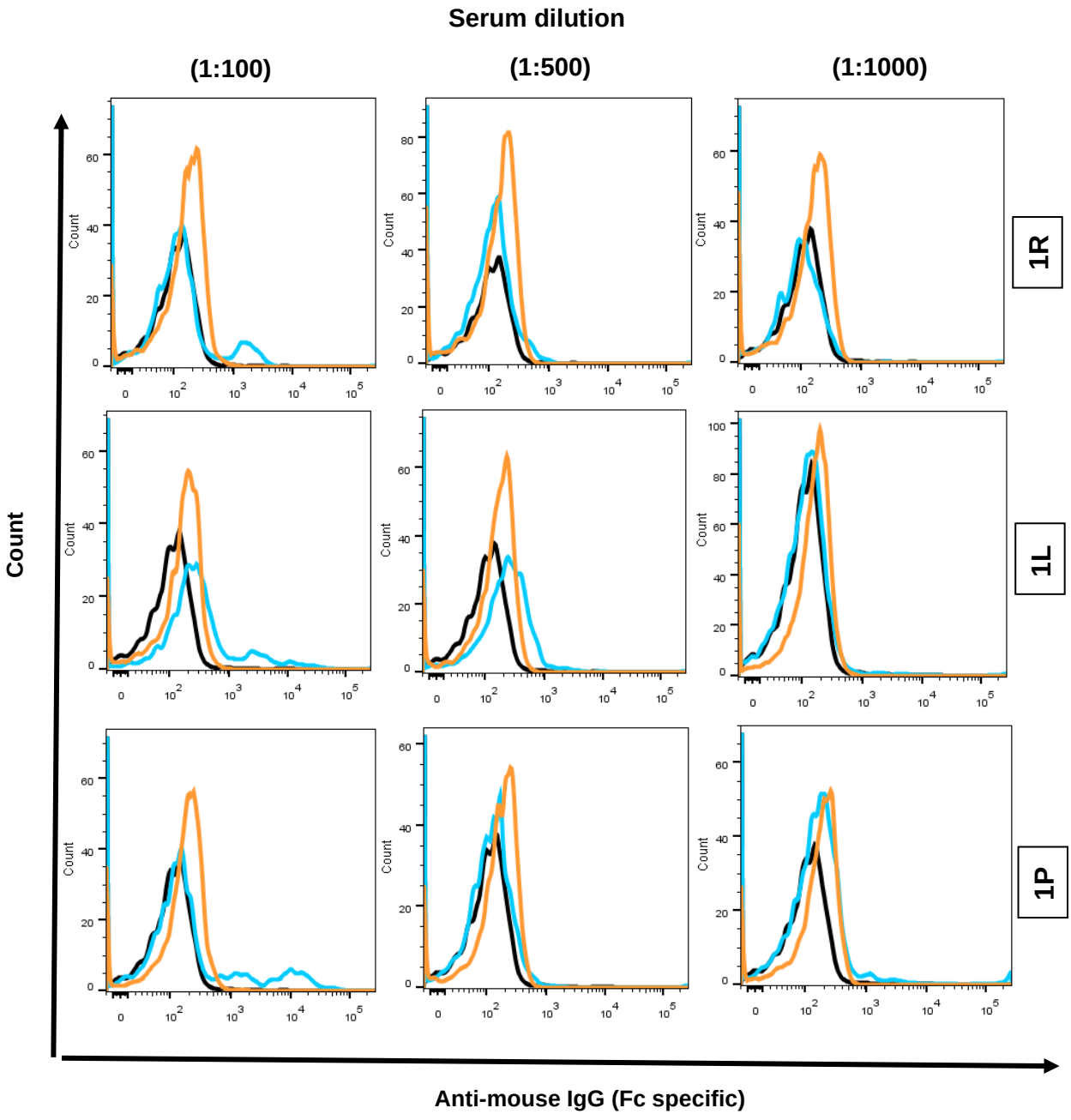

Figure 3. 6 IgG responses to TSPAN32 after 3rd and 4th DNA immunisation with TSPAN32 DNA.

The histograms represent the binding of TSPAN32 transfected cells (1x10^5 cells per well) with 1R,1L, and 1P mice sera at 1/100,1/500, 1/1000 dilutions after 3rd and 4th immunisation. An anti-mouse IgG Fc secondary antibody was used to detect anti-TSPAN32 IgG antibodies within the mice sera. **Black line** represents the negative control (normal mouse serum before immunisations); the **blue line** represents mice sera after third immunisation, and the **orange line** represents mice sera after fourth immunisation.

In order to improve IgG titre, two mice (1P and 1L) were boosted with TSPAN32 transfected NIH 3T3 cells via IP injection. A week after the boost, mouse sera were screened for the presence of IgG antibodies. Flow cytometry histograms shown in Figure 3.7 demonstrate that there was a minimal shift in MFI of IgG levels in the serum of the immunised mice at lower dilutions compared to the negative control, while there was no shift at higher dilutions. Therefore, due to the weak shift in MFI observed across all dilutions, the immunisation procedure was not pursued, and another immunisation method was required to obtain a highly specific anti- TSPAN32 antibody.

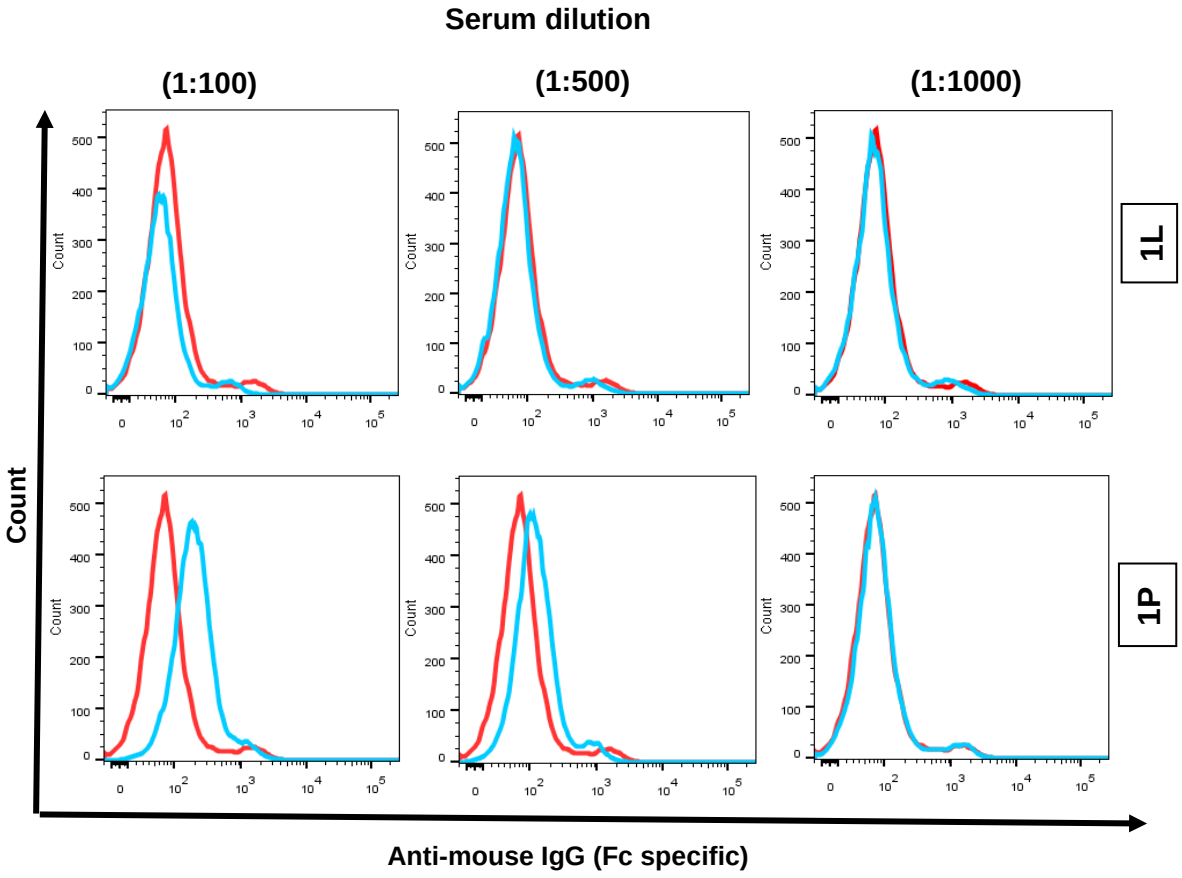

Figure 3. 7 1L and 1P mice IgG responses to TSPAN32 after IP boost.

TSPAN32 transfected NIH 3T3 cells (1x10^5 cells per well) were immunolabelled with 1L and 1P mice serum screening after the boost at serum dilutions 1/100,1/500, 1/1000, as presented in the histograms above. Then cells were incubated with secondary anti-mouse IgG Fc antibody to detect anti-TSPAN32 IgG antibodies within the mice sera. Red line represents the negative control (normal mouse serum before immunisations); the blue line represents mice sera after the boost.

3.2.3 TSPAN32 mice immunisation approaches: Immunising with plasma membrane glycolipid extraction

Immunisations with plasma membrane (PM) lipid extract is a novel immunisation method that has been successfully used by our colleagues in The University Of Nottingham Academic Oncology department to produce two mAbs (FG88.2 and FG88.7), recognising novel tumour-associated glycans with potent anti-tumour activity. [348] These mAbs were raised from mice immunised with PM lipid extract of COLO205 colorectal cancer cell line incorporated in liposomes as the immunogen formulation. Liposomes were used in these studies to immobilise antigens in order to protect them from degradation, creating the 'depot' effect as well as to help in antigen presentation. αGalCer was also incorporated in the liposomes as an adjuvant. αGalCer, a lipid extracted from marine sponge Agelas mauritianus, is a ligand for natural killer T-(NKT) cells. NKT cells are T-cells that express CD1d-restricted, lipid-specific T cell receptor. CD1d molecules are MHC-like molecules, expressed on APCs, that specialise in presenting lipid antigens to T-cells.[349] By incorporating both the lipid extracts and αGalCer in the liposomes, it is hypothesised that B-cell receptor would recognise the antigens presented on the liposomes and internalise them. Following that, B cells would process αGalCer and present it to NKT cells via CD1d molecules. Subsequently, activated NKT cells will provide help for B-cell activation, differentiation to plasma cells and eventually production of high titre specific antibodies. [350] This immunisation method was also used to develop functional anti-CD81 IgG antibodies. Hence, we decided to use a PM glycol-lipid extract of cells expressing TSPAN32 (activated T cells or TSPAN32 transfected NIH 3T3 cells) as an alternative immunisation method to gene gun immunisation to develop a mAb that recognises TSPAN32.

3.2.3.1 Immunising with plasma membrane glycolipid extraction of activated T cells

As previously mentioned, TSPAN32 is known to be restricted to hematopoietic cells, including T cells. The studies using TSPAN32 knockout mice suggest an immunoregulatory role of TSPAN32 on T cell proliferation similar to CTL-4 and PD-1.[320, 321] Therefore, we hypothesised that *in vitro* activation of T cells will increase the expression levels of TSPAN32, which will improve the chances to obtain an anti-TSPAN32 IgG response from mice immunised with PM glycolipid extract of these cells.

In this study, T cells were isolated from healthy donors and LRS cones, activated by anti-CD3 antibody and co-stimulated by anti-CD28 antibody for 48 hours. Flow cytometry dot plots in figure 3.8 A confirm that the majority of the isolated PBMCs used for the immunisations were T cells (CD8 and CD4) which also expresses CD69 and CD25 activation markers. Figure 3.8 B. represents the microscopic view of activated T-cells after 48 hours incubation with anti CD3/CD28 antibodies. These activated T cells were collected, and $1x10^8$ T cells were used to prepare PM lipid extract for each sample. The PM lipid extract was then incorporated into DOPC/DHP liposomes together with αGalCer as an adjuvant. Following sample preparations, three female BALB/c mice (2R, 2P and 2L) were bled to obtain the normal untreated serum, then they were immunised with the PM lipid extract of activated T cells via IP injection. Over 12 weeks, 2R, 2P and 2L mice were treated with six immunisations and boosted with TSPAN32 transfected NIH 3T3 cells. The immunisation scheme is shown in figure 3.8 C.

A

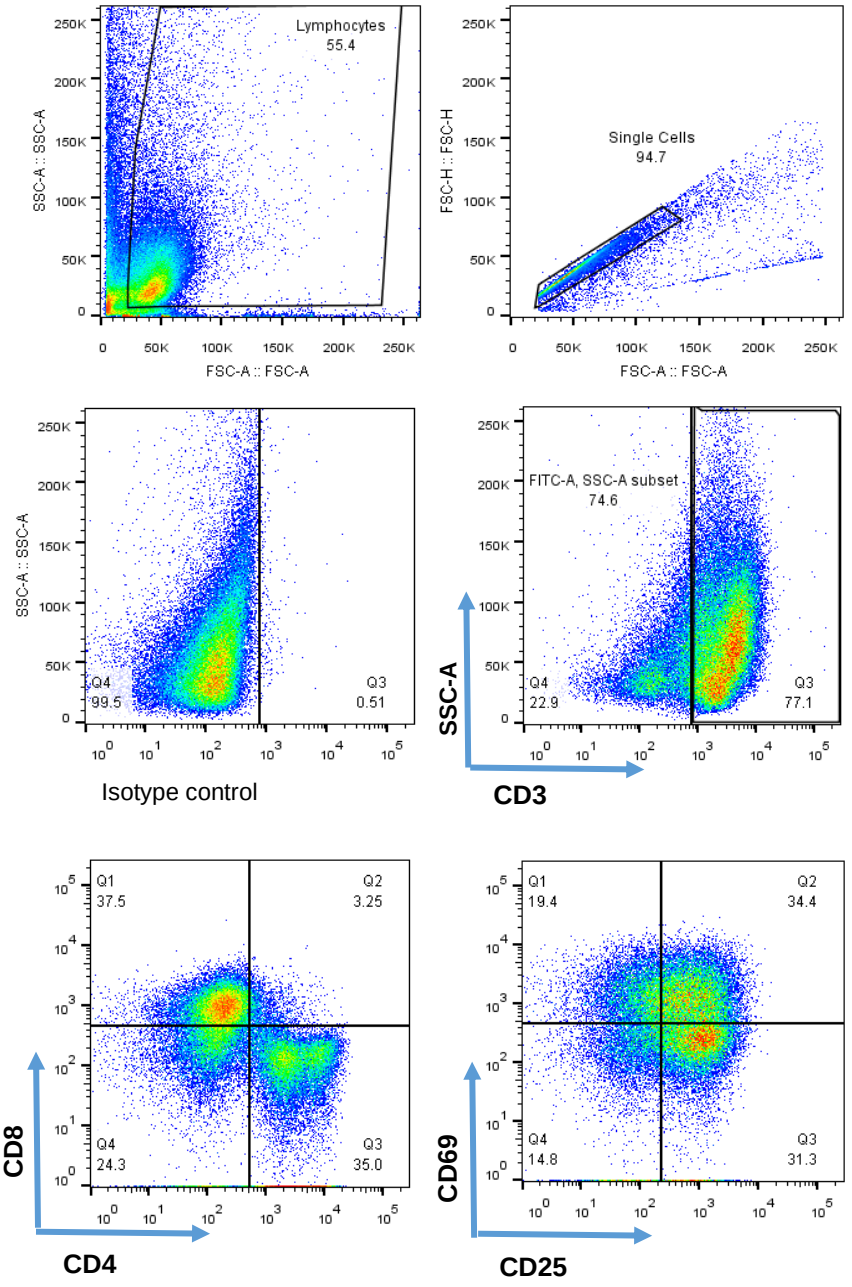
Lymphocytes
55.4
SSC-A :: SSC-A
FSC-A :: FSC-A
Single Cells
94.7
FSC-H :: FSC-H
FSC-A :: FSC-A
Q4
99.5
Q3
0.51
Isotype control
FITC-A, SSC-A subset
74.6
Q4
22.9
Q3
77.1
SSC-A
CD3
Q1
37.5
Q2
3.25
Q4
24.3
Q3
35.0
CD8
CD4
Q1
19.4
Q2
34.4
Q4
14.8
Q3
31.3
CD69
CD25

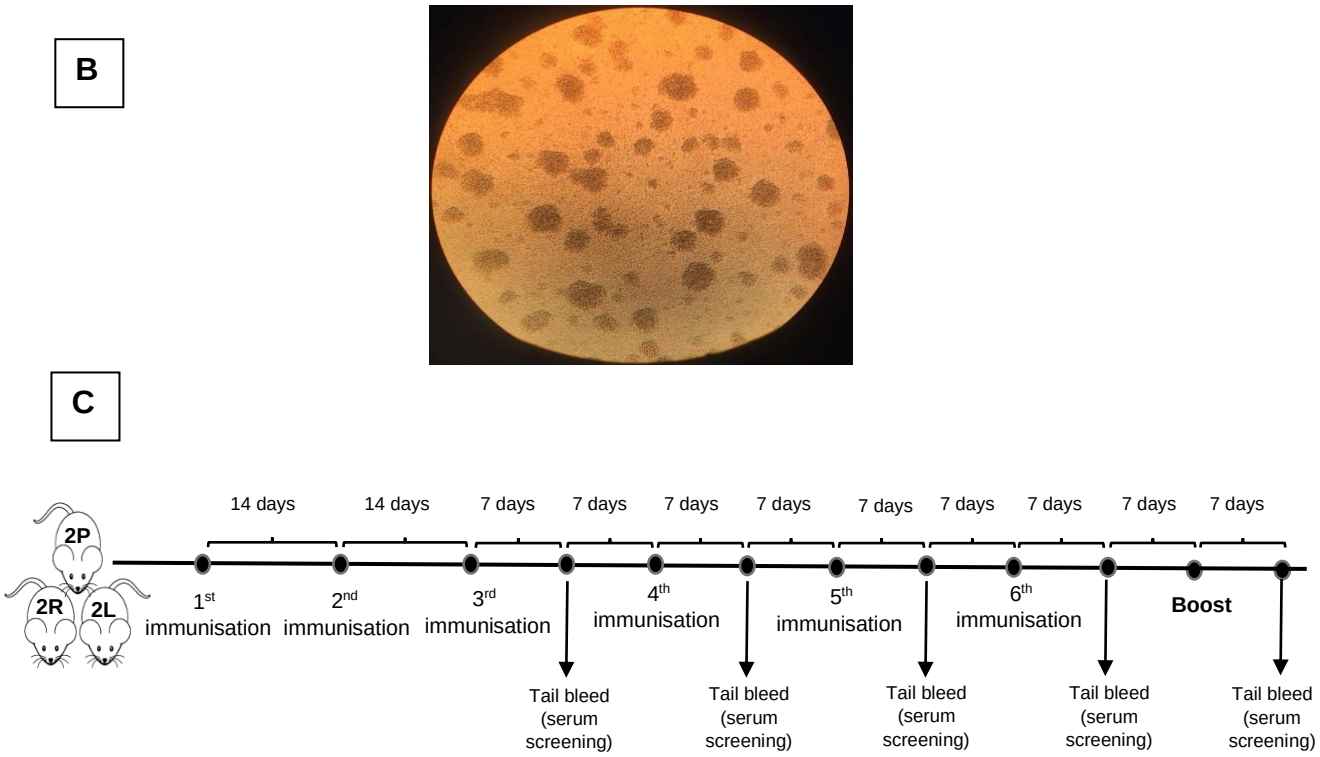

Figure 3. 8 Mice immunisation with PM glycolipid extract of activated T-cells.

(A) Dot plots represent the majority of PBMCs after activation (by anti-CD3/CD28 antibodies) for 48 hr are T-cells (CD4 and CD8) that express activation markers CD69 and CD25; **(B**) Microscopic view of activated T cells used to prepare PM glycolipid extract; **(C)**Immunisation scheme for 2R, 2P and 2L mice showing that mice were immunised six times with IP injection of PM glycolipid extraction of activated T cells and boosted with NIH 3T3 cells transfected with TSPAN32.

The PM lipid extraction of activated T cells was prepared and used to immunise mice via IP injection. The immunisation schedule is represented in table 3.2. The adjuvant αGalCer was incorporated with PM glycolipid extract for all the immunisations except the second immunisation due to its ability to aid B cell activation and differentiation into plasma cells needed to produce high antibody titres. For the second immunisation, we used anti-CD40 as the adjuvant to further enhance B cell maturation after the first immunisation. From the third immunisation onwards, mice were bled one week after each immunisation and sera were then screened for IgG (fc) binding to TSPAN 32 transfected NIH 3T3 cells by flow cytometry (figure 3.9 A).

Table 3. 2 Immunisation schedule of plasma membrane glycolipid extraction of activated T-cells for three mice [2R, 2P and 2L]. Mice were exposed to six immunisations of activated T cell pm glycolipid extract with the adjuvant, then boosted with NIH 3T3 cells transfected with TSPAN32 via IP injection.

(pm: plasma membrane; α-GalCer: alpha-galactosylceramide)

	Mouse 2R	**Mouse 2P**	**Mouse 2L**
1st immunisation	Activated T cell pm glycolipid extract ($1x10^8$) + α-GalCer	Activated T cell pm glycolipid extract ($1x10^8$) + α-GalCer	Activated T cell pm glycolipid extract ($1x10^8$) + α-GalCer
2nd Immunisation	Activated T cell pm glycolipid extract ($1x10^8$) + Anti-CD40	Activated T cell pm glycolipid extract ($1x10^8$) + Anti-CD40	Activated T cell pm glycolipid extract ($1x10^8$) + Anti-CD40
3rd immunisation	Activated T cell pm glycolipid extract ($1x10^8$) + α-GalCer	Activated T cell pm glycolipid extract ($1x10^8$) + α-GalCer	Activated T cell pm glycolipid extract ($1x10^8$) + α-GalCer
4th immunisation	Activated T cell pm glycolipid extract ($1x10^8$) + α-GalCer	Activated T cell pm glycolipid extract ($1x10^8$) + α-GalCer	Activated T cell pm glycolipid extract ($1x10^8$) + α-GalCer
5th immunisation	Activated T cell pm glycolipid extract ($1x10^8$) + α-GalCer	Activated T cell pm glycolipid extract ($1x10^8$) + α-GalCer	Activated T cell pm glycolipid extract ($1x10^8$) + α-GalCer
6th immunisation	Activated T cell pm glycolipid extract ($1x10^8$) + α-GalCer	Activated T cell pm glycolipid extract ($1x10^8$) + α-GalCer	Activated T cell pm glycolipid extract ($1x10^8$) + α-GalCer
Boost	-----	$1x\ 10^6$ of NIH 3T3 cells transfected with Tspan32 in 250ul PBS via I.P. injection	-----

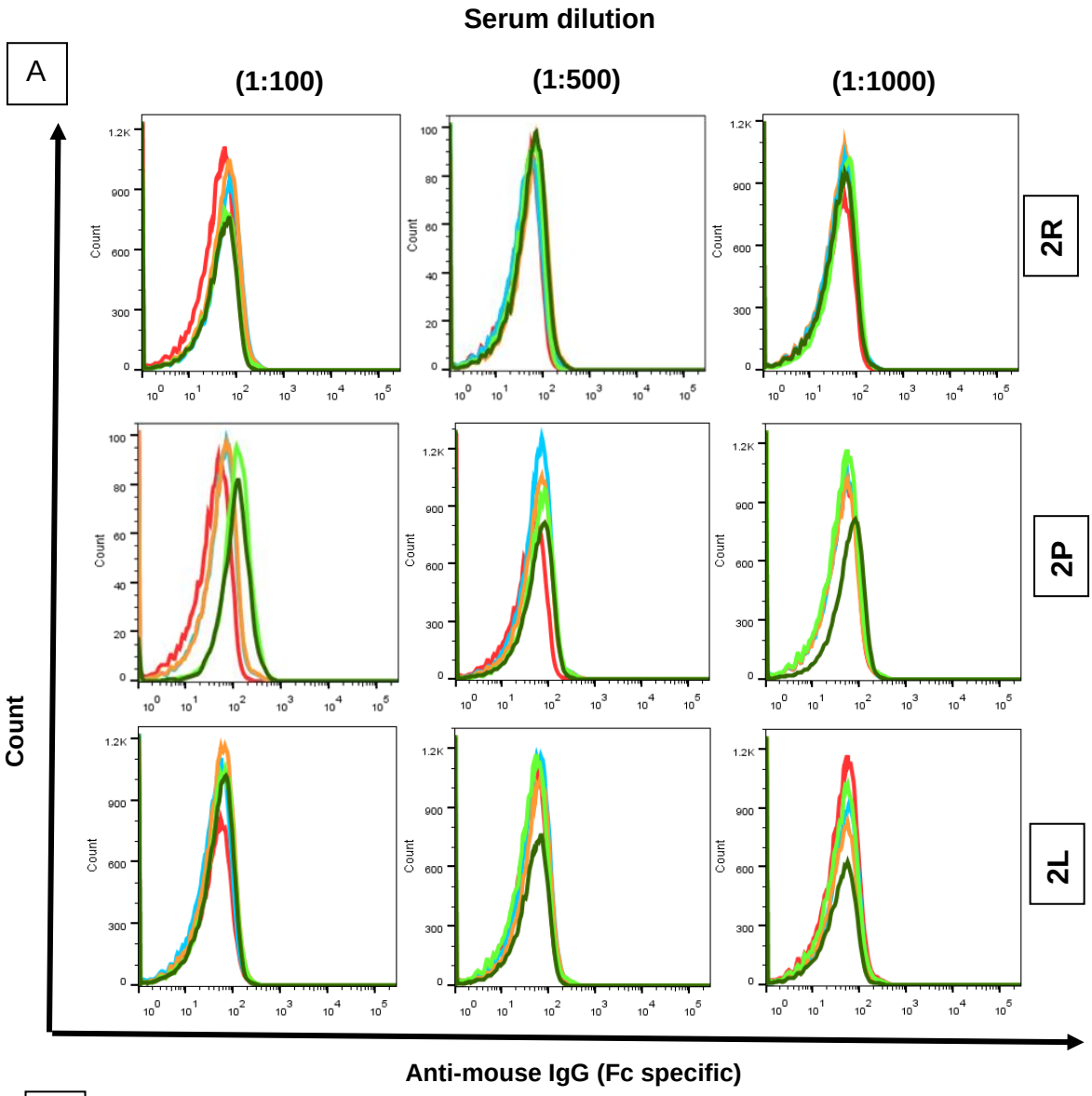

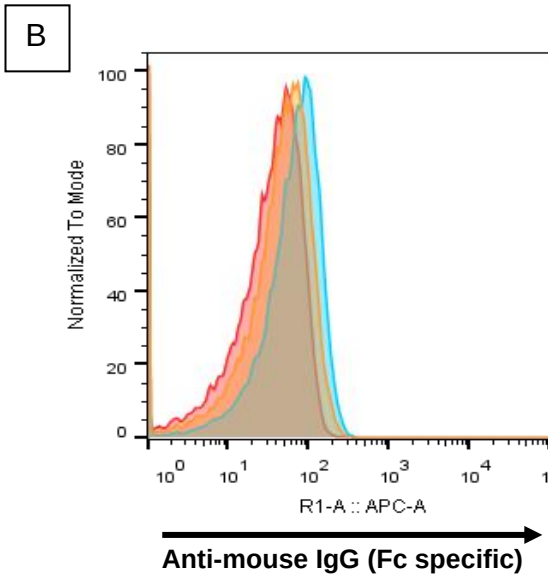

Subset Name		MFI
	TSPAN32 transfected NIH 3T3 cells incubated with 2P mouse serum after boost	41.6
	GFP only transfected NIH 3T3 cells incubated with 2P mouse serum after boost	64.5
	TSPAN32 transfected NIH 3T3 cells incubated with Normal untreated mouse serum (negative control)	24.4

Figure 3. 9 IgG responses to TSPAN32 transfected cells after mice immunisation with PM glycolipid extract from activated T cells.

(A) Histograms of mice 2R, 2P and 2L sera screened for the presence of IgG after the third (blue line), fourth (orange line), fifth (light green line) and sixth (dark green line) immunisations binding to TSPAN32 transfected cells compared to the negative control

(Normal untreated mouse serum; red line) ; **(B)** Histograms of 2P mouse serum screened for the presence of IgG after the boost (orange line) compared to the negative control (Normal untreated mouse serum; red line) binding to TSPAN32 transfected cells and GFP transfected cells (blue line)

Among all three mice, 2P mouse serum showed a slight increment of IgG levels after the sixth immunisation at 1/100 dilution compared to the negative control. Therefore, 2P mouse was boosted via IP injection with TSPAN32 transfected cells. Unfortunately, no significant difference in the MFI between the negative control and mouse serum after the boost was found. Hence, the procedure was terminated. (figure 3.9 B).

3.2.3.2 Immunising with plasma membrane glycolipid extraction from TSPAN32 transfected NIH 3T3 cells

The plasma membrane lipid extract of $5x10^7$ NIH 3T3 cells transfected with TSPAN32 was used to immunise 3R,3P and 3L mice. Six immunisations were performed, and mice sera were screened a week after the third, fourth, fifth and sixth immunisations. Immunisation scheme and schedule of 3R, 3P and 3L mice are shown in figure 3.10 and table 3.3, respectively. Upon serum screening for the immunised mice, 3P mouse showed a positive immune response at serum dilutions (1/100 and 1/500). The highest mouse IgG level was found after the sixth immunisation (figure 3.11 A). Based on these results, mice 3R and 3L were not pursued further. Mouse 3P was boosted with TSPAN32 transfected NIH 3T3 cells via IP injection.

Figure 3.11 B shows a considerable difference in the MFI between TSPAN32 transfected NIH 3T3 cells incubated with 3P negative control and the ones incubated with 3P mouse serum after the boost. Also, a significant mouse serum IgG binding was observed to TSPAN32 transfected NIH 3T3 cells compared to it's binding to GFP only transfected counterparts, indicating that 3P mouse serum IgG antibodies are

specific to TSPAN32. Following successful induction of an anti-TSPAN32 IgG immune response, the responding mouse (3P) was sacrificed, and its splenocytes fused for hybridoma generation.

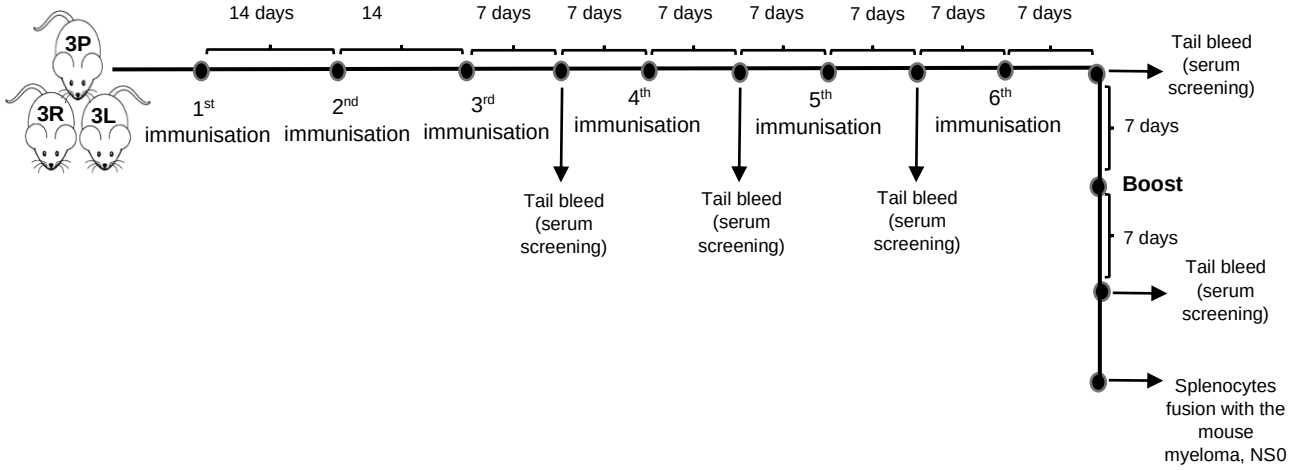

Figure 3. 10 Immunisation scheme for 3R, 3P and 3L mice with PM glycolipid extraction of TSPAN32 transfected NIH 3T3 cells.

The scheme shows that mice were immunised six times with IP injection of PM glycolipid extraction from TSPAN32 transfected NIH 3T3 cells and boosted with NIH 3T3 cells transfected with Tspan32. Mice were immunised every two weeks, and from the third immunisation onwards, mice were bled one week after each immunisation to determine the mice anti-TSPAN32 IgG response after each immunisation and the boost. Splenocytes from the boosted mouse with a positive anti-TSPAN32 IgG response were fused with mouse myeloma, NS0

Table 3. 3 Immunisation schedule of PM glycolipid extraction of TSPAN32 transfected NIH 3T3 cells for three mice [3R,3P and 3L]. Mice were exposed to six immunisations of TSPAN32 pm glycolipid extract with the adjuvant, then boosted with NIH 3T3 cells transfected with TSPAN32 via IP injection.

(PM: plasma membrane; α-GalCer: alpha-galactosylceramide)

	Mouse 3R	**Mouse 3P**	**Mouse 3L**
1st Immunisation	PM glycolipid extract of TSPAN32 trans. NIH cells ($5x10^7$) + α-GalCer	PM glycolipid extract of TSPAN32 trans. NIH cells ($5x10^7$) + α-GalCer	PM glycolipid extract of TSPAN32 trans. NIH cells ($5x10^7$) + α-GalCer
2nd immunisation	PM glycolipid extract of TSPAN32 trans. NIH cells ($5x10^7$) + Anti-CD40	PM glycolipid extract of TSPAN32 trans. NIH cells ($5x10^7$) + Anti-CD40	PM glycolipid extract of TSPAN32 trans. NIH cells ($5x10^7$) + Anti-CD40
3rd immunisation	PM glycolipid extract of TSPAN32 trans. NIH cells ($5x10^7$) + α-GalCer	PM glycolipid extract of TSPAN32 trans. NIH cells ($5x10^7$) + α-GalCer	PM glycolipid extract of TSPAN32 trans. NIH cells ($5x10^7$) + α-GalCer
4th immunisation	PM glycolipid extract of TSPAN32 trans. NIH cells ($5x10^7$) + Anti-CD40	PM glycolipid extract of TSPAN32 trans. NIH cells ($5x10^7$) + Anti-CD40	PM glycolipid extract of TSPAN32 trans. NIH cells ($5x10^7$) + Anti-CD40
5th immunisation	PM glycolipid extract of TSPAN32 trans. NIH cells ($5x10^7$) + α-GalCer	PM glycolipid extract of TSPAN32 trans. NIH cells ($5x10^7$) + α-GalCer	PM glycolipid extract of TSPAN32 trans. NIH cells ($5x10^7$) + α-GalCer
6th immunisation	PM glycolipid extract of TSPAN32 trans. NIH cells ($5x10^7$) + α-GalCer	PM glycolipid extract of TSPAN32 trans. NIH cells ($5x10^7$) + α-GalCer	PM glycolipid extract of TSPAN32 trans. NIH cells ($5x10^7$) + α-GalCer
Boost	-----	1x 10^6 of NIH 3T3 cells transfected with Tspan32 in 250ul PBS via I.P. injection	-----

A

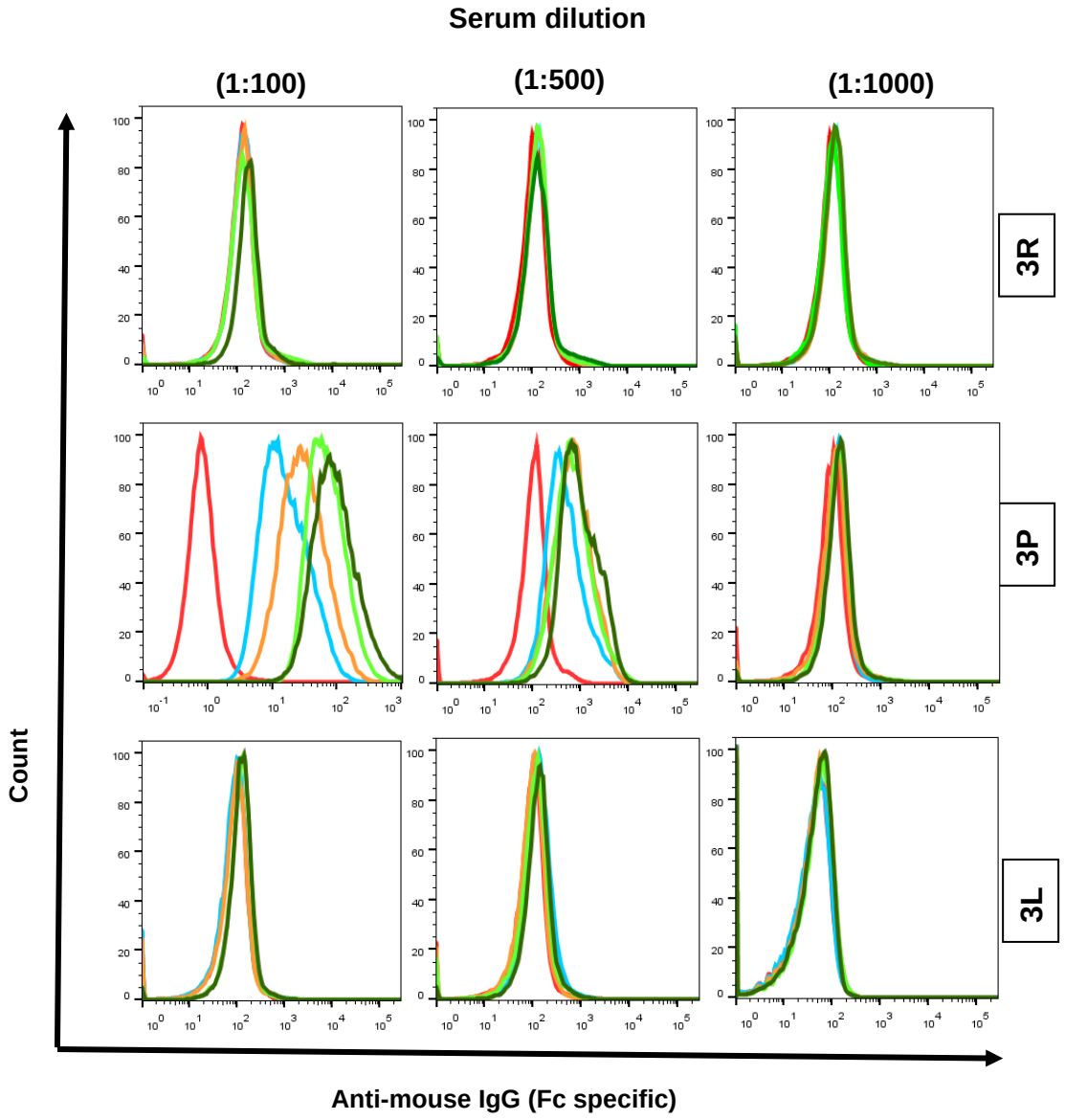

B

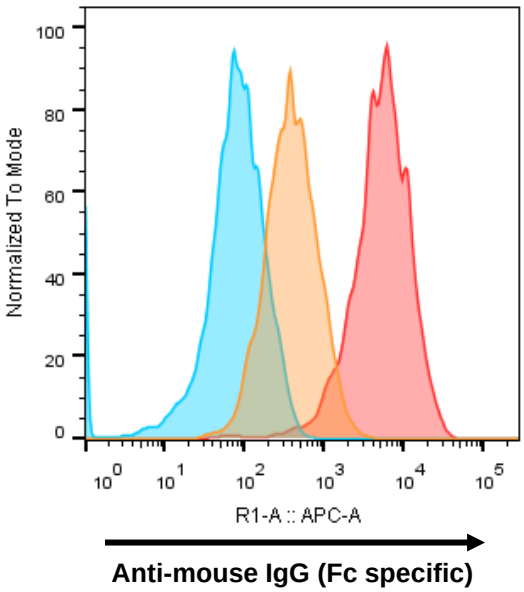

Subset Name	MFI
TSPAN32 transfected NIH 3T3 cells incubated with 3P mouse serum after boost	5232
GFP only transfected NIH 3T3 cells incubated with 3P mouse serum after boost	372
TSPAN32 transfected NIH 3T3 cells incubated with NMS of 3P mouse (negative control)	78.2

Figure 3. 11 IgG responses to TSPAN32 transfected cells after mice immunisation with PM glycolipid extract from TSPAN32 transfected NIH 3T3 cells.

(A) Histograms of mice 3R, 3P and 3L sera screened for the presence of IgG after the third (blue line), fourth (orange line), fifth (light green line) and sixth (dark green line) immunisations binding to TSPAN32 transfected cells compared to the negative control (Normal untreated mouse serum; red line) ; **(B**) Histograms of 3P mouse serum screened for the presence of IgG after the boost (red line) compared to the negative control (Normal untreated mouse serum; blue line) binding to TSPAN32 transfected cells and GFP transfected cells (orange line)

3.2.4 Assessment of hybridoma supernatants

For the purpose of developing mAb, splenocytes were isolated after the boost and fused with healthy NS0 myeloma cells to generate hybridoma. Following the first hybridoma screen, TSPAN32 transfected NIH 3T3 cells were stained with the supernatants of 188 hybridomas. Five hybridomas showed a positive IgG response to TSPAN32 transfected cells (figure 3.12 A and B). Hybridoma sample number 3, which had the best binding response, was single cloned into a 96- well plate while the rest of the hybridoma samples were stored. After two weeks of single cloning, four clones survived. Out of the four, three clones did not produce IgG specific to TSPAN32 transfected NIH 3T3 cells, while one clone was still producing specific IgG antibodies (figure 3.13 A). Unfortunately, the single positive clone was lost upon expanding it and was therefore not pursued further.

It should be noted that the single clone obtained from sample number 3 that was found to be producing IgG specific to TSPAN32 was selected using TSPAN32 transfected NIH 3T3. In order to confirm that the IgG produced by this single clone can recognise TSPAN32 expressed naturally on T cells, we treated activated T cells with the supernatant of the respective single clone (figure 3.13 B). Contrary to our expectations, no significant shift was observed on treating activated T cells with the supernatant of the positive clone.

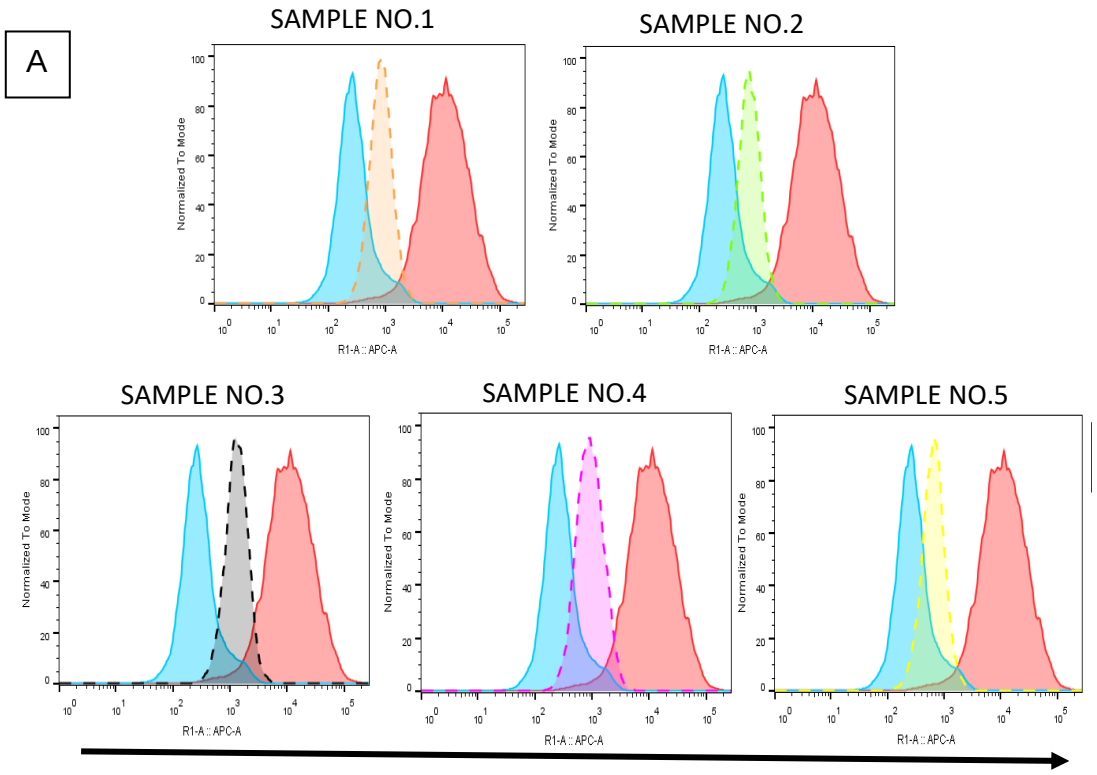

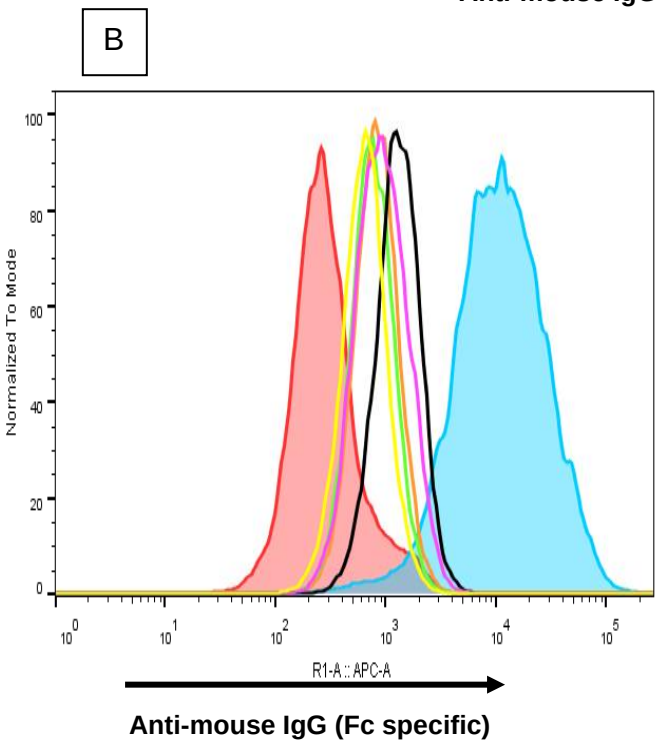

	Subset Name	MFI
	TSPAN32 transfected NIH 3T3 cells incubated with the supernatant of sample no.5	640
	TSPAN32 transfected NIH 3T3 cells incubated with the supernatant of sample no.4	897
	TSPAN32 transfected NIH 3T3 cells incubated with the supernatant of sample no.3	1285
	TSPAN32 transfected NIH 3T3 cells incubated with the supernatant of sample no.2	742
	TSPAN32 transfected NIH 3T3 cells incubated with the supernatant of sample no.1	818
	TSPAN32 transfected NIH 3T3 cells incubated with 3P mouse serum after boost	10834
	TSPAN32 transfected NIH 3T3 cells incubated with NMS of 3P mouse (negative control)	266

Figure 3. 12 Mouse 3P splenocytes fusion resulted in five hybridomas with positive IgG response to TSPAN32 transfected cells.

(A) Histograms of the supernatant of each hybridoma screened for the presence of anti-TSPAN32 IgG response compared to the negative control (normal untreated moue serum) and positive control (3P mouse serum after boost). **(B)** Histograms of the five hybridomas

together with the negative control and positive control to identify the hybridoma sample with the highest MFI shift compared to other hybridomas in order to use it for single-cell cloning procedure.

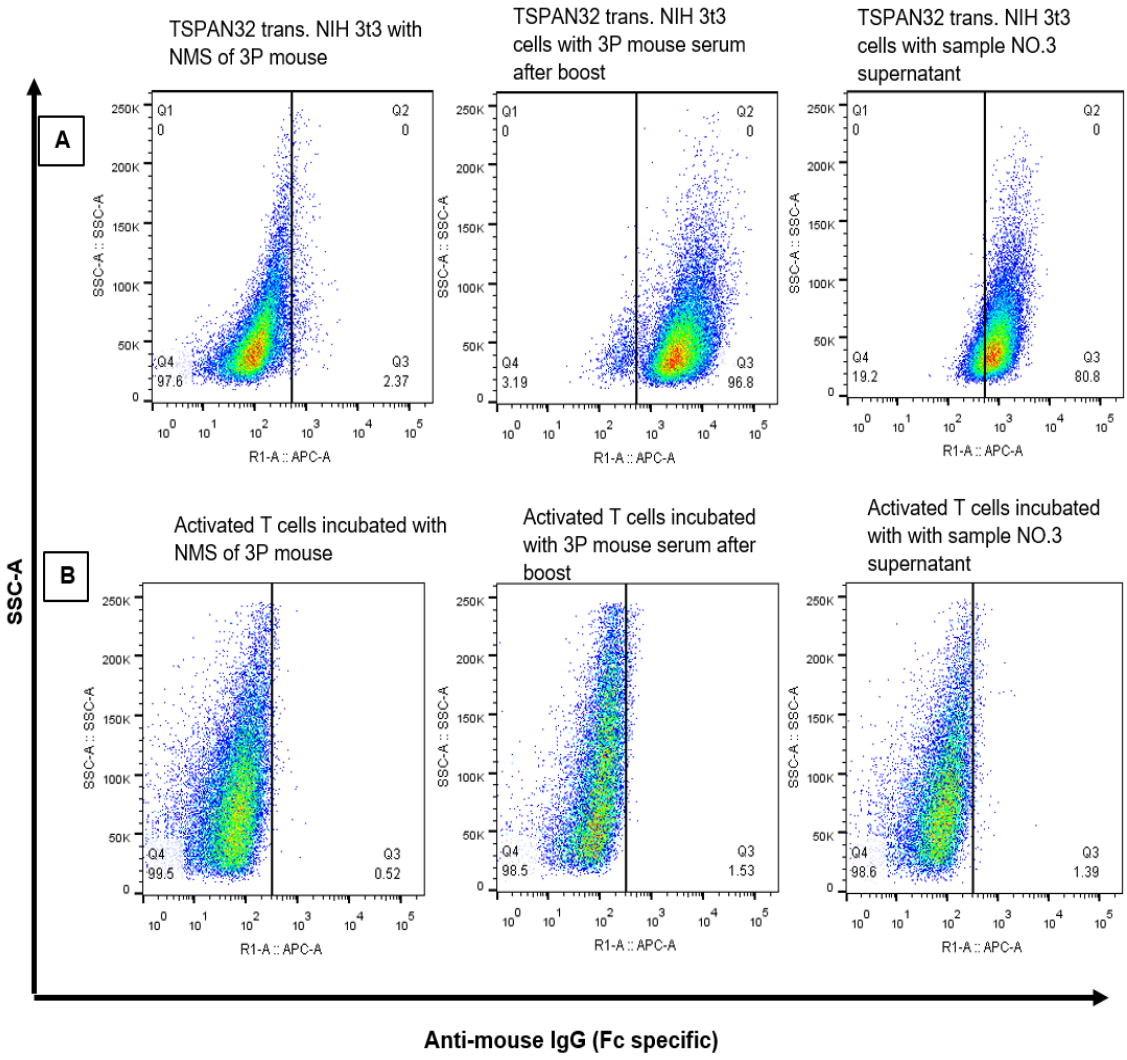

Figure 3. 13 Single-cell cloning of hybridoma no. 3 resulted in a single cell clone with positive IgG response to TSPAN32 .

Dot plots represent the binding of the supernatant from a single clone of sample no.3 with **(A)** TSPAN32 transfected NIH 3T3 and **(B)** activated T cells compared to the negative control and positive control (3P serum after boost).

3.3 Discussion:

Tetraspanins are cell membrane proteins that have been shown to be involved in regulatory actions within the immune system. The knockout mice of some tetraspanins resulted in the hyperproliferation of T cells, similar to effects seen in CTLA-4 and PD-1 KO mice. TSPAN32 is a member of tetraspanin superfamily. In a TSPAN32 KO mouse model, T cell activation was altered, indicating its role in the negative regulation of peripheral T-lymphocyte activation. In addition to that, the presence of TSPAN32 in high levels within T lymphocytes compared to other immune cells makes it a potential candidate to be a novel immune checkpoint. In this chapter, we have demonstrated three immunisation methods to develop a functional mAb against TSPAN32; Gene gun immunisation, immunisation with PM lipid extraction of activated T cells and immunisation with PM lipid extraction of TSPAN32 transfected NIH 3T3 cells. Among all immunisation approaches used, the most successful method involves the immunisation of mice with the purified extract of glycolipid enriched plasma membrane of NIH 3T3 cells transfected with TSPAN32. In contrast, DNA immunisation and the immunisation of PM lipid extraction of activated T cells did not yield an IgG response against TSPAN32. It is important to note that all the screening was done for IgG antibodies but not IgM , as IgG antibodies offer long and stable immunity, and their small size enables better infiltration into the tumour microenvironment.

Several studies have reported that antibody production against membrane proteins, including tetraspanin proteins, present unique difficulties due to the constrained three-dimensional presentation and limited solvent exposure of the available epitopes.[351, 352] However, successful attempts of developing a highly specific mAb to membrane proteins were reported using novel immunisation methods such as genetic immunisation[345, 346] and plasma membrane glycolipid immunisations.[353] In the present study, we have demonstrated that DNA- immunisation method was not

successful in producing anti-TSPAN32 antibody responses within the immunised mice. According to *Liu et al.*, many critical factors might affect the efficacy of the DNA immunisation technique, such as immunogen design, immunisation schedule delivery approach, the role of final boost immunisation and the use of immune modulators.[344] In this study, we have immunised mice with two bullets of DNA-gold nanocomplex in the abdominal area. In contrast, *Hansen et al.* have generated polyclonal antibodies for 17 membrane proteins expressed on two Biosafety Level 3 pathogens (*Francisella tularensis* and African swine fever virus) using a gene gun to immunise mice with two DNA-gold bullets through the ear skin.[354] The difference of the immunisation site might be a potential explanation why DNA immunisation was not effective to produce an immunogenic response to TSPAN32. However, there is yet no published data to compare the efficacy of antibody production or quality (e.g., affinity, specificity, or percent conformation-dependence) between the various DNA-based methods or using different immunisation sites (ear; abdomen; etc.).

Following the unsuccessful DNA immunisation, glycolipid from activated T cell PM was extracted and used for immunisation. The idea behind using this method of immunisation was that TSPAN32 is expressed naturally on T cells. The assumption that TSPAN32 was upregulated on T cell activation was based on studies that showed hyperproliferation of T cells in TSPAN32 knockout mice.[320, 321] However, PM lipid extract from active T cells did not result in a positive IgG response against TSPAN32. Interestingly, a recently published study by *Lombardo et al*.[355] showed that *in vitro* activation of T cells with anti-CD3/CD28 resulted in a downregulation of TSPAN32. This might explain the low IgG response observed in our study. The study by *Lombardo et al.* further went on to show that naïve T helper cells expressed higher levels of TSPAN32 compared to cytotoxic T cells.[355]These observations indicate that it might be beneficial to use PM glycolipid extract from naïve T cells to generate monoclonal IgG response specific to TSPAN32.

Though immunisation with PM glycolipid extract from activated T cells did not yield a positive TSPAN32 specific IgG response, immunisation with PM glycolipid extract from TSPAN32 transfected NIH 3T3 did yield a positive anti-tspan32 IgG response. Five hybridomas were obtained after the first screening process. Out of which one, sample number 3, was used further for single cloning. Out of the single clones obtained, only one single clone produced IgG specific to TSPAN32. This was confirmed using the supernatant of the single positive clone on TSPAN32 transfected NIH 3T3 cells. However, when the same supernatant was used to confirm this result on activated T cells, it did not yield a positive response. One of the reasons for this could be that activation of T cells resulted in downregulation of TSPAN32 expression, rendering them undetectable by the anti-TSPAN32 IgG antibodies present in the supernatant.

Furthermore, unpublished data shared kindly by Dr. Michael Tomlinson lab showed that tetraspanin mAbs generated using transient transfect cell lines, were unable to recognise or bind to the natural conformation of tetraspanins. They believe that overexpression of tetraspanins on transfected cells caused clustering of tetraspanins resulting in the generation of antibodies recognising only the clustered conformation of tetraspanins. These could be the possible explanations for the observation in figure 3.13. We recommend that the mAb developed against TSPAN32 be tested on naïve T cells and should be developed to recognise the native conformation on T cells. Developing a functional anti - TSPAN32 antibody would enable and support further studies looking at the immunoregulatory functions of TSPAN32.

Chapter 4: The prognostic role of tumour-infiltrating CD3+ and CD8+ T lymphocytes within different tumour regions

4.1 Introduction

The recent demonstration of the immune infiltrates characterisation (e.g. density, type, location within the tumour, phenotype and activation status) in patients treated with immunotherapy such as checkpoint blockade, could provide information to predict tumour progression and patient survival. [239, 356] Lymphocytes are located in specific areas within the tumour- microenvironment. For example, In non-small-cell lung cancer, colorectal cancer, head and neck cancers, T cells were found in the invasive margin and the tumour core. Whereas NK cells were distributed in the stroma, immature dendritic cells in the tumour core and B cells were mainly found in the invasive margin of growing tumours. [357, 358]

The density of intratumoral lymphocyte infiltrates in solid tumours is associated with good clinical outcome. High densities of CD3+ T cells and CD8+ cytotoxic T cells have been shown to be associated with prolonged disease-free survival. [237, 358, 359] In colorectal cancer, Simpson at el. [360] has previously published results showing that CD3+ T cells within the tumour nest and in the stromal region were significantly associated with improved prognoses. The role of CD8+T cells was examined on 133 CRC patients. The findings indicated that higher proliferative activity of CD8+ T cells was observed within cancer cell nests and that intratumoral CD8+TILs have a positive prognostic value in colorectal cancer. [236]

In 2006, Galon and colleagues investigated the relationship between the clinical outcome of CRC patients and the immune contexture (analysis of the functional orientation, location and density) of total T lymphocytes, CD8 T cell effector and

memory T cells (CD45RO) within the centre of the tumour (CT) and the invasive margin (IM). [239] The observations of the study showed a higher number of CD3+, CD8+ and CD45RO T cells within both CT and IM regions in patients without tumour recurrence in comparison with patients whose tumours had recurred. Moreover, a better prediction of patient survival was reported when the combined analysis of CT and IM [High density in CT and IM (HiHi) vs Low density in both regions (LoLo)] was used as compared to single region analysis (Hi vs Lo). [239, 240, 358]

In continuance with the above findings, Kirilovsky et al. have developed a prognostic score (Immunoscore) which depends on the distribution of CD3+ lymphocytes and CD8+ cytotoxic T cell density in the centre and invasive margin of the tumour. Patients were categorised from (I0 to I4) depending on the Immunoscore. [241, 361] For example, I0 refers to a tumour with low densities of CD3+ and CD8+ cells in CT and IM regions. I1, I2, I3 refers to tumours with one, two and three high densities, respectively. Whereas, patients with high densities of CD3 and CD8 in both tumour regions is classified I4. The results of this study concluded that patients' clinical outcome in terms of overall survival (OS) and disease-free survival (DFS), were significantly associated with the density and distribution of CD3+T cells and CD8+T cells in two tumour regions (CT and IM). Moreover, better clinical outcomes were observed with patients who had high immune cell density in both tumour regions (I4) compared to patients with (I3, I2, I1 or I0) Immunoscore. [356]

In addition to CRC, the prognostic value of the Immunoscore was significant and independent from other prognostic parameters in hepatocellular carcinoma and brain metastasis. [362, 363] Consequently, these initiatives will permit the implementation of the Immunoscore as a prerequisite necessary to use in a clinical setting to obtain an accurate prediction of a patient's prognosis and clinical response.

The importance of the distribution and location of T cell densities was further studied in a small cohort of CRCs patients with liver metastases. Detailed analysis of CD3+

cells, CD8+ cells and cytotoxic Granzyme B densities within different distance classes between the border of the tumour and adjacent normal tissue were performed. The findings of this study emphasised the localisation-dependent prognostic relevance of CD3+ and CD8+T cells, where a significant association of high cell densities and prolonged OS was observed in the proximal distance class (< 10 mm from tumour border). In contrast, no significant differences between high and low T cell infiltrates were found in other classes closer to the normal adjacent liver than tumour epithelium. [364]

Although many studies have been conducted to identify the proportion, distribution and function of different immune cells types in CT and IM regions of the tumour [242, 356, 365, 366] and distant metastasis [367] in colorectal cancer, the immune contexture of luminal side of the tumour (LS) and the adjacent normal tissue were yet unclear. In this study, the density of CD3+ cells, and CD8+ cells were quantified in three regions of the tumour (LS, CT and IM) and the adjacent normal tissue by using a validated image analysis workstation after immunostaining with specific antibodies to get a comprehensive evaluation of CD3+ and CD8+ T cells spatial heterogeneity within the tumour microenvironment and its clinical implication. It was hypothesised that the density of CD3+T cells and CD8+T cells in the LS of the tumour would have a prognostic value in colorectal cancer patients similar to CT and IM of the tumour. Thus, adding the information of immune cells proportion in LS into the combined regional analysis along with CT and IM will improve the prediction of patients' survival. Also, it was thought that CD3+ and CD8+T cells in the adjacent normal tissue of the tumour would function differently in comparison to the ones that exist or are in direct contact with tumour cells

4.2 Results:

4.2.1 Patient characteristics

The study cohort (Cohort 1) comprised 1000 cases of primary invasive CRC tissue. Samples were randomly selected in chronological order (year 2008 –2012). From each case, 3 cores of different regions of the tumour and one core from the adjacent normal epithelium (see figure 4.1) were collected to build a tissue microarray (TMA) with 4000 cores.

The patient cohort consisted of 568 men (57%) and 432 women (43%). The median age was 69 years (range 16-94). The mean follow-up period was 53.6 months. All cases were adenocarcinoma, and 89% were of moderate histological grade. (see table 4.1). Sixteen per cent of the patient cohort were TNM stage I, 40% were stage II, 32% were stage III, and 12% were TNM stage IV, comparable with previously published national numbers. [368, 369]

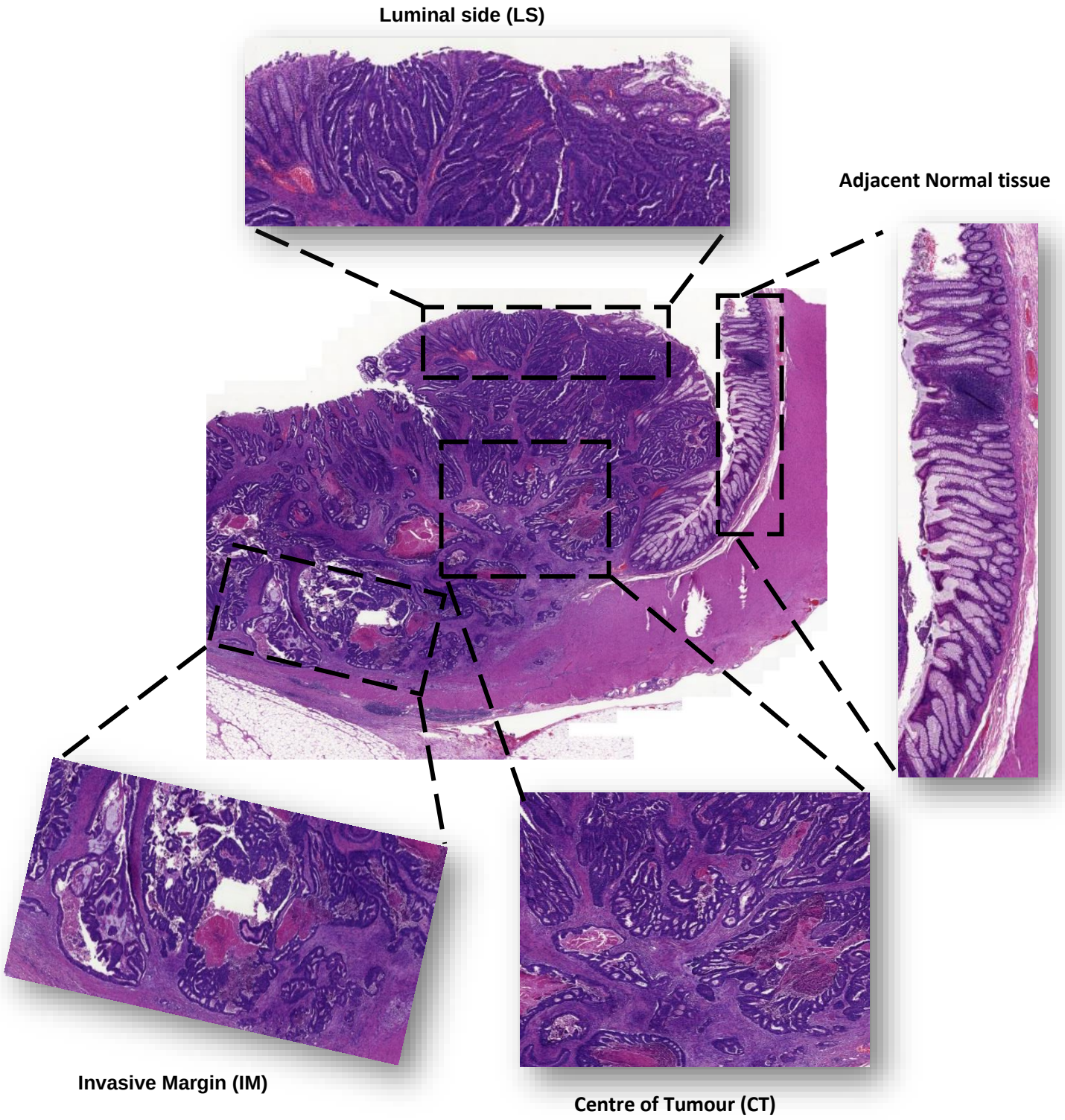

Figure 4. 1 TMA construction consisted of three Colorectal tumour regions.

LS is selected from the nearest area to the lumen; CT is selected from the middle area between the lumen and the edge of the tumour; IM is selected from the deepest area of the tumour, and adjacent normal tissue were collected from each case.

At the time of censoring for data analysis, 62% were alive, 18% of patients had died from cancer, and 20% had died from other causes. Evidence of extramural vascular invasion was documented in 49% of all tumours. Among all the clinicopathological parameters scored, tumour stage, nodal status, grade, the absence or presence of vascular invasion had a strongly significant influence on survival. The prognostic value of these factors is consistent with our previously published data. [360, 370]

Table 4. 1 Summary of the clinicopathological characteristics of the patient cohort (1). The correlation of the Clinic-pathological parameters such as sex, age, N -Regional lymph nodes, metastases, primary tumour location, TNM stage, extramural vascular invasion and microsatellite status, and the patient's survival. The log-rank test was used to test for significance. p- values <0.05 were considered statistically significant.

Clinic-pathological parameters		N (%)	Mean (DSS) months	SE	95% confidence interval		Survival distribution (Log Rank- Mantel cox) of overall colorectal patients	
					Lower	Upper	Chi-Square	P-value
Sex	Male	568 (56.8%)	99.9	1.861	92.9	100.2	1.51	0.219
	Female	432 (43.2%)	96.6	1.853	96.3	103.6		
	Overall	1000 (100%)	101.2	1.39	98.5	104		
Age	(≤69)	489	101.2	1.91	97.48	104.9	0.004	0.95
	(>69)	511	96.65	1.88	92.98	100.3		
	Overall	1000	101.2	1.39	98.51	103.9		
N -Regional lymph nodes	N0 (no lymph node metastasis)	570 (58.5%)	106.8	1.23	104.4	109.2	103.35	**<0.001**
	N1 (Regional lymph node metastasis)	405 (41.5%)	78.79	2.36	74.18	83.42		

	Overall	975 (100%)	96.26	1.313	93.69	98.83		
Metastases (M)	**M0 (no distant metastasis)**	881 (88.1%)	107.6	1.28	105.05	110.07	272.73	**<0.001**
	M1 (Distant metastasis)	119 (11.9%)	45.3	4.037	37.4	53.22		
	Overall	1000 (100%)	101.24	1.39	98.51	103.97		
Site of primary tumour	**Right colon**	461 (46.1%)	93.07	1.87	89.41	96.74	3.995	0.262
	Left colon	363 (36.3%)	99.53	2.33	94.95	104.117		
	Rectal	147 (14.7%)	98.02	2.76	92.61	103.44		
	Unknown	29 (2.9%)	103.82	5.08	93.85	113.8		
	Overall	1000 (100%)	101.24	1.39	98.51	103.97		
TNM stage	**I**	161 (16.1%)	119.2	1.28	116.7	121.7	307.781	**<0.001**
	II	402 (40.2%)	103.7	1.41	100.9	106.5		
	III	319 (31.9%)	88.8	2.36	84.15	93.43		
	IV	118 (11.8)	45.4	4.08	37.43	53.45		
	Overall	1000 (100%)	101.24	1.39	98.51	103.9		
Extramural vascular invasion	**Absence**	502 (50.9%)	110.9	1.48	108.0	113.8	56.655	**<0.001**
	Present	483 (49%)	84.1	2.07	80.13	88.3		
	Overall	985 (100%)	101	1.404	98.32	103.8		
Microsatellite status	**Microsatellite stable (MSS)**	818	100.6	1.54	97.59	103.6	2.082	0.149
	Microsatellite instable (MSI)	160	95.07	2.66	89.85	100.2		
	Overall	978	101.5	1.398	98.75	104.2		

4.2.2 CD3+ and CD8+ T lymphocytes expression and scoring in colorectal tumours.

Immunohistochemical staining of CD3 and CD8 biomarkers was conducted on 4000 colorectal TMA cores. Examples of cores with high and low CD3 and CD8 expression are shown in figure 4.2. The distribution of CD3+ and CD8+ T cell expression differs from case to case. Figure 4.2 A and B represent high intratumoral and stromal CD3+ and CD8+ Tcell densities, respectively. Furthermore, figure 4.3 C and D represent low intratumoral and stromal CD3+ and CD8+ Tcell densities, respectively.

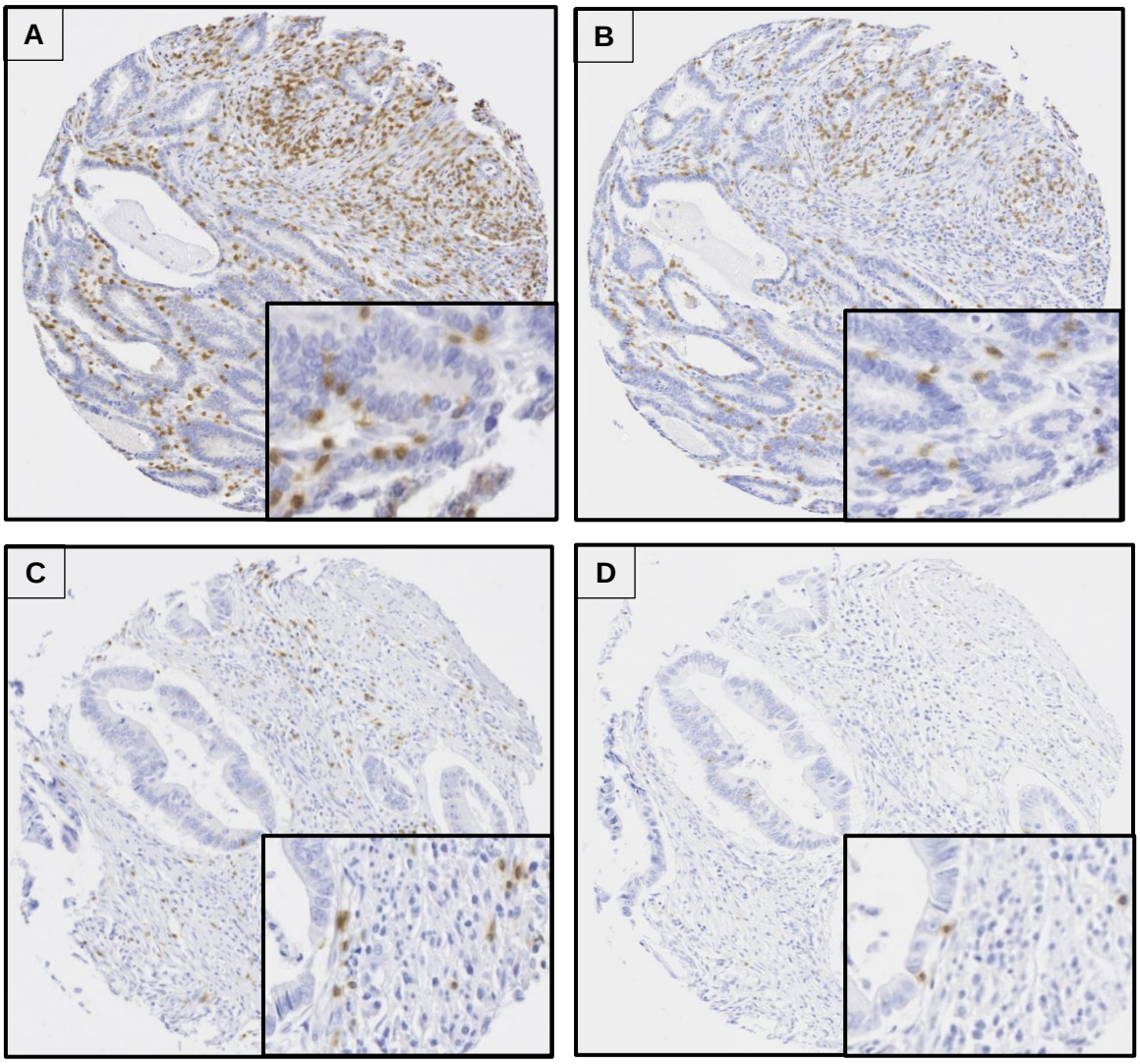

Figure 4. 2 Colorectal TMA cores stained with CD3 and CD8 biomarkers.

(A) Core with high CD3+ density**; (B)** Core with high CD8+ density**; (C)** Core with Low CD3+ density; **(D)** Core with Low CD8+ density. All ×100 original magnification (insets ×400 magnification)

Moreover, CD3+ and CD8+T cell numbers were counted per area of tumour seen in each core using the following formula, which we used in a previously published study [360] :

- T cell density = $\frac{\text{Total number of T cells}}{\text{Total size of the area (mm2)}}$

Intratumoral CD3+ and CD8+ Tcell densities were calculated by counting the total number of the positive cells in the area selected with blue (tumour) [shown in figure 4.3], then divided on the total size of that area. In contrast, stromal CD3+ and CD8+ T cell densities were calculated by counting the total number of the positive cells between the red (core outline) and blue areas then divided on the size of the stromal area (total size of the core minus size of the tumour). The scoring procedure was performed using an automated image analysis software (HALO®) due to the large size of our cohort (1000 patients, 4000 cores).

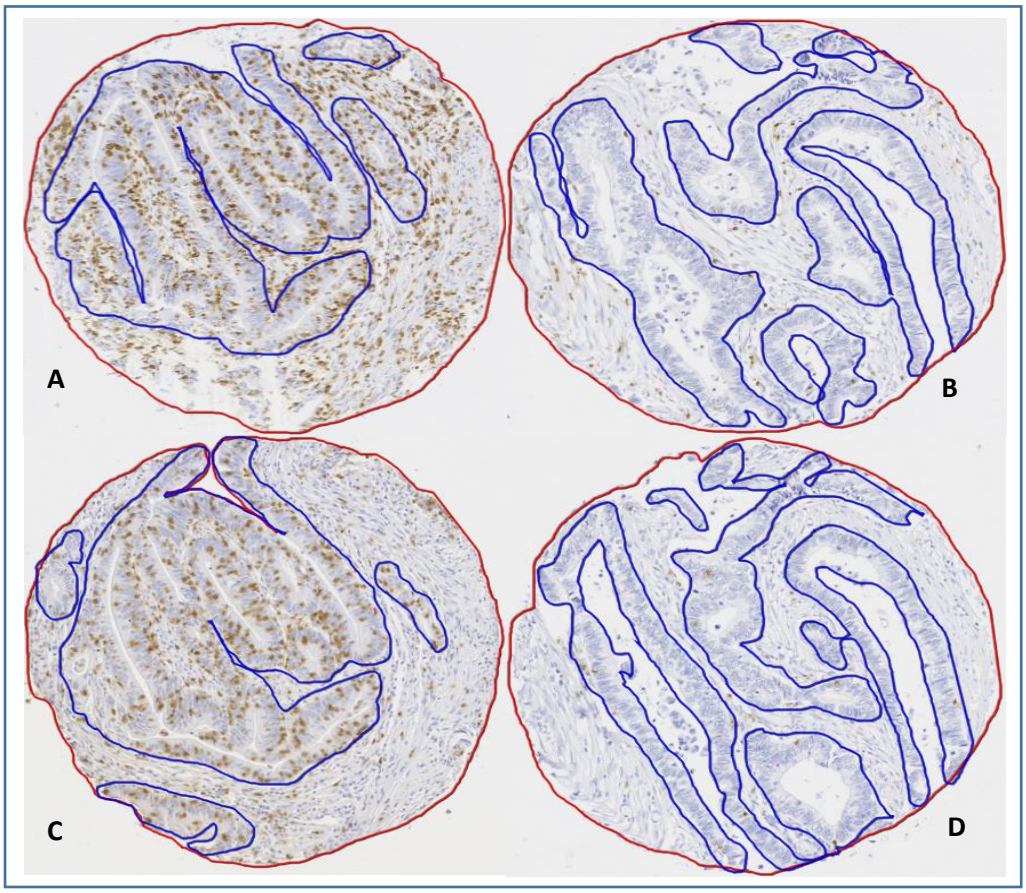

Figure 4. 3 CD3 and CD8 immunohistochemical staining of FFPE colorectal cancer cores using the ABC method.

Blue indicates specific tumour area; Red indicates total core areas. Cells within the tumour area (blue) are considered intratumoral. All other cells were counted as stromal. **(A)** Core with high intratumoral CD3+T cell level; **(B)** core with low intratumoral CD3+ T cell level; **(C)** Core with high intratumoral CD8+ T cell level; **(D)** core with low intratumoral CD8+ T cell level.

4.2.3 Training and validating digital image analysis software to count positive cells in different tissue segments

New digital pathology approaches have been adopted in recent years to replace conventional time-consuming manual scoring methods. Many studies utilised and validated HALO® software as a high-throughput and quantitative tissue analysis tool [371, 372, 373, 374]. In this study, HALO software was used to determine immune cell densities by classifying different tissue segments (tumour and stroma), and

automatically counting the number of positive cells within each distinct area and the size of that area. HALO® Tissue Classifier procedure is shown in figure 4.4. Tissue segmentation was performed using a machine learning algorithm based on texture, colour and contextual features of each segment. The software generates reports summarising the information (tissue types, number of positively stained cells, area size, etc.) of each core. Software training and generating data were kindly performed by Aušrinė Nestarenkait and Arvydas Laurinavičius from Vilnius University in Lithuania.

We manually scored 670 cores out of 4000 to validate HALO® scoring results. Intratumoral CD3+ and CD8+ T cell counts from both methods (manual and HALO®) were compared using Bland-Altman plots (Figure 4.5 A). These plots showed that there was no significant difference ($p > 0.05$) between zero and the mean difference of the two measurements for intraepithelial CD3, stromal CD3, intraepithelial CD8 and stromal CD8. The agreement bais with 95% confidence intervals (bais, SD±1.96) for intraepithelial CD3, Stromal CD3, intraepithelial CD8 and Stromal CD8 were [-1.405, (-7213,+69.32)], [-36, (-219.6,+146.4)], [- 1.129, (-27,+25.32)] and [-9.7, (-78.38,+58.96)], respectively. Also, we used Pearson correlation and linear regression plots (Figure 4.5.B) and found a significant positive correlation (Pearson, r > zero) between the manual scoring and HALO® scores for intraepithelial and stromal CD3+ and CD8+ T cells ($P<0.0001$).

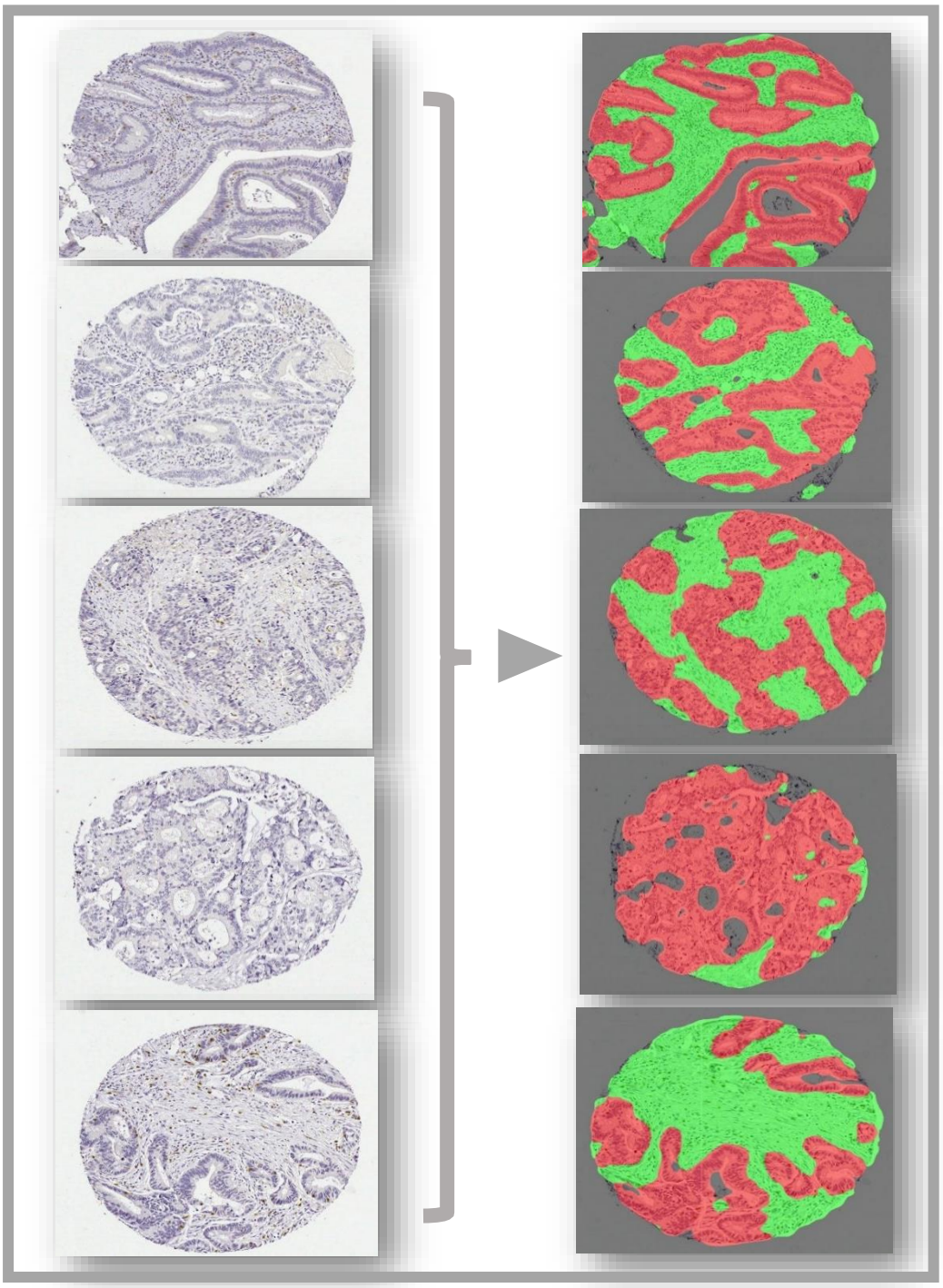

Figure 4. 4 Colorectal TMA cores classified using HALO® Tissue Classifier into three areas.

Red – tumour; green – stroma; black – background. Tissue types identification was based on texture, colour and contextual features. HALO software was trained to automatically count the number of positive cells within each distinct area and the size of that area.

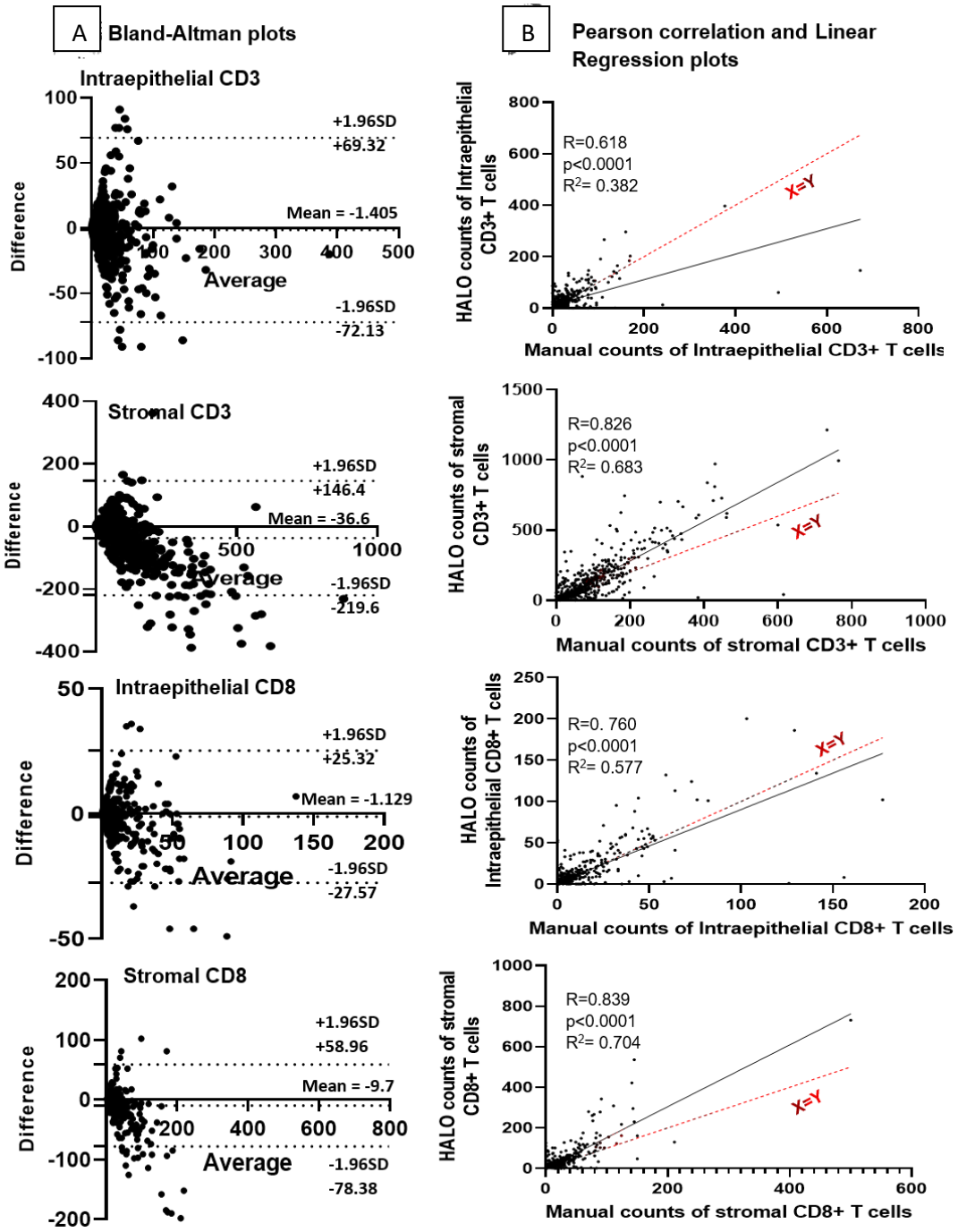

Figure 4. 5 Evaluation of the agreement between HALO and manual scoring methods using

(A) Bland-Altman plots with 95% confidence intervals on the limits of agreement and **(B)** Pearson correlation and linear regression plots for intraepithelial CD3, stromal CD3, intraepithelial CD8 and stromal CD8 manual counts vs HALO counts. R represents Pearson correlation co-efficient; p value <0.05 (shows a significant difference between zero and r) ; R2 (co-efficient of determination) evaluates the scatter of the data points around the fitted regression line (red dotted line).

4.2.4 Data distribution of CD3+ and CD8+ T cell densities in different tumour locations

Normality distribution tests were conducted to choose the most appropriate statistical analysis tests accordingly. We tested eight variables (Intratumoral CD3+ T cells and intratumoral CD8+ T cells in LS, CT, IM and adjacent normal tissue). A summary of normality distribution tests is shown in table 4.2. Z-values of Skewness and Kurtosis tests were more than 1.96, which indicates the data differ significantly from normality. [375] Shapiro-Wilk's test with p values <0.05 for all variables and the visual inspection of their histograms (figure 4.6) showed that intratumoral CD3+ and CD8+Tcell densities in LS, CT, IM and adjacent normal tissue were non-normally distributed (Skewed distribution).

Table 4. 2 Normality distribution tests of intratumoral CD3+ and CD8+T cells in LS, CT, IM and adjacent normal tissue. Skewness, Kurtosis and Shapiro-Wilk's tests were used to identify the normality of the distribution. Z-values >1.96 and p values <0.05 indicates that the data differ significantly from normality (non-normal distribution).

	Tumour region	**skewness**			**Kurtosis**			**Shapiro-Wilk**	
		statistics	Std. error	z-vlaue	statistics	Std. error	z-vlaue	statistics	Sig.
Intratumoral CD3+ T cells	**LS**	3.822	.085	44.9	22.269	.17	130.9	.617	<.001
	CT	4.475	.086	52.03	32.251	.171	188.6	.574	<.001
	IM	4.383	.085	51.6	25.849	.171	151.1	.553	<.001
	Adjacent normal tissue	9.043	.085	106.4	138.763	.17	816.2	.494	<.001
Intratumoral CD8+ T cells	**LS**	3.659	.083	44.08	16.323	.167	97.7	.553	<.001
	CT	4.091	.085	48.12	20.322	.17	119.5	.510	<.001
	IM	5.123	.085	60.27	34.883	.17	205.1	.454	<.001
	Adjacent normal tissue	3.733	.088	42.4	20.742	.176	117.8	.661	<.001

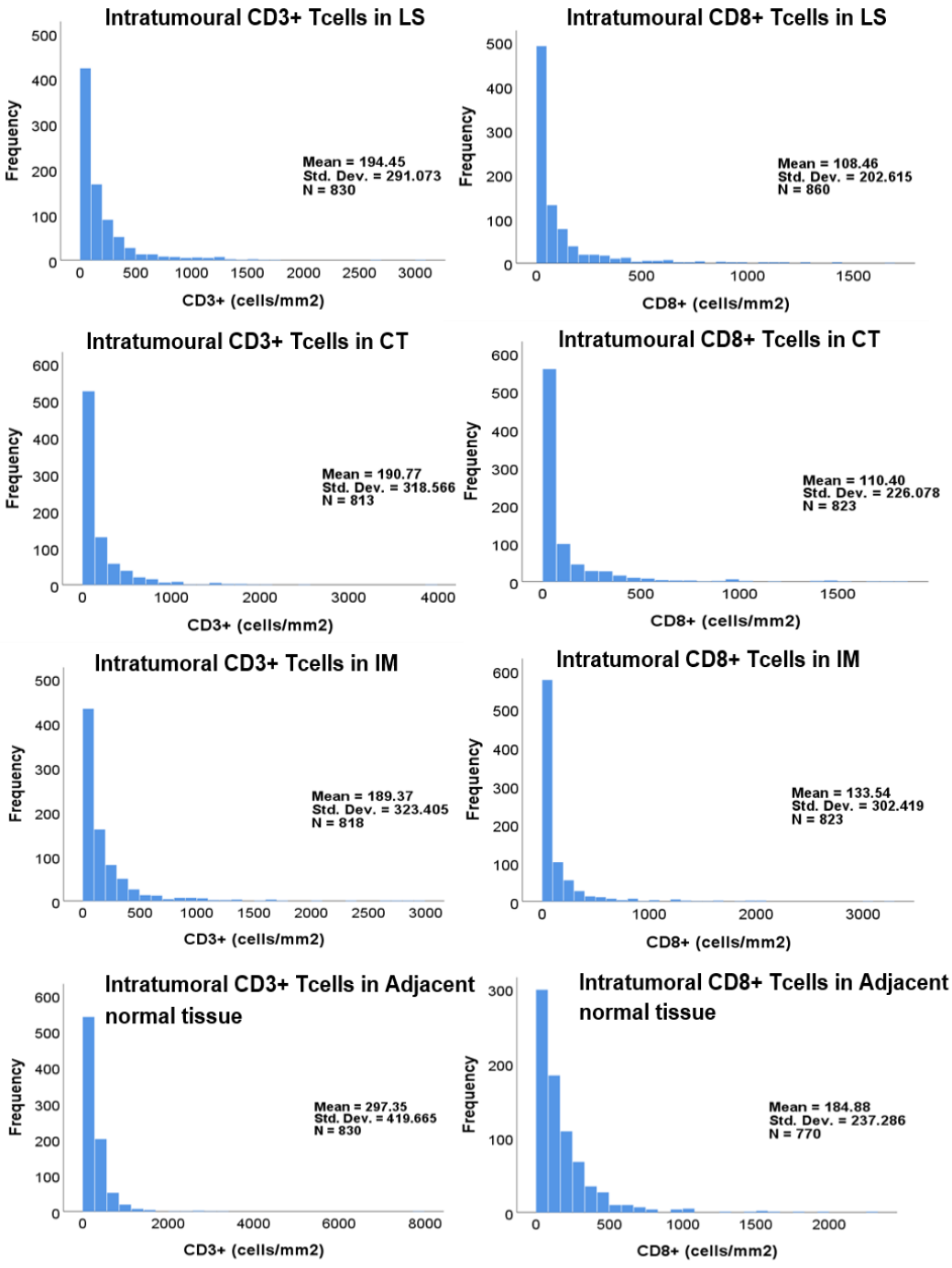

Figure 4. 6 Positively skewed histograms of intratumoral CD3+ and intratumoral CD8+ T cell densities in LS, CT, IM and Adjacent normal tissue.

4.2.5 Survival prediction of intraepithelial and stromal CD3+ and CD8+ T cells within three different tumour regions and adjacent normal tissue

The prognostic value of tissue infiltrating CD3+ and CD8+T cells in the tumour nest and stroma has been previously reported in CRCs patients. [236, 360] Moreover, Galon et al.[239, 366] performed a single regional analysis in two tumour regions (CT and IM) for CD3+ and CD8+ T cells each separately. They observed that high CD3+ or CD8+ T cell levels in either tumour region were associated with better patient survival rates. In continuous with these findings, the research of CD3+ lymphocytes heterogeneity, distribution and functional impact within the tumour was expanded in this study by performing a single regional analysis of CD3+ and CD8+T cell densities in LS, CT and IM tumour regions and the adjacent normal tissue from each patient. Similar to Galon et al.[239] and Anitei at el.[366], the minimum p-value approach was applied to obtain the cut-off points which give the best separation between the groups of patients (low vs. high) related to their disease-free survival outcome. The cut-off points for CD3+ and CD8+cell densities for LS, CT, IM and the adjacent normal tissue were estimated and used to divide patients into low and high groups of CD3+ and CD8+ infiltration. The expression of intraepithelial and stromal CD3+ and CD8+ lymphocytes in all regions, the number of patients in each group, mean survival data and cut-off values are summarised in table 4.3 and table 4.4.

Kaplan-Meier plots and the log-rank p-values in figure 4.7 and 4.8 show that the presence of high intraepithelial or stromal CD3+ cells or CD8+ T cell levels in LS, CT and IM regions correlate with improved disease-specific survival compared with low levels (P-values <0.05 were considered statistically significant). In contrast, no significant difference between high and low CD3+ or CD8+ cell infiltration were observed in the adjacent normal tissue.

Table 4. 3 Expression level of intraepithelial and stromal CD3+ T cells in LS, CT, IM and Adjacent normal tissue with mean survival (months) and cut-off values for all patient groups. CRC patients were categorised into high and low-density groups according to the cut off points of CD3 T cell density in each tumour location. [DSS: Disease-specific survival]

		Expression	Number	Mean DSS (Months)	Mean survival difference (Months)	Cut off point (cells/mm2)
LS	Intraepithelial CD3+ T cells	Low	89	79.3	24.5	<=8.9
		High	741	103.8		
	Stromal CD3+ T cells	Low	493	98.9	3	<=814
		High	335	101.9		
CT	Intraepithelial CD3+ T cells	Low	432	91.7	16	<=132.32
		High	381	107.7		
	Stromal CD3+ T cells	Low	531	91.9	19.7	<=826
		High	285	111.6		
IM	Intraepithelial CD3+ T cells	Low	415	91.3	14.7	<=121.2
		High	402	106		
	Stromal CD3+ T cells	Low	414	87.9	21.9	<=527
		High	418	109.8		
Adjacent normal tissue	Intraepithelial CD3+ T cells	Low	176	94.3	7.3	<=180
		High	654	101.6		
	Stromal CD3+ T cells	Low	305	92.2	11.4	<=582
		High	532	103.6		

Table 4. 4 Kaplan-Meier survival analysis of correlations between expression of intraepithelial and stromal CD8+T cells in LS, CT and IM and adjacent normal tissue and disease-specific survival. CRC patients were categorised into high and low-density groups according to the cut off points of CD8 T cell density in each tumour location. [DSS: Disease-specific survival]

		Expression	Number	Mean DSS (Months)	Cut off point (cells/mm2)
LS	Intraepithelial CD8+ T cells	Low	331	89.6	<= 17
		High	529	105.4	
	Stromal CD8+ T cells	Low	746	99.5	<=585
		High	104	107.1	
CT	Intraepithelial CD8+ T cells	Low	585	96.4	<=85
		High	238	104.6	
	Stromal CD8+ T cells	Low	666	98.5	<=382
		High	160	103.9	
IM	Intraepithelial CD8+ T cells	Low	710	98.3	<=260
		High	113	105.7	
	Stromal CD8+ T cells	Low	641	96.7	<=325
		High	209	105	
Adjacent normal tissue	Intraepithelial CD8+ T cells	Low	377	96.6	<=115
		High	393	99.3	
	Stromal CD8+ T cells	Low	183	92.1	<=105
		High	595	102.3	

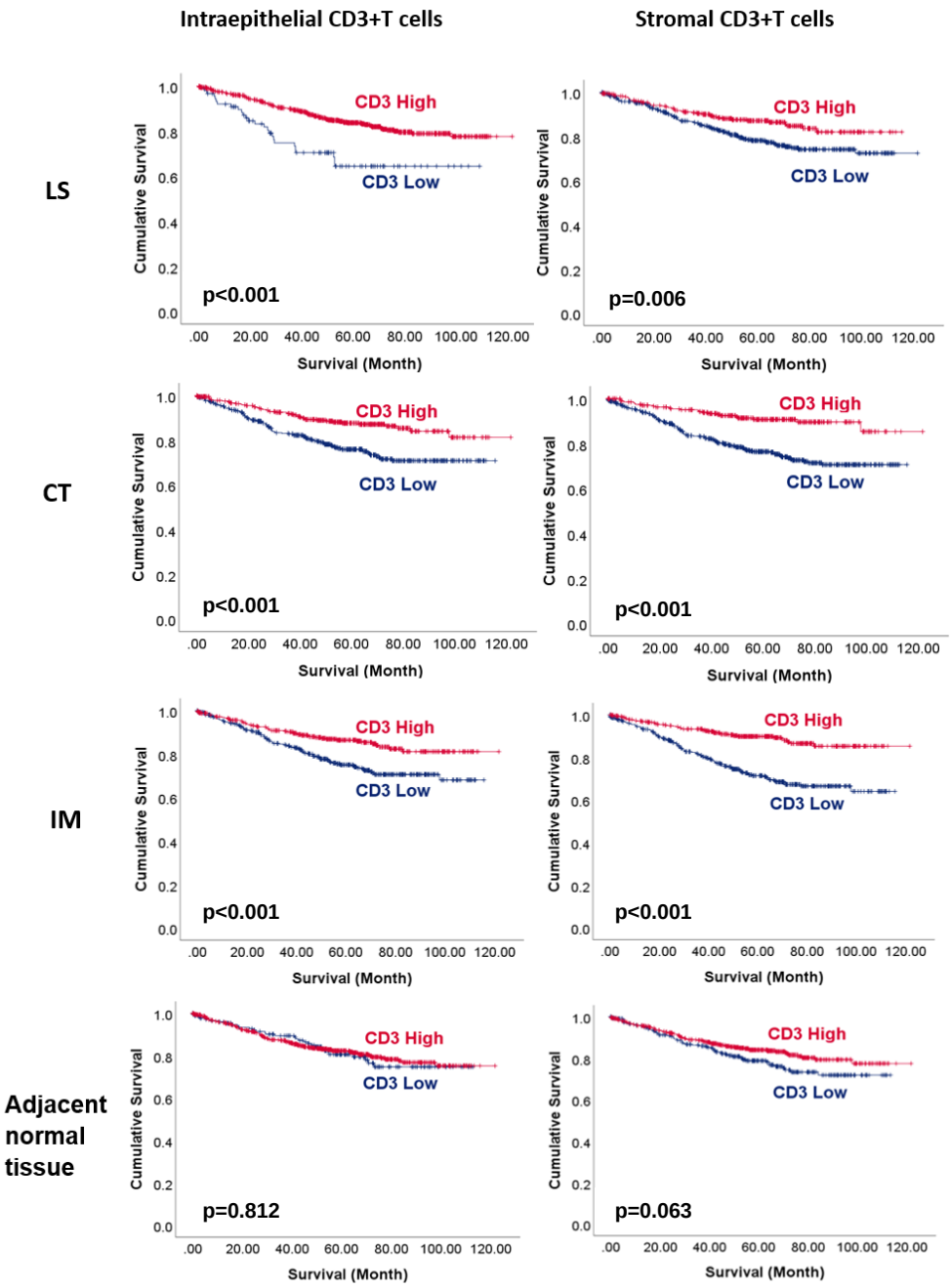

Figure 4. 7 Kaplan-Meier plots for disease-specific survival for intraepithelial and stromal CD3+T cells in three tumour regions

Intraepithelial and stromal infiltration of CD3+ T cells was significantly associated with DFS of CRC patients in the three tumoural regions but not the adjacent normal tissue. Log-rank test was used to test the statistical significance. p-value <0.05 was considered significant. LS: Luminal area; CT: Centre of the Tumour; IM: Invasive Margin and adjacent normal tissue.

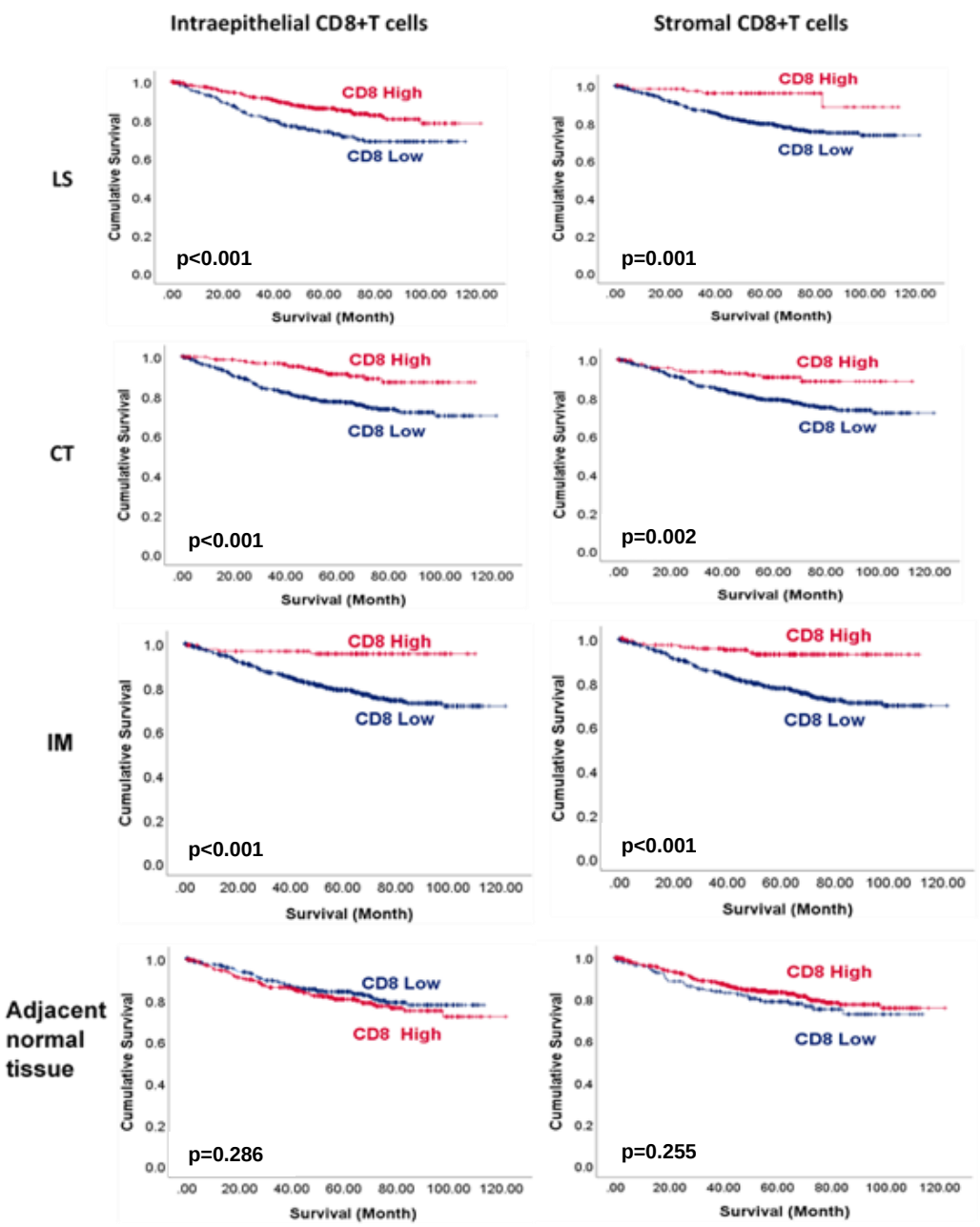

Figure 4. 8 Kaplan-Meier plots for disease-specific survival (DFS) for intraepithelial and stromal CD8+T cells in three tumour regions

Intraepithelial and stromal infiltration of CD8+T cells was significantly associated with DFS of CRC patients in the three tumoural regions but not the adjacent normal tissue. A log-rank test was used to test the statistical significance. P-value <0.05 was considered significant. LS: Luminal area; CT: Centre of the Tumour; IM: Invasive Margin and adjacent normal tissue.

4.2.6 Relationship between intratumoral CD3+ and CD8+ Tcell density and tumour recurrence within different tumour locations

The association between high CD3+ and CD8+ T cell infiltrates and lower frequency of tumour recurrence has been reported in several studies. [235, 376, 377] Galon and colleagues [239] compared the densities of CD3+and CD8+ T cells in CT and IM regions from patients with tumour recurrence and patients without tumour recurrence. They found that patients without recurrence had higher CD3+ and CD8+ T cell densities in each tumour region (CT and IM) than patients whose tumours had recurred. In order to confirm and expand on these findings, the median of CD3+ and CD8+ T cell densities in four tumour regions (LS, CT, IM and adjacent normal tissue) were estimated and compared between patients with tumour recurrence and patients without recurrence. Expectedly, the median of CD3+ and CD8+ T cell densities in LS, CT and IM regions was significantly higher in patients with no recurrence compared to the others (Figure 4.9. A and B). In contrast, no significant difference between the medians of the two patient groups was observed in the adjacent normal tissue. Mann Whitney (non-parametric) test was performed for this comparison, and p values < 0.05 were considered statistically significant.

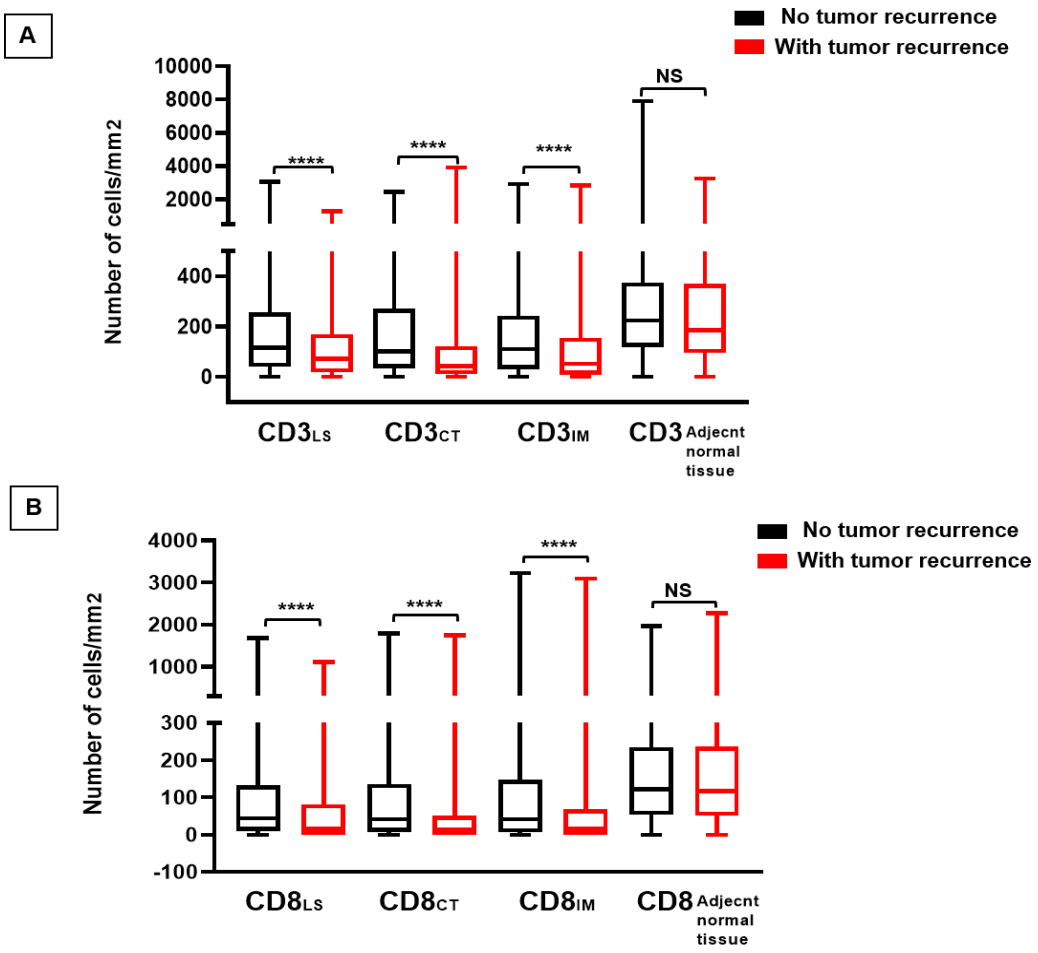

Figure 4. 9 Comparison of the median of (A) CD3+ T cell densities and (B) CD8+ T cell densities in the LS, CT, IM and Adjacent normal tissue from patients with tumour recurrence (red bars) or without tumour recurrence (black bars). The density of the cells was recorded as cells per mm^2. The middle line represents median densities. Mann Whitney U test was used for statistical comparisons. p-values <0.05 were considered statistically significant. (** represents p ≤ 0.0001, NS: non significant)**

4.2.7 Immunoscore and combined regional analysis of intraepithelial CD3 and CD8 T cell densities in LS, CT and IM regions

The role of Immunoscore as a predictive marker that supports and outperforms the AJCC/UICC TNM classification was evident in colorectal cancer by many studies. [241, 356, 366, 377] Thus, direct replication of the previous research and results of the Immunoscore and its association with patients' disease-free survival was performed on the new colorectal cohort to ensure data consistency and validate the scoring methods of this study. Patients were stratified according to their Immunoscore from I0 to I4. The classification was dependent on the total number of high densities observed (Figure 4.10 A). For example, the Immunoscore of patients with high densities of CD3+ and CD8+ T cells in CT and IM regions (4-Hi) was referred to as I4. Tumours with three high densities were classified as I3, and patients with low densities of both markers in CT and IM regions were referred to as I0 (0 Hi). [242, 366]

Kaplan–Meier plot (Figure 4.10 B) visualises the differences between disease-free survival for different Immunoscore categories (I0-I4). The log-rank test was used to calculate the significance among patient groups. Significant differences between patient groups for survival times were observed between different Immunoscore categories ($p < 0.001$). Patients with Immunoscore (I4) had prolonged survival time in comparison to other categories. Whereas, patients with Immunoscore (I0) experienced the poorest clinical outcome. Moreover, a combined regional analysis for each marker (CD3+ and CD8+) was conducted and expanded by combining the immune cell densities in three tumour regions (LS, CT and IM) instead of CT and IM regions only. [239, 366]

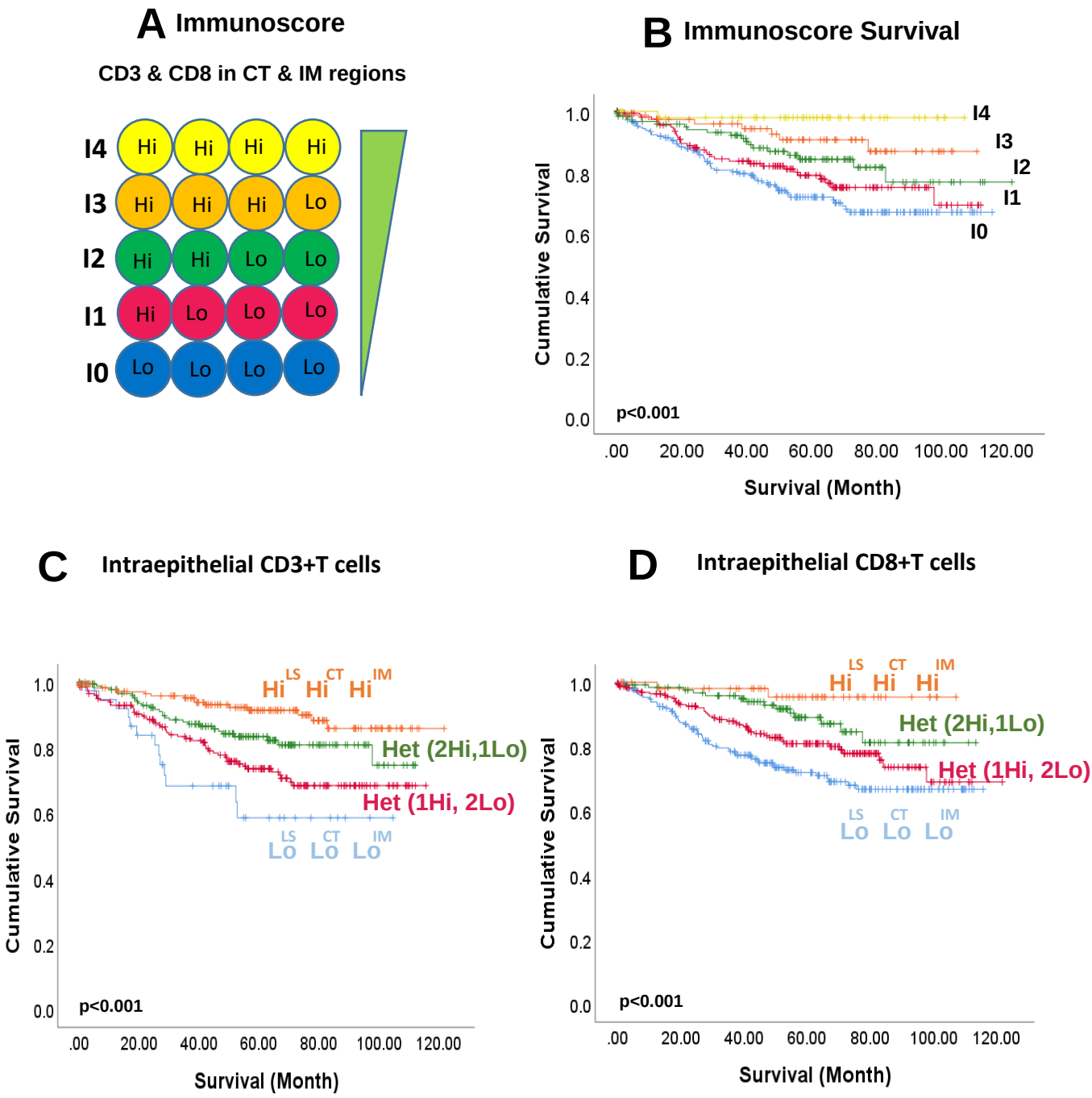

Figure 4. 10 Combined regional analysis of intra-epithelial CD3 and CD8+ T cell densities in LS, CT and IM regions.

(A) The Immunoscore stratifies tumour cores based on both CD3 and CD8 densities in CT and IM. The score ranges from (I0 to I4) depending on the total number of high densities observed of the two markers in two tumour regions. (Adapted from Galon.et al., 2012 [242]) **(B)** Kaplan-Meier curve showing the duration of disease-specific survival for Immunocore strata (I0, I1, I2, I3, I4). p values less than 0.05 were considered significant. **(C)** and **(D)** represents the combined analysis of intraepithelial CD3 and CD8 density in LS, CT and IM regions, respectively: orange line indicates high densities in all regions; green line indicates heterogeneous densities (2 regions with high density and one with low density); pink line

indicates heterogeneous densities 2 regions with low density and one with high density; blue line indicates low density in all regions.

According to the combined regional analysis, patients were divided into four groups: patients with high density of a marker in LS, CT and IM regions were classified (**Hi^{LS} Hi^{CT} Hi^{IM}**); patients with low density of such marker in all tumour regions were classified (**Lo^{LS} Lo^{CT} Lo^{IM}**); patients with heterogenous density (high density in two regions and low in one region) were classified "**(2Hi,1Lo)**" and patients with heterogenous density (high density in one region and low in two regions were classified "**(1Hi,2Lo)**". Kaplan–Meier plots (Figure.10 C and D) indicate that the combined regional analysis of immune cells in LS plus CT plus IM regions is more efficient to discriminate patient's outcome in comparison to single region analysis. Patients with high densities in all regions showed better association with patients' disease-free survival time compared to other patient groups (log-rank test, p <0.000)

4.2.8 Significant association of average CD3 and CD8 densities from three tumour regions and patient disease-free survival

Average CD3+ and CD8+ T cell densities in the tumour nest and stroma from LS, CT and IM regions were estimated to minimise the effect of immune cells heterogeneity and distribution on the prognostic role of CD3+ and CD8+ T cells on CRC patients' survival. The difference in survival probability between patients with low and high average density of Intraepithelial CD3+ T cells, stromal CD3+ T cells, Intraepithelial CD8+ T cells and stromal CD8+ T cells are shown in Figure 4.11. High average densities of intraepithelial and stromal CD3+ and CD8+ T cells were associated with improved survival compared to low average density of these markers. The association was statistically significant as the p values of the log-rank test were less than 0.05.

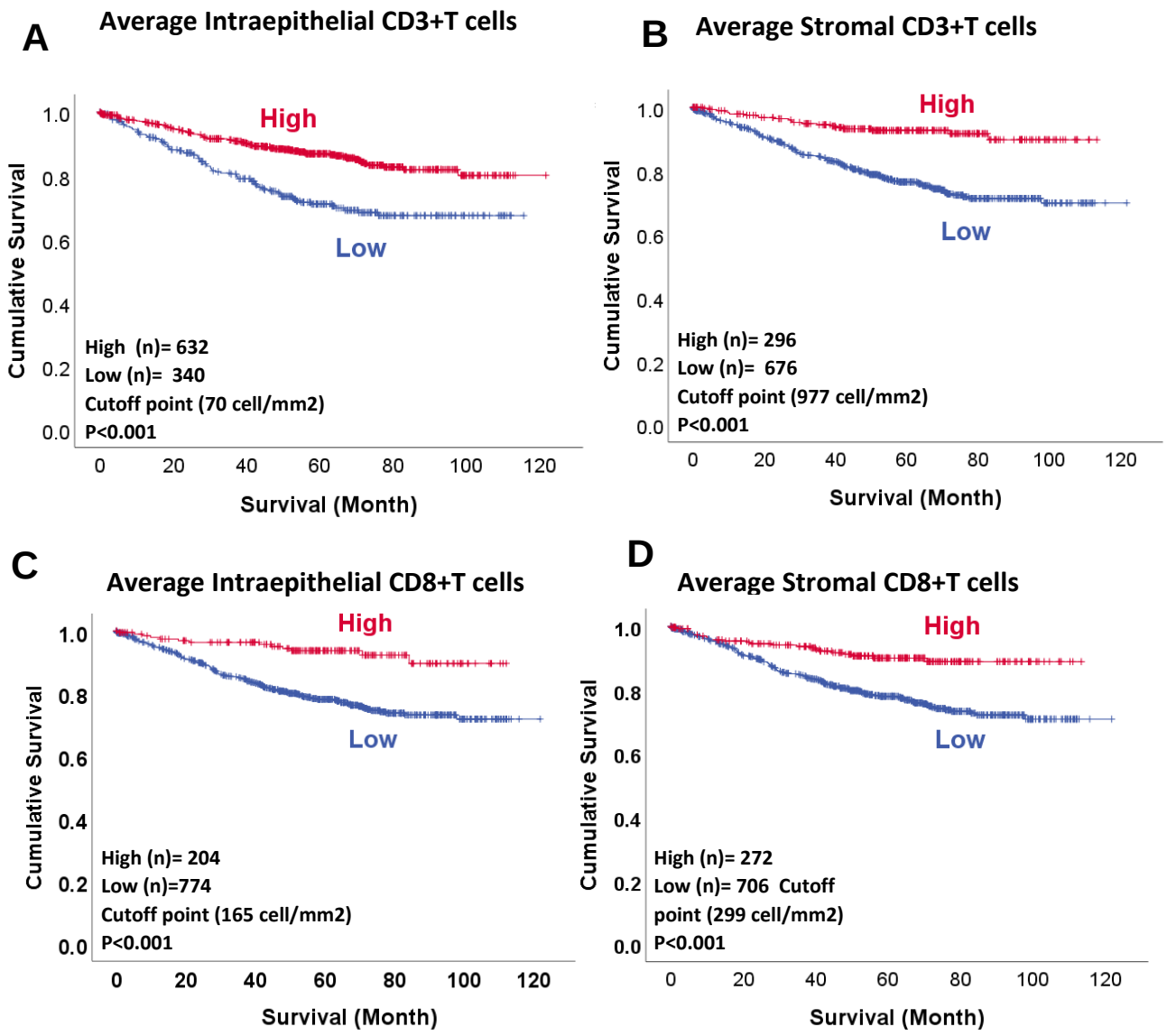

Figure 4. 11 The association of average CD3 and CD8 T cell densities from three tumour regions and patient disease-free survival.

Kaplan-Meier graphs for the duration of DFS according to **(A)** and **(B)** average of intraepithelial and stromal CD3+ cell density from LS, CT and IM tumour regions. **(C)** and **(D)** average of intraepithelial and stromal CD8+ T cell density from LS, CT and IM tumour regions. Log-rank test was used to test the statistical significance. P-value <0.05 was considered significant.

4.2.9 Correlation between intraepithelial CD3+ and CD8+T cells within different tumour regions and adjacent normal tissue

Following the above results, Chi-square tests were used to identify the correlations between CD3+ and CD8+ T cells within different tumour regions and the adjacent normal tissue. A strong correlation was seen between the average density of CD3+ and CD8+T cells from the three tumour regions (P<0.001; table 5). One hundred eighty-five tumours (94%) showed dense infiltrate of CD3+ and CD8+ T cells, while only 11 (6%) had a low level of CD3+ TILs and high CD8+ T cells. In contrast, 324 tumours (42%) had a low density of both markers. The correlation between CD3+ and CD8+T cells in the adjacent normal tissue was statistically significant (P<0.001; table 4.5). However, no significant correlation between CD3+ and CD8+T cells was found when one was in the tumour regions, and the other was in the adjacent normal tissue.

Table 4. 5 Correlations between average Intraepithelial CD3+ and CD8+ T cell densities from LS, CT and IM regions, and Intraepithelial CD3+ and CD8+ T cells in the adjacent normal tissue. The average density of each maker was calculated by dividing the total cell number of all tumour regions into the total tumour areas. Pearson's χ^2-tests were used to determine the significance of the correlation between different markers. p- values <0.05 were considered statistically significant.

		Average Intraepithelial CD8+ T cells			CD8+ T cells in adjacent normal tissue		
		Low (%)	High (%)	P-value	Low (%)	High (%)	P-Value
Average Intraepithelial CD3+ T cells	**Low**	324 (42%)	11 (6%)	**<0.001**	137 (37%)	119 (31%)	0.080
	High	441 (58%)	185 (94%)		233 (63%)	265 (69%)	
CD3+ T cells in adjacent normal tissue	**Low**	142 (21.8%)	30 (17.9%)	0.262	101 (27.8%)	39 (10.1%)	**<0.001**
	High	509 (78.2%)	138 (82.1%)		263 (72.2%)	347 (89.9%)	

4.2.10 Correlations with clinicopathological criteria and multivariate Cox regression models of average intraepithelial CD3+T cells and CD8+T cells in CRCs

The correlation of clinicopathological data with the average expression of CD3+ and CD8+T cells in the tumour nest is shown in table 4.6. A positive association was found between the prevalence of CD3+ and CD8+T cells, and microsatellite instability ($p<0.001$), the absence of regional lymph node metastasis ($p<0.001$), right-sided colon tumours ($p= 0.023$; $p= 0.002$, respectively.), lower TNM stage ($p<0.001$) and the absence of extramural vascular invasion ($p<0.001$). Also, a positive correlation was observed between the average intraepithelial and stromal CD3+ T cells ($p<0.001$), indicating that the more T cells found in the tumour tissue, the more likely T cells were to be found in the surrounding stroma. This observation is consistent with previously published data. [360] A similar significant correlation was seen between the average intraepithelial and stromal CD8+ T cells ($p<0.001$)

A multivariate Cox regression model integrating the influences of extramural vascular invasion, TNM stage, tumour grade and microsatellite status with intraepithelial CD3+ T cells, adjusting for their collective effect, indicates that the latter factor maintained its significant influence on prognosis (table 4.7) (HR=0.639, 95% CI 0.44 to 0.93; p=0.021). As CD3+ T cells, the expression of CD8+ T cells in the tumour tissue was shown to be a prognostic factor independent of the clinicopathological characteristics in table 4.8. (HR=0.38, 95% CI 0.195 to 0.74; p=0.004)

Table 4. 6 Summary of the correlations between clinicopathologic features (sex, age, N -Regional lymph nodes, metastases, primary tumour location, TNM stage, extramural vascular invasion and microsatellite status) and the expression of average Intraepithelial CD3+ and average Intraepithelial CD8+T cells in colorectal cancer. Pearson's χ^2-tests were used to determine the significance of the correlation between different markers. p- values <0.05 were considered statistically significant.

	Average Intraepithelial CD3+ T cells			**Intraepithelial CD8+ T cells**		
	Low (%)	**High (%)**	**P-value**	**Low (%)**	**High (%)**	**P-Value**
Sex						
Male	244 (44.6)	303 (55.4)	0.914	456 (82.6)	96 (17.4)	0.228
female	189 (44.3)	238 (55.7)		339 (79.6)	87 (20.4)	
Age diagnosis						
<=69	223 (45.3)	269 (54.7)	0.581	403 (81.6)	91 (18.4)	0.814
>69	210 (43.6)	272 (56.4)		392 (81)	92 (19)	
Tumour site						
Right colon	179 (39.3)	276 (60.7)	**0.023**	348 (76.7)	106 (23.3)	**0.002**
Left colon	175 (50)	175 (50)		300 (85.2)	52 (14.8)	
Rectal	66 (46.8)	75 (53.2)		123 (86)	20 (14)	
unknown	13 (46.4)	15 (53.6)		24 (82.8)	5 (17.2)	
Tumour grade (differentiation)						
well	6 (30)	14 (70)	0.204	19 (100)	0 (00)	0.097
Moderate	393 (45.5)	471 (54.5)		708 (81.6)	160 (18.4)	
poor	33 (37.1)	56 (62.9)		67 (74.4)	23 (25.6)	
Microsatellite status						
Negative	392 (48.9)	409 (51.1)	**<0.001**	683 (85.1)	120 (14.9)	**<0.001**
Positive	34 (21.7)	123 (78.3)		99 (62.7)	59 (37.3)	
Vascular invasion						
Absent	163 (33.3)	326 (66.7)	**<0.001**	373 (76)	118 (24)	**<0.001**
Present	266 (56.6)	204 (43.4)		412 (87.1)	61 (12.9)	
TNM stage						
1	43 (27.7)	112 (72.3)	**<0.001**	115 (72.3)	44 (27.7)	**<0.001**
2	163 (41.8)	227 (58.2)		312 (79.2)	82 (20.8)	
3	160 (50.8)	155 (49.2)		268 (85.6)	45 (14.4)	
4	67 (58.8)	47 (41.2)		100 (89.3)	12 (10.7)	
N -Regional lymph nodes						
N0 (no lymph node metastasis)	219 (39.7)	332 (60.3)	**<0.001**	433 (77.6)	125 (22.4)	**<0.001**
N1 (Regional lymph node metastasis)	212 (53.1)	187 (46.9)		344 (86.6)	53 (13.4)	

Table 4. 7 Multivariate Cox regression analysis model for vascular invasion, TNM stage, tumour grade, MSI status and average Intraepithelial CD3+ T cells. Multivariate analysis was performed by Cox regression proportional hazard analysis to test for confounders and the predictive independency of Intraepithelial CD3+ T cell infiltration from standard prognostic/predictive factors. The log-rank test was used to test for significance. p- values <0.05 were considered statistically significant.

Variable	HR	95% CI		p-value
		Lower	Upper	
TNM stage	3.304	2.561	4.263	<0.001
Vascular invasion	1.464	0.967	2.217	0.071
Tumour grade	1.946	1.15	3.294	0.013
MSI status	0.816	0.429	1.551	0.535
Intraepithelial CD3 T cells	0.582	0.406	0.833	**0.003**

Table 4. 8 Multivariate Cox regression analysis model for vascular invasion, TNM stage, tumour grade, MSI status and average Intraepithelial CD8+ T cells. Multivariate analysis was performed by Cox regression proportional hazard analysis to test for confounders and the predictive independency of Intraepithelial CD8+ T cell infiltration from standard prognostic/predictive factors. The log-rank test was used to test for significance. p- values <0.05 were considered statistically significant.

Variable	HR	95% CI		p-value
		Lower	Upper	
TNM stage	3.266	2.514	4.243	<0.001
Vascular invasion	1.472	0.963	2.25	0.074
Tumour grade	2.114	1.248	3.583	0.005
MSI status	0.90	0.478	1.696	0.745
Intraepithelial CD8 T cells	0.38	0.195	0.740	**0.004**

4.3 Discussion

The present study demonstrated a comprehensive analysis of CRC patients cohort, to validate the prognostic value of the clinicopathological parameters and immune cell heterogeneity in colorectal tumours. A significant influence on patients' survival was observed with tumour stage, grade and the absence or presence of vascular invasion. The majority of these predictive factors were reported previously by several studies.

[360, 370] Digital image analysis software (HALO®) was utilised to estimate immune cell densities in a timely and efficient manner. HALO® scoring was validated by a manually scored sample group (n=670 cores). Consequently, HALO® was considered as a reliable and reproducible scoring method.

As the immune infiltration in tumours is heterogeneous [356, 358, 367], this study investigated the role of intraepithelial and stromal CD3+ and CD8+ T cells in three different regions of the tumour and the adjacent normal tissue. The results of the single regional analysis for each location showed a significant association of intraepithelial and stromal CD3+ and CD8+ T cells with disease-free survival time when these markers were present in any region within the tumour but not in the adjacent normal tissue. In line with this observation, high intraepithelial CD3+ and CD8+ T cell infiltrate in LS, CT and IM regions were found in patients without tumour recurrence. Whereas, no relationship was seen between intraepithelial CD3+ and CD8+ T cell densities in the adjacent normal tissue and tumour recurrence. The prognostic value of Immunoscore and combined regional (LS plus CT plus IM) analysis of intraepithelial CD3+ and CD8+ T cell densities were demonstrated and shown to have an additive beneficial impact on predicting patients' survival over the single regional analysis of each tumour location.

Furthermore, the average densities of intraepithelial and stromal CD3+ and CD8+ T cells in all tumour regions were significantly associated with disease-free survival time depending mainly on immune cell density and excluding the distribution effect of these cells. The correlation between intraepithelial CD3+ and CD8+ T cells was shown to be statistically significant only when both the markers are present within the tumour regions or the adjacent normal tissue. Some of the prognostic clinicopathological parameters of this study were significantly associated with intraepithelial CD3+, and

CD8+ T cells present in the tumour regions. However, it was shown that these biomarkers (CD3 and CD8) are independent prognostic factors

The synergistic or opposing effects of the immune cell populations infiltrating human tumours may affect tumours differently depending on their molecular type and histological, their stage, the nature of the primary tumour or its metastases, or the microenvironment of the organ in which they grow. Additionally, the effect of each factor may be buffered by the existence of other immune cell populations at different densities. Hence, a comprehensive analysis to integrate immune cell-associated, tumour cell-associated, and microenvironment-associated parameters with clinical data (including treatment history, staging evolution and tumour histology) from large patient cohorts is required. [358, 378] In this study, a newly constructed, large cohort (n=1000) of CRC patients was analysed to assess the prognostic role of CD3+ and CD8+ infiltrates in patients' clinical outcome and to validate the predictive value of some clinicopathological parameters previously known as prognostic factors, to confirm the accuracy and efficacy of the scoring method and the analysis used in the current study.

In recent years, digital image analysis has emerged as a reliable, less time-consuming and reproducible alternative to manual scoring. [373] Several studies show high concordance between digital image analysis and manual scoring, especially with small tumour areas like tissue microarrays (TMAs) cores. [379, 380, 381] Therefore, a digital image analysis tool called (HALO®) was used in the study cohort, which consisted of 4000 TMA cores representing 1000 CRC patients. The software was trained to count CD3+ and CD8+ T cells within different tissue types (tumour tissue or stroma). In order to validate HALO scoring results, more than 15% of the study cohort was scored manually. HALO® scores significantly agreed and correlated with the manual scores of the sample group. As a result, this tool was utilised as the main scoring method for the whole cohort.

The effect of the host immune response on tumour recurrence, metastasis and invasion was evident by performing analyses of the *in situ* immune components and how these are distributed within human tumours. Indeed, immune infiltrates are heterogeneous between tumour types and are very diverse from patient to patient. [358] Accordingly, Galon et al. studied a series of tumours and concluded that the density, type and location of immune cells in CRC had better prognostic value than TNM stage classification. [240] Subsequently, several studies continued to investigate the previous observation by measuring the density of immune cells, and their distribution in the tumour core (CT) and the invasive margin (IM) of the tumour [239, 242, 356, 366, 377], and some were interested with the distance metastases of CRCs. The superiority of combined regional (CT plus IM) analysis over a single analysis of CD3+ and CD8+ T cells in each region in predicting the disease-free survival in CRC patients, had contributed to develop the Immunoscore, which can be measured by combining the density of CD3+ and CD8+T cells in the CT and IM regions. [356] Due to the prognostic impact of Immunoscore in patients with colon cancer, patients were stratified according to their immunoscore (I0 to I4) in the current study. Similar to the findings by Kirilovsky at el. [356] and Anitei at el. [366], a significant difference in patient survival time was shown between patients with different immunoscore, with an increase in disease-free survival time from I0 to I4.

Although a sufficient number of studies investigated immune cell density and distribution in CT and IM regions, there is a paucity of data regarding other sites of the tumour (such as the Luminal side of the tumour) or the normal epithelial tissue surrounding colorectal tumours. Therefore, the work of Galon and colleagues[239] was continued and expanded by measuring single and combined regional analysis of CD3+ and CD8+ T cells for LS, CT and IM tumour regions and the adjacent normal tissue of each tumour. In compliance with previous research and results, it was

shown, by performing the single regional analysis, that high intraepithelial and stromal CD3+ and CD8+ T cell infiltration in LS, CT or IM regions is associated with better clinical outcome. In contrast, the presence of dense intraepithelial and stromal CD3+ and CD8+ T cell infiltration in the adjacent normal tissue had no significant influence on patients' survival. This observation indicates that CD3+ and CD8+ T cells are considered as prognostic factors when they are located at any site within the tumour tissue (epithelium or stroma). Nevertheless, the predictive importance of the immune cells diminishes when found in the adjacent normal tissue from the tumour epithelium.

The present study illustrated that for each biomarker (CD3 and CD8), the combined analysis of LS plus CT plus IM regions improved the accuracy of prediction of DFS time for the different patient groups when compared to single-region analysis. Interestingly, patients were stratified into four distinctive groups by adding the immune cells density information of LS region into the combined analysis, showing better separation between the groups of patients according to DFS outcome in comparison to the combined analysis of two tumour regions (CT and IM) preformed by previous studies.[239, 366, 367]

A number of studies have been done to study the correlations between different types of immune cells, immune cells in different tissue types (epithelium and stroma), and immune cells and clinicopathological parameters.[235, 237, 360, 376, 382] Thus, the average density of intraepithelial and stromal CD3+ and CD8+ in LS, CT and IM regions were estimated, in order to minimise immune cell heterogeneity and distribution effect, and to compare the correlations performed in the current study with the literature. Our data have shown a strong positive correlation between intratumoral and stromal CD3+ cells, and the same observation was noted for CD8+ T cells. These observations align with Simpson et al. findings.[360] However, the same study suggested that the presence of high immune cell infiltration in the stromal area does

not correlate with patients survival. The opposite of this was shown in the current study, that is, high infiltration of CD3+ and CD8+ T cells in the stroma was associated with prolonged survival time in CRC patients. We believe that the reason for the contradictory results is that Simpson and colleagues used a semiquantitative scoring method in which cases were classified visually, according to the density of CD3+ cell infiltration in the stroma, as sparse, moderate or dense. In contrast, in the present study, validated automated software was used to measure the density of CD3+ cells by counting the number of cells per stromal area. Therefore, we suggest that our observation is more accurate and reproducible in comparison to the other.

A significant positive correlation between intraepithelial CD3+ and CD8+ T cells was shown in this study when both markers were present in any site of tumour regions or the adjacent normal tissue. However, no correlation was found between CD3+ cells density within the tumour tissue and CD8+ T cell density in the adjacent normal tissue, indicating that CD3+ and CD8+ T cell proportions correlate only when both are present in the same tissue type (cancerous or normal tissue). Although some clinicopathological parameters such as TNM stage, extramural vascular invasion, regional lymph node metastasis and microsatellite instability were shown to be strongly associated with the prevalence of CD3+ and CD8+T infiltrates, the results of intraepithelial CD3+ and CD8+ T cell Cox regression models indicate that these markers retained their significant influence on prognosis and were identified as independent prognostic factors.

Chapter 5: Investigating the predictive value of CD103 biomarker in colorectal cancer patients

5.1 Introduction

Accumulating evidence has shown the value of tumour-infiltrating lymphocytes (TIL) as a diagnostic, prognostic, and predictive biomarker in a wide range of cancers[239, 246, 383], particularly in colorectal cancer. [236, 360] Among different TIL types, CD8+ TILs are the major anti-tumour effector cells due to their direct role in killing the cancer cells by releasing cytotoxic molecules and cytokines. [384, 385] However, it was believed that some intratumoral CD8 T cells are not active participants in the immune response to the tumour and were considered as bystanders, while the ones which are functionally relevant to the anti-tumour response cells are CD8 cells that have recently engaged antigen (cytotoxic effector T cells) or previously engaged antigen (tissue-resident T cells).[386] In compliance with that, Ganesan et al. performed transcriptomic profiling of tumour-infiltrating CTLs from treatment-naive patients with lung cancer. It was shown that tumours with high TIL infiltration were associated with the upregulation of transcripts encoding products involved in TCR activation, concordant with the enrichment for presumed tumour-associated antigens specific CD8+T cells. They also found that tumours with a high CTL infiltration showed enrichment for transcripts linked to Tissue-resident T cells, such as CD103.[246]

Tissue-resident memory T cells (TRM) is an important subclass of TILs. Unlike the effector memory T cells that recirculate in the blood and can enter peripheral lymph nodes and non-lymphoid tissues, TRM cells influx peripheral tissues during primary responses and persists there (non-recirculating). In addition to their unique migratory

pattern, TRM cells express receptors and integrins such as CD69 and CD103 that help them maintain in tissue and distinguish them from circulating memory T cells. [385] CD103 also referred to as (Integrin αE), binds to the epithelial cell marker E-cadherin, hence favouring the location and retention of TRM in epithelial tumour regions in close contact with malignant cells. The CD103-E-cadherin interaction not only induces antigen recognition by enhancing T cell adhesion to certain cancer cells but also, promotes co-stimulation in activated cytotoxic T cells via the cooperation between the triggering signals and signalling mediated by TCR. [387]

An increased number of studies in various human cancers have shown a positive correlation between the presence of CD103+ population in the tumour tissues and survival of cancer patients. For example, a study carried out by Webb and colleagues showed that dense infiltration of CD103+ cells in the tumour was strongly associated with overall patient survival in high-grade ovarian cancer. [252] Moreover, Wang et al. presented that the presence of CD103+ tumour infiltrating lymphocytes is associated with tumour grade, size and ER/PR status of breast cancer, especially in basal like subtype. It should be noted that the same study claimed that CD8 status of tumour infiltrating lymphocytes showed less significant associations. In contrast, dual IHC staining for CD8+ and CD103+ tumour infiltrating lymphocytes proved to be a strong prognostic marker for relapse-free and overall survival. Similarly, the predictive value of CD103+ T cells was also demonstrated in non-small-cell lung cancer, bladder cancers, colorectal cancer and cervical cancer. [247, 248, 249, 388]

In colorectal cancer, several studies investigated the genomic, genetic and immune landscapes of the right-sided colon, left-sided colon and rectal cancers which may affect the clinical behaviour and patient treatment plan for each site. Many studies have reported that higher rates of microsatellite instability (MSI) and increased mutational burden was observed in right-sided colon cancers (RCRC) compared to the left-sided colon and rectal cancers (LCRC).[275, 389] Therefore, RCRCs are

predominantly characterised by microsatellite instability, while LCRCs are characterised by chromosomal instability.[279] The increment in the mutational and neoantigenic load in MSI-high CRCs is related to the defect in DNA mismatch repair mechanisms. These tumours have been associated with high levels of tumour-infiltrating lymphocytes, better survival rates and decreased risk of metastasis.[389] In 2015, a phase II study reported that mismatch-repair-deficient CRCs were found to respond to checkpoint inhibition, while no responses were observed with microsatellite stable counterparts.[390] Due to the high presence of such tumours in RCRC, it is believed that immunotherapies demonstrate more promising results with right-sided colon cancers than left-sided ones.[279]

Furthermore, Mlecnik et al. revealed, by performing integrative analyses of MSI and MSS colorectal tumours, that increased expression of immune-related genes was found with MSI patients. Nevertheless, a few MSI patients had a low expression of these genes in comparison to the rest of the MSI patients. Also, they reported that MSS patients were heterogeneous; some of these patients were found with high expression of immune genes, similar to MSI patients. Consequently, there was no significant difference in OS and risk of relapse in patients with MSI, and those with MSS and high immune expression (MSS-Hi), which demonstrate the superiority of Immunoscore over MSI in predicting survival and the presence of functional mutation-specific cytotoxic T cells.[274]

The Immune landscape of CRCs tumour microenvironment from different primary tumour location (right-sided, left-sided colon and rectal cancers) was further studied by Zhang and colleagues. Due to the similarities in gene expression and immune infiltration between left colon tumours and rectal tumours, they considered rectum cancer as left-side CRC in their subsequent analysis. Their findings illustrated that

the immune cell infiltration in right-side and left-side colorectal cancer is heterogeneous. For example, RCRCs were associated with higher levels of T lymphocyte subpopulations and enhanced cytotoxic potential compared to LCRCs. However, higher levels of CD56 NK cell infiltration were found in the left-side CRC, compared with that in right-side colon cancer. Interestingly, CD56 NK cell infiltration correlated strongly with good prognosis only in left-side CRC patients. The distinct immune landscapes between LCRC and RCRC could explain the primary CRC location-specific differences in disease prognosis and responses to treatments. [284]

Numerous studies have confirmed the predictive value of TRM cells in different cancer types. However, the role of TRMs in colorectal cancer, particularly between different primary locations of CRCs is still unclear. Thereby, a comprehensive analysis of the density, distribution and prognostic impact of CD103+ TILs on right-sided colon cancer, left-sided colon cancer and rectal cancer was conducted in this study. It was hypothesised that RCRCs would be associated with higher CD103+ TILs infiltration and the that CD103+ TILs would show better prognostic value in the right-sided colon tumours than those in the left-sided colon and rectal cancers.

5.2 Results

5.2.1 Patient cohorts

This study was conducted on two independent cohorts of CRC patients [Cohort (1), n= 1000; Cohort (2), n=462], to validate and confirm the results of the analysis. Patient characteristics and information of cohort (1) were discussed earlier in chapter 4 (4.2.1).

Patient characteristics of Cohort (2)

A tissue microarray (TMA) series of 462 primary invasive colorectal tumours were used. The samples were collected from January 1994 to December 2000. The mean

follow-up period was 58 months (range 1-200). Cohort (2) consisted of 266 men (58%) and 196 women (42%). The median age was 72 years (range 57-93). Patient characteristics of cohort (2) are summarised in Table 5.1. The majority of tumours (77%) were of a moderate histological grade, and 85% were adenocarcinomas. Sixteen percent of tumours in Cohort (2) were TNM stage I, 38% were TNM stage II, 34% were TNM stage III, and 12% were TNM stage IV. Evidence of extramural vascular invasion was documented in 76% of all tumours. Some clinicopathological parameters such as tumour stage, the presence or absence of vascular invasion and nodal status were strongly associated with patients' survival (p-value <0.001). The predictive impact of these factors was also noted in Cohort (1).

Table 5. 1 Summary of the clinicopathological characteristics of CRCs patient in cohort (2). The correlation of the Clinic-pathological parameters (sex, age, Tumour histological type, N -Regional lymph nodes, Nodal status, metastases, primary tumour location, TNM stage, extramural vascular invasion and microsatellite status, and the patient's survival. The log-rank test was used to test for significance. p- values <0.05 were considered statistically significant.

Clinic-pathological parameters		N (%)	Mean (DSS) months	SE	95% confidence interval		Survival distribution (Log Rank-Mantel cox) of overall colorectal patients	
					Lower	Upper	Chi-Square	P-value
Sex	**Male**	266 (58%)	106.91	6.07	95.007	118.827	0.107	0.743
	Female	196 (42%)	107.85	6.55	95.017	120.695		
	Total	462 (100%)	109.97	4.54	101.068	118.875		
Age	**(<72)**	243 (52.6%)	110.74	5.97	99.041	122.445	.072	0.788
	(≥72)	219 (47.4%)	100.27	6.15	88.206	112.345		
	Total	462 (100%)	109.9	4.54	101.068	118.875		
	Adenocarcinoma	392 (85%)	106.8	4.63	97.71	115.895	11.276	0.024

Tumour histological type	**Mucinous adenocarcinoma**	51 (11%)	115.908	13.68	89.096	142.719		
	Columnar adenocarcinoma	4 (1%)	87.250	39.885	9.076	165.424		
	Signet ring mucinous adenocarcinoma	7 (1.5%)	30.429	10.950	8.966	51.891		
	Unknown	8 (1.7%)	32.000	10.774	10.883	53.117		
	Total	462 (100%)	109.972	4.543	101.068	118.875		
Nodal status (UICC)	**0**	242 (52.4%)	144.790	5.697	133.623	155.957	93.919	**<0.001**
	1	109 (23.6%)	80.877	8.296	64.618	97.136		
	2	84 (18.2%)	49.839	8.075	34.011	65.666		
	unknown	27 (5.8%)	45.56	10.3	25.26	65.869		
	Total	462 (100%)	109.972	4.543	101.068	118.875		
TNM stage	**I**	72 (16%)	143.57	8.195	127.51	159.63	91.509	**<0.001**
	II	174 (38%)	144.87	6.943	131.27	158.48		
	III	155 (34%)	82.56	6.96	68.90	96.207		
	IV	54 (12%)	9.304	1.21	6.92	11.68		
	Overall	462 (100%)	109.97	4.543	101.068	118.87		
Extramural vascular invasion	**Absence**	224 (48%)	121.809	5.877	110.291	133.327	42.459	**<0.001**
	Present	128 (28%)	65.911	7.573	51.068	80.753		
	Unknown	110 (24%)	120.974	9.262	102.821	139.128		
	Overall	462 (100%)	109.972	4.543	101.068	118.875		
Microsatellite status	**Microsatellite stable (MSS)**	211 (90%)	114.7	6.78	100.7	127.356	1.250	0.263
	Microsatellite instability (MSI)	24 (10%)	86.03	16.4	53.80	118.268		
	Overall	235 (100%)	111.9	6.40	99.39	124.517		

5.2.2 CD103+ T lymphocytes expression and scoring in colorectal tumours.

Immunohistochemical staining of CD103 was conducted on Cohort (1) and Cohort (2). Antibody optimisation was determined by staining a set of whole tissue sections. The optimal staining of CD103+ TILs in human tonsil tissue and colorectal cancer whole tissue sections is shown in Figure 5.1. (A) and (B). The distribution of CD103+ TILs in the normal tonsil tissue was observed mainly in the interfollicular area, similar to CD3 and CD8 T cell distribution pattern shown earlier in chapter 4. Figure 5.1 (C) and (D) represent a high and low CD103+ expression in colorectal TMA cores, respectively. Furthermore, CD103+ TIL densities in the tumour tissue and the surrounding stroma were calculated using the same formula we used to score CD3+ and CD8+ T cells previously (total number of CD103+ TILs per area divided on the total size of that area). Figure 5.2 shows the intratumoral CD103+ TILs (positive cells within the blue selected area) and stromal CD103+ TILs (positive cells located in the area between the red outline and blue selected area).

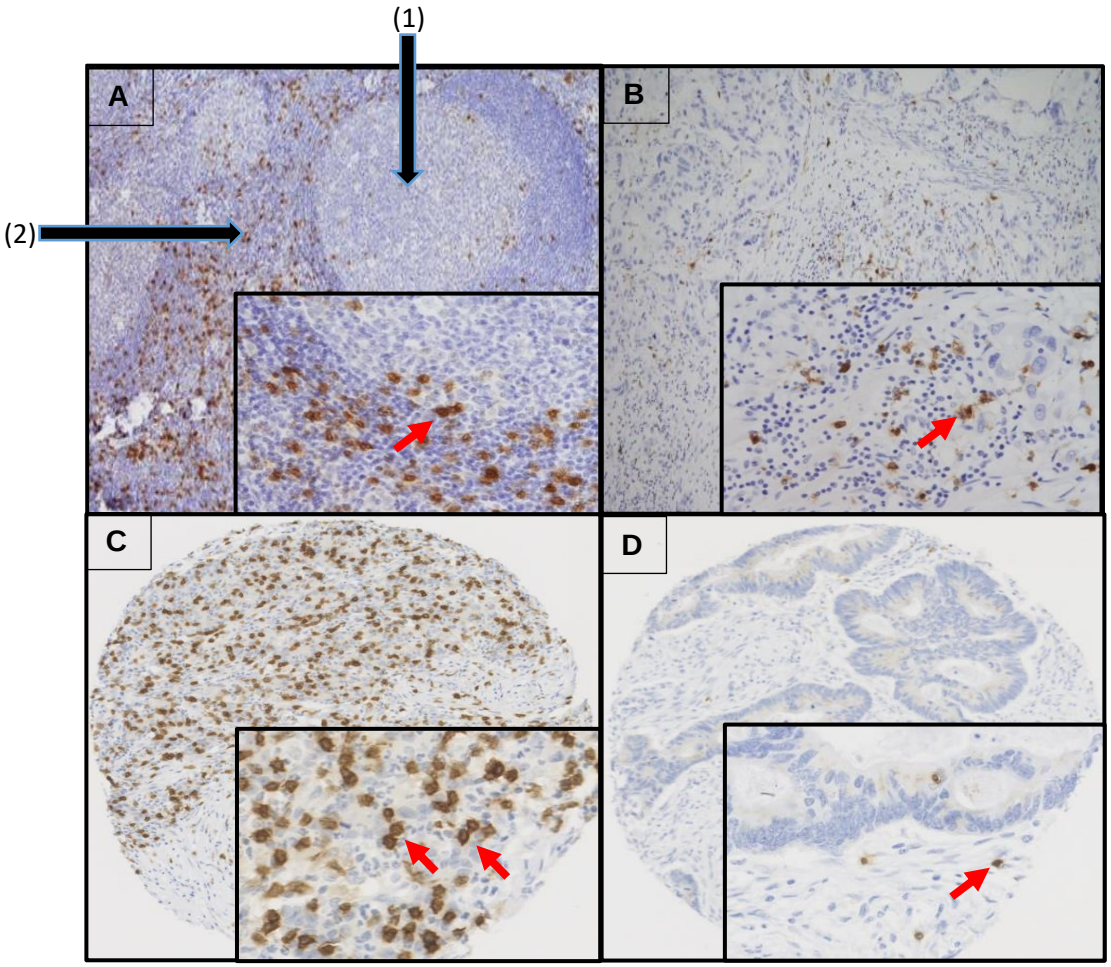

Figure 5. 1 (A) CD103+ expression in tonsil whole tissue section. The black arrows represent (1) follicular region and (2) interfollicular region; (B) CD103+ expression in whole colorectal tumour section; (C) Colorectal TMA Core with high CD103+ density; (D) Colorectal TMA Core with low CD103+ density. Red arrows show samples of positive cells. All ×200 original magnification (insets ×400 magnification)

In Cohort (1), the average density of intratumoral and stromal CD103+ TILs was calculated (combining the density of CD103+ TILs from LS, CT and IM tumour regions). Due to the similarity between the function and distribution of Immune cells within different tumour regions demonstrated earlier. The intratumoral and stromal CD103+ TILs density for Cohort (2) were determined from one core per patient, and then CD103+ scores from both cohorts were compared to validate the prognostic

value and distribution of CD103+ TILs in all CRCs cases and between different primary tumour locations (right colon, left colon and rectal tumours).

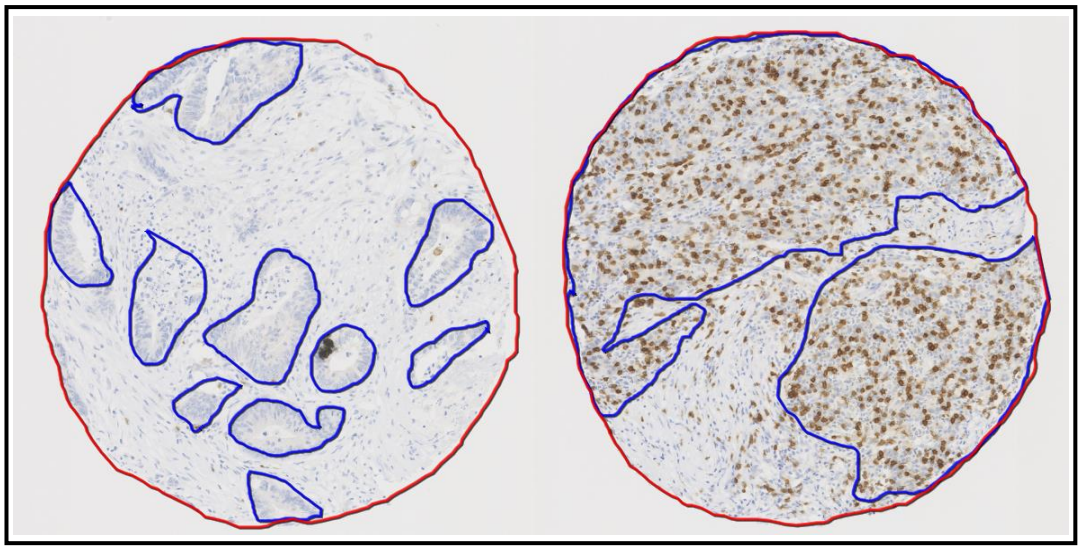

Figure 5. 2 Examples of different expression levels of CD103+ in formalin-fixed paraffin embedded colorectal cancer cores.

Red lines are indicating the total core areas; blue lines present the tumour area in the core. Only the positive cells within the blue perimeter were counted as intratumoral CD103+ TILs. All other cells were considered to be stromal.

5.2.3 The predictive significance of CD103+ T lymphocytes in all colorectal tumours patients.

Patients in Cohort (1) and Cohort (2) were categorised into high and low CD103+ density groups in accordance with a cut-off value determined by X-tile software. For both cohorts, low CD103+ TILs density group (Cohort (1), n=411; Cohort (2), n= 168) in the tumour nests was defined as ≤177 cells/mm², whereas high intratumoral CD103+ TIL density group (Cohort (1), n=541; Cohort (2), n= 59) was defined as >177 cells/mm². For stromal CD103+ TILs, patients were classified in the low-density group (Cohort (1), n=210; Cohort (2), n=40) if the density in the surrounding stroma was

≤139 cell/mm² and those who had densities >139 cell/mm² were considered in the high-density group (Cohort (1), n=743; Cohort (2), n=187).

Kaplan-Meier plots and log-rank test (p values) in Figure 5.3 A and B show a statistically significant difference in patient disease-specific survival (DSS) between patients with high intratumoral CD103+ (mean DSS 107.6 months) and stromal CD103+ (mean DSS 110.9 months) density group and the ones with low intratumoral CD103+ (mean DSS 92.5 months) and stromal CD103+ density group (mean DSS 91 months) in Cohort (1). In contrast, figure 5.3 C shows a trend towards a significantly longer DSS in tumours with high intratumoral CD103+ infiltration (mean DSS 129.5 months) versus tumours with low intratumoral CD103+ infiltration (mean DSS 100.2 months). However, no significant difference in survival was noted between patients with tumours displaying either low (mean DSS 93.3 months) or high (mean DSS 114.2 months) expression of CD103+ in the stroma for Cohort (2) (figure 5.3 D).

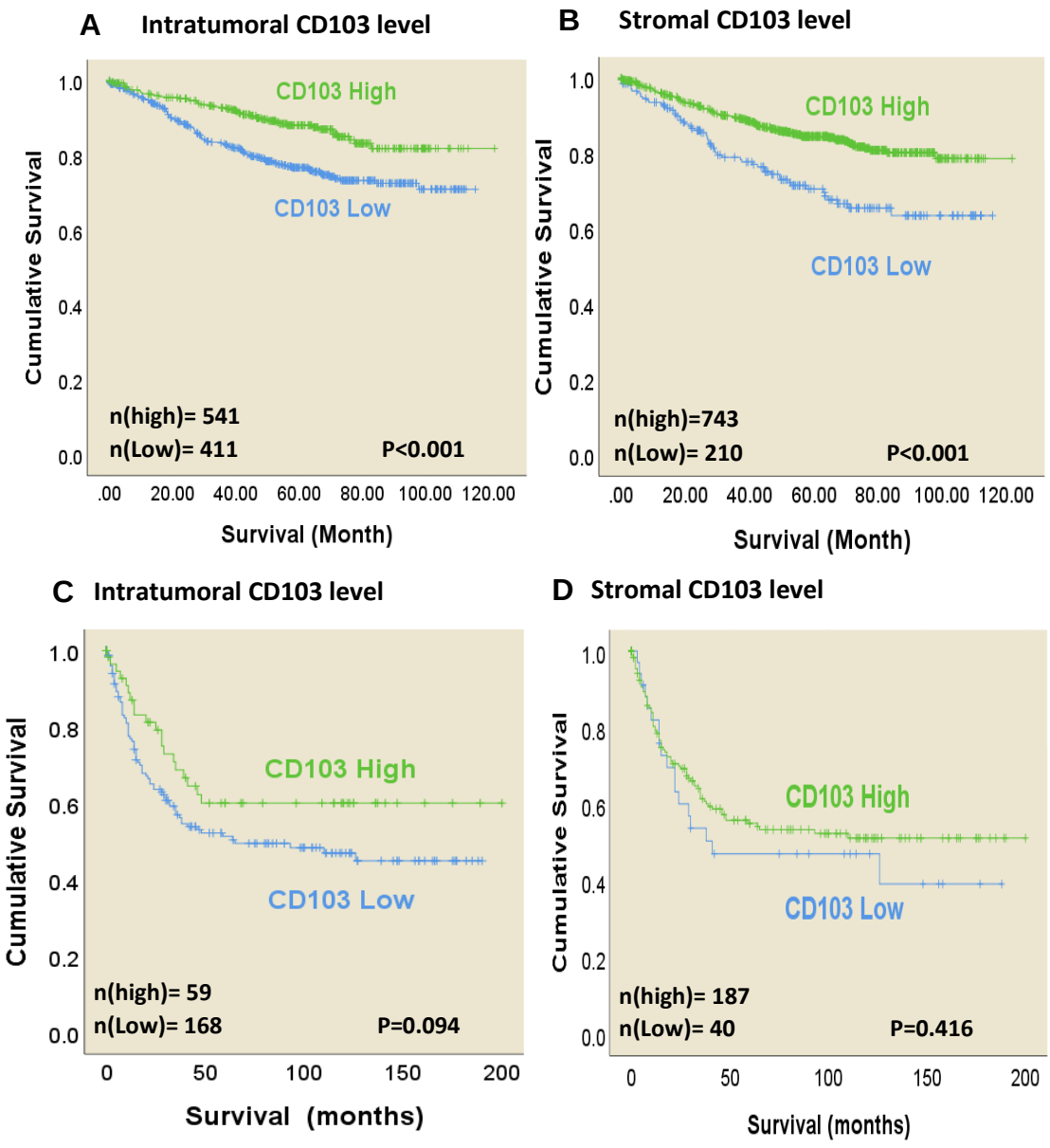

Figure 5. 3 Kaplan-Meier plots represent disease-specific survival probability for the high density group verus low density group of : (A) Intratumoural CD103+ TILs in Cohort (1); (B) Stromal CD103+ TILs in Cohort (1); (C) Intratumoural CD103+ TILs in Cohort (2); (D) Intratumoural CD103+ TILs in Cohort (2). p values <0.05 were considered statistically significant

5.2.4 Correlations of intratumoral CD103+ TILs levels with clinicopathological variables and other immune cell infiltrates

We further analysed the relationship between CD103+ TILs and other immune cells infiltrates (CD3+ and CD8+ TILs). Pearson correlation analyses showed that intraepithelial CD103 strongly correlated with intraepithelial CD3+ and CD8+ TILs (p=0.000, table 5.2). Fifty-nine per cent of tumours in $CD3^{hi}$ density group had high CD103+ TILs levels, while 75% of tumours in $CD8^{hi}$ density group showed high CD103+ TILs levels. Also, it was found that some clinicopathological variables such as tumour primary site, tumour grade, microsatellite status, vascular invasion, TNM stage and the regional lymph node metastasis were significantly associated with CD103+ TILs (p<0.05, table 5.2).

Table 5. 2 Correlations between intraepithelial CD103 TILs and other intratumoral immune infiltrates and the clinicopathological parameters in cohort (1). The average density of CD103+ TILs was calculated by dividing the total cell number of all tumour regions on the total tumour areas. Pearson's χ^2-tests were used to determine the significance of the correlation between different markers. p- values <0.05 were considered statistically significant.**

		Average Intraepithelial CD103+ T cells			
		Low (%)	**High (%)**	**Pearson Chi-Square**	**P-value**
Average Intraepithelial CD3+ T cells	**Low**	282 (86.2%)	45 (13.8%)	173.56	**<0.001**
	High	253 (41%)	356 (59%)		
Average Intraepithelial CD8+ T cells	**Low**	604 (80%)	150 (20%)	157.956	**<0.001**
	High	49 (25%)	148 (75%)		
Gender	**Male**	306 (56.9%)	232 (43.1%)	.001	.972
	Female	235 (56.8%)	179 (43.2%)		

Age diagnosis	**<=69**	269 (56.3%)	209 (43.7%)	.119	.730
	>69	272 (57.4%)	202 (42.6%)		
Tumour site	**Right colon**	226 (51.5%)	213 (48.5%)	11.313	**.010**
	Left colon	208 (60.8%)	134 (39.25%)		
	Rectal	92 (64.8%)	50 (35.2%)		
Tumour grade (differentiation)	**Well**	10 (52.6%)	9 (47.4%)	6.344	**.042**
	Moderate	492 (58.2%)	354 (41.8%)		
	Poor	38 (44.2%)	48 (55.85%)		
Microsatellite status	**MSS**	482 (61.6%)	300 (38.4%)	49.523	**<0.001**
	MSI	48 (31%)	107 (69%)		
Vascular invasion	**Absent**	231 (48.3%)	247 (51.7%)	32.493	**<0.001**
	Present	307 (66.7%)	153 (33.3%)		
TNM stage	**1**	62 (40%)	93 (60%)	32.757	**<0.001**
	2	217 (55.9%)	171 (44.1%)		
	3	184 (60.5%)	120 (39.5%)		
	4	78 (74.3%)	27 (25.7%)		
N -Regional lymph nodes	**N0 (no lymph node metastasis)**	293 (53.7%)	253 (46.3%)	8.827	**.003**
	N1 (Regional lymph node metastasis)	243 (63.4%)	140 (36.6%)		

** Correlation tests were conducted on Cohort (1) only due to the lack of information about CD3+ and CD8+ TILs in Cohort (2)

5.2.5 The impact of colorectal cancer sidedness and microsatellite instability on patient survival

Several studies have reported conflicting results regarding the prognostic impact of tumour sidedness in colorectal cancer. However, the survival difference between

right-sided colon cancer, left-sided colon cancer and rectal cancers remains controversial. In this study, the role of tumour sidedness and microsatellite instability in colorectal tumours were investigated by performing a univariate analysis of each factor. Kaplan-Meier curves in figure 5.4.A indicate that there is no significant difference in patient survival between right colon cancers (mean DSS 93 months), left colon cancer (mean DSS 99.5 months) and rectal cancer (mean DSS 98 months) in Cohort (1). In conformity with the data obtained on Cohort (1), figure 5.4 (B) shows that there is no difference in the mean DSS between patients with different primary location in Cohort (2) (mean DSS for RCRC is 106.3 months; LCRC is 108.3 months; RC 105.3 months; p=0.686).

The role of MSI status in CRCs as a predictive tool was investigated in the two independent cohorts. Interestingly, no significant correlation between patients' survival and MSI status was observed in both cohorts for all CRC cases (Figure 5.4 C and D). However, plotting survival curves among different primary tumour locations demonstrated a significant prognostic value of MSI status only in patients with RCRC (Figure 5.4 E, p= 0.016), while patients with LCRC had no significant difference in mean DSS between MSI and MSS tumours. The latter analysis was conducted on Cohort (1) only due to the limited number of MSI cases in LCRC patients of Cohort (2).

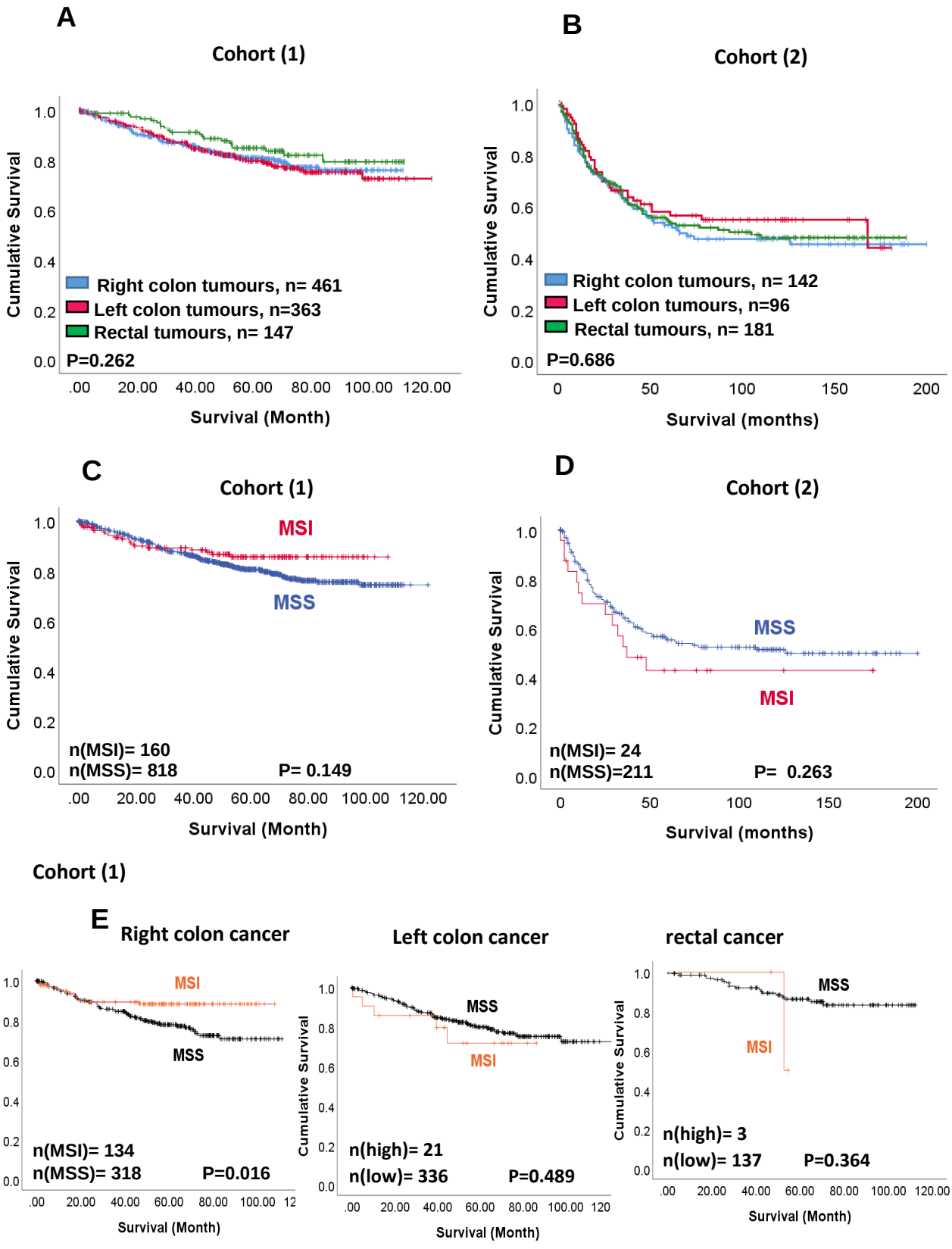

Figure 5. 4 Kaplane-Meier plots for disease-specific survival for (A) patients with right colon cancer, left colon cancer and rectal cancers in Cohort (1) ; (B) patients with right colon cancer, left colon cancer and rectal cancers in Cohort (2); (C) patients with MSI and MSS colorectal tumours in Cohort (1); (D) patients with MSI and MSS colorectal tumours in Cohort (2). (E) patients with MSI and MSS tumours in the right colon cancer, left colon and rectal cancers in Cohort (1). Log-rank test was used to test the statistical significance. p values <0.05 were considered statistically significant

5.2.6 CD8+ and CD103+ TILs infiltration between different colorectal cancer sidedness and microsatellite instability status tumours

Although It has been confirmed that CRC prognosis varies significantly based on the primary tumour locations (PTLs), we demonstrated earlier that colorectal cancer sidedness and microsatellite instability status by themselves are not the main contributors to these survival differences. Accordingly, we hypothesised that the differences in genetic alterations between different PTLs lead to significant differences in immune infiltration, which might mediate some of these survival differences between the right side- colon and left-side-colon and rectal cancers. Thus, we compared the average densities of CD8+ TILs and CD103+ TILs among CRCs from different PTLs. Figure 5.5 A demonstrates significantly higher levels of intraepithelial CD8+ and CD103+ TILs in the right-side colon tumours (median density:CD8=65.5 ; CD103= 172 cells/mm^2) compared to the left side colon (median density:CD8=36.4; CD103= 125 cells/mm^2) and rectal tumours (median density:CD8=35.5; CD103= 113.6 cells/mm^2).

As previously demonstrated in studies on CRC tumours, right-sided
colon cancers had higher rates of microsatellite instability[275]. Therefore, we also compared the numbers of intraepithelial CD8+ and CD103+ TILs between MSI patients and MSS patients. As per our expectations, lower median densities of intraepithelial CD8+ and CD103+ TILs were observed in MSS tumours (39 and 120 cells/mm^2, respectively) compared to MSI tumours (106 and 365 cells/mm^2, respectively). Moreover, intraepithelial CD103+ TILs levels were significantly higher in both MSI and MSS tumours than intraepithelial CD8+ TILs (figure 5.5 B), which indicates the presence of intraepithelial CD103+CD8-TILs within CRCs.

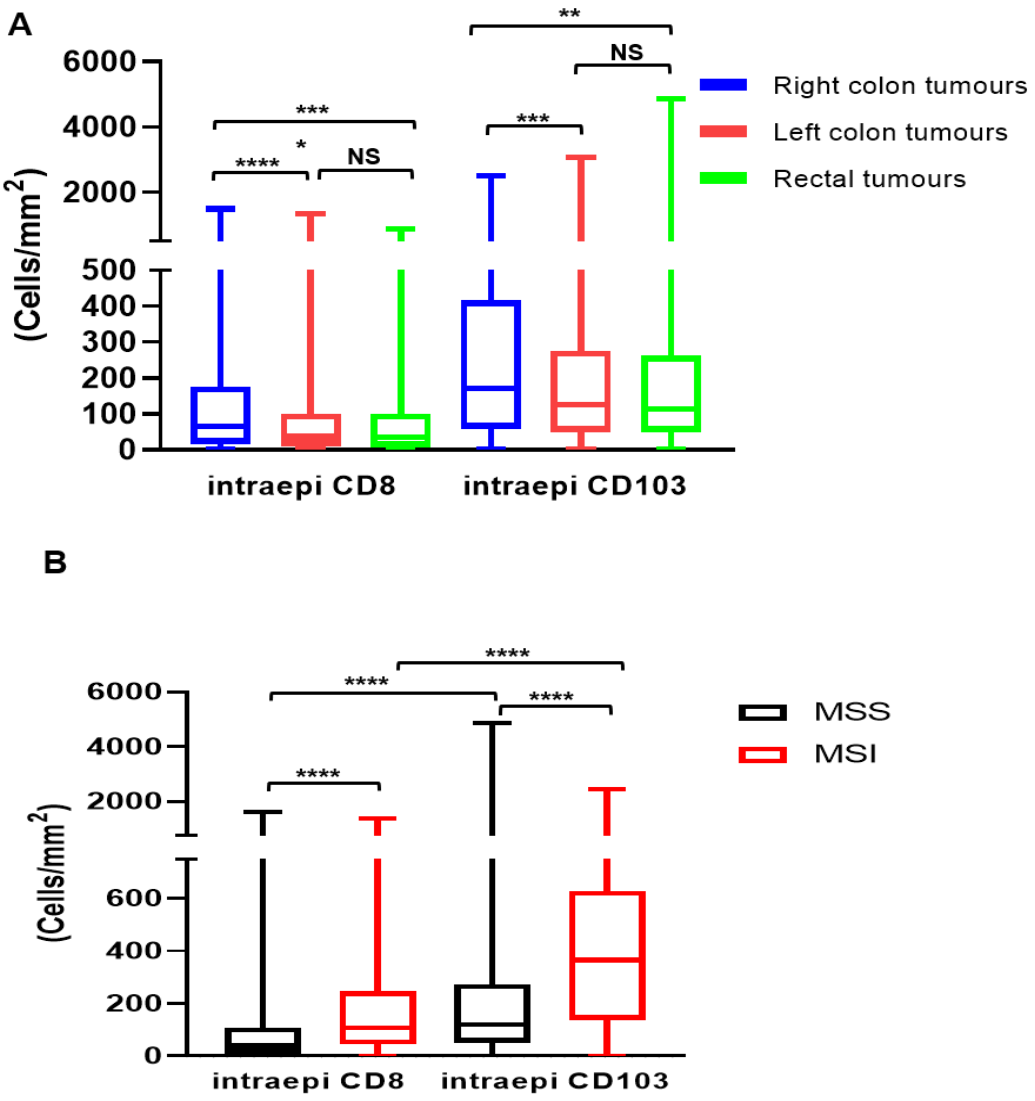

Figure 5. 5 Comparison of intraepithelial CD8+TILs and CD103+ TILs densities between (A) right colon cancer, left colon cancer and rectal cancers (B) MSI and MSS colorectal tumours.

The density of the cells was recorded as cells per mm^2. The middle line represents median densities. Mann-Whitney test was performed to test for significance. ns if $p > 0.05$, *$p \leq 0.05$, ** $p \leq 0.01$,*** $p \leq 0.001$, **** $p \leq 0.0001$

5.2.7 Enhanced CD103+ cells response in the right colon cancer

Following the above results, the predictive impact of heterogeneous CD103+ infiltration among different CRC primary tumour locations was determined and confirmed on patients from Cohort 1 and Cohort 2. In accordance with our hypothesis, Kaplan- Meier plots in Figure 5.6 (A) show that the presence of high intraepithelial CD103+ TILs significantly predicts DSS in right-sided colon tumours, while no significant difference in DSS was found between $CD103^{hi}$ and $CD103^{lo}$ density groups in the left-sided colon and rectal cancers from Cohort 1. These observations were confirmed in Cohort 2 (Figure 5.6 B).

In a Cox multivariate regression model (Table 5.3) combining the prognostic clinicopathological variables (TNM stage, vascular invasion and tumour grade), MSI status and intraepithelial CD103+ TILs in right colon cancers of cohort 1, only TNM stage, tumour grade and intraepithelial CD103+ TILs remained significant for DFS in RCRC patients. In contrast, vascular invasion were no longer significant ($p > 0.05$) for DFS in those patients. In conclusion, intraepithelial CD103+ TILs was found as an independent prognostic factor, whereas the predictive value of MSI status in RCRC patients was dependent on the TNM stage, tumour grade and intraepithelial CD103+ TILs.

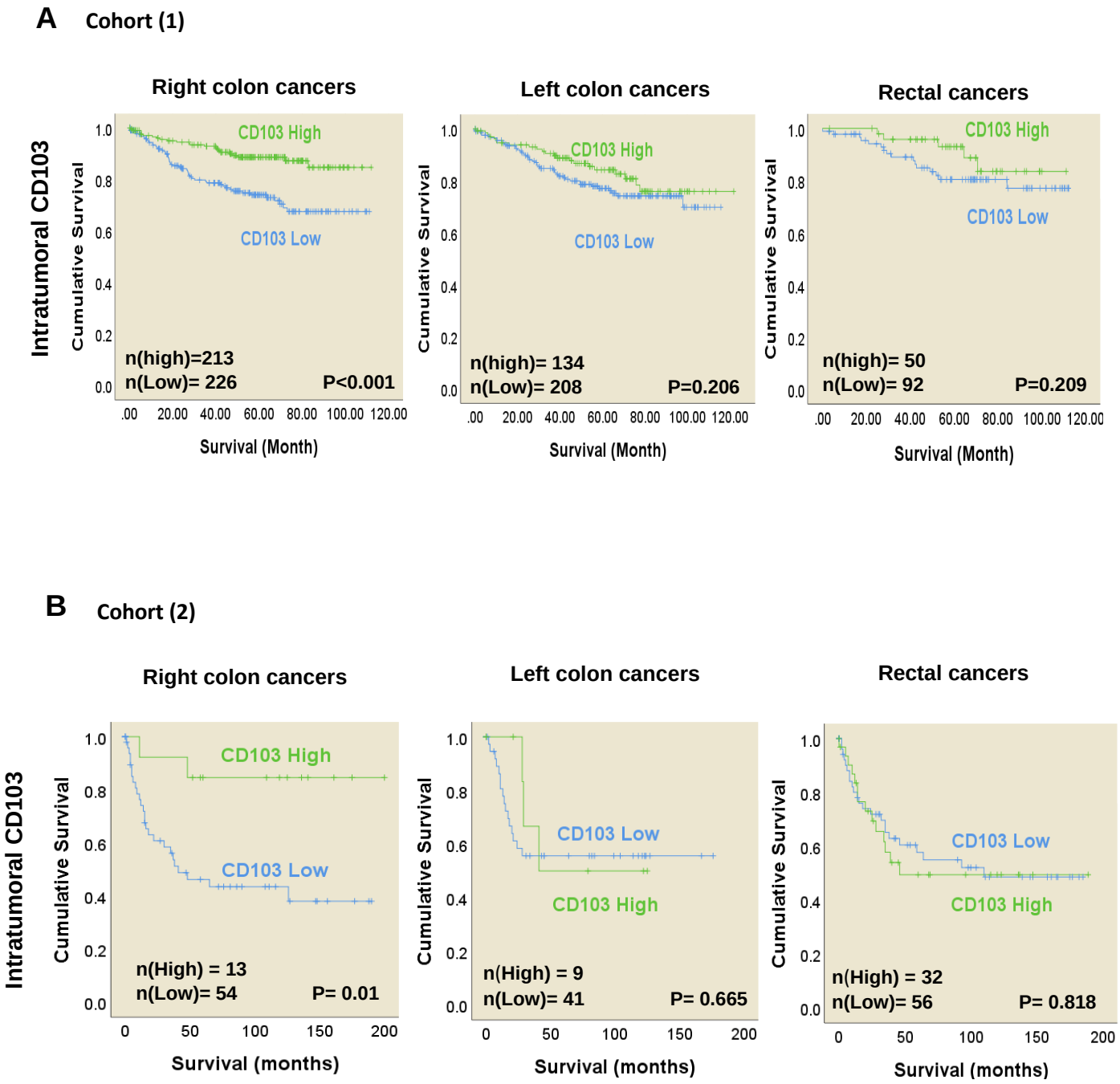

Figure 5. 6 (A and B) Kaplan- Meier plots representing the prognostic effect of CD103 in the right colon cancer, left colon cancer and rectal cancers from Cohort (1) and Cohort (2), respectively. RCRCs patients in both CRC cohorts showed better survival rates with high CD103+ TIL density within the tumour nest. A Log-rank test was used to test significance. p values less than 0.05 were considered significant.

Table 5. 3 Multivariate Cox regression analysis model for vascular invasion, TNM Stage, tumour grade, MMR status and combined Intraepithelial CD103+ cells in RCRCs. Multivariate analysis was performed by Cox regression proportional hazard analysis to test for confounders and the predictive independency of Intraepithelial CD103+ T cell infiltration from standard prognostic/predictive factors. The log-rank test was used to test for significance. p- values <0.05 were considered statistically significant.

Variable	HR	95% CI		P-value
		Lower	Upper	
TNM stage	3.102	2.384	4.038	<0.001
Vascular invasion	1.478	0.960	2.276	0.076
Tumour grade	2.415	1.373	4.245	0.002
MMR status	1.010	0.514	1.982	0.978
Intraepithelial CD103+ TILs	0.374	0.215	0.651	**0.001**

5.3 Discussion

In this study, the role of CD103+ TILs as a prognostic and predictive factor in CRCs in general and specifically between different primary locations (right-sided colon, left-sided colon and rectal cancers) was demonstrated and confirmed in two independent cohorts. Despite the controversial debate on the differences in disease prognosis and responses to treatments between the right-side colon and left-side colon and rectal cancers, we confirmed that neither the primary tumour location nor MSI status was the direct predictor of patient survival. Accordingly, we suggested that the significant differences in the genetic alterations promoted the heterogeneous immune infiltration among PTLs, which might be a superior predictor of patient survival. Therefore, we compared the average density of intraepithelial CD8+ TILs and CD103+ TILs between different PTLs and MSI status of CRCs. Right-sided colon tumours were associated with significantly higher infiltration of intraepithelial CD8+ TILs and CD103+ TILs

compared to left-side colon and rectal cancers. Furthermore, we have shown that MSI tumours, which are predominantly found in the right-sided colon tumours, have more levels of intraepithelial CD8+ TILs and CD103+ TILs than those with MSS. High infiltration of intraepithelial CD103+ TILs was an independent predictor of patient survival in the right-sided colon tumours only.

The characterisation, proliferation and function of TRM cells have been extensively studied in recent years. There are a few studies providing evidence that greater density of CD103+ TILs in tumours was predictive of a better survival outcome in various types of solid tumours. [247, 248, 249, 252] In CRC, the prognostic significance of CD103+ TRM cells was investigated by a limited number of studies with small sample size.[388] Thus, two large independent cohorts (cohort 1, n= 1000; cohort 2, n=462) were used in this study to determine and confirm the role of CD103 TILs in CRCs. Our results showed that high average density of intraepithelial and stromal CD103+ TILs was associated with better patient survival in all cases of CRCs.

Similar to the distribution pattern of CD3+ T cells and CD8+ T cells we mentioned earlier (chapter 4) in the normal tonsil tissue, CD103+ TILs were located mainly in the interfollicular area where most of the T cell populations are. This observation indicates that the majority of CD103+ cells are a subset of CD8+ T cells. Similar findings were reported by *Wang, B. et al.,* who showed that CD103+ TILs were significantly associated with CD8 TILs and showed a related distribution pattern to CD8+ TILs within breast cancer tissues.[249] In CRC, we confirmed that intraepithelial CD103 TILs strongly correlated with intraepithelial CD3+ TILs and CD8+ TILs. However, several studies revealed that two CD103+ TILs subsets were present in the intestine, which are CD103+CD8+ and CD103+CD4+ TILs, with a lesser proportion of the latter subset.[391, 392]

Recently, the PTL of CRC has drawn attention due to various biological and clinical differences, including embryonic origin, vascular supply, disease prognosis and the response to treatments.[279, 284] Several studies revealed that patients with advanced RAS wild-type left-sided colon or rectal cancers have a better prognosis than those with right-sided colon cancers.[393, 394] According to *Qiu, M.Z. et al.* [395], right-sided colon cancer patients were older, more often females, with larger tumour sizes, more advanced T and N stage, and more poorly differentiated tumours compared to left-sided colon or rectal cancers. However, a study conducted by *Weiss et al.* illustrated that after adjusting for various variables, no overall difference in 5-year mortality between right- and left-sided colon cancer was observed.[396] In this study, we aimed to investigate the role of colorectal tumour sidedness as an independent predictive factor with the entire CRC cohort with no specific subdivisions. Our results demonstrated that there is no significant difference in DSS between patients with right-sided colon, left-sided colon or rectal cancers, which indicates that different PTL does not have a direct effect on patients' survival.

Following the above results, we compared DSS of patients with MSI tumours and MSS tumours across all CRC cases. Interestingly, no relationship was found between MSI status and disease prognosis. This observation contradicts with some published studies, which reported an independent prognostic value of the microsatellite instability status for survival.[397] Thereby, we further investigated the prognostic significance of MSI status among different PTLs. Patients with MSI tumours showed prolonged survival only in right-sided colon cancer. The explanation for the latter observation could be related to the fact that MSI tumours are significantly more in RCRCs. In contrast, much lower MSI cases were found in the left-sided colon or rectal cancers.[275, 279] Another suggestion is that microsatellite instability might influence the clinical outcome in right-sided colon cancer by increasing the presence and functionality of tumour specific effector memory T cells.[274]

The heterogeneous immune infiltration of CD8+ TILs and CD103+ TILs between right-sided colon cancers, left-sided colon or rectal cancers were reported in this study. Significantly higher numbers of intraepithelial CD8+ TILs and CD103+ TILs were found in patients with right-sided colon cancers in comparison to the left-sided colon or rectal cancers. Expectedly, intraepithelial CD8+ TILs and CD103+ TILs levels were higher in MSI tumours compared to MSS counterparts. The prognostic significance and cytotoxic activity of CD8+ TILs in right-sided colon cancers was illustrated by Zhang, L and colleagues. In contrast, they found that left-sided colon or rectal cancers were associated with a higher degree of infiltration of the antitumour CD56 NK cell subpopulation and that the presence of these cells significantly correlated with patient survival.[284] In this study, we focused on the prognostic value of intraepithelial CD103+ TILs among different PTLs of CRCs. By conducting univariate and multivariate analyses, we confirmed that intraepithelial CD103+ TILs is an independent predictor of patient survival in right-sided colon cancers, whereas no relationship between intraepithelial CD103+ TILs and patient survival was observed in the left-sided colon or rectal cancers.

Finally, we have demonstrated that intraepithelial CD103+ TILs levels were significantly higher than intraepithelial CD8+ TILs regardless of tumour sidedness or MSI status of CRCs. Thus, we suggest that intraepithelial CD103+ TILs consisted of CD103+CD8+ TILs and CD103+CD8-TILs subsets in CRCs. The importance of CD103+CD8+ TILs as a stronger prognostic factor with favourable prognosis in comparison to single positive subsets was reported in high-grade ovarian cancers and basal like-breast cancers.[249, 252] Accordingly, our next step is to focus on the localisation and function of CD103+CD8+TILs subset by utilising a reliable multi-staining tool, which facilitates the detection of triple, double and single positive TILs.

Chapter 6: Identification and Immunolocalisation of tumour- reactive resident CD8 T Cells in the right, left colon cancer and rectal cancer

6.1 Introduction

The heterogeneity of the immune contexture and phenotypic profiles of tumour-infiltrating lymphocytes (TILs) between patients or individual tumours have resulted in unpredictable responses to immunotherapy. [398, 399, 400, 401] In 2009, Camus et al. first classified primary CRCs according to the quantity of TILs present within the tumour into three major immune coordination profiles (hot, altered and cold). The 2-year risk of relapse for these three types of tumour was 10%, 50% and 80%, respectively. [245] According to *Galon et al.*, the terms 'hot' and 'cold' are generally used to refer to T cell- infiltrated, inflamed but non- infiltrated, and non- inflamed tumours, reflecting well the lower (I0) and the higher (I4) the Immunoscore categories.[239] The altered phenotype included two distinct patterns — 'excluded' and 'immunosuppressed'. [402] These four characteristic subgroups emerged to potentially represent a practical tool to direct treatment approaches.

Numerous studies have investigated the significance of different phenotypic profiles of TILs in a wide variety of solid tumours. Among different TILs types, tumour-infiltrating CD8+ T cells showed the utmost importance in anti-tumour immunity and were considered as one of the best predictors of survival in many cancer types.[247, 403, 404, 405, 406] Further research conducted on different CD8 TILs subtypes in breast cancer, NSCLC and HGSC, illustrated the prognostic superiority of resident memory CD103+CD8+ TILs and suggested that this subset contained tumour-reactive CD8 T cells, in comparison to CD8+ TILs lacking CD103.[247, 250, 252] Moreover, a study

conducted by *Ganesan et al*. using transcriptomic profiling of CTLs from patients with lung tumours, showed that CD103+ CD8 TILs were highly activated, had features of enhanced cytotoxicity and proliferation, and displayed a TRM gene signature. Interestingly, it was reported that hot tumours (heavily infiltrated with TILs) showed enrichment for TRM cells. Heavily infiltrated tumour with CD8+ and CD103+ TILs were associated with higher expression of molecules which are effective targets of immunotherapy (such as PDCD1, TIM3 and LAG3), and molecules with important functions in modulating the magnitude and specificity of anti-tumour immune responses (such as CD39; a cell-surface ectonucleotidase that dephosphorylates ATP to AMP). [246]

The role of CD39 in tumour specificity was investigated by a few studies. According to Simoni and colleagues, a population of tumour infiltrating CD8+ T cells in the lung and colorectal cancers were not specific for tumour antigens and described as 'bystanders'. These bystanders CD8+ TILs were characterised by diverse phenotypes that overlap with tumour specific cells, recognise a broad range of epitopes unrelated to cancer, and lack CD39 expression.[255] Therefore, CD8+CD39+TILs were considered tumour specific T cells. This subset was enriched in the expression of genes related to exhaustion and cell proliferation, justified by the presence of chronic antigen stimulation. [407, 408, 409] Although all the tumour-specific CD8+ TILs obtained resident memory T cell-like features and expressed various co-stimulatory and inhibitory receptors, such as PD-1, CTL-4 and TIM-3. Many of the bystander CD8+ TILs also expressed CD103, suggesting that tumour infiltrating CD8+CD103+TILs were present as both tumour specific and bystander CD8+ TILs.[255]

Furthermore, *Van Duijn et al.* suggested that the expression of CD39 does not indicate exhaustion only; it also reflects the activation of CD8+TILs. This speculation was based on their observation that CD8+CD39+ TILs were able to produce more

IFN-γ compared to CD8+CD39− TILs in both atherosclerotic lesions and spleen. However, CD39 can catalyse the conversion of ATP to adenosine, which has been shown to have immunosuppressive activity. [253, 410] Interestingly, CD39 inhibition induced by sodium metatungstate (POM-1) showed a dose-dependent increase in IFN production by all CD8+ TILs population with a higher increment in CD8+CD39- TILs in comparison to CD8 TILs with high CD39 expression. This observation suggests that CD39 expression may modulate the cytokine responses of both CD39+ and CD39- cells by affecting autocrine and paracrine adenosine signalling. [254]

Recently, a unique tumour microenvironment specific population of CD8+ T-cells co-expressing CD39 and CD103 was identified and studied by Duhen et al. within head and neck tumours. They reported that, in comparison to DP (CD8+CD103+CD39-) T-cells and SP (CD8+CD103-CD39-) T-cells, TP (CD8+CD103+CD39+) T-cells express high levels of exhaustion markers, have a distinct TCR repertoire, own a high frequency of tumour-reactive cells, display a TRM gene signature and are capable of recognising and killing autologous tumour cells. Also, a greater overall survival in head and neck cancer patients was found when associated with high TP T-cells density compared to other subtypes.[258]

In the previous chapter, we showed that CD8TILs and CD103+ TILs were more infiltrated into RCRCs compared to LCRCs. Also, CD103+ TILs were found to be independent predictors of patient survival in RCRCs only. According to the studies discussed above, CD8+ TILs and CD103+ TILs are heterogeneous populations consisted of bystander subsets and specific subsets of TILs that are responsible for recognising and killing cancer cells. In this chapter, we hypothesised that recently activated tumour specific TRM cells recognised by the co-expression of CD39 and CD103 on CD8TILs would be the most important tumour infiltrating CD8+TILs subtype that obtains an additive benefit to CRCs patients' clinical outcome regardless

of the conventional Immunoscore status (hot vs cold) or the tumour sidedness of CRCs. In order to examine our hypothesis, we conducted a multiplex detection method to localise and quantify four different CD8+ TILs subtypes (CD8+CD103+CD39+ T cells, CD8+CD103+CD39- T cells, CD8+CD103-CD39+ T cells and CD8+CD103-CD39- T cells). Then the numbers of CD8+TILs subtypes were compared based on tumour segmentation (epithelial or stromal), PTL (right colon, left colon and rectal tumours and microsatellite instability status (MSI vs MSS tumours). Finally, overall survival analysis using Kaplan- Meier curves of the four different CD8+ TILs subtypes in all CRCs cases, different PTLs and different TIL density 'Hot vs cold' tumours was performed in this chapter. By doing so, we aimed for a better understanding of the role of different CD8 TILs subtypes in CRCs, as the focus of this study was to identify and recognise new effective immunotherapy targets.

6.2 Results

6.2.1 Multiplex IHC staining for simultaneous detection of CD8, CD103 and CD39 markers

The development of multiplex detection systems such as multiplex Immunohistochemistry/Immunofluorescence (mIHC/IF) technique overcame the limitations associated with conventional IHC, like the capacity to label only one marker per tissue section and high inter-observer variability. [411] TSA-based mIHC/IF, a relative novel strategy, allows performing multiple sequential staining without the concern of cross-reactivity.[412] Therefore, this technique enables simultaneous antibody-based detection and quantification of the expression of up to six protein markers and a nuclear counterstain on a single tissue section.[413] Here, TSA-based mIHC/IF method was utilised for simultaneous detection of 3 biomarkers (CD8, CD103 and CD39) within a single tissue section. An eight-step workflow of the

multiplex detection technique (Figure 6.1) was adopted and implemented to identify, localise, and quantify different cell phenotypes within the TME of CRCs.

Figure 6.1 A, B and C represent the TMA construction of cohort (1) used for this study. Cohort (1) consisted of 4000 TMA cores representing four different locations: the luminal side of the tumour, centre of the tumour, invasive margin and adjacent normal tissue of 1000 colorectal cancer patients. The patient characteristics of cohort (1) were mentioned earlier in chapter (4). Next, TMA slides were treated with three sequential cycles of CD8, CD39 and CD103 antibodies and paired with opal fluorophores 520, 570 and 690, respectively. Then nuclear counterstain of the tissue was conducted with DAPI (Figure 6.1 D). The optimisation of the multiplex staining was mainly concentrated on the order of adding the primary antibodies, blocking duration, pairing the appropriate opal fluorophore to the target antigen, and opal staining duration. The optimisation of these factors is detailed in chapter (2). Multispectral imaging was performed using Vectra 3 automated Imaging System, together with the Phenochart™ whole slide contextual viewer (Figure 6.1 E and F). Digital scanning enabled us to visualise, detect, and measure fluorophores intensity for each TMA core. Furthermore, inForm®, an automated image analysis software, was utilised to analyse multispectral images generated from the previous steps. This software is associated with a spectral unmixing engine. Unmixing feature helped us to identify and separate weakly expressing and overlapping signals from background autofluorescence. Also, we compared the expression of CD8, CD103 and CD39 monoplex staining within the tumour tissue in two different settings: IHC (DAP) view and fluorescence view, to confirm and validate the staining efficacy and specificity for each marker separately (Figure. 6.2).

We next sought to identify and quantify cell phenotypes within tumour epithelium and stroma using the inForm® software (Figure 6.1 G). inForm® is an automated image

analysis software used to visualise and quantify biomarkers accurately in tissue sections. This software, distinguished by a powerful unmixing engine, allows the separation and measurement of overlapping markers in multiplex assays. Using multiplex fluorescence view, six different cell phenotypes TP (CD39+CD103+CD8+), DP (CD103+CD8+), DP (CD39+CD8+), SP (CD8+), SP (CD103+) and SP (CD39+) cells were identified within the tumour microenvironment (figure 6.3). After identifying and visualising different cell phenotypes, inForm® project (1) was initiated to enable biomarker analysis in the 4000 CRC TMA cores. inForm® projects consist of automated, trainable algorithms to perform three analytical steps: tissue segmentation, cell segmentation, and identification of multiple markers within a sample (phenotyping). Figure 6.2 represents inForm® project (1) training steps. The tissue segmentation step involved automated detection and segmentation of specific tissue types depending on tissue morphologies, enabling recognition algorithms to learn and determine different areas for each core. The software labelled tumour epithelium tissue red, whereas the stromal tissue was labelled green. Next, the cell segmentation step was performed regardless of staining heterogeneity and background levels. This step identifies individual cell types in densely packed, complex morphologies for accurate phenotyping (figure 6.4 and figure 6.5).

The phenotyping step was conducted by training and optimising inForm® software to detect and quantify different TIL phenotype subsets. A colour coding system was used to label these subsets, as shown in figure 6.6. TP CD8+CD103+CD39+, DP CD8+CD103+, DP CD8+CD39+, SP CD8+, SP CD103+ and SP CD39+ TILs were labelled with dark blue, light blue, magenta, green, red and yellow dots, respectively. Furthermore, project (1) outputs were reviewed by manually checking all the steps (tissue segmentation, cell segmentation and cell phenotyping) for each TMA. The rejected cores were corrected in a new project, called project (2). Figure 6.7 shows some rejected cores in project (1) being corrected in project (2).

Out of 4000 colorectal TMA cores, 3708 cores were accepted, while the rest were rejected due to loss of tissue, absence of tumour tissue or inaccurately trained even after applying project (2). The data from the accepted cores were merged and processed through R program to produce phenoptrReports. These reports presented a summary of the immune cells densities within the tumour epithelium and stromal tissue for all cores. (figure. 6.1 H).

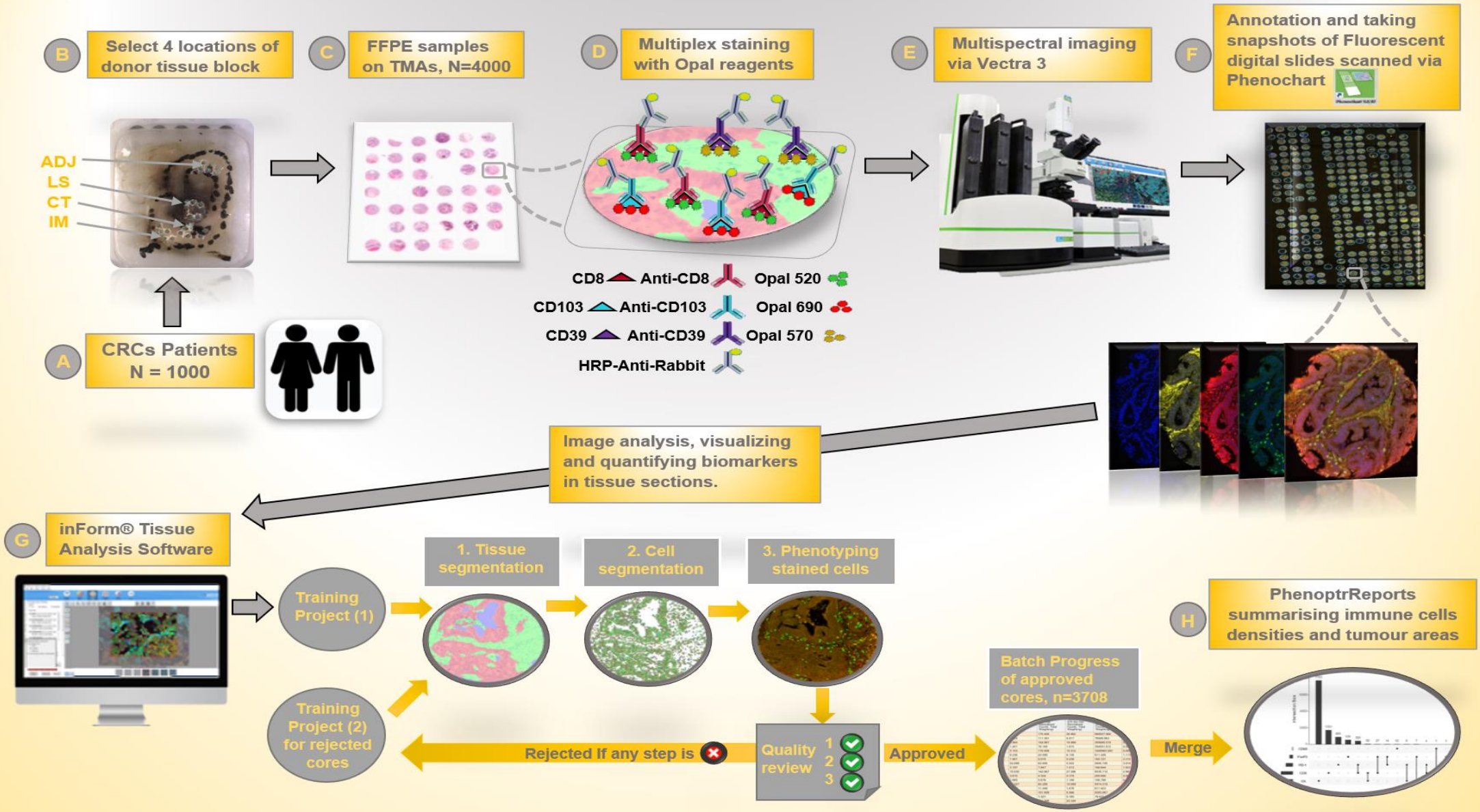
B
Select 4 locations of donor tissue block
C
FFPE samples on TMAs, N=4000
D
Multiplex staining with Opal reagents
E
Multispectral imaging via Vectra 3
F
Annotation and taking snapshots of Fluorescent digital slides scanned via Phenochart
ADJ
LS
CT
IM
A
CRCs Patients N = 1000
CD8 Anti-CD8 Opal 520
CD103 Anti-CD103 Opal 690
CD39 Anti-CD39 Opal 570
HRP-Anti-Rabbit
Image analysis, visualizing and quantifying biomarkers in tissue sections.
G
inForm® Tissue Analysis Software
Training Project (1)
Training Project (2) for rejected cores
1. Tissue segmentation
2. Cell segmentation
3. Phenotyping stained cells
Rejected If any step is
Quality review 1 2 3
Approved
Batch Progress of approved cores, n=3708
Merge
H
PhenoptrReports summarising immune cells densities and tumour areas

Figure 6. 1 Eight steps workflow representing Multiplex detection methodology.

(**A)** CRC primary tumours from 1000 patients (Males 57%,females 43%). **(B)** Samples extracted four different locations of donor tissue block. **(C)** TMA Construction consists of 4000 cores. **(D)** Multiplex staining with Opal 4-color IHC Kit anti-CD8, anti-CD39 and anti-CD103 antibodies were paired with Opal 520, 570 and 690, respectively. **(E)** Vectra 3 Imaging System used for multispectral imaging. **(F)** Phenochart™ viewer was used for annotation and taking snapshots of whole slides. **(G)** inForm® software was used to detect and quantify different phenotypes within the TMA core. InForm® training project enabled tissue and cell segmentation and phenotyping stained cells automatically. The quality of the project outcome was checked, and a new project was used to correct the rejected cores. **(H)** PhenotrReports calculated the densities of the stained cells and the tumour (epithelium and stroma) area

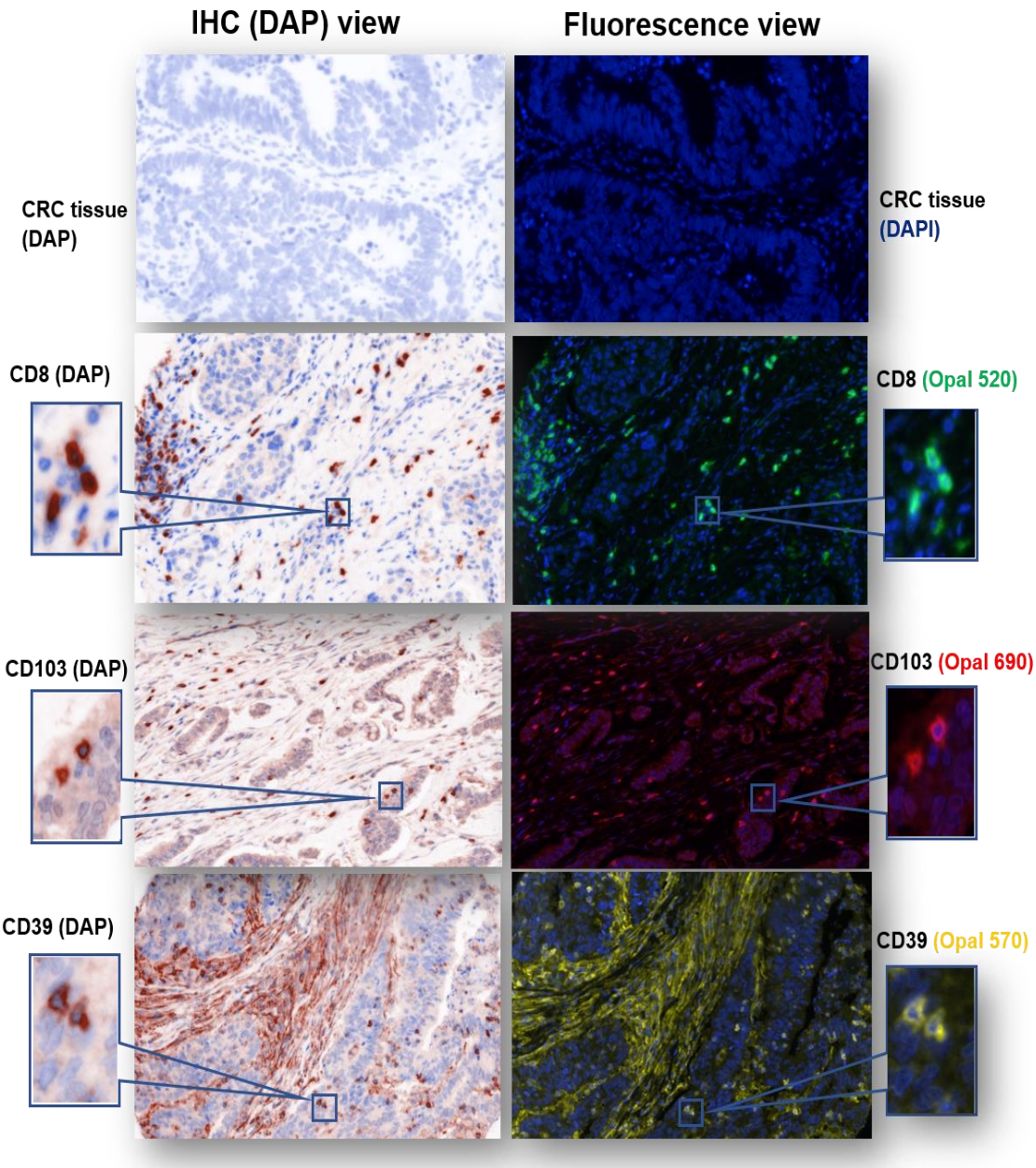

Figure 6. 2 The monoplex expression of CD8, CD103 and CD39 markers within CRCs tissue using DAP view and fluorescence view.

Fluorescence view visualises (1) CRCs tissue nuclear counterstain with DAPI in dark blue; (2) CD8+ cells paired with Opal 520 in green; (3) CD103+ cells paired with Opal 690 in red; (4) CD39+ cells paired with Opal 570 in yallo. Snapshots from each view for positive cells within the same location in tumour tissue were taken using Inform software.

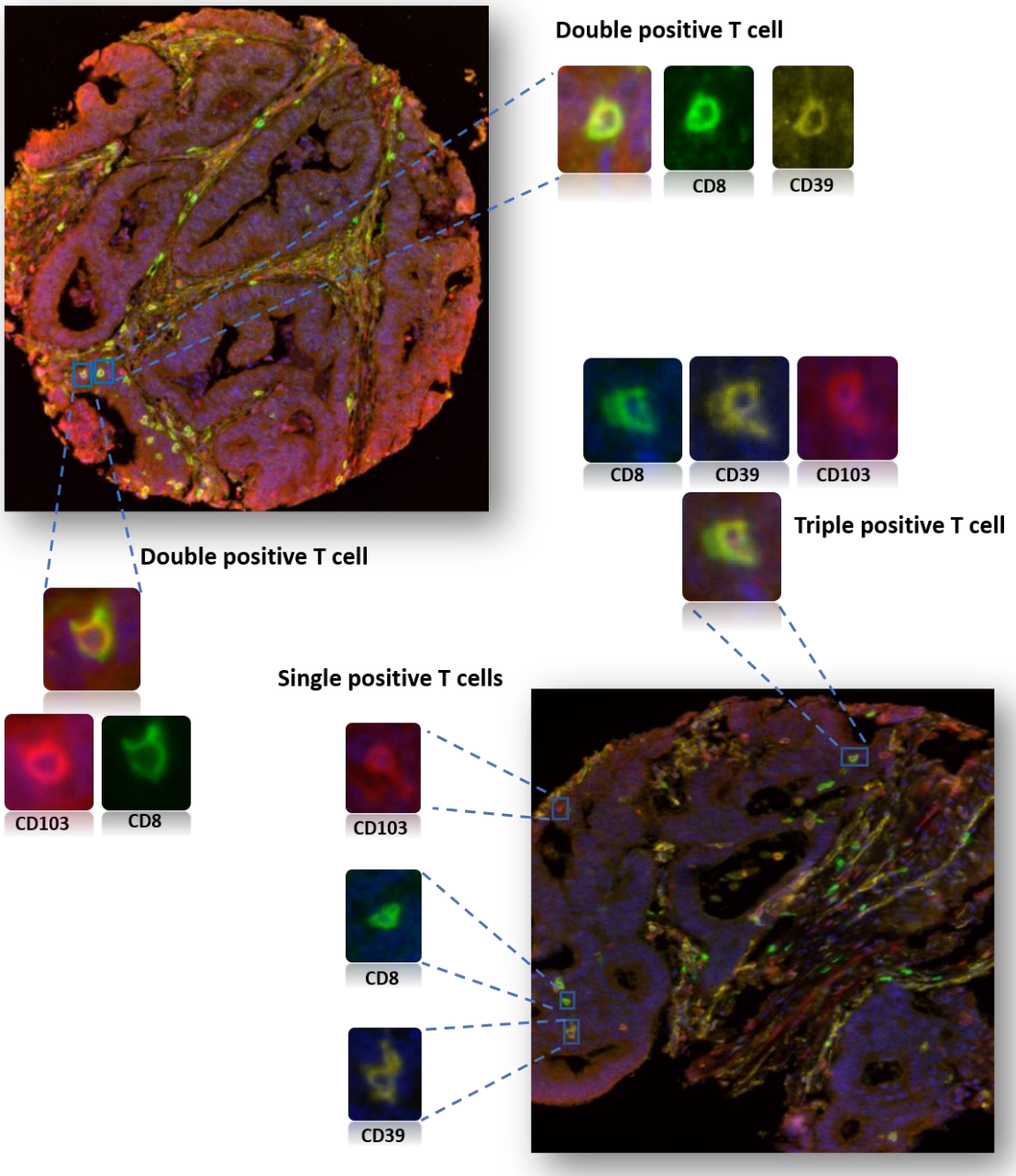

Figure 6. 3 Multiplex view of different CRC TMA cores presenting triple, double and single stained T cells with CD8 (green), CD103 (red) and CD39 (yellow) biomarkers.

Different immune cells phenotypes were Identified and localised within CRCs tissue using multiplex fluorescence view.

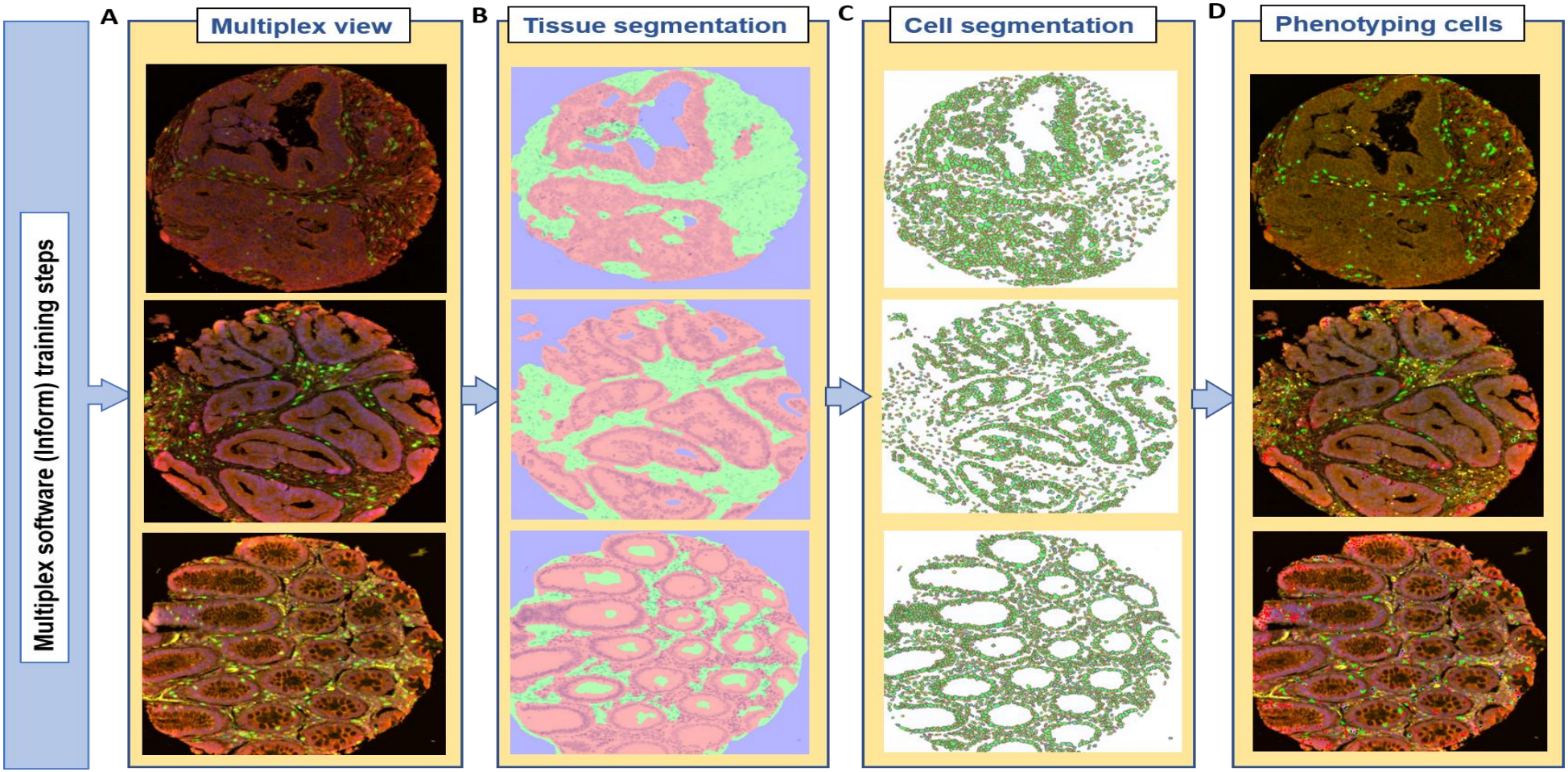

Figure 6. 4 InForm training stages were used to automate the detection and segmentation of CRC tissues through powerful patented pattern recognition algorithms.

(A) represents a multiplex view of tumour core with multistained T cells, **(B)** Tissue segmentation of tumour epithelium (red) and stroma (green). **(C)** Cell segmentation was used to identify individual cell types for accurate phenotyping. **(D)** Cell phenotyping was used to detect and quantify different TIL phenotype subsets.

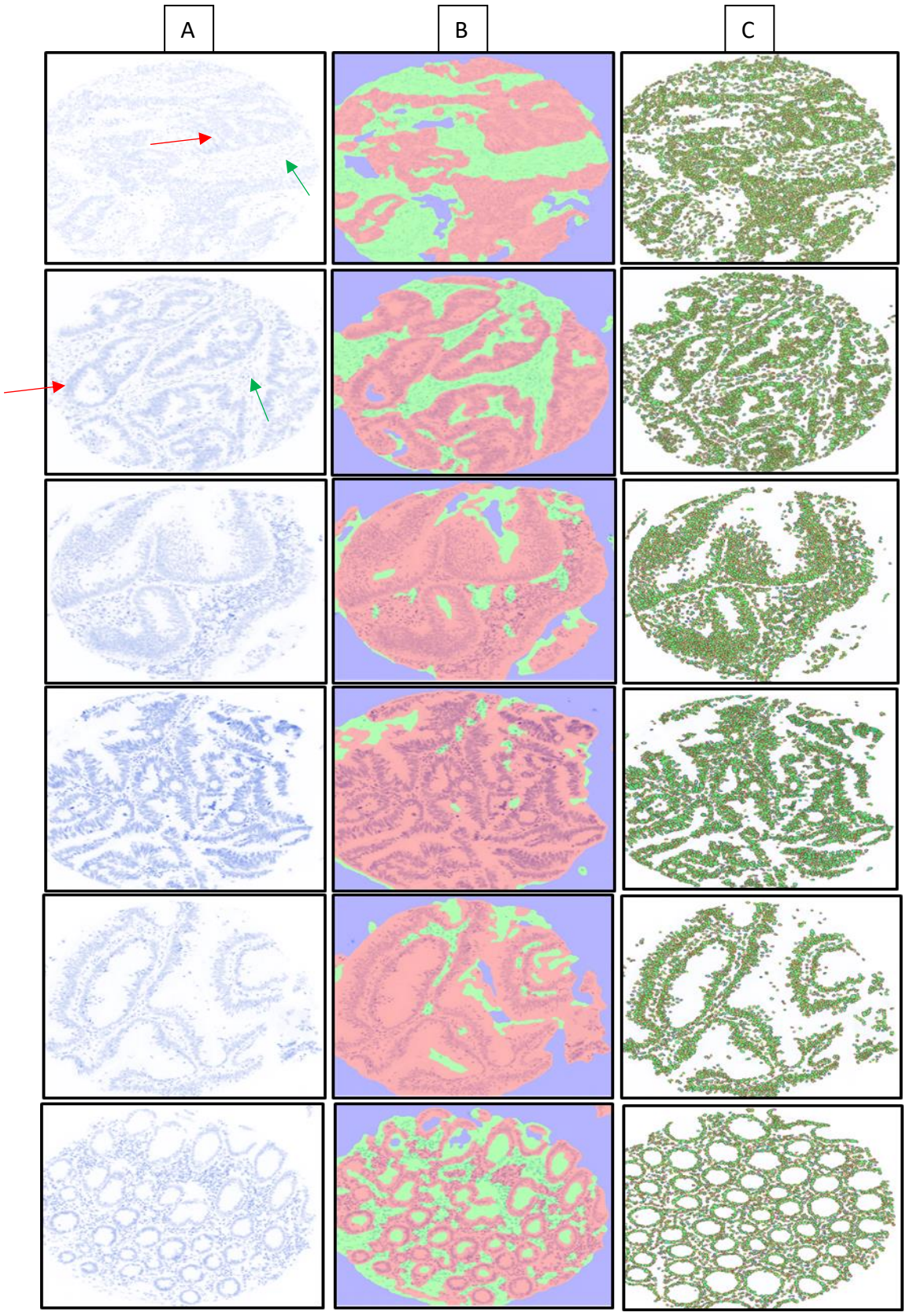

Figure 6. 5 Examples of tissue and cell segmentation compared to standard IHC DAP view.

(A) DAP view CRC TMA showing the epithelium (red arrow) and stromal areas (green arrow)**. (B)** Colorectal cancer TMA into epithelium (red) and stroma (green) using colour coding segments **(C)** All cells segmented individually for accurate cell phenotyping

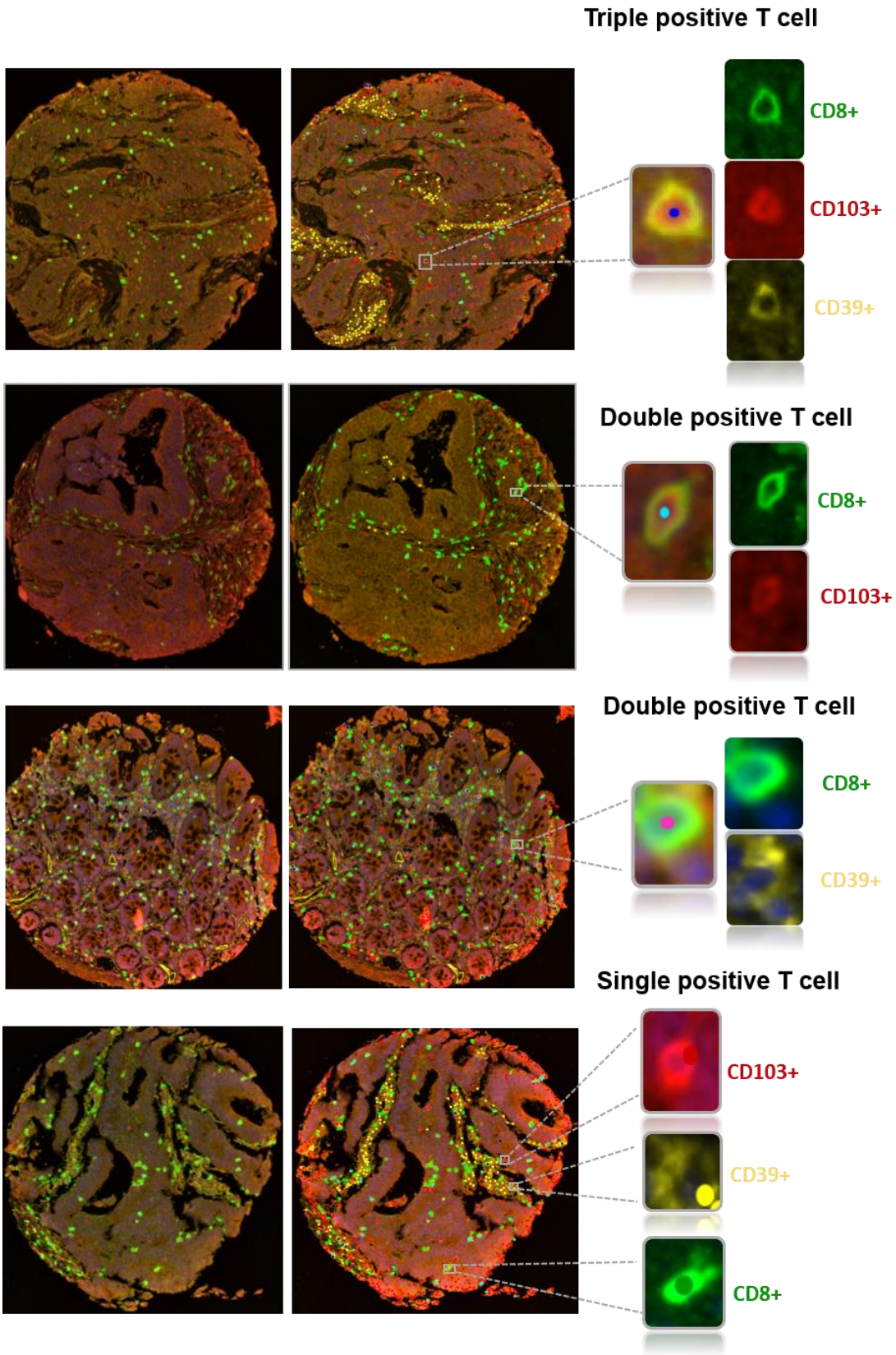

Figure 6. 6 Training and phenotyping multi-stained and single stained cells using colouring- code method on infrom software.

inForm® was trained to detect and quantify six different TILs phenotypes: TP CD8+CD103+CD39+(dark blue), DP CD8+CD103+ (turquoise), DP CD8+CD39+(magenta), SP CD8+ (green), SP CD103+ (red) and SP CD39+(yellow) TILs.

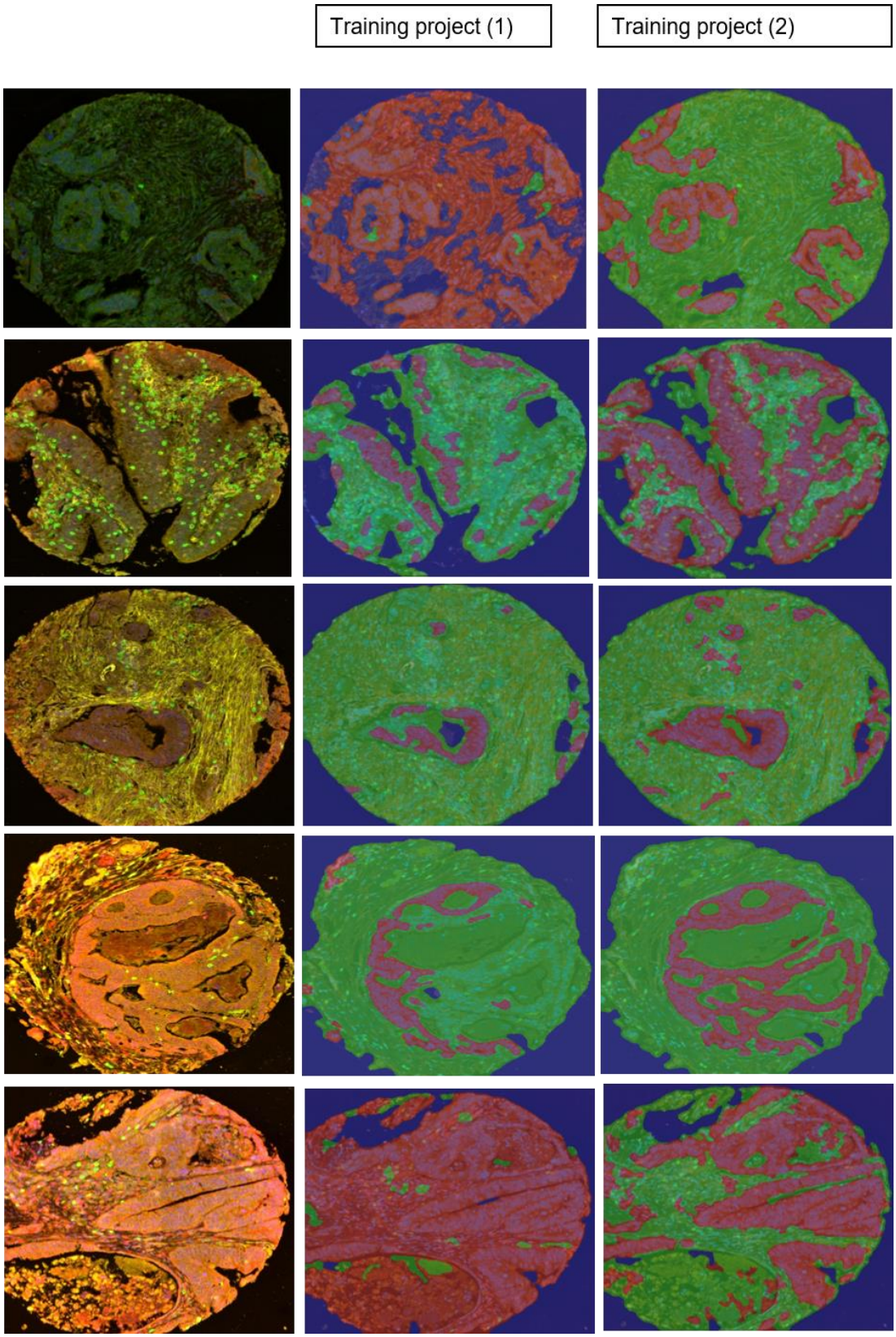

Figure 6. 7 Examples of rejected cores from Project (1) and their corrected matches from Project (2).

The majority of the rejected cores showed inaccurate tissue segmentation from project (1). The rejected cores were corrected in project (2) to obtain better tissue segmentation.

6.2.2 TRM subsets preferentially localised to the intraepithelial compartment within the tumour microenvironment of CRCs

As mentioned earlier, six phenotype subsets were identified, localised, and quantified across CRCs' tumour microenvironment using inform software. However, the focus of the present study was mainly on CD8+ phenotype subsets; therefore, SP CD103+ and SP CD39+ TILs were excluded. Figure 6.8 represent a comparison of the densities of CD8+ T-cells phenotypes (TP CD8+CD103+CD39+, DP CD8+CD103+, DP CD8+CD39+ and SP CD8+ CD103-CD39- TILs) in tumour epithelium and stroma. The results show that TRM subsets (TP CD8+CD103+CD39+T cells and DP CD8+CD103+CD39- T cells) were localised significantly more within the tumour epithelium when compared to the stroma. Interestingly, there was no significant difference in cells number per mm^2 of CD8+ CD103-CD39+ T cells between epithelium and stroma ($p > 0.05$). SP CD8+CD39-CD103- T cells were predominantly present in the stroma, and fewer numbers were seen in the epithelium ($p < 0.0001$).

Although non-resident CD8+ T-cells subsets (lacking CD103) were more infiltrated in CRCs' tumour microenvironment, we hypothesised that these subsets obtain lower prognostic significance than TP CD8+CD103+CD39+ T cells and DP CD8+CD103+CD39- T cells subsets. Therefore, the next step was to determine the prognostic impact of CD8+ T-cells phenotypes on the overall survival of CRCs patients.

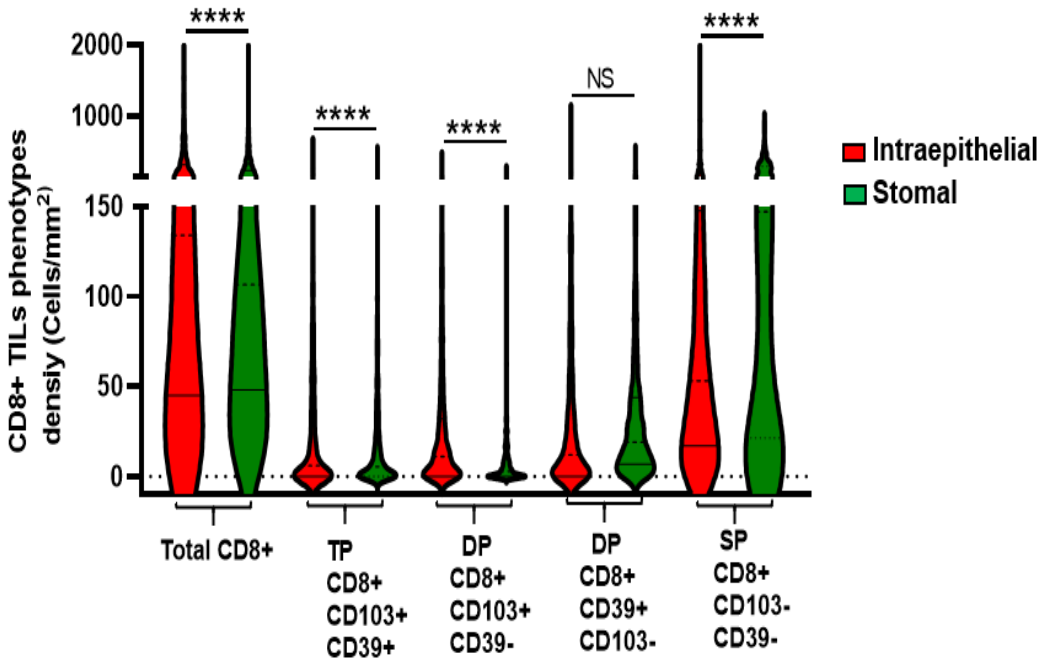

Figure 6. 8 Comparison of the average density of different CD8+ T cell phenotypes in tumour epithelium (red violins) and stroma (green violins) from tissue microarrays of cohort (1).

The violins represent total CD8+ T-cells; TP CD8+CD103+CD39+ T cells; DP CD8+CD103+CD39- T cells; DP CD8+CD103-CD39+ T cells and SP CD8+CD103-CD39- T cells. The density of CD8+ T cells phenotypes was calculated as the number of positive cells per mm^2 of epithelial and stromal tissue. Wilcoxon test was applied to determine the difference in median density of different CD8+ T cell phenotypes. (NS represents $p>0.05$, **** represents $p \leq 0.0001$).

6.2.3 Prognostic significance of different CD8+ T cell phenotypes in colorectal tumours

The prognostic role of CD8+ TILs and CD103+ TILs in CRCs was discussed in previous chapters. However, this chapter aims to identify the prognostic role of different phenotypic profiles of CD8+ TILs in CRCs patients. After analysing the Kaplan Meier survival curves, we found that tumours with high epithelial and stromal total CD8+ T cell infiltration were associated with better survival (Figure 6.9 and 6.10), which is in line with our previous findings using conventional IHC staining (chapter 4.2.8). Furthermore, analysing the four different $CD8^+$ T cell phenotypes CD8+CD103+CD39+(TP); CD8+CD103+CD39-(DP103); CD8+CD103-CD39+(DP39), CD8+CD103-CD39- (SP) showed that the presence of high intraepithelial density of any of these phenotypes was significantly associated with better disease-free survival in CRCs patients (Figure 6.9). In contrast, TP $CD8^+CD103^+CD39^+$ T cells and DP CD8+CD103+CD39- T cells were the only subsets that showed prognostic significance when highly infiltrated in the stroma. (Figure 6.10).

Comparing the prognostic impact of different CD8+TILs phenotypes in the tumour epithelium was further studied by estimating the 10-year survival rates of each phenotype using SPSS software. Among all CD8+ TILs phenotypes, high intraepithelial infiltration of TP cells had the highest survival rate at 10 years after disease diagnosis (92%), whereas lower survival rates were associated DP CD8+CD103+, DP CD8+CD39+ and SP CD8+ CD103-CD39- TILs (86%, 78% and 79%, respectively).

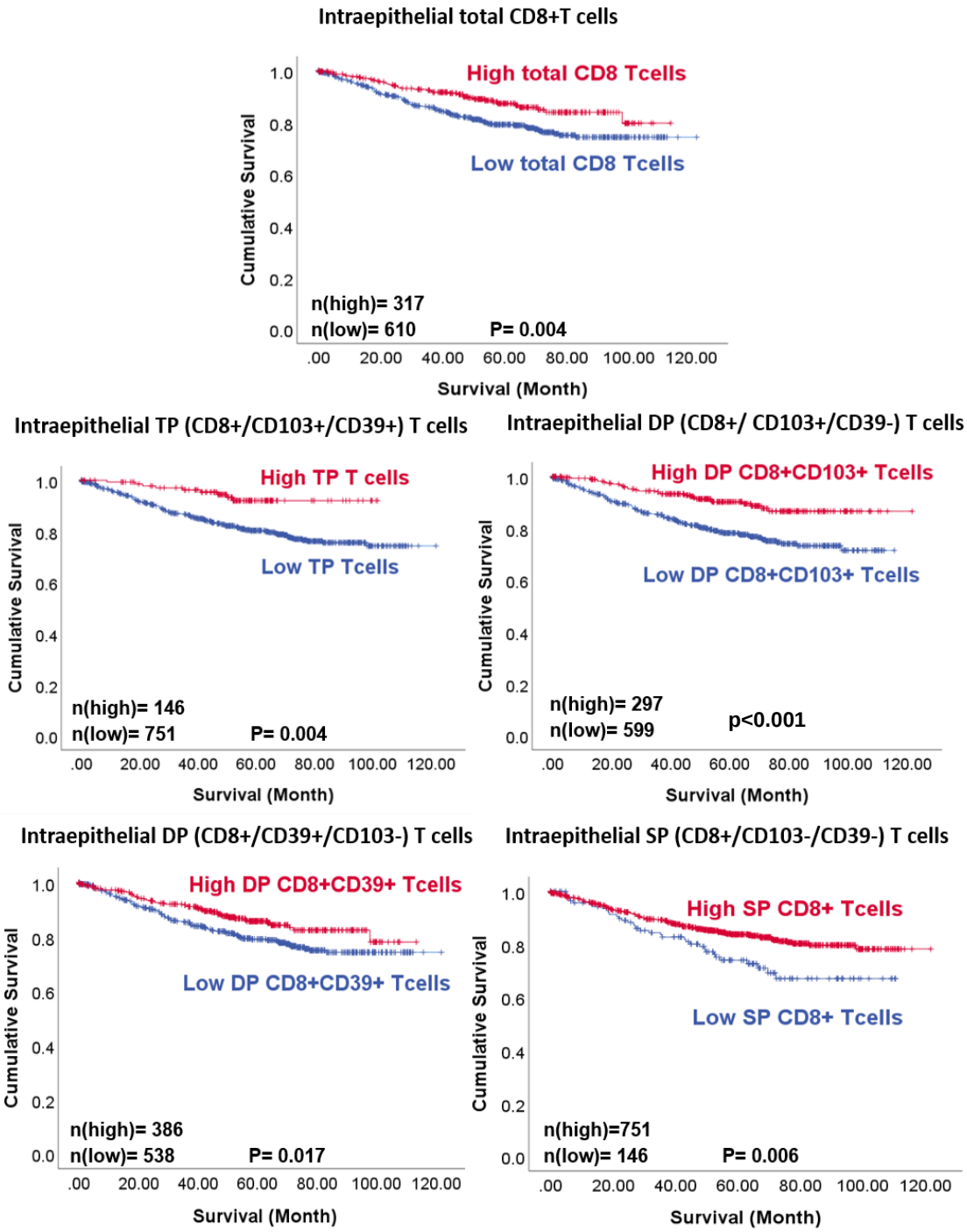

Figure 6. 9 Kaplan-Meier plots for disease specific survival for total CD8+ T cells, TP CD8+CD103+CD39+ T cells, DP CD8+CD103+CD39- T cells, DP CD8+CD39+CD103-T cells and SP CD8+CD103-CD39- T cells in tumour epithelium. p values <0.05 were considered statistically significant.

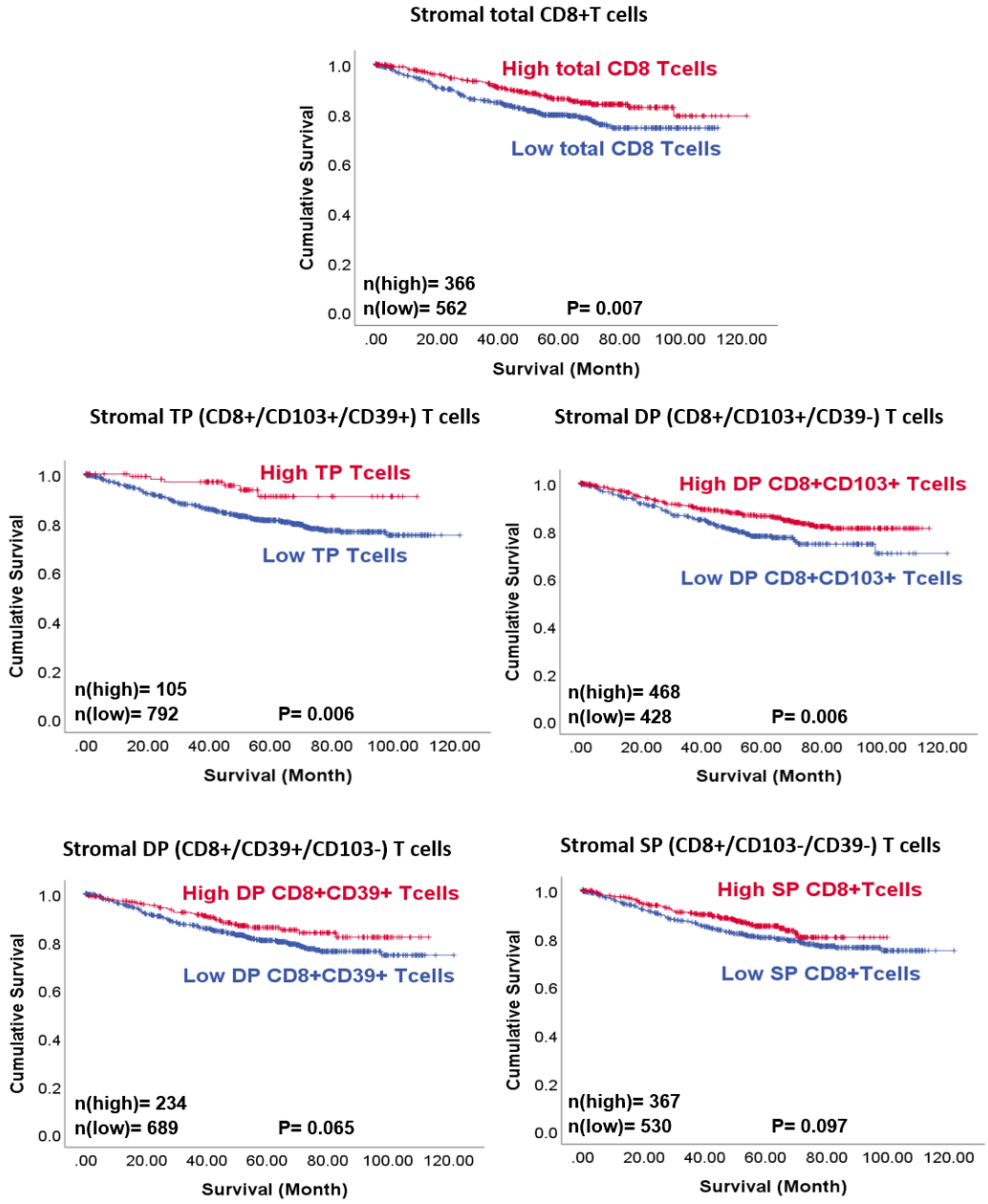

Figure 6. 10 Kaplan-Meier plots for disease specific survival for total CD8+ T cells, TP CD8+CD103+CD39+ T cells, DP CD8+CD103+CD39- T cells, DP CD8+CD39+CD103- T cells and SP CD8+CD103-CD39- T cells in stroma. p values <0.05 were considered statistically significant

The correlation between clinicopathological data of Cohort (1) and CD8+ phenotypes subsets (TP CD8+CD103+CD39+ T cells, DP CD8+CD103+CD39- T cells, DP CD8+CD39+CD103- T cells and SP CD8+CD103-CD39- T cells) is shown in table (6.1 a and b). All four CD8+ T cell phenotypes were significantly correlated ($p< 0.05$) with TNM stage, tumour metastases, vascular invasion, and microsatellite instability status of the tumours. TRM subsets only (TP CD8+CD103+CD39+T cells and DP CD8+CD103+CD39- T cells) were significantly associated with primary tumour location (right side colon, left side colon or rectal cancer). Tumour grade and the presence of regional lymph node metastasis were significantly associated with DP CD8+CD103+CD39- T cells and SP CD8+CD103-CD39- T cells (subsets lacking CD39 expression) compared to the other subsets where no significant correlation was observed between them and these factors ($p>0.05$)

Table 6.2, 6.3, 6.4, 6.5 and 6.6 represent Cox multivariate regression models for each CD8+ phenotype combined with the prognostic clinicopathological variables (TNM stage, vascular invasion and tumour grade) and MSI status. The results demonstrated that only the TRM subsets (TP CD8+CD103+CD39+ T cells and DP CD8+CD103+CD39- T cells) were independent prognostic factors in CRCs.

Table 6. 1a Correlations between the expression of intraepithelial TP CD8+CD103+CD39+T cells, DP CD8+CD103+CD39- T cells, DP CD8+CD39+CD103-T cells and SP CD8+CD103-CD39- T cells, and clinicopathologic features in CRCs. Pearson's χ^2-tests were used to determine the significance of the correlation. p- values <0.05 were considered statistically significant.

	Intraepithelial TP CD8+CD103+CD39+ T cells			Intraepithelial DP CD8+CD103+ CD39- T cells			Intraepithelial TP CD8+CD103+CD39+ T cells			Intraepithelial DP CD8+CD103+ CD39- T cells		
	Low (%)	High (%)	P-value	Low (%)	High (%)	P-value	Low (%)	High (%)	P-value	Low (%)	High (%)	P-value
Sex												
Male	424 (56.5)	85 (58.2)	0.694	342 (57.1)	167 (56.2)	0.805	311 (57.8)	214 (55.4)	0.474	75 (51.4)	434 (57.8)	0.09
female	327 (43.5)	61 (41.8)		257 (42.9)	130 (43.8)		227 (42.2)	172 (44.6)		71 (48.6)	317 (42.2)	
Age diagnosis												
<=69	44 (81.5)	10 (18.5)	0.645	36 (6)	18 (6.1)	0.976	38 (7.1)	21 (5.4)	0.320	14 (9.6)	40 (5.3)	0.057
>69	707 (83.9)	136 (16.1)		563 (94)	279 (93.9)		500 (92.9)	365 (94.6)		132 (90.4)	711 (94.7)	
Tumour site												
Right colon	327 (43.5)	88 (60.3)	0.001	257 (42.9)	158 (53.2)	0.017	234 (43.5)	195 (50.5)	0.196	59 (40.4)	356 (47.4)	0.132
Left colon	284 (37.8)	42 (28.8)		227 (37.9)	98 (33)		203 (37.7)	130 (33.7)		63 (43.2)	263 (35)	
Rectal	111 (14.8)	16 (11)		96 (16)	31 (10.4)		82 (15.2)	51 (13.2)		17 (11.6)	110 (14.6)	
unknown	29 (3.9)	0 (0)		19 (3.2)	10 (3.4)		19 (3.5)	10 (2.6)		7 (4.8)	22 (2.9)	
Tumour grade (differentiation)												
well	13 (1.7)	4 (2.7)	0.683	7 (1.2)	10 (3.4)	0.003	12 (2.2)	5 (1.3)	0.427	1 (0.7)	16 (2.1)	0.013
Moderate	674 (89.9)	131 (89.7)		551 (92.1)	253 (85.2)		484(90)	344 (89.4)		141(96.6)	664 (88.5)	
poor	63 (8.4)	11 (7.5)		40 (6.7)	34 (11.4)		42 (7.8)	36 (9.4)		4 (2.7)	70 (9.3)	

Table 6. 2b Correlations between the expression of intraepithelial TP CD8+CD103+CD39+T cells, DP CD8+CD103+CD39- T cells, DP CD8+CD39+CD103-T cells and SP CD8+CD103-CD39- T cells, and clinicopathologic features in CRCs. Pearson's χ^2-tests were used to determine the significance of the correlation. p- values <0.05 were considered statistically significant.

	Intraepithelial TP CD8+CD103+CD39+ T cell			Intraepithelial DP CD8+CD103+ CD39- T cells			Intraepithelial DP CD8+CD103-CD39+ T cells			Intraepithelial SP CD8+CD103- CD39- T cells		
	Low (%)	High (%)	P-value	Low (%)	High (%)	P-value	Low (%)	High (%)	P-value	Low (%)	High (%)	P-value
Microsatellite instability status												
Negative	631 (85)	109 (75.7)	0.006	518 (87.2)	221 (75.9)	<.001	465 (87.2)	297 (78.4)	<.001	139 (95.2)	601 (81.2)	<.001
Positive	111 (15)	35 (24.3)		76 (12.8)	70 (24.1)		68 (12.8)	82 (21.6)		7 (4.8)	139 (18.8)	
Vascular invasion												
Absent	370 (50.1)	84 (58.3)	0.006	279 (47.4)	175 (59.7)	0.001	251 (46.9)	214 (56.9)	0.003	61 (42.1)	393 (53.3)	0.014
Present	369 (49.9)	60 (41.7)		310 (52.6)	118 (40.3)		284 (53.1)	162 (43.1)		84 (57.9)	345 (46.7)	
TNM stage												
1	118 (15.7)	30 (20.5)	0.015	84 (14)	64 (21.5)	0.007	76 (14.1)	73 (18.9)	0.014	18 (12.3)	130 (17.3)	<.001
2	305 (40.6)	62 (42.5)		241 (40.2)	125 (42.1)		213 (39.6)	164 (42.5)		41 (28.1)	326 (43.4)	
3	238 (31.7)	49 (33.6)		202 (33.7)	85 (28.6)		176 (32.7)	119 (30.8)		60 (41.1)	227 (30.2)	
4	90 (12)	5 (3.4)		72 (12)	23 (7.7)		73 (13.6)	30 (7.8)		27 (18.5)	68 (9.1)	
Metastases (M)												
M0 (no distant metastasis)	660 (87.9)	141 (96.6)	0.002	526 (87.8)	274 (92.3)	0.043	464 (86.2)	356 (92.2)	0.005	119 (14.9)	682 (85.1)	0.002
M1 (Distant metastasis)	91 (12.1)	5 (3.4)		73 (12.2)	23 (7.7)		74 (13.8)	30 (7.8)		27 (28.1)	69 (71.9)	
N -Regional lymph nodes												
N0 (no lymph node metastasis)	426 (58.4)	94 (65.3)	0.122	327 (55.9)	192 (66.7)	0.002	302 (56.8)	231 (62.4)	0.089	119 (81.5)	682 (90.8)	<.001
N1 (Regional lymph node metastasis)	304 (41.6)	50 (34.7)		258 (44.1)	96 (33.3)		230 (43.2)	139 (37.)		27 (18.5)	69 (9.2)	

Table 6. 3 Multivariate Cox regression analysis model for vascular invasion, TNM stage, tumour grade, MSI status and Intraepithelial Triple positive (CD8+CD103+CD39+) T cells. Multivariate analysis was performed by Cox regression proportional hazard analysis to test for confounders and the predictive independency of Intraepithelial TP T cell infiltration from standard prognostic/predictive factors. The log-rank test was used to test for significance. p- values <0.05 were considered statistically significant.

Variable	HR	95% CI		p- value
		Lower	Upper	
TNM stage	3.429	2.738	4.295	<0.001
Vascular invasion	1.588	1.095	2.302	0.015
Tumour grade	2.624	1.537	4.480	<0.001
MSI status	0.656	0.369	1.163	0.149
Total Intraepithelial TP CD8+CD103+CD39+ T cells	0.449	0.228	0.883	**0.02**

Table 6. 4 Multivariate Cox regression analysis model for vascular invasion, TNM stage, tumour grade, MSI status and Intraepithelial DP (CD8+CD103+CD39-) T cells. Multivariate analysis was performed by Cox regression proportional hazard analysis to test for confounders and the predictive independency of Intraepithelial DP (CD8+CD103+CD39-) T cell infiltration from standard prognostic/predictive factors. The log-rank test was used to test for significance. p- values <0.05 were considered statistically significant.

Variable	HR.	95% CI		p- value
		Lower	Upper	
TNM stage	3.401	2.714	4.262	<0.001
Vascular invasion	1.514	1.042	2.198	0.029
Tumour grade	2.890	1.685	4.954	<0.001
MSI status	0.642	0.361	1.142	0.131
Total Intraepithelial DP CD8+CD103+CD39- T cells	0.506	0.330	0.776	**0.002**

Table 6. 5 Multivariate Cox regression analysis model for vascular invasion, TNM stage, tumour grade, MSI status and Intraepithelial DP (CD8+ CD39+CD103-) T cells. Multivariate analysis was performed by Cox regression proportional hazard analysis to test for confounders and the predictive independency of Intraepithelial DP (CD8+ CD39+CD103-) T cell infiltration from standard prognostic/predictive factors. The log-rank test was used to test for significance. p- values <0.05 were considered statistically significant.

Variable	HR	95% CI		p-value
		Lower	Upper	
TNM stage	3.281	2.63	4.093	<0.001
Vascular invasion	1.707	1.179	2.471	0.005
Tumour grade	2.333	1.404	3.878	0.001
MSI status	0.696	0.402	1.206	0.196
Total Intraepithelial DP CD8+CD39+CD103- T cells	0.861	0.610	1.216	0.395

Table 6. 6 Multivariate Cox regression analysis model for vascular invasion, TNM stage, tumour grade, MSI status and Intraepithelial SP (CD8+CD103-CD39-) T cells. Multivariate analysis was performed by Cox regression proportional hazard analysis to test for confounders and the predictive independency of Intraepithelial SP (CD8+CD103-CD39-) T cell infiltration from standard prognostic/predictive factors. The log-rank test was used to test for significance. p- values <0.05 were considered statistically significant.

Variable	HR	95% CI		p- value
		Lower	Upper	
TNM stage	3.49	2.776	4.387	<0.001
Vascular invasion	1.591	1.096	2.310	0.015
Tumour grade	2.723	1.597	4.643	<0.001
MSI status	0.637	0.357	1.135	0.126
Total Intraepithelial SP CD8+CD103-CD39-T cells	0.951	0.642	1.411	0.804

6.2.4 TP CD8+ T cell phenotype maintain it's prognostic significance among different primary tumour locations in CRCs: RCRCs vs LCRCs

We previously mentioned that CRCs originating from different PTL obtain different immune landscapes and different responsiveness to immunotherapy. Therefore, it was hypothesised that high infiltration of CD8+ TILs phenotypes would affect the survival of RCRCs and LCRCs patients differently. The intraepithelial and stromal infiltration of total CD8+TILs did not predict survival in LCRC patients. However, only intraepithelial and stromal infiltration of TP CD8+CD103+CD39+T cells showed a positive correlation to the survival of LCRC patients (refer to figure 6.11 and 6.12, respectively). In contrast, high infiltration of all intraepithelial CD8+ T cell phenotypes was significantly correlated better prognosis in RCRC patients.

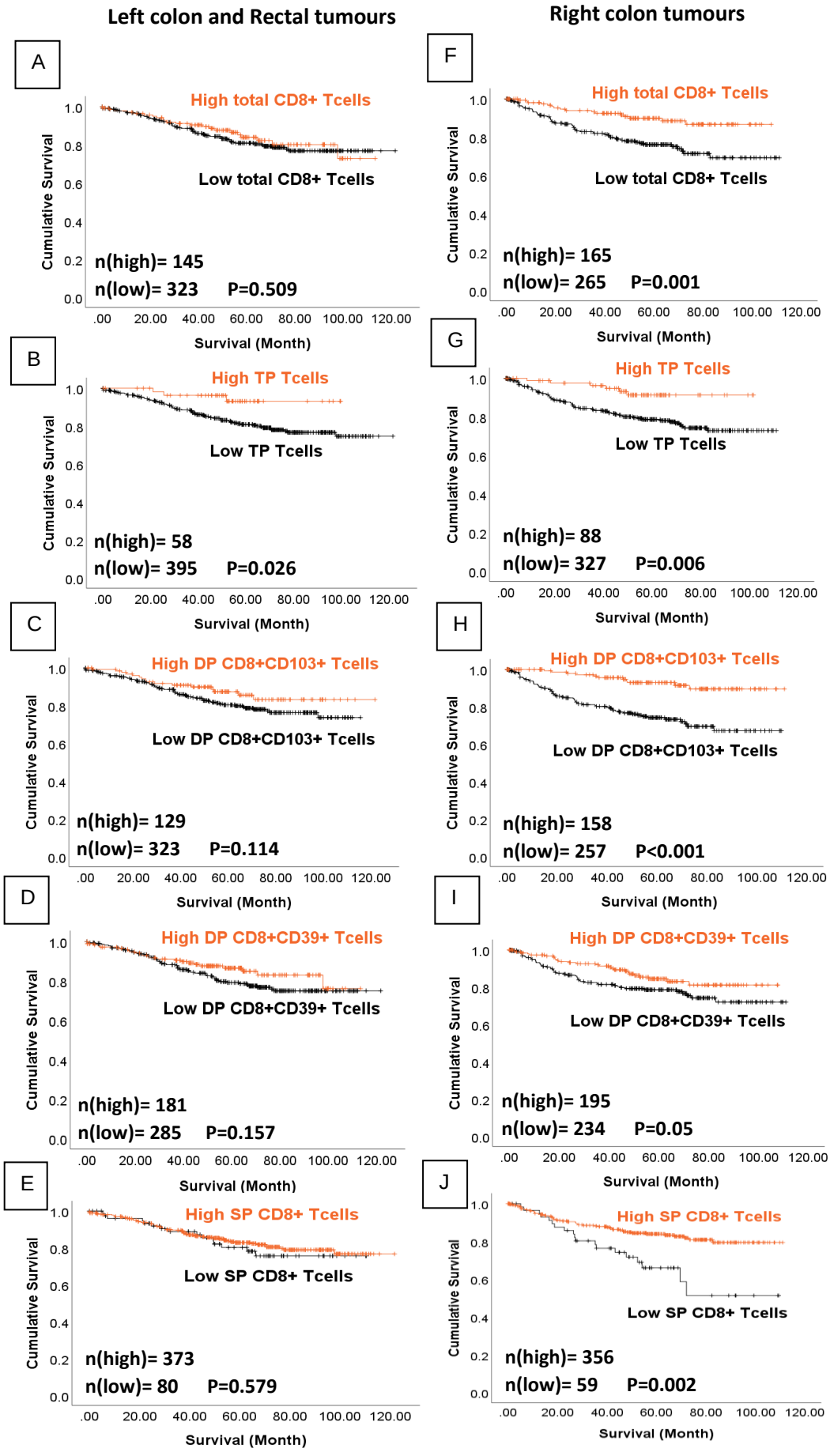
Left colon and Rectal tumours
Right colon tumours
A
High total CD8+ Tcells
Low total CD8+ Tcells
n(high)= 145
n(low)= 323 P=0.509
F
High total CD8+ Tcells
Low total CD8+ Tcells
n(high)= 165
n(low)= 265 P=0.001
B
High TP Tcells
Low TP Tcells
n(high)= 58
n(low)= 395 P=0.026
G
High TP Tcells
Low TP Tcells
n(high)= 88
n(low)= 327 P=0.006
C
High DP CD8+CD103+ Tcells
Low DP CD8+CD103+ Tcells
n(high)= 129
n(low)= 323 P=0.114
H
High DP CD8+CD103+ Tcells
Low DP CD8+CD103+ Tcells
n(high)= 158
n(low)= 257 P<0.001
D
High DP CD8+CD39+ Tcells
Low DP CD8+CD39+ Tcells
n(high)= 181
n(low)= 285 P=0.157
I
High DP CD8+CD39+ Tcells
Low DP CD8+CD39+ Tcells
n(high)= 195
n(low)= 234 P=0.05
E
High SP CD8+ Tcells
Low SP CD8+ Tcells
n(high)= 373
n(low)= 80 P=0.579
J
High SP CD8+ Tcells
Low SP CD8+ Tcells
n(high)= 356
n(low)= 59 P=0.002
Cumulative Survival
Survival (Month)
0.0
0.2
0.4
0.6
0.8
1.0
.00
20.00
40.00
60.00
80.00
100.00
120.00

Figure 6. 11 Kaplan-Meier survival plots showing the association between intraepithelial infiltration of different CD8TILs subsets and disease-free survival (months) of patients with LCRC (A,B,C,D,E) and RCRC (F,G,H,I,J), respectively.

No significant association between the infiltration total CD8+TILs (A), DP CD8+CD103+ TILs (C), DP CD8+CD39+ (D) and SP CD8+CD103-CD39- TILs (E) and survival of patients with LCRC. A significant correlation between the infiltration TP TILs (B) and survival of LCRC patients was observed. A significant correlation between the infiltration of total CD8+TILs (F), TP TILs (G) DP CD8+CD103+ TILs (H), DP CD8+CD39+ (I) and SP CD8+CD103-CD39- TILs (J) and survival of patients with RCRC was observed. P-values <0.05 were considered statistically significant.

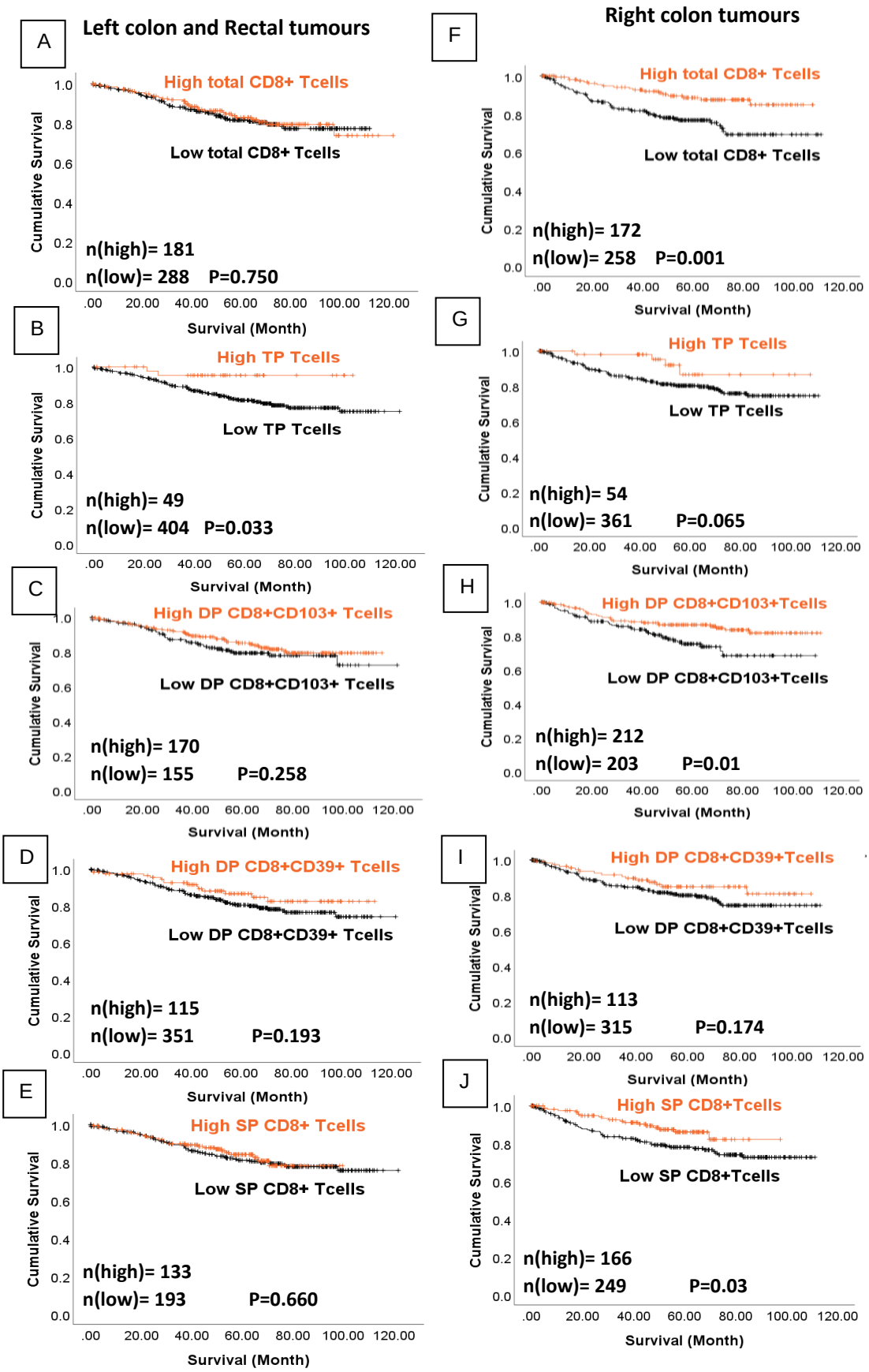
A
Left colon and Rectal tumours
High total CD8+ Tcells
Low total CD8+ Tcells
n(high)= 181
n(low)= 288 P=0.750
B
High TP Tcells
Low TP Tcells
n(high)= 49
n(low)= 404 P=0.033
C
High DP CD8+CD103+ Tcells
Low DP CD8+CD103+ Tcells
n(high)= 170
n(low)= 155 P=0.258
D
High DP CD8+CD39+ Tcells
Low DP CD8+CD39+ Tcells
n(high)= 115
n(low)= 351 P=0.193
E
High SP CD8+ Tcells
Low SP CD8+ Tcells
n(high)= 133
n(low)= 193 P=0.660
F
Right colon tumours
High total CD8+ Tcells
Low total CD8+ Tcells
n(high)= 172
n(low)= 258 P=0.001
G
High TP Tcells
Low TP Tcells
n(high)= 54
n(low)= 361 P=0.065
H
High DP CD8+CD103+Tcells
Low DP CD8+CD103+Tcells
n(high)= 212
n(low)= 203 P=0.01
I
High DP CD8+CD39+Tcells
Low DP CD8+CD39+Tcells
n(high)= 113
n(low)= 315 P=0.174
J
High SP CD8+Tcells
Low SP CD8+Tcells
n(high)= 166
n(low)= 249 P=0.03
Cumulative Survival
Survival (Month)

Figure 6. 12 Kaplan-Meier survival plots showing the association between stromal infiltration of different CD8TILs subsets and disease-free survival (months) of patients with LCRC (A,B,C,D,E) and RCRC (F,G,H,I,J), respectively.

No significant association between the stromal infiltration total CD8+TILs (A), DP CD8+CD103+ TILs (C), DP CD8+CD39+ TILs (D) and SP CD8+CD103-CD39- TILs (E) and survival of patients with LCRC. A significant correlation between the infiltration TP TILs (B) and survival of LCRC patients was observed. A significant correlation between the infiltration of total CD8+TILs (F), DP CD8+CD103+ TILs (H), and SP CD8+CD103-CD39- TILs (J) and survival of patients with RCRC. Meanwhile, no significant correlation between stromal infiltration of TP TILs (G) and DP CD8+CD39+ (I) and survival of patients with RCRC was seen. p values <0.05 were considered statistically significant.

6.2.5 CD8+ T-cells phenotypes landscape of the tumour Microenvironment from right-sided and left-sided colon cancers

In order to assess the immune landscape and distribution of the different CD8+TILs subsets within the tumour microenvironment (epithelium and stroma), the average densities of the respective CD8+TILs subsets were determined using the multiplex IHC and Inform software. Mann-Whitney U test was used to compare the average densities of CD8 TILs subsets between RCRCs and LCRCs. The findings illustrated that intraepithelial total CD8+ T-cells were presented more in the right-side colon tumours compared to left-sided ones, which is consistent with our previous observation in chapter (5).

It was interesting to see despite that the total CD8TILs density was higher in the RCRCs, only the TP CD8+ TILs and DP CD8+CD39+ TILs densities were significantly higher in the epithelium of the RCRC. DP CD8+CD103+ T cells and SP CD8+CD103-CD39- T cells did not show a significant difference in the distribution between RCRC and LCRC. A role of the upregulated CD39 expression on the TP TILs and DP CD8+CD39+TILs can be implied for the above observation.

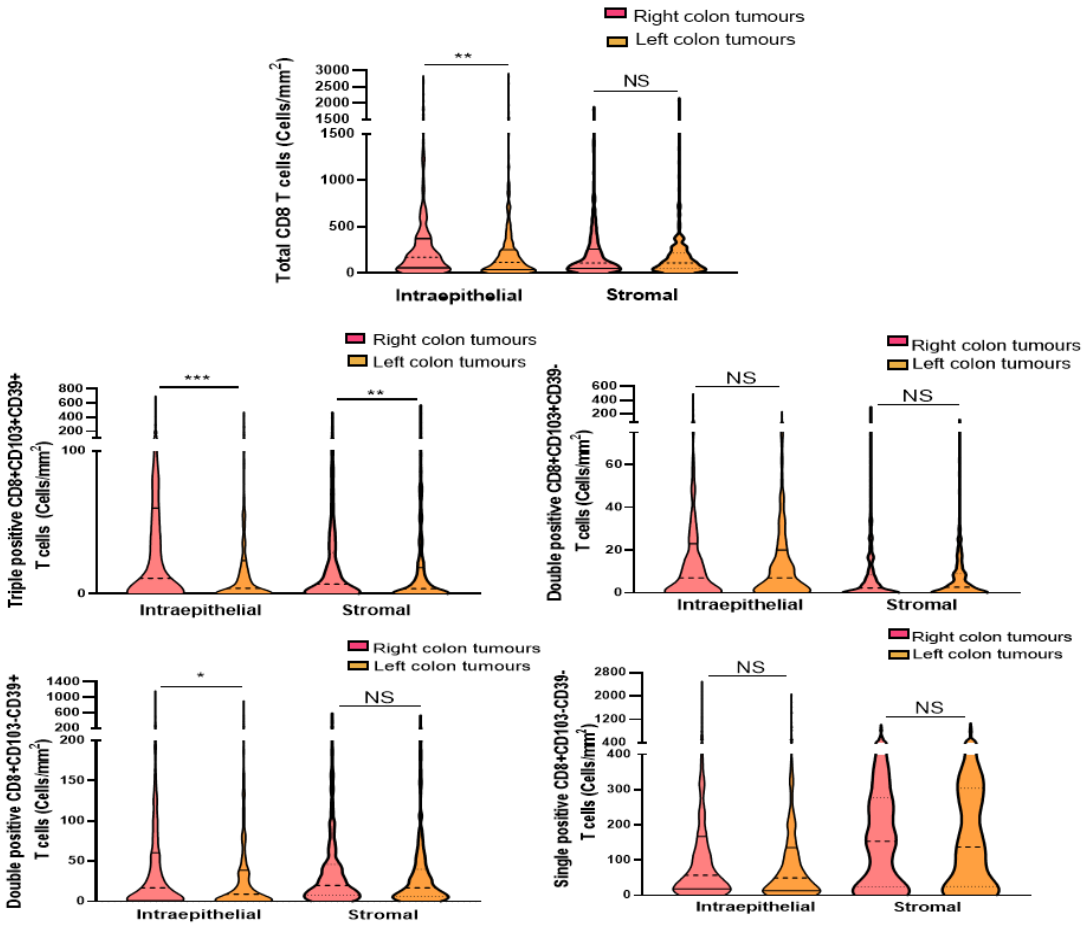

Figure 6. 13 Comparison of the average densities of different CD8 TILs subsets between RCRC and LCRC in the epithelium and stroma.

The orange violin represents LCRCs, and the red violin represents RCRC. Significant differences in the total CD8TILs, TP and DP CD8+CD39+TILs subsets in the intraepithum were found between the right and Left colorectal tumours. The density of TP TILs infiltrating the stroma was significantly higher in RCRC compared to LCRC. The Mann-Whitney U test was used to calculate the significance between the average densities of different CD8 TILs in RCRC and LCRC. P-values <0.05 were considered statistically significant.

6.2.6 MSI Tumours are heavily infiltrated with CD8+ T-cells subsets

It is well known that MSI tumours are more predominant in RCRC[279]. In the previous result, we looked at the average density of different CD8TILs subsets between RCRCs and LCRCs. However, not all RCRCs might have an MSI high status and not all LCRCs might have an MSI low/MSS status. Therefore, in order to further specify our search. We assessed the average densities of different CD8TILs subsets in MSI vs MSS characterised tumours. All four CD8+ T cells subsets were found to be significantly higher in TME (epithelium and stroma) of patients with MSI tumours. The only exclusion to this was stromal SP CD8+CD103-CD39- T cells where there was no significant difference (p = 0.4514) between numbers in MSI and MSS patients.

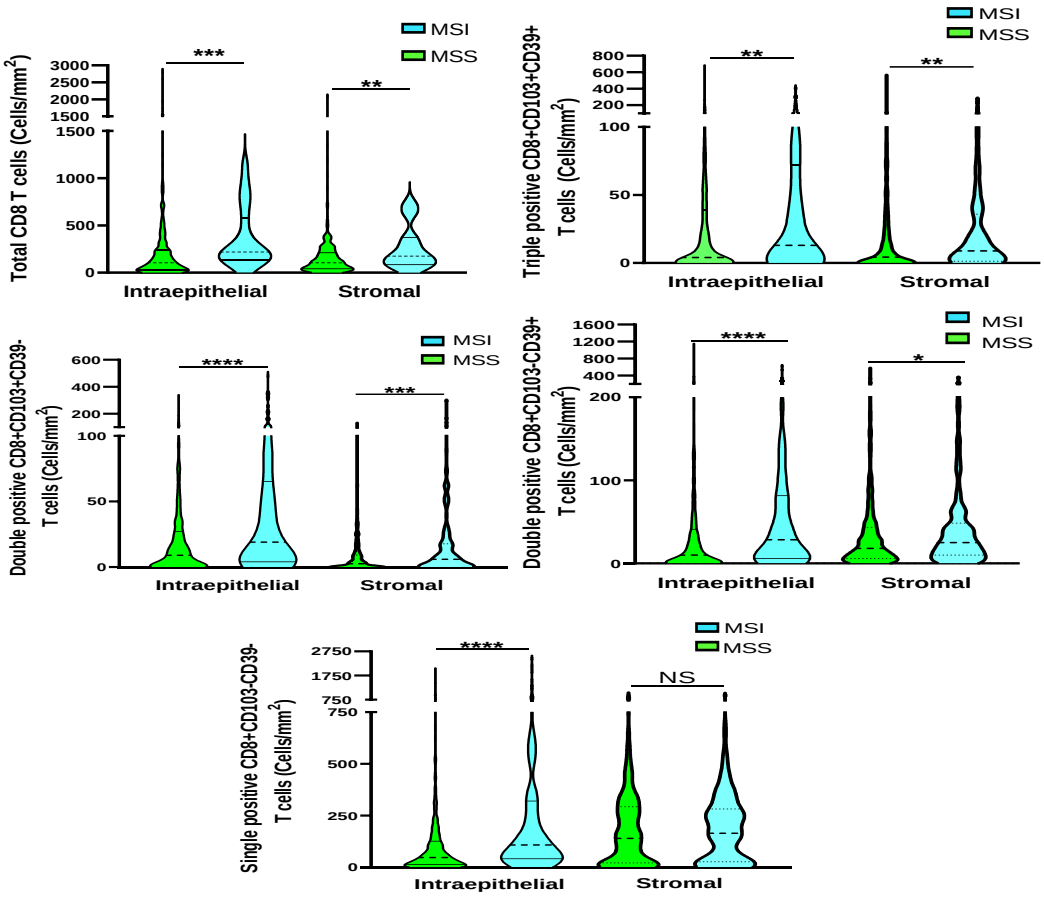

Figure 6. 14 Comparison of average densities of different CD8 TILs subsets in the epithelium and stroma between MSI and MSS tumours.

The blue violin represents MSI tumours, and the green violin represents MSS tumours. The average densities of all CD8+ TILs subsets were significantly higher in the MSI tumour, with

the exception of SP CD8+TILs in the stroma. The Mann-Whitney U test was used to calculate the significance between the average densities of different CD8 TILs in MSI and MSS tumours. P-values <0.05 were considered statistically significant.

6.2.7 The superiority of immune infiltration quality (cell type) over immune infiltration density in CRCs.

Several studies including our study have shown that a positive correlation exists between total CD8 TILs infiltration and survival of cancer patients. [235, 236, 237, 376] The study by *Galon et al.* suggests that total CD8+ T cell infiltration can be consider as a marker for hot tumours, which further positively correlates with survival. Low infiltration of CD8+ T cells was suggested to be a marker for cold tumours and negatively correlate with survival.[241] Although our findings support the above study, we hypothesised that the correlation between high CD8 T cell infiltration and survival is mainly dependent on the TP infiltrating T cell subset. In order to test this hypothesis, we classified cohort (1) CRCs patients into four groups according to total CD8+ T cells subsets and TP CD8+CD103+CD39+ T cell density in the tumour. The cohort was classified into the following groups.

- **Group 1:** High total CD8+ T cells, High TP T cells (Hot tumours, high expression of TP T cells)

- **Group 2:** Low total CD8+ T cells, High TP T cells (Cold tumours, high expression of TP T cells)

- **Group 3:** High total CD8+ T cells, Low TP T cells (Hot tumours, Low expression of TP T cells)

- **Group 4:** Low total CD8+ T cells, High TP T cells (Cold tumours, Low expression of TP T cells)

Survival analysis of these four groups using Kaplan Meier curves (figure 6.15) showed that patients with group 1 tumours were associated with better clinical outcome than patients from group 3 and group 4. In contrast, no significant difference in DSS was observed between group1 and group 2 patients. The latter finding indicated that hot and cold tumours act the same if associated with high expression of TP T cells.

Although both group 1 and group 3 are heavily infiltrated tumours (hot tumours), the difference in survival between these two groups shows that the presence of TP TILs in high density in group 1 tumours is the reason of having prolonged survival compared to group 3. Both findings indicate that having the right type of CD8+ TILs is more critical than infiltration density. It is possible that in group 3, patients were highly infiltrated with 'bystander' CD8+ TILs or cancer unspecific CD8+ TILs. It is important to note that SP CD8+CD103-CD39- T cell subset was the highest component of this group. Another reason could be that the TME of group 3 tumours is immunosuppressive, therefore reducing the cytotoxicity and prognostic impact of CD8+ TILs phenotypes presented in this group. In order to test the latter theory, we quantified the expression of CD39 (As it is considered an indicator of adenosine) in the tumour stroma of all the four groups.

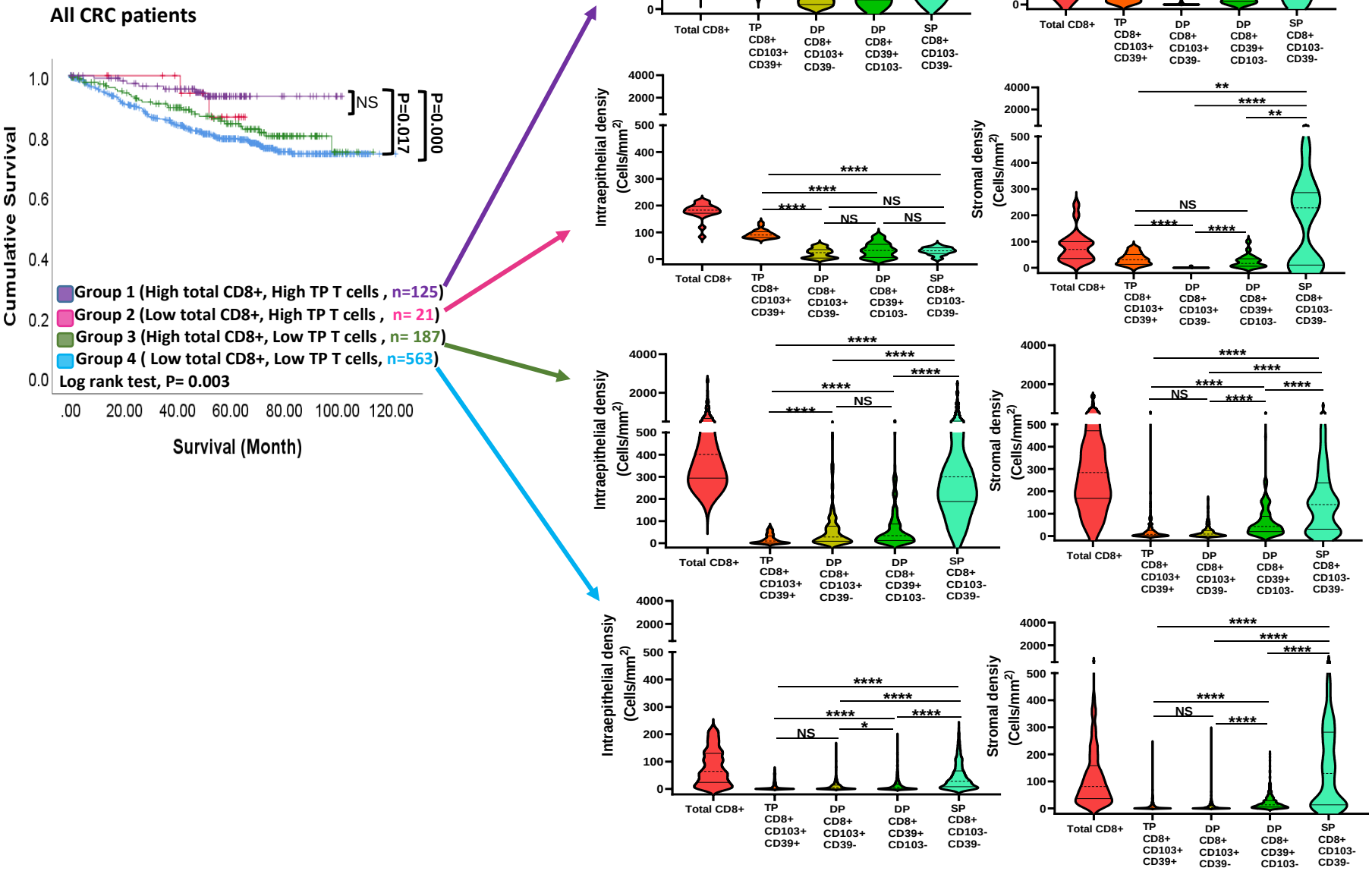
All CRC patients
Cumulative Survival
1.0
0.8
0.6
0.4
0.2
0.0
NS
P=0.017
P=0.000
Group 1 (High total CD8+, High TP T cells , n=125)
Group 2 (Low total CD8+, High TP T cells , n= 21)
Group 3 (High total CD8+, Low TP T cells , n= 187)
Group 4 (Low total CD8+, Low TP T cells, n=563)
Log rank test, P= 0.003
.00 20.00 40.00 60.00 80.00 100.00 120.00
Survival (Month)
Intraepithelial densiy (Cells/mm2)
Stromal densiy (Cells/mm2)
Total CD8+
TP CD8+ CD103+ CD39+
DP CD8+ CD103+ CD39-
DP CD8+ CD39+ CD103-
SP CD8+ CD103- CD39-

Figure 6. 15 Classification of CRC cohort depending on total CD8 TILs and TP TILs infiltration into the TME followed by the assessment of their correlation to survival using Kaplan Meier curves.

Better survival was seen between high total CD8 TILs and TP TILs infiltration with survival (group 1). Poor survival was observed on low infiltration of total CD8 TP TILs infiltration (group 4). A significant difference in survival of CRC patients was observed between group 1 and group 3 ($p=0.017$) and between group 1 and group 3 ($p<0.0001$). Log-rank test was used to test the statistical significance ($p=0.003$). The violin plots represent the average densities of the respective CD8+ TIL subsets in the TME for each of the four groups. P-values <0.05 were considered statistically significant.

6.2.8 The presence of immunosuppressive tumour environment in group (3) patients

CD39 is an important exhaustion marker expressed on lymphocytes in the epithelium of the tumour. It is a rate-limiting enzyme that aids the conversion of ATP into adenosine with the help of CD73. Adenosine is an inhibitory molecule that makes the tumour microenvironment immunosuppressive. CD39 is expressed on a wide range of cell types in the stroma, as seen in our multiplex staining. In order to further understand the observation seen in (figure 6.15) the average density of SP CD39+ cells in the stroma was compared across all four groups of the cohort. Among all four groups, the highest SP CD39+ cells density was found in the stroma of group 3 patients (as shown in figure 6.16). This could explain the low survival seen in group 3 patients that have high intraepithelial total CD8+TILs infiltration and low TP TILs infiltration. The high CD39 expression in the stroma may contribute to the immunosuppression in the TME of group 3 patients. Interestingly, the lowest density of stromal CD39+ cells was observed with group 2 and group 1 patients, which can be a reason for better survival observed in these groups due to reduced immunosuppression.

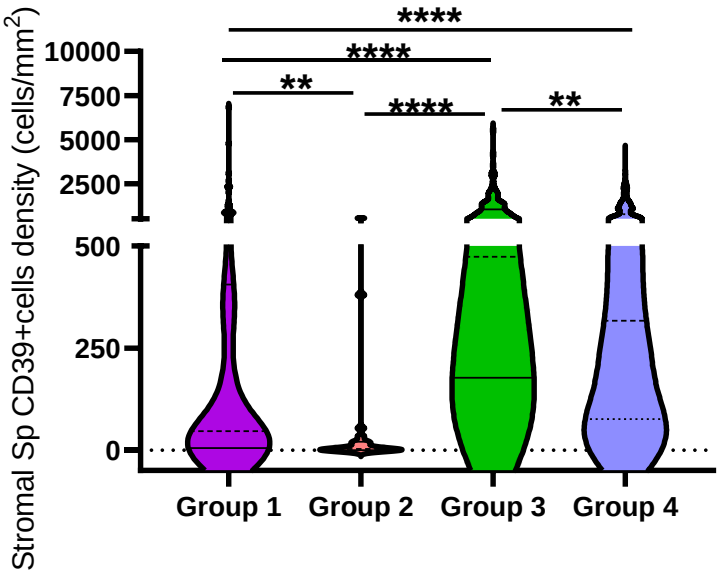

Figure 6. 16 Comparison of average densities of SP CD39+ cells in the stroma of group 1, group 2, group 3 and group 4 tumours.

The average density of SP CD39+ cells was significantly higher in group 3 patients (green violin). Mann Whitney U test was used for statistical comparisons. p-values <0.05 were considered statistically significant. (*p ≤0.05, ** p ≤ 0.01,*** p ≤ 0.001, **** p ≤ 0.0001)

6.2.9 Groups overall survival differs between RCRC and LCRC patients.

On studing the survival pattren of group 1, group 2, group 3 and group 4 CRC patients. Group 1 and group 2 showed better survival compared to group 3 and group 4. To study if the same survival patterns were observed between RCRC and LCRC, survival analysis of the four groups using Kaplan Meier plots was performed for RCRC and LCRC patients (figure 6.17).

In LCRC, Kaplan Meier survival curve showed that group 1 was significantly better in predicting patient survival than group 3 and group 4, which is consistent with the previous result for cohort (1). However, the survival analysis for the four groups in RCRCS was different. Groups1, 2 and 3 in the RCRC had no significant difference in patient survival but showed significantly better prognostic impact compared to group 4 (cold tumours).

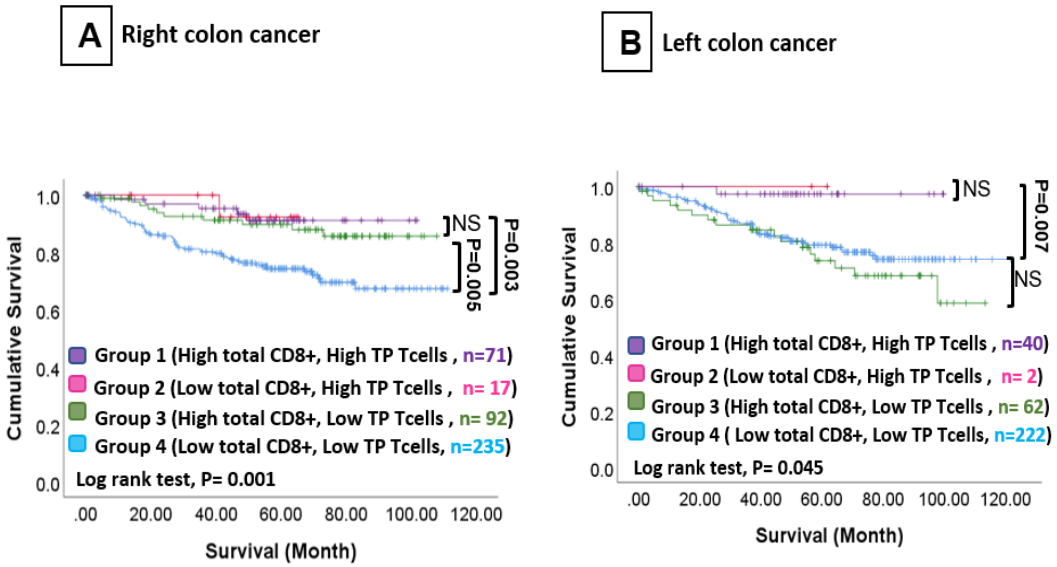

Figure 6. 17 Comparison of survival curves for group 1, group 2, group 3 and group 4 between RCRC and LCRC.

(A) Kaplan Meier plots of group 1, group 2, group 3 showed better survival than group 4 in RCRC. **(B)** Kaplan Meier plots of group 1, group 2 showed better survival than group 3 and group 4 in LCRC. Log rank test was used to determine overall significance. p-values <0.05 were considered statistically significant.

6.2.10 Overview of CD8+ phenotypes from different tumour locations (LS, CT, IM and AJD) within the four groups classification

The differences in the distribution of cytotoxic T cells, Th17 cells, B cells, macrophages, and natural killer (NK) cells between different tumour regions (CT and IM) were previously highlighted by Mlecnik et al. in MSI and MSS colorectal tumours.[274] Moreover, in chapter 4 of this thesis, we have shown the prognostic value of combined regional analysis of intraepithelial CD3+ and CD8+ T cell densities in three tumour regions (LS, CT, and IM) over the single regional analysis of each region. Here, we sought to determine the differences in the distribution of CD8 T cell phenotypes in the three tumour regions (LS, CT and IM) and the adjacent normal tissue of CRCs patients from the four groups mentioned above. The reason for this is to find out if CD8 T cell phenotypes preferentially accumulate in a certain region within the tumour or are highly infiltrated throughout.

The violin plots in figure 6.18 A depict a comparison of total CD8+ TILs densities (all phenotypes) in LS, CT, IM and the adjacent normal tissue of CRCs patients group 1,2,3 and 4. Interestingly, no significant difference was found between the median densities of total CD8+ TILs in LS, CT and IM regions of CRCs patients stratified in group 1,2 and 3. However, group 4 tumours showed lower total CD8+ infiltration in the core of the tumour compared to the other regions. Comparing the infiltration of total CD8+TIL in tumour regions and the adjacent normal tissue of group1 and group 4, it was noticed that in group 1 the density of total CD8+ TILs was concentrated more within the tumour regions than the adjacent normal tissue. In contrast, in group 4 the adjacent normal tissue obtained significantly higher numbers of total CD8+ TILs than within the tumour tissue. Moreover, the heatmaps in figure 6.19 B visualise and confirm the above violin plots depicting matching it by presenting the density of total CD8+ TILs for each core and each individual in all four groups.

Similarly, we analysed the distribution of CD8+ phenotypes (TP CD8+CD103+CD39+ T cells, DP CD8+CD103+ T cells, DP CD8+CD39+ T cells and SP CD8+T cells) in LS, CT, IM and the adjacent normal tissue of tumours from group 1, 2, 3 and 4. Figure 6.19 shows that In the exception of group 4, no difference in TP T cells distribution was observed between LS, CT and IM tumour regions. The adjacent normal tissue of group 1 tumours had lower infiltration of TP T cells than tumour regions. These observations go in line with the distribution pattern of total CD8+ TILs showed above.

The adjacent normal tissue in group1 and 3, had higher infiltration of TP T cells than LS, CT and IM areas. Group 1 in figure 6.20 and figure 6.21 illustrate no difference in intraepithelial infiltration of DP CD8+CD103+ T cells and DP CD8+CD39+ T cells within all four regions (LS, CT, IM and the adjacent normal tissue). However, SP CD8+ TILs infiltration was significantly concentrated in CT and IM regions compared to LS and the adjacent normal tissue showing a different pattern of distribution in group1 tumours than other CD8+ TILs phenotypes (figure 6.22). Comparing group 1 and 3 from figure 6.22 confirms that the infiltration of SP CD8+ TILs is higher in group 3 compared to group 1 in all tumour regions of these groups.

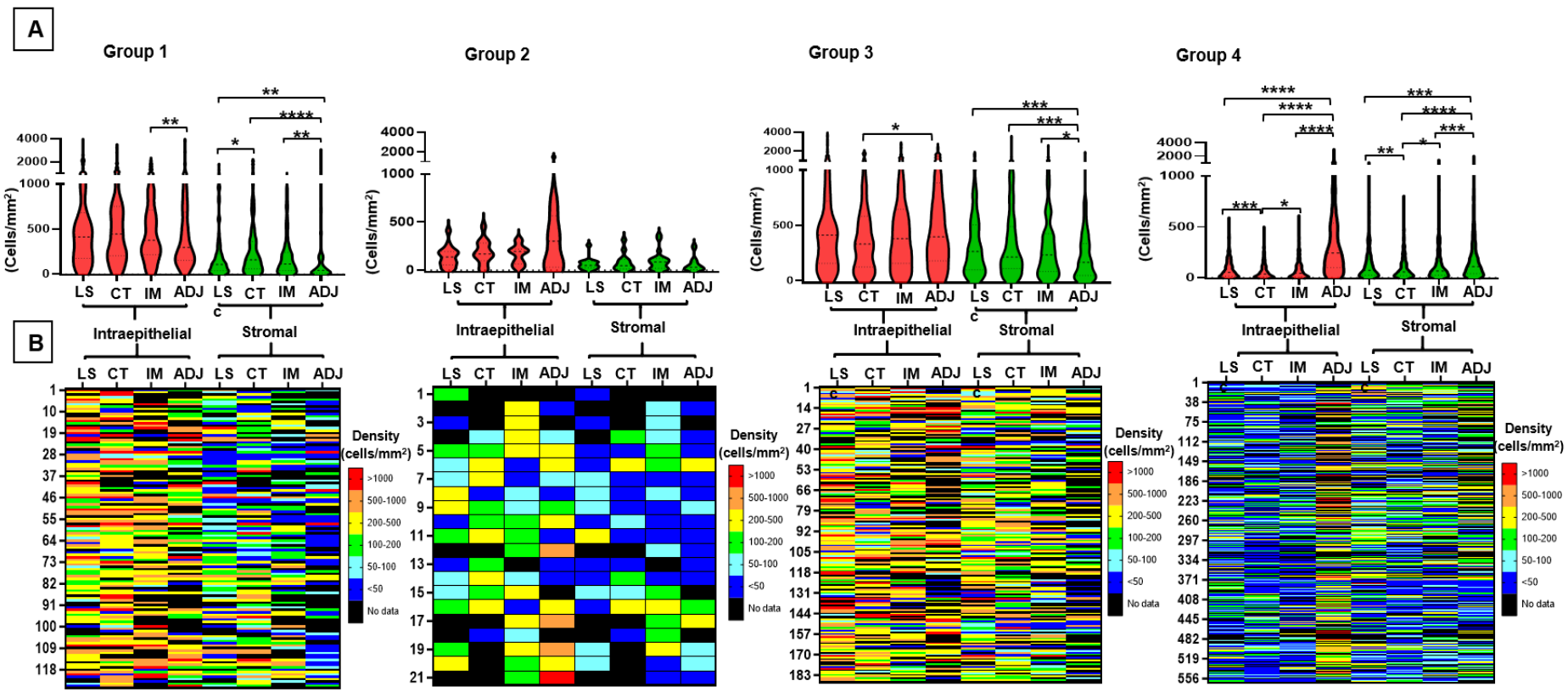

Figure 6. 18 Comparison of median density of total CD8+TILs in different regions of the tumour (LS, CT, IM and ADJ) between different groups of CRC cohort.

(A) The violin plots represent the median density of total CD8 TILs in the respective tumour region matched to the density of total CD8 TILs infiltrating the same tumour region in each patient mapped one below each other in the heat maps **(B).** Group 1 tumours (hot tumours) had significantly higher total CD8 TILs infiltration in the LS, CT and IM as compared to ADJ. The opposite was observed in group 4 tumours (Cold tumours) that had significantly higher total CD8 TILs infiltration in the AJD. Mann Whitney U test was used to test for significance. p- values <0.05 were considered statistically significant. (*p ≤0.05, ** p ≤ 0.01,*** p ≤ 0.001, **** p ≤ 0.0001)

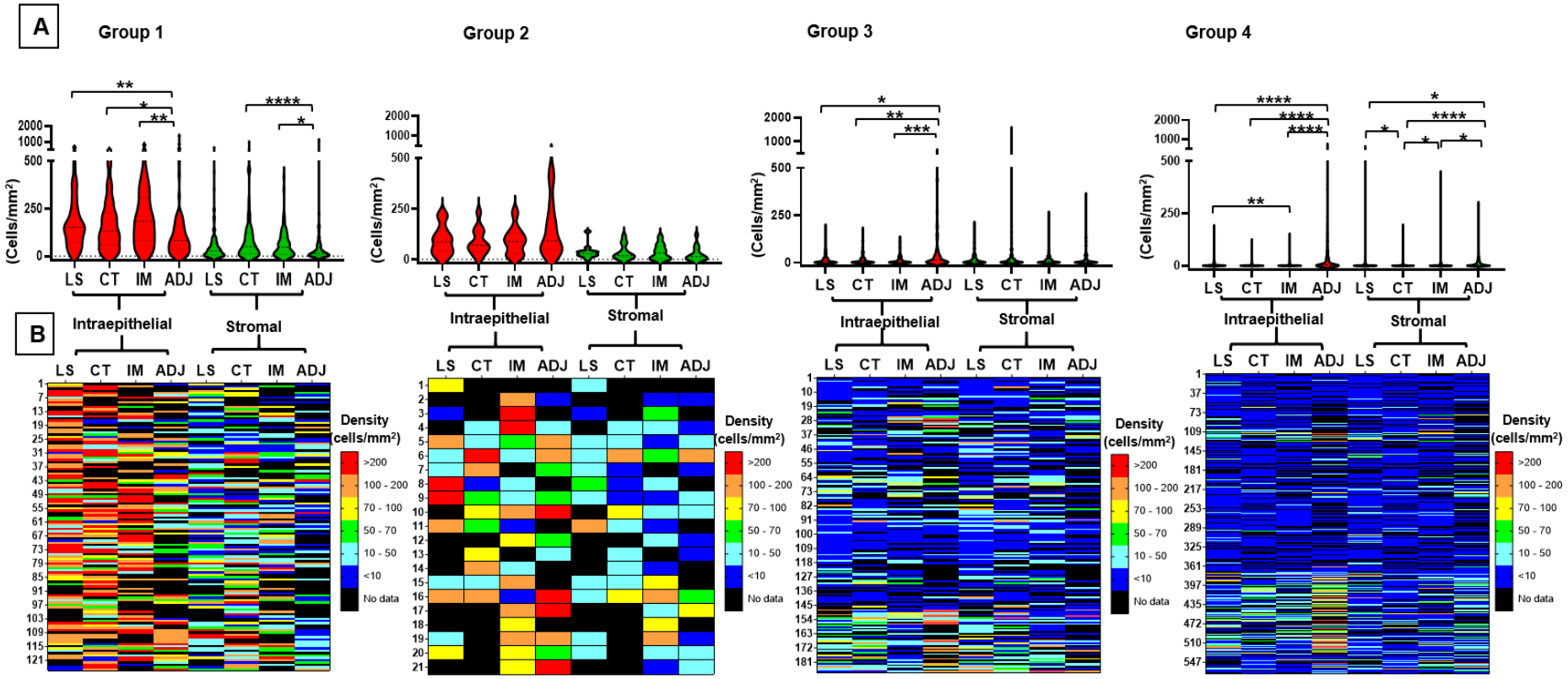

Figure 6. 19 Comparison of median density of TP TILs in different regions of the tumour (LS, CT, IM and ADJ) between different groups of CRC cohort.

(A) The violin plots represent the median density of TP TILs in the respective tumour region matched to the density of TP TILs infiltrating the same tumour region in each patient in the heat maps **(B).** Group 1 tumours (hot tumours) had significantly higher TP TILs infiltration in the LS, CT and IM as compared to ADJ. Meanwhile, group 3 and group 4 tumours had significantly higher TP TILs infiltration in the AJD as compared to other regions of the tumour. Mann Whitney U test was used to test for significance. p- values <0.05 were considered statistically significant. (*p ≤0.05, ** p ≤ 0.01,*** p ≤ 0.001, **** p ≤ 0.0001)

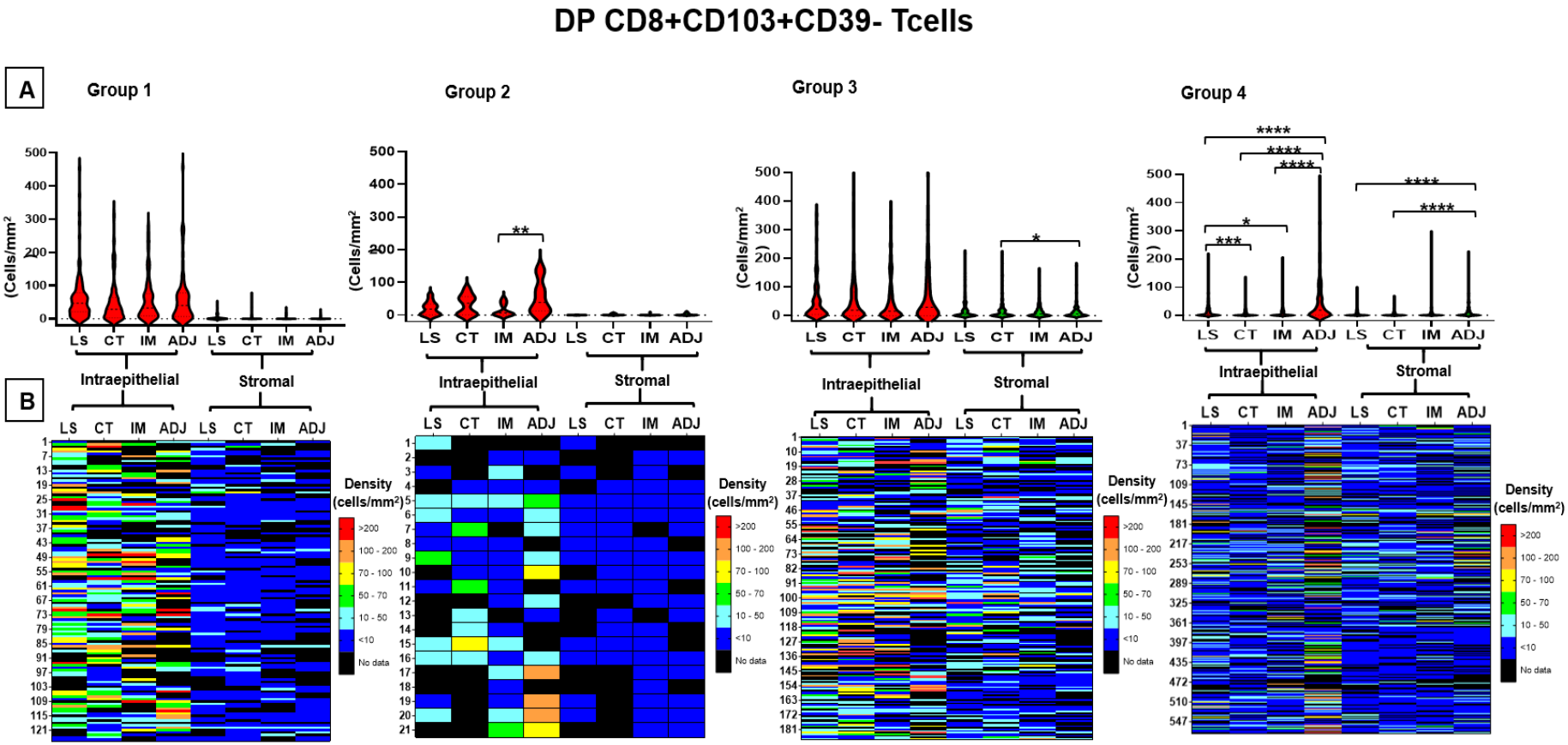

Figure 6. 20 Comparison of median density of DP CD8+CD103+CD39- TILs in different regions of the tumour (LS, CT, IM and ADJ) of the four groups of CRC cohort.

(A) The violin plots represent the median density of DP CD8+CD103+CD39- TILs in the respective tumour region matched to the respective density in each patient in the heat maps **(B).** The median density of DP CD8+CD103+CD39- TILs in the ADJ was significantly higher in group 4 patients as compared to the infiltration in the regions of the tumour. Mann Whitney U test was used to test for significance. P -values <0.05 were considered statistically significant. (*p ≤0.05, ** p ≤ 0.01,*** p ≤ 0.001, **** p ≤ 0.0001)

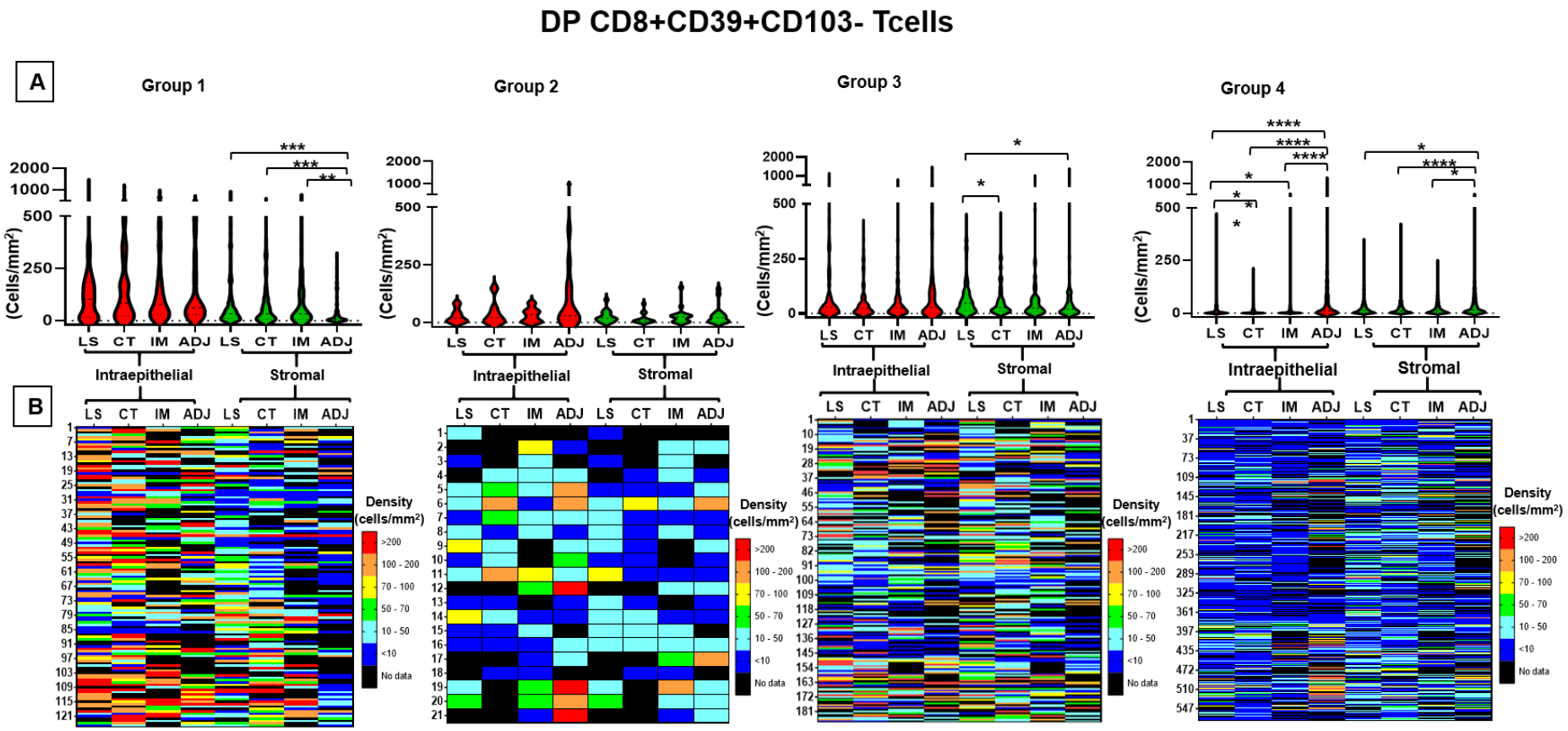

Figure 6. 21 Comparison of median density of DP CD8+CD39+CD103- TILs in different regions of the tumour (LS, CT, IM and ADJ) of the four groups of CRC cohort.

(A) The violin plots represent the median density of DP CD8+CD39+CD103- TILs in the respective tumour region matched to the respective density in each patient in the heat maps **(B).** The median density of DP CD8+CD39+CD103- TILs in the ADJ was significantly higher in group 4 patients as compared to the infiltration in the regions of the tumour. Mann Whitney U test was used to test for significance. P-values <0.05 were considered statistically significant. (*p ≤0.05, ** p ≤ 0.01,*** p ≤ 0.001, **** p ≤ 0.0001)

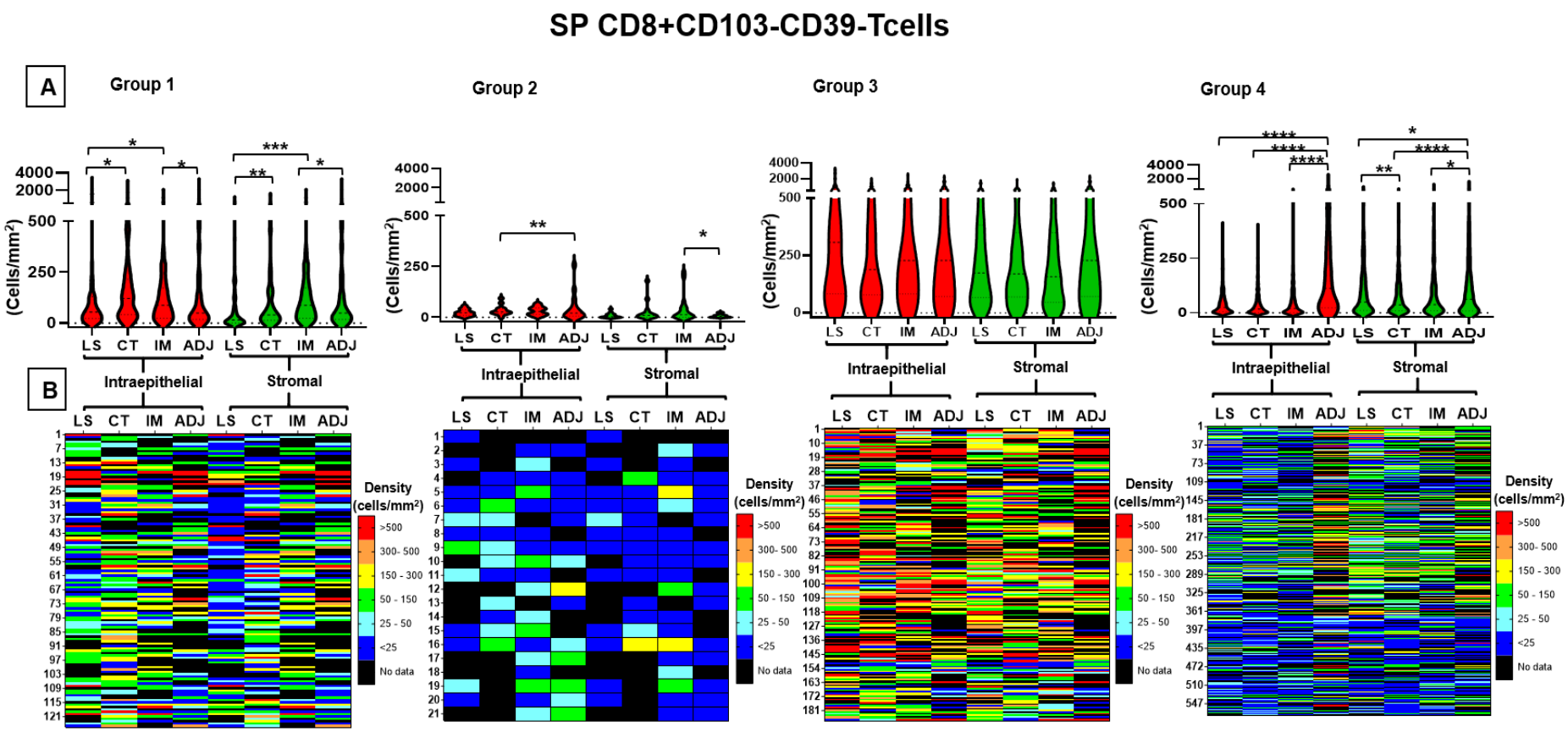

Figure 6. 22 Comparison of median density of SP CD8+TILs in different regions of the tumour (LS, CT, IM and ADJ) between different groups of CRC cohort.

(A) The violin plots represent the median density of SP CD8 TILs in the respective tumour region matched to the density of sp CD8 TILs infiltrating the same tumour region in each patient in the heat maps **(B).** Group 1 tumours (hot tumours) had significantly higher SP CD8 TILs infiltration in the CT and IM as compared to LS and ADJ. In contrast, group 4 tumours (Cold tumours) had significantly higher SP CD8 TILs infiltration in the ADJ as compared to other regions of the tumour. Mann Whitney U test was used to test for significance. P-values <0.05 were considered statistically significant. (*p ≤0.05, ** p ≤ 0.01,*** p ≤ 0.001, **** p ≤ 0.0001)

Table 6. 7 Summary of the CD8 TILs phenotypes distributed across tumour regions in group 1, group 2, group 3 and group 4 and the prognostic correlation between the four groups and patient survival in the CRC cohort.

	Total CD8+ T cells/ TP T cells	All CRCs cases	Left colon tumours	Right colon tumours	Distribution across tumour regions											
					LS			CT			IM			ADJ		
		Prognostic impact	Prognostic impact	Prognostic impact	Total CD8	TP	SP	Total CD8	TP	SP	Total CD8	TP	SP	Total CD8	TP	SP
Group 1	High/High	Good	Good	Good	High	High	Low	High	High	High	High	High	High	High	High	Low
Group 2	Low/High	Good	Good	Good	Low	High	Low	Low	High	Low	Low	High	Low	Low	High	Low
Group 3	High/Low	Poor	Poor	Good	High	Low	High	High	Low	High	High	Low	High	High	Low	High
Group 4	Low/ Low	Poor	Poor	Poor	Low	Low	Low	Low	Low	Low	Low	Low	Low	High	High	High

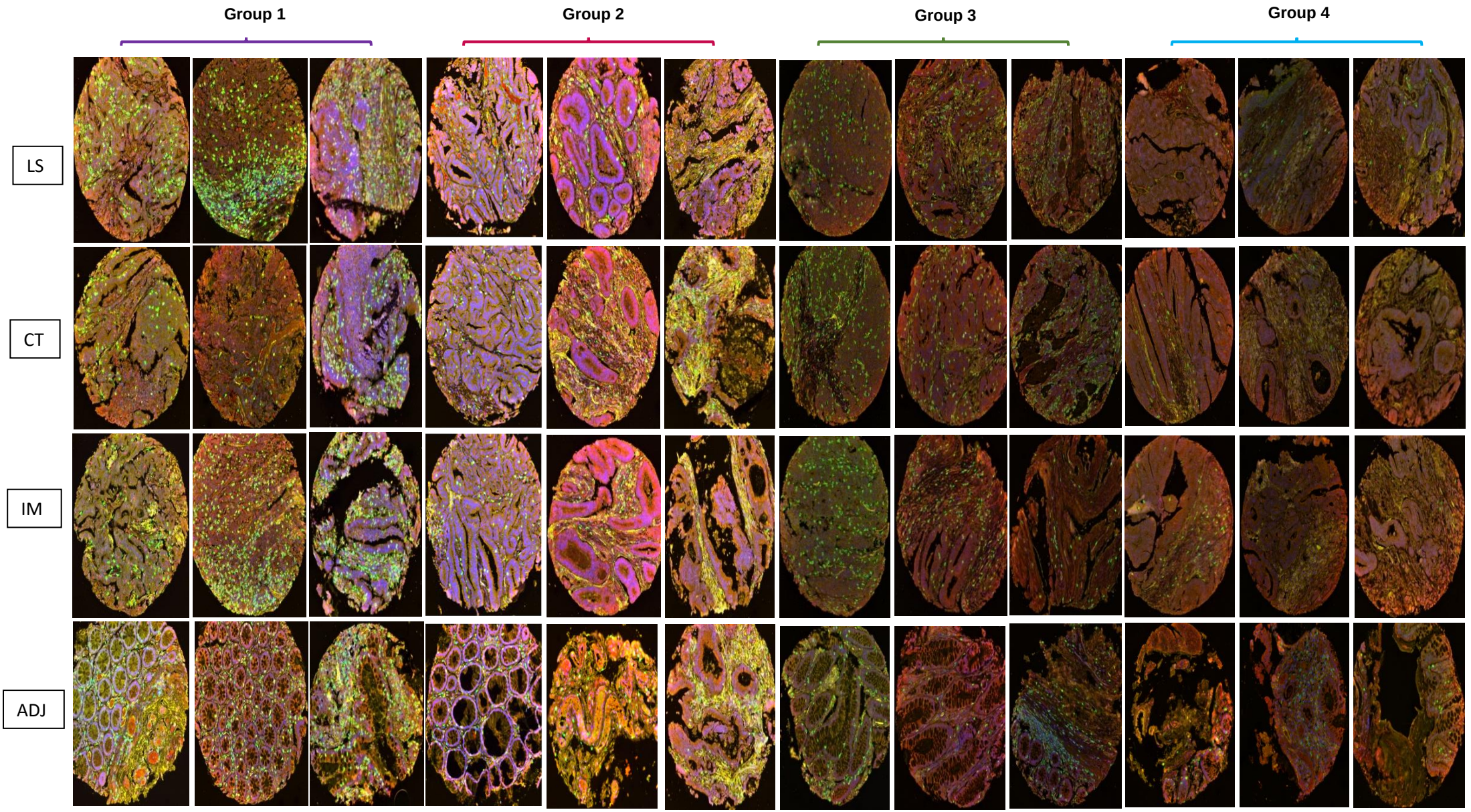

Figure 6. 23 Multiplex view of different tumour regions for patients in group 1, group 2, group 3 and group 4 of the CRC cohort. Each group represents sample staining for three individual patients.

6.3 Discussion

In this chapter, we present the largest study yet to compare the landscape and prognostic significance of recently activated tumour specific TRM cells and other CD8+ TILs phenotypes within the tumour microenvironment of colorectal tumours. Using multiplex immunohistochemistry staining, followed by training using advanced image-analysis software, tumour infiltrated CD8 T cell populations, co-expressing CD103 and/or CD39 on their surface, were detected and quantified within tumour epithelium and stroma of each TMA core. The findings of our comprehensive analysis demonstrated the superiority of recently activated tumour specific TRM cells (CD8+CD103+CD39+) as a predictive marker compared to other CD8+ phenotypes in colorectal cancer. Also, recently activated TRM CD8 T-cells were shown to be an independent predictor of survival. Due to various differences between RCRCs and LCRCs, further analysis of CD8+ TILs phenotypes between different PTLs was conducted. Among all CD8+ TILs phenotypes, recently activated TRM CD8-T cells were shown to be the only phenotype that predicted survival in both RCRCS and LCRCs. A group of hot tumours were found to be heavily infiltrated with total CD8 TILs throughout but with low infiltration of recently activated TRM CD8 T-cells. In LCRCs, the aforementioned group was associated with a poor prognosis compared to hot tumours that were heavily infiltrated with recently activated TRM CD8 T-cells. However, the presence of recently activated TRM CD8 T-cells within hot tumours was not mandatory for a better prognosis in RCRCs.

Identifying the immune contexture and phenotypic profiles of tumour infiltrating lymphocytes within the tumour microenvironment has a crucial role in predicting patients survival and tumours response to immunotherapy.[255] Heavily T cell infiltrated tumours (‘Hot’ tumours), reflecting Immunoscore I4, have been associated with

favourable tumour prognosis.[245] Tumour infiltrating CD8 T-cells are recognised as the best predictors of survival. However, CD8 TILs represent a heterogeneous cell population, including tumour-specific T cells and bystander T cells.[255, 258] In solid tumours, Duhen and colleagues reported that CD8+ TILs co-expressing of CD39 and CD103 were identified as recently activated Tumour reactive TRM. Using flow cytometric analysis, this unique population was found predominantly within the tumour microenvironment, whereas low levels of TP CD8+TILs were detected in the prepared blood and uninvolved LN. In our study, using multiplex detection system enabled us to get a deeper look into the distribution and localisation of TP CD8TILs and other CD8+TILs phenotypes within the epithelial and stromal tissue of TME of CRCs. The results showed that TRM subsets (CD8+CD103+CD39+/-) were preferentially localised in the intraepithelial compartment compared to the stromal area of TME, which could be due to the interaction between CD103 and E-cadherin on epithelial cells. This observation goes in line with the work of Webb et al.[252] and Wang et al.[250], both studies showed the ratio of intraepithelial to stromal density was significantly higher for CD103 as compared with CD8 in breast and ovarian tumours.

In this chapter, we explored the relationship between different CD8+ TILs subsets infiltration within the tumour microenvironment (epithelium and stroma) of CRCs and patient survival (DSS). It was shown that all CD8+ TILs phenotypes were associated with better survival when heavily infiltrated within the tumour epithelium in CRCs patients. Nevertheless, TP TILs were found to obtain better predictive significance by showing a higher 10-year survival rate compared to other CD8+TILs phenotypes. Furthermore, the Cox multivariate regression models, performed for each CD8+ phenotype combined with the prognostic clinicopathological variables, illustrated that TP TILs and DP CD103+CD8+TILs are the only phenotypes considered as an independent prognostic marker in CRCs. The latter observation is consistent with *Ganesan et al.*[246] and *Duhen et al.*[258] results. They found that highly infiltrated tumours

with CD8 TILs co-expressing CD103 and CD39 were associated with better prognosis in lung, head and neck tumours. According to *Ganesan et al.,* CD103+CD8+ T cells within highly infiltrated tumours are highly activated and proliferating (high expression levels of CD69+, 4-1 BB and Ki-67), co-express CD39 marker, associated with increased cytotoxic activity and displayed TRM gene signature in multiple solid tumours.[246] Moreover, Duhen and colleagues suggested that the expression of CD39 within CD103+CD8+ TILs population is crucial to enrich for tumour-reactive CD8 T cells, as the CD103+CD8+ TILs lacking CD39 expression showed little reactivity to autologous tumour cells.[258]

Some clinicopathological factors of the study cohort, such as TNM staging, tumour metastases, vascular invasion, and microsatellite instability status of the tumours, were significantly associated with all CD8+ T cell phenotypes. However, only TP and DP CD8+CD103+T cell subsets were correlated to PTL compared to non-resident T cells. This confirms the correlation reported earlier between CD103+ TILs and PTL in chapter (5). Hence, this study aimed to investigate the prognostic impact of CD8+ TILs phenotypes when infiltrated in different PTLs (RCRCs and LCRCs). In LCRCs, the only CD8TILs subset that predicted survival was the TP TILs cells. Whereas in RCRCs, highly infiltrated tumours with either CD8TILs subsets were associated with better prognosis.

In order to rule out the possibility that the distribution pattern of CD8+ TILs subsets within RCRCs and LCRCs was the reason for the latter observation, we compared the average infiltration densities of CD8+ TILs subsets between RCRCs and LCRCs and found that intraepithelial TP and DP CD39+CD8+TILs showed significantly higher intraepithelial infiltration in RCRCs compared to LCRCs. In contrast, no difference in DP CD103+CD8+ TILs and SP CD8+ TILs was observed between different PTLs. This suggests that part of DP CD103+CD8+TILs and SP CD8+TILs populations in LCRCs were cancer unrelated TILs (recognise epitopes unrelated to cancer) which

could be due to the lack of CD39. The study by *Simoni et al.*, suggest that CD39 expression is high on tumour neoantigen-specific CD8+TILs. They further demonstrated that CD39 upregulation on CD8TILs was indicative of chronic antigen stimulation in the TME. However, it should be kept in mind that these observations were made using a small sample size (n=2).[255] Having a lower TP TILs infiltration in LCRCs than RCRCs but still maintaining its' prognostic significance confirms that this unique T cell subset obtains higher tumour cytotoxic activity than the DP CD103+CD8+TILs, DP CD39+CD8+TILs and SP CD8+TILs.

A recent review by Galon and Bruni focused on the tumour's immune contexture and immunoscore as a critical indicator for the effectiveness of immunotherapies approaches. They believed that hot tumours (highly infiltrated with T cells) obtain characteristics that predict better survival and better response to immunotherapies in comparison to immunosuppressed and cold tumours.[245] Although we agree that the density of immune cells infiltration in the tumour site is vital, we speculated that the specificity and the phenotype of TILs are as important as the number of TILs, if not superior to indicate better patient survival and immunotherapy responsiveness. To validate this theory, tumours were classified into four groups depending on the infiltration density of total CD8+ TILs and TP TILs within the tumour epithelium tissue. Patients with tumours with high TP TILs infiltration showed better survival rates regardless of total CD8+ TILs infiltration.

According to the conventional classification of hot tumours (high infiltration of CD8 TILs), group 1 and 3 should be considered hot tumours. Whereas Group 2 and 4 were classified as cold tumours (low infiltration of CD8 TILs). However, we suggest that tumours with high infiltration of activated tumour specific resident TILs (TP TILs) should be considered hot tumours regardless of the infiltration densities of other CD8+ TILs phenotypes. In contrast, group 3 should be defined as 'lukewarm' tumours

due to the high density of CD8+ TILs populations (in exception of TP TILs) within the tumour tissue, but in terms of patients survival, no significant difference was observed between group 3 tumours and group 4 (cold) tumours. Furthermore, hot tumours (group1) had total CD8+TILs infiltration and TP TILs infiltration in all tumour regions (LS, CT and IM) except the adjacent normal tissue. In contrast, the cold tumours (group 4) had higher total CD8+TILs infiltration and TP TILs infiltration the adjacent normal tissue but not in the other regions of the tumour. We also assessed the average density of SP CD39+ cells in the stroma of all the four groups' CRCs. The high expression of CD39 in the stroma of group 3 tumours explains the poor prognosis observed due to immunosuppression caused by adenosine accumulation. Therefore, it might be useful to target CD39 in group 3 tumours to overcome the immunosuppression, which might improve patient survival of that group.

Survival analyses for group 1, group 2, group 3 and group 4 in RCRC and LCRC was performed. In RCRC that has tumour mutational burden and high MSI status, thus having high neoantigens, patients in group 1, group 2, and group 3 were associated with a better prognosis than group 4 patients. However, LCRC patients with only high TP TILs (group1 and group2) showed a better prognosis. It is interesting to note that group 3 patients who had low TP TILs infiltration but high total CD8 infiltration had a better prognosis in RCRCs and a poor prognosis in LCRCs. The reason behind the difference observed in the survival analyses of group 3 between RCRC and LCRC is unclear. It could be due to the differences in the mutational burden, tumour neoantigen, genetic mutations or other immune cells in the TME that were out of the scope of this study. The focus of this study was assessing different phenotypes of the cytotoxic T cell populations in CRC. Assessing other immune infiltrate like CD4+ T cell phenotypes that could play an important role in survival was not part of this study which is a limitation. Future studies should look at incorporating the different immune cell phenotypes observed in the TME to assess their prognostic potential.

Chapter 7: Final discussion

Colorectal cancer harbours enormous heterogeneity, with spatial and temporal differences in genetic alterations, epigenetic regulation, and tumour microenvironment. A better understanding of the frequency and distribution of immune cells infiltration, genetic alterations and microenvironment differences in CRCs would govern the treatment approaches for this disease. In this study, we have demonstrated that high CD3 and CD8 TILs infiltration in any region within the colorectal tumour (LS, CT and IM) but not in the adjacent normal tissue predicts better disease-free survival time. We have also demonstrated that MSI tumours, which are predominantly found in the right-sided colon tumours, have more levels of intraepithelial CD8 TILs and CD103 TILs than those with MSS, and that CD103 TILs was an independent predictor of patient survival in RCRC. Importantly, we are reporting for the first time that a specific subset of CD8TILs co-expressing CD103 and CD39, identified as tumour reactive TRM cells, was the only subset associated with better prognosis in both LRCR and RCRC patients.

Although various therapies are available for the treatment of advanced colorectal cancer, survival rates for these patients remain very poor. The standard conventional treatments for colorectal tumours are surgery, chemotherapy and radiotherapy. Based on the progression and localisation of the disease, these treatments can be used in combination.[414, 415, 416] For localised cancer or whenever the tumour location is accessible, total mesorectal excision through transanal and laparoscopic surgery approaches are often the treatment options for this group. Nevertheless, complete removal of all tumour cells is often not possible. About 61% to 66% of stage II and III CRC patients require further treatments with adjuvant therapy (chemotherapy and/or

radiotherapy)[417]. Due to the unspecificity and cytotoxicity of these treatments, patients may suffer from many side effects. Moreover, 54% of patients relapse even after neoadjuvant treatment [418, 419]. Therefore, targeted therapeutics and immunotherapies, especially for metastatic advanced CRC cases, have been developed and combined with conventional chemotherapy to improve the overall survival among these patients.

CRC patients with different primary tumour locations respond differently to the adjuvant therapy combinations. When conventional chemotherapy is combined with targeted therapeutics, especially with anti-EGFR agents (cetuximab and panitumumab), LCRC tumours have better outcomes than RCRC tumours.[279] In contrast, immunotherapies such as Anti-PD-1 inhibitors (pembrolizumab and nivolumab) seem to have more promising results in RCRC patients compared to LCRC patients, which were non-responsive to any immunotherapeutic agents. The responsiveness of RCRC tumours to immunotherapies is justified by the unique characteristics of these tumours, like having high microsatellite instability status, which leads to a higher number of mutations and thereby a higher number of neoepitopes for T cell recognition leading to a higher likelihood of having highly activated lymphocytic microenvironment – so called “hot tumours”.[275, 279] Moreover, MSI-High CRC tumours have a high density of Tbet-positive Th1 T cells, higher expression of the chemokines CCL5, CXCL9, and CXCL10, and upregulation of a range of immune checkpoint genes (CTLA4, PDL1, PDL2, LAG3, and TIM3) relative to MSS tumours [420].

In 2017, the FDA approved pembrolizumab and nivolumab as monotherapy to treat deficient mismatch repair/microsatellite instability-high (dMMR/MSI-high) CRCs, CTL-4 inhibitors (Ipilimumab and tremelimumab) did not show any significant benefit alone in CRC patients. However, ipilimumab in combination with nivolumab showed an improved survival benefit in MSI-high CRCs, and therefore the combination of these immunotherapies was approved in 2018 for this group of CRCs patients.

Our study proposes several potential approaches to convert LCRC tumours into more immunogenic ones and improve their responsiveness to immunotherapies. The first approach is to convert the cold microenvironment of LCRC tumours into hot microenvironment by treating these tumours with a combination of CTL-4 inhibitor and Anti-PD-1 inhibitor. According to the Nobel laureate Professor James Allison, immune checkpoint inhibitors showed significant survival benefit mostly in tumours with a high mutational burden (TMB), such as melanoma, which tend to be responsive because there are neoantigens available for targeting by reinvigorated T cells, while those with low TMB demonstrate limited clinical responses. However, he suggested that a combination of anti–CTLA-4 plus anti–PD-1 checkpoint blockade utilises cellular mechanisms partially distinct from monotherapies, indicating that tumours with low TMB might respond differently with combinational immunotherapies than monotherapies.[291]

The practical application of this was demonstrated in a recent study conducted by *Sharma et al.*[292] on Metastatic castration-resistant prostate cancer (mCRPC). It has been reported that mCRPC is immunologically cold and predominantly resistant to immune checkpoint therapy due to few tumour-infiltrating T cells. Therefore, Ipilimumab (anti-CTLA-4) or anti-PD-1/PD-L1 monotherapy failed to show a significant benefit in mCRPC. However, a significant survival benefit was observed with mCRPC patients when treated with an ipilimumab/nivolumab combination. They found that the treatment of ipilimumab turned prostate tumours from cold to hot, with increased tumour penetration by activated T cells. Nevertheless, increased PD-1/PD-L1 expression was observed with prostate tumours as a compensatory inhibitory pathway to ipilimumab. Therefore, the treatment with nivolumab anti-PD-1/PD-L1 protected the immune response induced by ipilimumab resulting in an enhanced efficacy when used both treatments together than using each individually.[292]

Previous studies conducted on melanoma tumours have also revealed that monotherapies targeting CTLA-4 and PD-1 regulate specific CD4 and CD8 T cell subsets, which contribute to the therapeutic effect of both therapies. Th1-like PD-1+ ICOS+ TBET+ CD4 effector T cell population expanded following anti–CTLA-4 but not anti–PD-1 monotherapy. In contrast, phenotypically exhausted (PD-1^{high} Lag3+ Tim3+) CD8 T cells expanded in response to anti–PD-1 monotherapy. Interestingly, despite displaying a highly exhausted phenotype, nearly 20% of PD-1^{high} Lag3+ Tim3+ CD8 T cells were actively proliferating regardless of therapy. These data support a model in which phenotypically exhausted CD8 T cells still functionally contribute to antitumor responses.[291, 421]

In line with the latter observation, recent studies revealed that among the heterogeneous CD8 TILs populations, CD8 TIL co-expressing CD39+ and CD103 subset was chronically activated with exhaustion characteristics, enriched for tumour recognition and immune specific tumour killing. In chapter 6, we have discussed the prognostic role TP CD8+ TILs and other CD8 TILs subsets (DP CD103+CD8+, DP CD39+CD8+ and SP CD8+ TILs) between different CRC sidedness. In LCRC patients, TP CD8+ TILs were the only CD8 TILs subset to show a better prognosis when expressed highly within the tumour epithelium and stroma. Moreover, heavily infiltrated LCRCs with total CD8+TILs in the absence of recently activated TRM (TP CD8 TILs) were shown not to have any significant benefit of survival compared to LCRC with low tumour infiltrated microenvironment (cold). Thereby, we suggest that in addition to converting LCRCs from cold tumours into hot ones, another potential approach to improve patient survival and obtain a better response to immunotherapies in LCRC patients is by re-stimulating and expanding the recently activated TRM subset within the tumour microenvironment of LCRCs.

The activated phenotype of the TP CD39+C103+CD8 TILs and their skewed TCR repertoire strongly suggest that these cells recognise their cognate antigen within the tumour microenvironment. However, TP CD39+C103+CD8 TILs were associated with the highest expression of activation/exhaustion markers (e.g., PD-1, CTLA-4 and TIM-3) due to the chronic TCR stimulation within the tumour. Sustained expression of these checkpoints molecules can have detrimental effects on the downregulate the cytotoxic activity of these cells resulting in tumour outgrowth.[258] Therefore, checkpoint inhibitors could inhibit the recently activated tumour-specific TRM cells, allowing them to fully exert their effector function. To address this hypothesis, it would be of interest to determine the frequency and/or activation status of the TP CD39+C103+CD8 TILs within the tumours following anti-PD-1 and anti- CTLA-4 monotherapy or a combination of both therapies.

Several studies reported that the expression of CD39 on CD8TILs indicate the tumour specificity of that subset, and it reflects the most activated CD8+ T-cells.[255, 410] According to *Duhen et al.*, CD39 expression levels on TP CD8TILs is the highest compared to other subsets. However, CD39 has been known as an ectonucleotidase that hydrolyses extracellular ATP and ADP into AMP, which is then processed into adenosine by CD73. Adenosine is a potent immunoregulator and, when binding to A2A receptors on T lymphocytes, it enhances the accumulation of intracellular cAMP, thereby dampening T-cell activation.[422] Interfering with the adenosine pathway via blockade of the CD39/CD73 axis or adenosine receptors on T cells within the tumour microenvironment might be another promising therapeutic strategy to increase the function/potency of the TP CD8 TIL.

A recent study conducted on mice with atherosclerosis by *van Duijn et al.*[254] demonstrated that CD39 inhibition using the small molecule inhibitor sodium

metatungstate (POM-1) increased the IFN-γ production by all CD8+TILs populations and mainly in the subsets lacking CD39. Interestingly, the expression levels of CD39 were also slightly increased upon treatment with POM-1.[254] As previously mentioned, CD39 is constitutively expressed by Foxp3+ Treg cells and suppression of Th1 and Th17 responses in an adenosine-dependent manner have been well documented for CD39+ Treg cells. Based on the aforementioned findings, we speculate that using anti- CD39 inhibitor might obtain dual effect, expanding and enhancing the cytotoxic activity of TP CD8TILs and reducing the suppression activity of CD39+ Treg cells. Therefore, future studies should consider anti-CD39 inhibitors as a potential treatment for LCRC patients alone or combined with other checkpoint inhibitors.

Currently, there are over 1,100 clinical trials testing the efficacy of PD-1 blockade agents in combination with other therapies.[423] These include over 250 combining therapeutic agents targeting CTLA-4 and PD-1, as well as combinations with novel agents targeting other T cell costimulatory molecules (e.g., TIM-3, LAG3, OX-40).[291] In addition to these molecules, there are other potential receptors on T-cells, such as tetraspanin proteins that could be targeted for therapeutic antibodies. Several members of the tetraspanin family have been implicated in the regulation of T-cells.

The knock-out of some tetraspanins in mice results in the hyperproliferation of T cells, similar to effects seen in CTLA-4 and PD-1 KO mice. TSPAN32 is a member of tetraspanin proteins in which T cell hyperproliferation was observed during KO.[320, 321] This observation has led to the belief that TSPAN32 obtain a negative regulatory role in T cell proliferation which could be targeted as checkpoint inhibitors in cancer immunotherapy. In our study, we have demonstrated that immunisation with plasma membrane extraction of TSPAN32 transfected cells was successful to produce an anti-TSPAN32 immune response in BALB/c mice. However, further efforts are

needed to develop mAb that recognises TSPAN32 to determine the functional role of TSPAN32 on the proliferation of T cells in general and on TP CD8 TILs in particular.

Growing evidence suggests that the adoptive transfer of antigen-specific CD8 TILs might represent an effective strategy in the fight against malignancies, such as melanoma and chronic viral infections.[424] As discussed earlier, TP CD8TILs are tissue-resident and found only within the tumour microenvironment and absent or present at very low frequency in the peripheral blood and an uninvolved LN. Therefore, in vitro expansion of recently activated TRM cells and transferred it back to the patient might be challenging to achieve. However, in vivo expansion of recently activated TRM cells might be implemented by converting other CD8TILs subsets into TP CD8TILs within the tumour microenvironment. In order to achieve that, we need to investigate the transcription pathways of TP CD8TILs and understand which transcription factors are involved in defining the characteristics and function of this unique subset. Then we can target these pathways with small molecules to increase the TP CD8TILs density within the TME of LCRCs. Alternatively, identifying TCR sequences within the TP CD8 TILs that specifically recognise tumour antigens may aid in TCR engineering approaches that would lead to a personalised tumour therapy in LCRC patients or within tumours that have failed approved treatments.

Molecular profiling of RCRC and LCRC tumours (including mutational analysis for BRAF, KRAS, NRAS, PIK3CA, POLE, POLD1 and others) has become increasingly important to obtain a proper treatment plan for patients with advanced stages. It has been reported that right-sided colon cancers have higher *BRAF*, *POLE, POLD1* and *PIK3CA* mutation rates compared to LCRC. In contrast, RAS mutations (KRAS, NRAS) were more presented in LRCR. Moreover, *TP53* and *APC* were significantly more frequently mutated in LCRCs than RCRCs[275, 279]. A recent study conducted by *Lal et al.*[420] revealed a link between the immune landscape and CRCs

different mutation types in addition to the MSI status and the presence of neoantigen. They found that CRC tumours with *POLE* and *POLD1* mutations predict a high-level expression of T helper cell and class II-related genes together alongside a range of chemokines (*CX3CL1, CXCL9, CXCL10*) and immune inhibitory checkpoint molecules (PD-L1, PD-L2, LAG3, TIM3 and CTLA4), which suggests a combination checkpoint blockade therapy may be required to improve efficacy in such tumours. In contrast, *RAS* mutant (KRAS, NRAS) tumours were associated with relatively poor immune infiltration and low inhibitory molecule expression. In this setting, checkpoint inhibitors could be less efficacious, highlighting the need for novel strategies in this group of patients.[420]

In line with *Lal et al.* observations, Liao and colleagues showed that oncogenic KRAS mutation drives an immune suppressive activity in CRCs by suppressing the expression of interferon regulatory factor 2 (IRF2), a negative regulator of the CXCL3 chemokine expression, which leads to enhanced expression of CXCL3 and recruitment of suppressive myeloid cells, and subsequent resistance to immune checkpoint blockade.[425] These findings suggest that immune cells infiltration and the responsiveness to ICB mono- or combinational therapy might be governed by the mutational type of CRC, in addition to CRC sidedness and MSI status. Thereby, further investigation of the correlation between recently activated tumour-specific TRM cells and CRCs different mutation types is required to obtain a better prediction and optimisation of immunotherapies efficacy in CRCs.

From the above studies, it is evident that different CD8+ and CD4+ TILs subtypes exist and function within the tumour microenvironment. From our study, we see that the presence of recently activated tumour specific TRM cells is an independent predictor of survival. Therefore expanding or increasing the infiltration of this subset into the tumour microenvironment can be beneficial for treating solid tumours, especially the cold ones. It is curious to think that there might be other subsets like

recently activated tumour specific TRM cells that not yet have been identified that could be of clinical significance and target cancer cells. There are strong implications from our study and some of the studies discussed above that high CD8 infiltration does not necessarily imply that all the T cells infiltrating specifically attack cancer cells. There might be some T cells that may act as bystander populations while specific T cell populations like recently activated tumour specific TRM cells subset might be the actively cytotoxic population in the TME. Therefore, targeting these specific cytotoxic T cell subsets in the TME to improve their functionality using combination therapies should be the focus of the future treatment strategies.

References

1. Charles A Janeway, J., Paul Travers, Mark Walport, and Mark J Shlomchik. *Janeway's immunobiology*. Garland Science: New York, 2012.

2. Delves, P.J. & Roitt, I.M. The immune system. First of two parts. *The New England journal of medicine* **343**, 37-49 (2000).

3. Kuby, J.A.O.J.P.S.A.S.P.P.J.J. *Kuby immunology*. W.H. Freeman: New York 2012.

4. Miller, J. The discovery of thymus function and of thymus-derived lymphocytes. *Immunological reviews* **185**, 7-14 (2002).

5. Miller, J. Events that led to the discovery of T-cell development and function - A personal recollection. *Tissue antigens* **63**, 509-517 (2004).

6. Miller, J.F. The golden anniversary of the thymus. *Nature reviews. Immunology* **11**, 489-495 (2011).

7. Wu, L. *et al.* CD4 expressed on earliest T-lineage precursor cells in the adult murine thymus. *Nature* **349**, 71-74 (1991).

8. Wu, L., Antica, M., Johnson, G.R., Scollay, R. & Shortman, K. Developmental potential of the earliest precursor cells from the adult mouse thymus. *The Journal of experimental medicine* **174**, 1617-1627 (1991).

9. Benz, C. & Bleul, C. A multipotent precursor in the thymus maps to the branching point of the T versus B lineage decision. *The Journal of experimental medicine* **202**, 21 - 31 (2005).

10. Igarashi, H., Gregory, S.C., Yokota, T., Sakaguchi, N. & Kincade, P.W. Transcription from the RAG1 locus marks the earliest lymphocyte progenitors in bone marrow. *Immunity* **17**, 117-130 (2002).

11. Schlenner, S. *et al.* Fate Mapping Reveals Separate Origins of T Cells and Myeloid Lineages in the Thymus. *Immunity* **32**, 426-436 (2010).

12. Petrie, H.T. & Zúñiga-Pflücker, J.C. Zoned out: functional mapping of stromal signaling microenvironments in the thymus. *Annual review of immunology* **25**, 649-679 (2007).

13. Shortman, K., Egerton, M., Spangrude, G.J. & Scollay, R. The generation and fate of thymocytes. *Seminars in immunology* **2**, 3-12 (1990).

14. Feyerabend, T.B. *et al.* Deletion of Notch1 converts pro-T cells to dendritic cells and promotes thymic B cells by cell-extrinsic and cell-intrinsic mechanisms. *Immunity* **30**, 67-79 (2009).

15. Han, H. *et al.* Inducible gene knockout of transcription factor recombination signal binding protein-J reveals its essential role in T versus B lineage decision. *International immunology* **14**, 637-645 (2002).

16. Hozumi, K. *et al.* Delta-like 4 is indispensable in thymic environment specific for T cell development. *The Journal of experimental medicine* **205**, 2507-2513 (2008).

17. Koch, U. *et al.* Delta-like 4 is the essential, nonredundant ligand for Notch1 during thymic T cell lineage commitment. *The Journal of experimental medicine* **205**, 2515-2523 (2008).

18. Capone, M., Hockett, R.D., Jr. & Zlotnik, A. Kinetics of T cell receptor beta, gamma, and delta rearrangements during adult thymic development: T cell receptor rearrangements are present in CD44(+)CD25(+) Pro-T thymocytes. *Proc Natl Acad Sci U S A* **95**, 12522-12527 (1998).

19. Livák, F., Tourigny, M., Schatz, D.G. & Petrie, H.T. Characterization of TCR gene rearrangements during adult murine T cell development. *Journal of immunology (Baltimore, Md. : 1950)* **162**, 2575-2580 (1999).

20. Burtrum, D.B., Kim, S., Dudley, E.C., Hayday, A.C. & Petrie, H.T. TCR gene recombination and alpha beta-gamma delta lineage divergence: productive TCR-beta rearrangement is neither exclusive nor preclusive of gamma delta cell development. *Journal of immunology (Baltimore, Md. : 1950)* **157**, 4293-4296 (1996).

21. Porritt, H.E., Gordon, K. & Petrie, H.T. Kinetics of steady-state differentiation and mapping of intrathymic-signaling environments by stem cell transplantation in nonirradiated mice. *The Journal of experimental medicine* **198**, 957-962 (2003).

22. Borgulya, P., Kishi, H., Uematsu, Y. & von Boehmer, H. Exclusion and inclusion of alpha and beta T cell receptor alleles. *Cell* **69**, 529-537 (1992).

23. Singer, A., Adoro, S. & Park, J.-H. Lineage fate and intense debate: myths, models and mechanisms of CD4- versus CD8-lineage choice. *Nature Reviews Immunology* **8**, 788-801 (2008).

24. Veillette, A., Zúñiga-Pflücker, J.C., Bolen, J.B. & Kruisbeek, A.M. Engagement of CD4 and CD8 expressed on immature thymocytes induces activation of intracellular tyrosine phosphorylation pathways. *The Journal of experimental medicine* **170**, 1671-1680 (1989).

25. Starr, T.K., Jameson, S.C. & Hogquist, K.A. Positive and Negative Selection of T Cells. *Annual review of immunology* **21**, 139-176 (2003).

26. Cerottini, J.C., Nordin, A.A. & Brunner, K.T. Specific in vitro cytotoxicity of thymus-derived lymphocytes sensitized to alloantigens. *Nature* **228**, 1308-1309 (1970).

27. Zinkernagel, R.M. & Doherty, P.C. Immunological surveillance against altered self components by sensitised T lymphocytes in lymphocytic choriomeningitis. *Nature* **251**, 547-548 (1974).

28. Golstein, P., Wigzell, H., Blomgren, H. & Svedmyr, E.A. Cells mediating specific in vitro cytotoxicity. II. Probable autonomy of thymus-processed lymphocytes (T cells) for the killing of allogeneic target cells. *The Journal of experimental medicine* **135**, 890-906 (1972).

29. Cantor, H. & Boyse, E.A. Functional subclasses of T lymphocytes bearing different Ly antigens. II. Cooperation between subclasses of Ly+ cells in the generation of killer activity. *The Journal of experimental medicine* **141**, 1390-1399 (1975).

30. Kisielow, P. *et al.* Ly antigens as markers for functionally distinct subpopulations of thymus-derived lymphocytes of the mouse. *Nature* **253**, 219-220 (1975).

31. Shiku, H. *et al.* Expression of T-cell differentiation antigens on effector cells in cell-mediated cytotoxicity in vitro. Evidence for functional heterogeneity related to the surface phenotype of T cells. *The Journal of experimental medicine* **141**, 227-241 (1975).

32. Shimonkevitz, R., Kappler, J., Marrack, P. & Grey, H. Antigen recognition by H-2-restricted T cells. I. Cell-free antigen processing. *The Journal of experimental medicine* **158**, 303-316 (1983).

33. Gotch, F., Rothbard, J., Howland, K., Townsend, A. & McMichael, A. Cytotoxic T lymphocytes recognize a fragment of influenza virus matrix protein in association with HLA-A2. *Nature* **326**, 881-882 (1987).

34. Yewdell, J.W., Bennink, J.R., Smith, G.L. & Moss, B. Influenza A virus nucleoprotein is a major target antigen for cross-reactive anti-influenza A virus cytotoxic T lymphocytes. *Proc Natl Acad Sci U S A* **82**, 1785-1789 (1985).

35. Hickman, H.D. *et al.* Direct priming of antiviral CD8+ T cells in the peripheral interfollicular region of lymph nodes. *Nature immunology* **9**, 155-165 (2008).

36. Chtanova, T. *et al.* Dynamics of T cell, antigen-presenting cell, and pathogen interactions during recall responses in the lymph node. *Immunity* **31**, 342-355 (2009).

37. John, B. *et al.* Dynamic Imaging of CD8(+) T cells and dendritic cells during infection with Toxoplasma gondii. *PLoS pathogens* **5**, e1000505 (2009).

38. Parish, I.A. & Kaech, S.M. Diversity in CD8(+) T cell differentiation. *Current opinion in immunology* **21**, 291-297 (2009).

39. Mescher, M.F. *et al.* Signals required for programming effector and memory development by CD8+ T cells. *Immunol Rev* **211**, 81-92 (2006).

40. Zhang, N. & Bevan, M.J. CD8(+) T cells: foot soldiers of the immune system. *Immunity* **35**, 161-168 (2011).

41. Pamer, E. & Cresswell, P. Mechanisms of MHC class I--restricted antigen processing. *Annual review of immunology* **16**, 323-358 (1998).

42. Wong, P. & Pamer, E.G. CD8 T cell responses to infectious pathogens. *Annual review of immunology* **21**, 29-70 (2003).

43. Srivastava, P. Interaction of heat shock proteins with peptides and antigen presenting cells: chaperoning of the innate and adaptive immune responses. *Annual review of immunology* **20**, 395-425 (2002).

44. Lefrançois, L., Altman, J.D., Williams, K. & Olson, S. Soluble Antigen and CD40 Triggering Are Sufficient to Induce Primary and Memory Cytotoxic T Cells. *The Journal of Immunology* **164**, 725-732 (2000).

45. Kurts, C. Cross-presentation: inducing CD8 T cell immunity and tolerance. *Journal of molecular medicine (Berlin, Germany)* **78**, 326-332 (2000).

46. Fehres, C.M., Unger, W.W., Garcia-Vallejo, J.J. & van Kooyk, Y. Understanding the biology of antigen cross-presentation for the design of vaccines against cancer. *Frontiers in immunology* **5**, 149 (2014).

47. Andersen, M.H., Schrama, D., Thor Straten, P. & Becker, J.C. Cytotoxic T cells. *The Journal of investigative dermatology* **126**, 32-41 (2006).

48. Nagata, S. Fas-mediated apoptosis. *Advances in experimental medicine and biology* **406**, 119-124 (1996).

49. Trapani, J.A. & Smyth, M.J. Functional significance of the perforin/granzyme cell death pathway. *Nature Reviews Immunology* **2**, 735-747 (2002).

50. Osińska, I., Popko, K. & Demkow, U. Perforin: an important player in immune response. *Central-European journal of immunology* **39**, 109-115 (2014).

51. Halle, S. *et al.* In Vivo Killing Capacity of Cytotoxic T Cells Is Limited and Involves Dynamic Interactions and T Cell Cooperativity. *Immunity* **44**, 233-245 (2016).

52. Wiedemann, A., Depoil, D., Faroudi, M. & Valitutti, S. Cytotoxic T lymphocytes kill multiple targets simultaneously via spatiotemporal uncoupling of lytic and stimulatory synapses. *Proceedings of the National Academy of Sciences* **103**, 10985-10990 (2006).

53. Kuhn, J.R. & Poenie, M. Dynamic polarization of the microtubule cytoskeleton during CTL-mediated killing. *Immunity* **16**, 111-121 (2002).

54. Klebanoff, C.A., Gattinoni, L. & Restifo, N.P. CD8+ T-cell memory in tumor immunology and immunotherapy. *Immunol Rev* **211**, 214-224 (2006).

55. Durgeau, A., Virk, Y., Corgnac, S. & Mami-Chouaib, F. Recent Advances in Targeting CD8 T-Cell Immunity for More Effective Cancer Immunotherapy. *Frontiers in immunology* **9**, 14 (2018).

56. Reading, J.L. *et al.* The function and dysfunction of memory CD8(+) T cells in tumor immunity. *Immunol Rev* **283**, 194-212 (2018).

57. Gravano, D.M. & Hoyer, K.K. Promotion and prevention of autoimmune disease by CD8+ T cells. *Journal of autoimmunity* **45**, 68-79 (2013).

58. Overwijk, W.W. *et al.* Tumor regression and autoimmunity after reversal of a functionally tolerant state of self-reactive CD8+ T cells. *The Journal of experimental medicine* **198**, 569-580 (2003).

59. Gattinoni, L. *et al.* Acquisition of full effector function in vitro paradoxically impairs the in vivo antitumor efficacy of adoptively transferred CD8+ T cells. *The Journal of clinical investigation* **115**, 1616-1626 (2005).

60. den Boer, A.T. *et al.* The tumoricidal activity of memory CD8+ T cells is hampered by persistent systemic antigen, but full functional capacity is regained in an

antigen-free environment. *Journal of immunology (Baltimore, Md. : 1950)* **172**, 6074-6079 (2004).

61. Yee, C. *et al.* Adoptive T cell therapy using antigen-specific CD8+ T cell clones for the treatment of patients with metastatic melanoma: in vivo persistence, migration, and antitumor effect of transferred T cells. *Proc Natl Acad Sci U S A* **99**, 16168-16173 (2002).

62. Willcox, A., Richardson, S.J., Bone, A.J., Foulis, A.K. & Morgan, N.G. Analysis of islet inflammation in human type 1 diabetes. *Clinical and experimental immunology* **155**, 173-181 (2009).

63. Wong, C.P. *et al.* Identical beta cell-specific CD8(+) T cell clonotypes typically reside in both peripheral blood lymphocyte and pancreatic islets. *Journal of immunology (Baltimore, Md. : 1950)* **178**, 1388-1395 (2007).

64. Lucchinetti, C. *et al.* Inflammatory Cortical Demyelination in Early Multiple Sclerosis. *The New England journal of medicine* **365**, 2188-2197 (2011).

65. Coles, A.J. *et al.* Alemtuzumab vs. interferon beta-1a in early multiple sclerosis. *The New England journal of medicine* **359**, 1786-1801 (2008).

66. Huseby, E.S. *et al.* A pathogenic role for myelin-specific CD8(+) T cells in a model for multiple sclerosis. *The Journal of experimental medicine* **194**, 669-676 (2001).

67. Rep, M.H. *et al.* Treatment with depleting CD4 monoclonal antibody results in a preferential loss of circulating naive T cells but does not affect IFN-gamma secreting TH1 cells in humans. *The Journal of clinical investigation* **99**, 2225-2231 (1997).

68. McKinney, E.F. *et al.* A CD8+ T cell transcription signature predicts prognosis in autoimmune disease. *Nature medicine* **16**, 586-591, 581p following 591 (2010).

69. Claman, H.N., Chaperon, E.A. & Triplett, R.F. Thymus-marrow cell combinations. Synergism in antibody production. *Proceedings of the Society for Experimental Biology and Medicine. Society for Experimental Biology and Medicine (New York, N.Y.)* **122**, 1167-1171 (1966).

70. Miller, J.F. & Mitchell, G.F. Cell to cell interaction in the immune response. I. Hemolysin-forming cells in neonatally thymectomized mice reconstituted with thymus or thoracic duct lymphocytes. *The Journal of experimental medicine* **128**, 801-820 (1968).

71. Mitchell, G.F. & Miller, J.F. Cell to cell interaction in the immune response. II. The source of hemolysin-forming cells in irradiated mice given bone marrow and

thymus or thoracic duct lymphocytes. *The Journal of experimental medicine* **128**, 821-837 (1968).

72. Nossal, G.J., Cunningham, A., Mitchell, G.F. & Miller, J.F. Cell to cell interaction in the immune response. 3. Chromosomal marker analysis of single antibody-forming cells in reconstituted, irradiated, or thymectomized mice. *The Journal of experimental medicine* **128**, 839-853 (1968).

73. Raff, M.C. Role of Thymus-derived Lymphocytes in the Secondary Humoral Immune Response in Mice. *Nature* **226**, 1257-1258 (1970).

74. Howard, M. *et al.* Identification of a T cell-derived b cell growth factor distinct from interleukin 2. *The Journal of experimental medicine* **155**, 914-923 (1982).

75. Paul, W.E. & Ohara, J. B-cell stimulatory factor-1/interleukin 4. *Annual review of immunology* **5**, 429-459 (1987).

76. Mosmann, T.R., Cherwinski, H., Bond, M.W., Giedlin, M.A. & Coffman, R.L. Two types of murine helper T cell clone. I. Definition according to profiles of lymphokine activities and secreted proteins. *Journal of immunology (Baltimore, Md. : 1950)* **136**, 2348-2357 (1986).

77. Cantor, H. & Boyse, E.A. Regulation of cellular and humoral immune responses by T-cell subclasses. *Cold Spring Harbor symposia on quantitative biology* **41 Pt 1**, 23-32 (1977).

78. Elgueta, R. *et al.* Molecular mechanism and function of CD40/CD40L engagement in the immune system. *Immunol Rev* **229**, 152-172 (2009).

79. Gay, D. *et al.* Functional interaction between human T-cell protein CD4 and the major histocompatibility complex HLA-DR antigen. *Nature* **328**, 626-629 (1987).

80. Doyle, C. & Strominger, J.L. Interaction between CD4 and class II MHC molecules mediates cell adhesion. 1987. *Journal of immunology (Baltimore, Md. : 1950)* **184**, 5935-5938 (2010).

81. Laidlaw, B.J., Craft, J.E. & Kaech, S.M. The multifaceted role of CD4(+) T cells in CD8(+) T cell memory. *Nature reviews. Immunology* **16**, 102-111 (2016).

82. Rajasagi, N.K. *et al.* CD4+ T cells are required for the priming of CD8+ T cells following infection with herpes simplex virus type 1. *Journal of virology* **83**, 5256-5268 (2009).

83. Smith, C.M. *et al.* Cognate CD4(+) T cell licensing of dendritic cells in CD8(+) T cell immunity. *Nature immunology* **5**, 1143-1148 (2004).

84. Janssen, E.M. *et al.* CD4+ T cells are required for secondary expansion and memory in CD8+ T lymphocytes. *Nature* **421**, 852-856 (2003).

85. Phares, T.W. *et al.* CD4 T cells promote CD8 T cell immunity at the priming and effector site during viral encephalitis. *Journal of virology* **86**, 2416-2427 (2012).

86. Janssen, E.M. *et al.* CD4+ T cells are required for secondary expansion and memory in CD8+ T lymphocytes. *Nature* **421**, 852-856 (2003).

87. Shedlock, D.J. & Shen, H. Requirement for CD4 T cell help in generating functional CD8 T cell memory. *Science* **300**, 337-339 (2003).

88. Sun, J.C. & Bevan, M.J. Defective CD8 T cell memory following acute infection without CD4 T cell help. *Science* **300**, 339-342 (2003).

89. Charles A Janeway, J., Paul Travers, Mark Walport, and Mark J Shlomchik. *Immunobiology: The Immune System in Health and Disease*. Garland Science: New York, 2001.

90. Caccamo, N., Dieli, F., Wesch, D., Jomaa, H. & Eberl, M. Sex-specific phenotypical and functional differences in peripheral human Vgamma9/Vdelta2 T cells. *Journal of leukocyte biology* **79**, 663-666 (2006).

91. Chien, Y.-h., Iwashima, M., Kaplan, K.B., Elliott, J.F. & Davis, M.M. A new T-cell receptor gene located within the alpha locus and expressed early in T-cell differentiation. *Nature* **327**, 677-682 (1987).

92. Hayday, A. *et al.* Structure, organization, and somatic rearrangement of T cell gamma genes. *Cell* **40**, 259-269 (1985).

93. Hoytema van Konijnenburg, D.P. & Mucida, D. Intraepithelial lymphocytes. *Current biology : CB* **27**, R737-r739 (2017).

94. Groh, V. *et al.* Human lymphocytes bearing T cell receptor gamma/delta are phenotypically diverse and evenly distributed throughout the lymphoid system. *The Journal of experimental medicine* **169**, 1277-1294 (1989).

95. Parker, C.M. *et al.* Evidence for extrathymic changes in the T cell receptor gamma/delta repertoire. *The Journal of experimental medicine* **171**, 1597-1612 (1990).

96. Constant, P. *et al.* Stimulation of human gamma delta T cells by nonpeptidic mycobacterial ligands. *Science* **264**, 267-270 (1994).

97. Tanaka, Y. *et al.* Nonpeptide ligands for human gamma delta T cells. *Proc Natl Acad Sci U S A* **91**, 8175-8179 (1994).

98. Morita, C.T., Jin, C., Sarikonda, G. & Wang, H. Nonpeptide antigens, presentation mechanisms, and immunological memory of human Vgamma2Vdelta2 T cells: discriminating friend from foe through the recognition of prenyl pyrophosphate antigens. *Immunol Rev* **215**, 59-76 (2007).

99. Idrees, A.S. *et al.* Comparison of γδ T cell responses and farnesyl diphosphate synthase inhibition in tumor cells pretreated with zoledronic acid. *Cancer science* **104**, 536-542 (2013).

100. Uldrich, A.P. *et al.* CD1d-lipid antigen recognition by the γδ TCR. *Nature immunology* **14**, 1137-1145 (2013).

101. Bai, L. *et al.* The majority of CD1d-sulfatide-specific T cells in human blood use a semiinvariant Vδ1 TCR. *European journal of immunology* **42**, 2505-2510 (2012).

102. Tyler, C.J., Doherty, D.G., Moser, B. & Eberl, M. Human Vγ9/Vδ2 T cells: Innate adaptors of the immune system. *Cellular immunology* **296**, 10-21 (2015).

103. Caccamo, N. *et al.* Differentiation, phenotype, and function of interleukin-17-producing human Vγ9Vδ2 T cells. *Blood* **118**, 129-138 (2011).

104. Davey, M.S. *et al.* Human neutrophil clearance of bacterial pathogens triggers anti-microbial γδ T cell responses in early infection. *PLoS pathogens* **7**, e1002040 (2011).

105. Agrati, C. *et al.* Activated V gamma 9V delta 2 T cells trigger granulocyte functions via MCP-2 release. *Journal of immunology (Baltimore, Md. : 1950)* **182**, 522-529 (2009).

106. Davey, M.S. *et al.* Microbe-specific unconventional T cells induce human neutrophil differentiation into antigen cross-presenting cells. *Journal of immunology (Baltimore, Md. : 1950)* **193**, 3704-3716 (2014).

107. Legendre, V. *et al.* Selection of phenotypically distinct NK1.1+ T cells upon antigen expression in the thymus or in the liver. *European journal of immunology* **29**, 2330-2343 (1999).

108. Burdin, N. *et al.* Selective ability of mouse CD1 to present glycolipids: alpha-galactosylceramide specifically stimulates V alpha 14+ NK T lymphocytes. *Journal of immunology (Baltimore, Md. : 1950)* **161**, 3271-3281 (1998).

109. Schofield, L. *et al.* CD1d-restricted immunoglobulin G formation to GPI-anchored antigens mediated by NKT cells. *Science* **283**, 225-229 (1999).

110. Joyce, S. *et al.* Natural ligand of mouse CD1d1: cellular glycosylphosphatidylinositol. *Science* **279**, 1541-1544 (1998).

111. Budd, R.C. *et al.* Developmentally regulated expression of T cell receptor beta chain variable domains in immature thymocytes. *The Journal of experimental medicine* **166**, 577-582 (1987).

112. Fowlkes, B.J. *et al.* A novel population of T-cell receptor alpha beta-bearing thymocytes which predominantly expresses a single V beta gene family. *Nature* **329**, 251-254 (1987).

113. Ceredig, R., Lynch, F. & Newman, P. Phenotypic Properties, Interleukin 2 Production, and Developmental Origin of a ``Mature'' Subpopulation of Lyt-2⁻ L3T4⁻mouse Thymocytes. *Proceedings of the National Academy of Sciences of the United States of America* **84**, 8578-8582 (1987).

114. Arase, H., Arase, N., Nakagawa, K., Good, R.A. & Onoé, K. NK1.1+ CD4+ CD8- thymocytes with specific lymphokine secretion. *European journal of immunology* **23**, 307-310 (1993).

115. Yoshimoto, T. & Paul, W.E. CD4pos, NK1.1pos T cells promptly produce interleukin 4 in response to in vivo challenge with anti-CD3. *The Journal of experimental medicine* **179**, 1285-1295 (1994).

116. Gumperz, J.E. *et al.* Murine CD1d-restricted T cell recognition of cellular lipids. *Immunity* **12**, 211-221 (2000).

117. Makino, Y., Kanno, R., Ito, T., Higashino, K. & Taniguchi, M. Predominant expression of invariant V alpha 14+ TCR alpha chain in NK1.1+ T cell populations. *International immunology* **7**, 1157-1161 (1995).

118. Godfrey, D.I., MacDonald, H.R., Kronenberg, M., Smyth, M.J. & Kaer, L.V. NKT cells: what's in a name? *Nature Reviews Immunology* **4**, 231-237 (2004).

119. Gumperz, J.E., Miyake, S., Yamamura, T. & Brenner, M.B. Functionally distinct subsets of CD1d-restricted natural killer T cells revealed by CD1d tetramer staining. *The Journal of experimental medicine* **195**, 625-636 (2002).

120. Lee, P.T., Benlagha, K., Teyton, L. & Bendelac, A. Distinct functional lineages of human V(alpha)24 natural killer T cells. *The Journal of experimental medicine* **195**, 637-641 (2002).

121. O'Reilly, V. *et al.* Distinct and overlapping effector functions of expanded human CD4+, CD8α+ and CD4-CD8α- invariant natural killer T cells. *PloS one* **6**, e28648 (2011).

122. Treiner, E. *et al.* Selection of evolutionarily conserved mucosal-associated invariant T cells by MR1. *Nature* **422**, 164-169 (2003).

123. Rahimpour, A. *et al.* Identification of phenotypically and functionally heterogeneous mouse mucosal-associated invariant T cells using MR1 tetramers. *The Journal of experimental medicine* **212**, 1095-1108 (2015).

124. Treiner, E. *et al.* Mucosal-associated invariant T (MAIT) cells: an evolutionarily conserved T cell subset. *Microbes and infection* **7**, 552-559 (2005).

125. Treiner, E. *et al.* Selection of evolutionarily conserved mucosal-associated invariant T cells by MR1. *Nature* **422**, 164-169 (2003).

126. Kjer-Nielsen, L. *et al.* MR1 presents microbial vitamin B metabolites to MAIT cells. *Nature* **491**, 717-723 (2012).

127. Xiao, X. & Cai, J. Mucosal-Associated Invariant T Cells: New Insights into Antigen Recognition and Activation. *Frontiers in immunology* **8**, 1540 (2017).

128. van Wilgenburg, B. *et al.* MAIT cells are activated during human viral infections. *Nat Commun* **7**, 11653 (2016).

129. Gold, M.C. *et al.* Human mucosal associated invariant T cells detect bacterially infected cells. *PLoS biology* **8**, e1000407 (2010).

130. Ussher, J.E. *et al.* CD161++ CD8+ T cells, including the MAIT cell subset, are specifically activated by IL-12+IL-18 in a TCR-independent manner. *European journal of immunology* **44**, 195-203 (2014).

131. Dusseaux, M. *et al.* Human MAIT cells are xenobiotic-resistant, tissue-targeted, CD161hi IL-17-secreting T cells. *Blood* **117**, 1250-1259 (2011).

132. Tang, X.Z. *et al.* IL-7 licenses activation of human liver intrasinusoidal mucosal-associated invariant T cells. *Journal of immunology (Baltimore, Md. : 1950)* **190**, 3142-3152 (2013).

133. Kurioka, A. *et al.* MAIT cells are licensed through granzyme exchange to kill bacterially sensitized targets. *Mucosal Immunology* **8**, 429-440 (2015).

134. Willing, A., Jäger, J., Reinhardt, S., Kursawe, N. & Friese, M.A. Production of IL-17 by MAIT Cells Is Increased in Multiple Sclerosis and Is Associated with IL-7 Receptor Expression. *Journal of immunology (Baltimore, Md. : 1950)* **200**, 974-982 (2018).

135. Held, K. *et al.* αβ T-cell receptors from multiple sclerosis brain lesions show MAIT cell-related features. *Neurology(R) neuroimmunology & neuroinflammation* **2**, e107 (2015).

136. Sakaguchi, S. *et al.* Foxp3+ CD25+ CD4+ natural regulatory T cells in dominant self-tolerance and autoimmune disease. *Immunol Rev* **212**, 8-27 (2006).

137. Workman, C.J., Szymczak-Workman, A.L., Collison, L.W., Pillai, M.R. & Vignali, D.A. The development and function of regulatory T cells. *Cellular and molecular life sciences : CMLS* **66**, 2603-2622 (2009).

138. Sakaguchi, S., Wing, K. & Miyara, M. Regulatory T cells - a brief history and perspective. *European journal of immunology* **37 Suppl 1**, S116-123 (2007).

139. Sakaguchi, S. Naturally arising CD4+ regulatory t cells for immunologic self-tolerance and negative control of immune responses. *Annual review of immunology* **22**, 531-562 (2004).

140. Churlaud, G. *et al.* Human and Mouse CD8(+)CD25(+)FOXP3(+) Regulatory T Cells at Steady State and during Interleukin-2 Therapy. *Frontiers in immunology* **6**, 171 (2015).

141. Vuddamalay, Y. & van Meerwijk, J.P. CD28(-) and CD28(low)CD8(+) Regulatory T Cells: Of Mice and Men. *Frontiers in immunology* **8**, 31 (2017).

142. Vieyra-Lobato, M.R., Vela-Ojeda, J., Montiel-Cervantes, L., López-Santiago, R. & Moreno-Lafont, M.C. Description of CD8(+) Regulatory T Lymphocytes and Their Specific Intervention in Graft-versus-Host and Infectious Diseases, Autoimmunity, and Cancer. *Journal of immunology research* **2018**, 3758713 (2018).

143. Lee, J. *et al.* Induction of Immunosuppressive CD8(+)CD25(+)FOXP3(+) Regulatory T Cells by Suboptimal Stimulation with Staphylococcal Enterotoxin C1. *Journal of immunology (Baltimore, Md. : 1950)* **200**, 669-680 (2018).

144. Sakaguchi, S., Sakaguchi, N., Asano, M., Itoh, M. & Toda, M. Immunologic self-tolerance maintained by activated T cells expressing IL-2 receptor alpha-chains (CD25). Breakdown of a single mechanism of self-tolerance causes various

autoimmune diseases. *Journal of immunology (Baltimore, Md. : 1950)* **155**, 1151-1164 (1995).

145. Liu, W. *et al.* CD127 expression inversely correlates with FoxP3 and suppressive function of human CD4+ T reg cells. *The Journal of experimental medicine* **203**, 1701-1711 (2006).

146. Fontenot, J.D., Gavin, M.A. & Rudensky, A.Y. Foxp3 programs the development and function of CD4+CD25+ regulatory T cells. *Nature immunology* **4**, 330-336 (2003).

147. Hori, S., Nomura, T. & Sakaguchi, S. Control of regulatory T cell development by the transcription factor Foxp3. *Science* **299**, 1057-1061 (2003).

148. Bruder, D. *et al.* Neuropilin-1: a surface marker of regulatory T cells. *European journal of immunology* **34**, 623-630 (2004).

149. Wing, K. *et al.* CTLA-4 control over Foxp3+ regulatory T cell function. *Science* **322**, 271-275 (2008).

150. Ronchetti, S. *et al.* Glucocorticoid-induced tumour necrosis factor receptor-related protein: a key marker of functional regulatory T cells. *Journal of immunology research* **2015**, 171520 (2015).

151. Booth, N.J. *et al.* Different proliferative potential and migratory characteristics of human CD4+ regulatory T cells that express either CD45RA or CD45RO. *Journal of immunology (Baltimore, Md. : 1950)* **184**, 4317-4326 (2010).

152. Venken, K. *et al.* Natural naive CD4+CD25+CD127low regulatory T cell (Treg) development and function are disturbed in multiple sclerosis patients: recovery of memory Treg homeostasis during disease progression. *Journal of immunology (Baltimore, Md. : 1950)* **180**, 6411-6420 (2008).

153. Fritzsching, B. *et al.* Naive regulatory T cells: a novel subpopulation defined by resistance toward CD95L-mediated cell death. *Blood* **108**, 3371-3378 (2006).

154. Valmori, D., Merlo, A., Souleimanian, N.E., Hesdorffer, C.S. & Ayyoub, M. A peripheral circulating compartment of natural naive CD4 Tregs. *The Journal of clinical investigation* **115**, 1953-1962 (2005).

155. Curotto de Lafaille, M.A. & Lafaille, J.J. Natural and adaptive foxp3+ regulatory T cells: more of the same or a division of labor? *Immunity* **30**, 626-635 (2009).

156. Knoechel, B., Lohr, J., Kahn, E., Bluestone, J.A. & Abbas, A.K. Sequential development of interleukin 2-dependent effector and regulatory T cells in response

to endogenous systemic antigen. *The Journal of experimental medicine* **202**, 1375-1386 (2005).

157. Chen, W. *et al.* Conversion of peripheral CD4+CD25- naive T cells to CD4+CD25+ regulatory T cells by TGF-beta induction of transcription factor Foxp3. *The Journal of experimental medicine* **198**, 1875-1886 (2003).

158. Huang, H., Ma, Y., Dawicki, W., Zhang, X. & Gordon, J.R. Comparison of induced versus natural regulatory T cells of the same TCR specificity for induction of tolerance to an environmental antigen. *Journal of immunology (Baltimore, Md. : 1950)* **191**, 1136-1143 (2013).

159. Yadav, M. *et al.* Neuropilin-1 distinguishes natural and inducible regulatory T cells among regulatory T cell subsets in vivo. *The Journal of experimental medicine* **209**, 1713-1722, s1711-1719 (2012).

160. Weiss, J.M. *et al.* Neuropilin 1 is expressed on thymus-derived natural regulatory T cells, but not mucosa-generated induced Foxp3+ T reg cells. *The Journal of experimental medicine* **209**, 1723-1742, s1721 (2012).

161. van den Broek, T., Borghans, J.A.M. & van Wijk, F. The full spectrum of human naive T cells. *Nature Reviews Immunology* **18**, 363-373 (2018).

162. den Braber, I. *et al.* Maintenance of peripheral naive T cells is sustained by thymus output in mice but not humans. *Immunity* **36**, 288-297 (2012).

163. Mestas, J. & Hughes, C.C. Of mice and not men: differences between mouse and human immunology. *Journal of immunology (Baltimore, Md. : 1950)* **172**, 2731-2738 (2004).

164. Larbi, A. & Fulop, T. From "truly naïve" to "exhausted senescent" T cells: when markers predict functionality. *Cytometry. Part A : the journal of the International Society for Analytical Cytology* **85**, 25-35 (2014).

165. Mahnke, Y.D., Brodie, T.M., Sallusto, F., Roederer, M. & Lugli, E. The who's who of T-cell differentiation: human memory T-cell subsets. *European journal of immunology* **43**, 2797-2809 (2013).

166. Motamedi, M., Xu, L. & Elahi, S. Correlation of transferrin receptor (CD71) with Ki67 expression on stimulated human and mouse T cells: The kinetics of expression of T cell activation markers. *Journal of immunological methods* **437**, 43-52 (2016).

167. Pepper, M. & Jenkins, M.K. Origins of CD4(+) effector and central memory T cells. *Nature immunology* **12**, 467-471 (2011).

168. Sallusto, F., Lenig, D., Förster, R., Lipp, M. & Lanzavecchia, A. Two subsets of memory T lymphocytes with distinct homing potentials and effector functions. *Nature* **401**, 708-712 (1999).

169. Appay, V., van Lier, R.A., Sallusto, F. & Roederer, M. Phenotype and function of human T lymphocyte subsets: consensus and issues. *Cytometry. Part A : the journal of the International Society for Analytical Cytology* **73**, 975-983 (2008).

170. Masopust, D., Vezys, V., Marzo, A.L. & Lefrançois, L. Preferential localization of effector memory cells in nonlymphoid tissue. *Science* **291**, 2413-2417 (2001).

171. Sallusto, F., Geginat, J. & Lanzavecchia, A. Central memory and effector memory T cell subsets: function, generation, and maintenance. *Annual review of immunology* **22**, 745-763 (2004).

172. Song, K. *et al.* Characterization of subsets of CD4+ memory T cells reveals early branched pathways of T cell differentiation in humans. *Proc Natl Acad Sci U S A* **102**, 7916-7921 (2005).

173. Geginat, J., Lanzavecchia, A. & Sallusto, F. Proliferation and differentiation potential of human CD8+ memory T-cell subsets in response to antigen or homeostatic cytokines. *Blood* **101**, 4260-4266 (2003).

174. Weiskopf, D. *et al.* Dengue virus infection elicits highly polarized CX3CR1+ cytotoxic CD4+ T cells associated with protective immunity. *Proc Natl Acad Sci U S A* **112**, E4256-4263 (2015).

175. Gordon, C.L. *et al.* Tissue reservoirs of antiviral T cell immunity in persistent human CMV infection. *The Journal of experimental medicine* **214**, 651-667 (2017).

176. Libri, V. *et al.* Cytomegalovirus infection induces the accumulation of short-lived, multifunctional CD4+CD45RA+CD27+ T cells: the potential involvement of interleukin-7 in this process. *Immunology* **132**, 326-339 (2011).

177. Tian, Y. *et al.* Unique phenotypes and clonal expansions of human CD4 effector memory T cells re-expressing CD45RA. *Nature Communications* **8**, 1473 (2017).

178. Verma, K. *et al.* Human CD8+ CD57- TEMRA cells: Too young to be called "old". *PloS one* **12**, e0177405 (2017).

179. Jiang, X. *et al.* Skin infection generates non-migratory memory CD8+ T(RM) cells providing global skin immunity. *Nature* **483**, 227-231 (2012).

180. Beura, L.K. *et al.* T Cells in Nonlymphoid Tissues Give Rise to Lymph-Node-Resident Memory T Cells. *Immunity* **48**, 327-338.e325 (2018).

181. Kumar, B.V. *et al.* Human Tissue-Resident Memory T Cells Are Defined by Core Transcriptional and Functional Signatures in Lymphoid and Mucosal Sites. *Cell reports* **20**, 2921-2934 (2017).

182. Mackay, L.K. *et al.* Hobit and Blimp1 instruct a universal transcriptional program of tissue residency in lymphocytes. *Science* **352**, 459-463 (2016).

183. Mueller, S.N. & Mackay, L.K. Tissue-resident memory T cells: local specialists in immune defence. *Nature reviews. Immunology* **16**, 79-89 (2016).

184. Iborra, S. *et al.* Optimal Generation of Tissue-Resident but Not Circulating Memory T Cells during Viral Infection Requires Crosspriming by DNGR-1(+) Dendritic Cells. *Immunity* **45**, 847-860 (2016).

185. Nakanishi, Y., Lu, B., Gerard, C. & Iwasaki, A. CD8+ T lymphocyte mobilization to virus-infected tissue requires CD4+ T-cell help. *Nature* **462**, 510-513 (2009).

186. Wu, T.C. *et al.* Reprogramming tumor-infiltrating dendritic cells for CD103+ CD8+ mucosal T-cell differentiation and breast cancer rejection. *Cancer immunology research* **2**, 487-500 (2014).

187. Amsen, D., Van Gisbergen, K., Hombrink, P. & van Lier, R. Tissue-resident memory T cells at the center of immunity to solid tumors. *Nature immunology* **19** (2018).

188. Sheridan, B.S. *et al.* Oral infection drives a distinct population of intestinal resident memory CD8(+) T cells with enhanced protective function. *Immunity* **40**, 747-757 (2014).

189. Masopust, D., Vezys, V., Wherry, E.J., Barber, D.L. & Ahmed, R. Cutting edge: gut microenvironment promotes differentiation of a unique memory CD8 T cell population. *Journal of immunology (Baltimore, Md. : 1950)* **176**, 2079-2083 (2006).

190. Skon, C.N. *et al.* Transcriptional downregulation of S1pr1 is required for the establishment of resident memory CD8+ T cells. *Nature immunology* **14**, 1285-1293 (2013).

191. Mackay, L.K. *et al.* Cutting Edge: CD69 Interference with Sphingosine-1-Phosphate Receptor Function Regulates Peripheral T Cell Retention. *The Journal of Immunology* **194**, 2059-2063 (2015).

192. Cheuk, S. *et al.* CD49a Expression Defines Tissue-Resident CD8(+) T Cells Poised for Cytotoxic Function in Human Skin. *Immunity* **46**, 287-300 (2017).

193. Gebhardt, T. *et al.* Memory T cells in nonlymphoid tissue that provide enhanced local immunity during infection with herpes simplex virus. *Nature immunology* **10**, 524-530 (2009).

194. Ray, S.J. *et al.* The collagen binding alpha1beta1 integrin VLA-1 regulates CD8 T cell-mediated immune protection against heterologous influenza infection. *Immunity* **20**, 167-179 (2004).

195. Goodison, S., Urquidi, V. & Tarin, D. CD44 cell adhesion molecules. *Molecular pathology : MP* **52**, 189-196 (1999).

196. Boutet, M. *et al.* TGFβ Signaling Intersects with CD103 Integrin Signaling to Promote T-Lymphocyte Accumulation and Antitumor Activity in the Lung Tumor Microenvironment. *Cancer research* **76**, 1757-1769 (2016).

197. Thaiss, C.A., Semmling, V., Franken, L., Wagner, H. & Kurts, C. Chemokines: a new dendritic cell signal for T cell activation. *Frontiers in immunology* **2**, 31 (2011).

198. Kalinski, P. Dendritic cells in immunotherapy of established cancer: Roles of signals 1, 2, 3 and 4. *Current opinion in investigational drugs (London, England : 2000)* **10**, 526-535 (2009).

199. Corthay, A. A three-cell model for activation of naïve T helper cells. *Scandinavian journal of immunology* **64**, 93-96 (2006).

200. Wang, C., Sun, W., Ye, Y., Bomba, H.N. & Gu, Z. Bioengineering of Artificial Antigen Presenting Cells and Lymphoid Organs. *Theranostics* **7**, 3504-3516 (2017).

201. Koretzky, G.A. Multiple roles of CD4 and CD8 in T cell activation. *Journal of immunology (Baltimore, Md. : 1950)* **185**, 2643-2644 (2010).

202. Wooldridge, L. *et al.* Interaction between the CD8 coreceptor and major histocompatibility complex class I stabilizes T cell receptor-antigen complexes at the cell surface. *The Journal of biological chemistry* **280**, 27491-27501 (2005).

203. Artyomov, M., Lis, M., Devadas, S., Davis, M.M. & Chakraborty, A. CD4 and CD8 binding to MHC molecules primarily acts to enhance Lck delivery. *Proceedings of the National Academy of Sciences* **107**, 16916 - 16921 (2010).

204. Li, Q.J. *et al.* CD4 enhances T cell sensitivity to antigen by coordinating Lck accumulation at the immunological synapse. *Nature immunology* **5**, 791-799 (2004).

205. Brownlie, R.J. & Zamoyska, R. T cell receptor signalling networks: branched, diversified and bounded. *Nature Reviews Immunology* **13**, 257-269 (2013).

206. Smith-Garvin, J.E., Koretzky, G.A. & Jordan, M.S. T cell activation. *Annual review of immunology* **27**, 591-619 (2009).

207. Huse, M. The T-cell-receptor signaling network. *Journal of cell science* **122**, 1269-1273 (2009).

208. Zhang, W. *et al.* Essential role of LAT in T cell development. *Immunity* **10**, 323-332 (1999).

209. Balagopalan, L., Coussens, N.P., Sherman, E., Samelson, L.E. & Sommers, C.L. The LAT story: a tale of cooperativity, coordination, and choreography. *Cold Spring Harbor perspectives in biology* **2**, a005512 (2010).

210. Pham, N.L., Badovinac, V.P. & Harty, J.T. Differential role of "Signal 3" inflammatory cytokines in regulating CD8 T cell expansion and differentiation in vivo. *Frontiers in immunology* **2**, 4 (2011).

211. Curtsinger, J.M. & Mescher, M.F. Inflammatory cytokines as a third signal for T cell activation. *Current opinion in immunology* **22**, 333-340 (2010).

212. Keppler, S.J., Rosenits, K., Koegl, T., Vucikuja, S. & Aichele, P. Signal 3 cytokines as modulators of primary immune responses during infections: the interplay of type I IFN and IL-12 in CD8 T cell responses. *PloS one* **7**, e40865 (2012).

213. Boomer, J.S. & Green, J.M. An enigmatic tail of CD28 signaling. *Cold Spring Harbor perspectives in biology* **2**, a002436 (2010).

214. Crawford, A. & Wherry, E.J. The diversity of costimulatory and inhibitory receptor pathways and the regulation of antiviral T cell responses. *Current opinion in immunology* **21**, 179-186 (2009).

215. Mir, M.A. *Chapter 1 - Introduction to Costimulation and Costimulatory Molecules. In: Developing Costimulatory Molecules for Immunotherapy of Diseases.* . Academic Press, 2015.

216. Sharpe, A.H. Mechanisms of costimulation. *Immunol Rev* **229**, 5-11 (2009).

217. Grosso, J.F. & Jure-Kunkel, M.N. CTLA-4 blockade in tumor models: an overview of preclinical and translational research. *Cancer immunity* **13**, 5 (2013).

218. Walker, L.S. & Sansom, D.M. The emerging role of CTLA4 as a cell-extrinsic regulator of T cell responses. *Nature reviews. Immunology* **11**, 852-863 (2011).

219. Tai, X., Van Laethem, F., Sharpe, A.H. & Singer, A. Induction of autoimmune disease in CTLA-4^{−/−} mice depends on a specific CD28 motif that is required for in vivo costimulation. *Proceedings of the National Academy of Sciences* **104**, 13756-13761 (2007).

220. Walker, L.S. & Sansom, D.M. Confusing signals: recent progress in CTLA-4 biology. *Trends in immunology* **36**, 63-70 (2015).

221. Tai, X. *et al.* Basis of CTLA-4 function in regulatory and conventional CD4(+) T cells. *Blood* **119**, 5155-5163 (2012).

222. Burleson SCM, F.R., Mannie MD, Olmstead SG, Van Scott MR. *Chapter 35 - The Immune Basis of Allergic Lung Disease.In: Comparative Biology of the Normal Lung (Second Edition).* Academic Press: San Diego, 2015.

223. Chen, L. & Flies, D.B. Molecular mechanisms of T cell co-stimulation and co-inhibition. *Nature Reviews Immunology* **13**, 227-242 (2013).

224. Curtsinger, J.M., Lins, D.C. & Mescher, M.F. Signal 3 determines tolerance versus full activation of naive CD8 T cells: dissociating proliferation and development of effector function. *The Journal of experimental medicine* **197**, 1141-1151 (2003).

225. Curtsinger, J.M. *et al.* Inflammatory cytokines provide a third signal for activation of naive CD4+ and CD8+ T cells. *Journal of immunology (Baltimore, Md. : 1950)* **162**, 3256-3262 (1999).

226. de Groot, R. *et al.* Viral dsRNA-activated human dendritic cells produce IL-27, which selectively promotes cytotoxicity in naive CD8+ T cells. *Journal of leukocyte biology* **92**, 605-610 (2012).

227. Boomershine, C. & Zwilling, B. Macrophage Antimycobacterial Activity, Effects of Stress on. 2007; 2007.

228. Swann, J.B. & Smyth, M.J. Immune surveillance of tumors. *The Journal of clinical investigation* **117**, 1137-1146 (2007).

229. Tian, T., Olson, S., Whitacre, J.M. & Harding, A. The origins of cancer robustness and evolvability. *Integrative biology : quantitative biosciences from nano to macro* **3**, 17-30 (2011).

230. Mlecnik, B., Bindea, G., Pagès, F. & Galon, J. Tumor immunosurveillance in human cancers. *Cancer metastasis reviews* **30**, 5-12 (2011).

231. Finn, O.J. Immuno-oncology: understanding the function and dysfunction of the immune system in cancer. *Annals of oncology : official journal of the European Society for Medical Oncology* **23 Suppl 8**, viii6-9 (2012).

232. Piersma, S.J. *et al.* High number of intraepithelial CD8+ tumor-infiltrating lymphocytes is associated with the absence of lymph node metastases in patients with large early-stage cervical cancer. *Cancer research* **67**, 354-361 (2007).

233. Kohrt, H.E. *et al.* Profile of immune cells in axillary lymph nodes predicts disease-free survival in breast cancer. *PLoS medicine* **2**, e284 (2005).

234. Chen, D.S. & Mellman, I. Oncology meets immunology: the cancer-immunity cycle. *Immunity* **39**, 1-10 (2013).

235. Glaire, M.A. *et al.* Tumour-infiltrating CD8+ lymphocytes and colorectal cancer recurrence by tumour and nodal stage. *British Journal of Cancer* **121**, 474-482 (2019).

236. Naito, Y. *et al.* CD8+ T Cells Infiltrated within Cancer Cell Nests as a Prognostic Factor in Human Colorectal Cancer. *Cancer research* **58**, 3491-3494 (1998).

237. Sato, E. *et al.* Intraepithelial CD8+ tumor-infiltrating lymphocytes and a high CD8+/regulatory T cell ratio are associated with favorable prognosis in ovarian cancer. *Proceedings of the National Academy of Sciences of the United States of America* **102**, 18538-18543 (2005).

238. Chiba, T. *et al.* Intraepithelial CD8+ T-cell-count becomes a prognostic factor after a longer follow-up period in human colorectal carcinoma: possible association with suppression of micrometastasis. *Br J Cancer* **91**, 1711-1717 (2004).

239. Galon, J. *et al.* Type, Density, and Location of Immune Cells Within Human Colorectal Tumors Predict Clinical Outcome. *Science* **313**, 1960-1964 (2006).

240. Galon, J., Fridman, W.H. & Pagès, F. The adaptive immunologic microenvironment in colorectal cancer: a novel perspective. *Cancer research* **67**, 1883-1886 (2007).

241. Galon, J. *et al.* Cancer classification using the Immunoscore: a worldwide task force. *Journal of translational medicine* **10**, 205 (2012).

242. Galon, J. *et al.* The immune score as a new possible approach for the classification of cancer. *Journal of translational medicine* **10**, 1 (2012).

243. Angell, H.K., Bruni, D., Barrett, J.C., Herbst, R. & Galon, J. The Immunoscore: Colon Cancer and Beyond. *Clinical cancer research : an official journal of the American Association for Cancer Research* **26**, 332-339 (2020).

244. Marliot, F. *et al.* Analytical validation of the Immunoscore and its associated prognostic value in patients with colon cancer. *Journal for immunotherapy of cancer* **8**, e000272 (2020).

245. Galon, J. & Bruni, D. Approaches to treat immune hot, altered and cold tumours with combination immunotherapies. *Nature reviews. Drug discovery* **18**, 197-218 (2019).

246. Ganesan, A.P. *et al.* Tissue-resident memory features are linked to the magnitude of cytotoxic T cell responses in human lung cancer. *Nature immunology* **18**, 940-950 (2017).

247. Djenidi, F. *et al.* CD8+CD103+ tumor-infiltrating lymphocytes are tumor-specific tissue-resident memory T cells and a prognostic factor for survival in lung cancer patients. *Journal of immunology (Baltimore, Md. : 1950)* **194**, 3475-3486 (2015).

248. Komdeur, F.L. *et al.* CD103+ tumor-infiltrating lymphocytes are tumor-reactive intraepithelial CD8+ T cells associated with prognostic benefit and therapy response in cervical cancer. *Oncoimmunology* **6**, e1338230 (2017).

249. Wang, B. *et al.* CD103+ Tumor Infiltrating Lymphocytes Predict a Favorable Prognosis in Urothelial Cell Carcinoma of the Bladder. *The Journal of urology* **194**, 556-562 (2015).

250. Wang, Z.-Q. *et al.* CD103 and Intratumoral Immune Response in Breast Cancer. *Clinical Cancer Research* **22**, 6290-6297 (2016).

251. Dumauthioz, N., Labiano, S. & Romero, P. Tumor Resident Memory T Cells: New Players in Immune Surveillance and Therapy. *Frontiers in immunology* **9** (2018).

252. Webb, J.R., Milne, K., Watson, P., Deleeuw, R.J. & Nelson, B.H. Tumor-infiltrating lymphocytes expressing the tissue resident memory marker CD103 are associated with increased survival in high-grade serous ovarian cancer. *Clinical cancer research : an official journal of the American Association for Cancer Research* **20**, 434-444 (2014).

253. Gupta, P.K. *et al.* CD39 Expression Identifies Terminally Exhausted CD8+ T Cells. *PLoS pathogens* **11**, e1005177 (2015).

254. van Duijn, J. *et al.* CD39 identifies a microenvironment-specific anti-inflammatory CD8(+) T-cell population in atherosclerotic lesions. *Atherosclerosis* **285**, 71-78 (2019).

255. Simoni, Y. *et al.* Bystander CD8+ T cells are abundant and phenotypically distinct in human tumour infiltrates. *Nature* **557**, 575-579 (2018).

256. Canale, F.P., Ramello, M.C. & Montes, C.L. CD39 as a marker of pathogenic CD8+ T cells in cancer and other chronic inflammatory diseases. *Oncoscience* **5**, 65-66 (2018).

257. Zhao, H., Bo, C., Kang, Y. & Li, H. What Else Can CD39 Tell Us? *Frontiers in immunology* **8** (2017).

258. Duhen, T. *et al.* Co-expression of CD39 and CD103 identifies tumor-reactive CD8 T cells in human solid tumors. *Nature Communications* **9**, 2724 (2018).

259. Rawla, P., Sunkara, T. & Barsouk, A. Epidemiology of colorectal cancer: incidence, mortality, survival, and risk factors. *Przeglad gastroenterologiczny* **14**, 89-103 (2019).

260. Kobayashi, H. *et al.* Characteristics of recurrence after curative resection for T1 colorectal cancer: Japanese multicenter study. *Journal of gastroenterology* **46**, 203-211 (2011).

261. Hurwitz, H. *et al.* Bevacizumab plus irinotecan, fluorouracil, and leucovorin for metastatic colorectal cancer. *The New England journal of medicine* **350**, 2335-2342 (2004).

262. Van Cutsem, E. *et al.* Cetuximab and chemotherapy as initial treatment for metastatic colorectal cancer. *The New England journal of medicine* **360**, 1408-1417 (2009).

263. Douillard, J.Y. *et al.* Randomized, phase III trial of panitumumab with infusional fluorouracil, leucovorin, and oxaliplatin (FOLFOX4) versus FOLFOX4 alone as first-line treatment in patients with previously untreated metastatic colorectal cancer: the PRIME study. *Journal of clinical oncology : official journal of the American Society of Clinical Oncology* **28**, 4697-4705 (2010).

264. Guan, Z.Z. *et al.* Efficacy and safety of bevacizumab plus chemotherapy in Chinese patients with metastatic colorectal cancer: a randomized phase III ARTIST trial. *Chinese journal of cancer* **30**, 682-689 (2011).

265. Samelis, G.F., Ekmektzoglou, K.A., Tsiakou, A. & Konstadoulakis, M. The continuation of bevacizumab following disease progression in patients with metastatic colorectal cancer offers a survival benefit. *Hepato-gastroenterology* **58**, 1968-1971 (2011).

266. Davies, R.L., Grosse, V.A., Kucherlapati, R. & Bothwell, M. Genetic analysis of epidermal growth factor action: assignment of human epidermal growth factor receptor gene to chromosome 7. *Proc Natl Acad Sci U S A* **77**, 4188-4192 (1980).

267. Hagan, S., Orr, M.C. & Doyle, B. Targeted therapies in colorectal cancer-an integrative view by PPPM. *The EPMA journal* **4**, 3 (2013).

268. Vilar, E. & Gruber, S.B. Microsatellite instability in colorectal cancer-the stable evidence. *Nature reviews. Clinical oncology* **7**, 153-162 (2010).

269. Duval, A. & Hamelin, R. Mutations at coding repeat sequences in mismatch repair-deficient human cancers: toward a new concept of target genes for instability. *Cancer research* **62**, 2447-2454 (2002).

270. Williams, D.S. *et al.* Nonsense mediated decay resistant mutations are a source of expressed mutant proteins in colon cancer cell lines with microsatellite instability. *PloS one* **5**, e16012 (2010).

271. Yamamoto, H. & Imai, K. Microsatellite instability: an update. *Archives of toxicology* **89**, 899-921 (2015).

272. Setaffy, L. & Langner, C. Microsatellite instability in colorectal cancer: clinicopathological significance. *Polish journal of pathology : official journal of the Polish Society of Pathologists* **66**, 203-218 (2015).

273. Buecher, B. *et al.* Role of microsatellite instability in the management of colorectal cancers. *Digestive and liver disease : official journal of the Italian Society of Gastroenterology and the Italian Association for the Study of the Liver* **45**, 441-449 (2013).

274. Mlecnik, B. *et al.* Integrative Analyses of Colorectal Cancer Show Immunoscore Is a Stronger Predictor of Patient Survival Than Microsatellite Instability. *Immunity* **44**, 698-711 (2016).

275. Salem, M.E. *et al.* Comparative molecular analyses of left-sided colon, right-sided colon, and rectal cancers. *Oncotarget* **8**, 86356-86368 (2017).

276. San Roman, A.K. & Shivdasani, R.A. Boundaries, junctions and transitions in the gastrointestinal tract. *Experimental cell research* **317**, 2711-2718 (2011).

277. Gualco, G., Reissenweber, N., Cliché, I. & Bacchi, C.E. Flat elevated lesions of the colon and rectum: a spectrum of neoplastic and nonneoplastic entities. *Annals of diagnostic pathology* **10**, 333-338 (2006).

278. Nawa, T. *et al.* Differences between right- and left-sided colon cancer in patient characteristics, cancer morphology and histology. *Journal of gastroenterology and hepatology* **23**, 418-423 (2008).

279. Baran, B. *et al.* Difference Between Left-Sided and Right-Sided Colorectal Cancer: A Focused Review of Literature. *Gastroenterology research* **11**, 264-273 (2018).

280. Kang, S.P. *et al.* Pembrolizumab KEYNOTE-001: an adaptive study leading to accelerated approval for two indications and a companion diagnostic. *Annals of oncology : official journal of the European Society for Medical Oncology* **28**, 1388-1398 (2017).

281. Diaz, L.A. *et al.* Pembrolizumab therapy for microsatellite instability high (MSI-H) colorectal cancer (CRC) and non-CRC. *Journal of Clinical Oncology* **35**, 3071-3071 (2017).

282. Overman, M.J. *et al.* Nivolumab in patients with metastatic DNA mismatch repair-deficient or microsatellite instability-high colorectal cancer (CheckMate 142): an open-label, multicentre, phase 2 study. *The Lancet. Oncology* **18**, 1182-1191 (2017).

283. Andre, T. *et al.* Combination of nivolumab (nivo) + ipilimumab (ipi) in the treatment of patients (pts) with deficient DNA mismatch repair (dMMR)/high microsatellite instability (MSI-H) metastatic colorectal cancer (mCRC): CheckMate 142 study. *Journal of Clinical Oncology* **35**, 3531-3531 (2017).

284. Zhang, L. *et al.* Immune Landscape of Colorectal Cancer Tumor Microenvironment from Different Primary Tumor Location. *Frontiers in immunology* **9**, 1578 (2018).

285. Pico de Coaña, Y., Choudhury, A. & Kiessling, R. Checkpoint blockade for cancer therapy: revitalizing a suppressed immune system. *Trends in molecular medicine* **21**, 482-491 (2015).

286. Beyersdorf, N., Kerkau, T. & Hünig, T. CD28 co-stimulation in T-cell homeostasis: a recent perspective. *ImmunoTargets and therapy* **4**, 111-122 (2015).

287. Eggermont, A.M. *et al.* Adjuvant ipilimumab versus placebo after complete resection of high-risk stage III melanoma (EORTC 18071): a randomised, double-blind, phase 3 trial. *The Lancet. Oncology* **16**, 522-530 (2015).

288. Chen, D.S. & Mellman, I. Elements of cancer immunity and the cancer–immune set point. *Nature* **541**, 321-330 (2017).

289. Fessas, P., Lee, H., Ikemizu, S. & Janowitz, T. A molecular and preclinical comparison of the PD-1-targeted T-cell checkpoint inhibitors nivolumab and pembrolizumab. *Seminars in oncology* **44**, 136-140 (2017).

290. Eggermont, A.M. *et al.* Prolonged Survival in Stage III Melanoma with Ipilimumab Adjuvant Therapy. *The New England journal of medicine* **375**, 1845-1855 (2016).

291. Wei, S.C. *et al.* Combination anti-CTLA-4 plus anti-PD-1 checkpoint blockade utilizes cellular mechanisms partially distinct from monotherapies. *Proc Natl Acad Sci U S A* **116**, 22699-22709 (2019).

292. Sharma, P. *et al.* Nivolumab Plus Ipilimumab for Metastatic Castration-Resistant Prostate Cancer: Preliminary Analysis of Patients in the CheckMate 650 Trial. *Cancer cell* **38**, 489-499.e483 (2020).

293. Tarrant, J.M., Robb, L., van Spriel, A.B. & Wright, M.D. Tetraspanins: molecular organisers of the leukocyte surface. *Trends in immunology* **24**, 610-617 (2003).

294. Hemler, M.E. Tetraspanin functions and associated microdomains. *Nature Reviews Molecular Cell Biology* **6**, 801-811 (2005).

295. Beckwith, K.A., Byrd, J.C. & Muthusamy, N. Tetraspanins as therapeutic targets in hematological malignancy: a concise review. *Frontiers in physiology* **6**, 91 (2015).

296. Charrin, S. *et al.* Differential stability of tetraspanin/tetraspanin interactions: role of palmitoylation. *FEBS letters* **516**, 139-144 (2002).

297. Berditchevski, F., Odintsova, E., Sawada, S. & Gilbert, E. Expression of the Palmitoylation-deficient CD151 Weakens the Association of α3β1 Integrin with the Tetraspanin-enriched Microdomains and Affects Integrin-dependent Signaling*. *Journal of Biological Chemistry* **277**, 36991-37000 (2002).

298. Ono, M., Handa, K., Withers, D.A. & Hakomori, S. Glycosylation effect on membrane domain (GEM) involved in cell adhesion and motility: a preliminary note on functional alpha3, alpha5-CD82 glycosylation complex in ldlD 14 cells. *Biochemical and biophysical research communications* **279**, 744-750 (2000).

299. Ono, M., Handa, K., Withers, D.A. & Hakomori, S.-i. Motility Inhibition and Apoptosis Are Induced by Metastasis-suppressing Gene Product CD82 and Its Analogue CD9, with Concurrent Glycosylation. *Cancer research* **59**, 2335-2339 (1999).

300. Scholz, C.J., Sauer, G. & Deissler, H. Glycosylation of tetraspanin Tspan-1 at four distinct sites promotes its transition through the endoplasmic reticulum. *Protein and peptide letters* **16**, 1244-1248 (2009).

301. Levy, S. & Shoham, T. Protein-protein interactions in the tetraspanin web. *Physiology (Bethesda, Md.)* **20**, 218-224 (2005).

302. Haining, E.J. *et al.* The TspanC8 subgroup of tetraspanins interacts with A disintegrin and metalloprotease 10 (ADAM10) and regulates its maturation and cell surface expression. *The Journal of biological chemistry* **287**, 39753-39765 (2012).

303. Levy, S. Function of the tetraspanin molecule CD81 in B and T cells. *Immunologic research* **58**, 179-185 (2014).

304. Imai, T., Kakizaki, M., Nishimura, M. & Yoshie, O. Molecular analyses of the association of CD4 with two members of the transmembrane 4 superfamily, CD81 and CD82. *Journal of immunology (Baltimore, Md. : 1950)* **155**, 1229-1239 (1995).

305. Todd, S.C., Lipps, S.G., Crisa, L., Salomon, D.R. & Tsoukas, C.D. CD81 expressed on human thymocytes mediates integrin activation and interleukin 2-dependent proliferation. *Journal of Experimental Medicine* **184**, 2055-2060 (1996).

306. Rocha-Perugini, V. *et al.* CD81 controls sustained T cell activation signaling and defines the maturation stages of cognate immunological synapses. *Molecular and cellular biology* **33**, 3644-3658 (2013).

307. Deng, J., Dekruyff, R.H., Freeman, G.J., Umetsu, D.T. & Levy, S. Critical role of CD81 in cognate T–B cell interactions leading to Th2 responses. *International immunology* **14**, 513-523 (2002).

308. Witherden, D.A., Boismenu, R. & Havran, W.L. CD81 and CD28 Costimulate T Cells Through Distinct Pathways. *The Journal of Immunology* **165**, 1902-1909 (2000).

309. Miyazaki, T., Müller, U. & Campbell, K.S. Normal development but differentially altered proliferative responses of lymphocytes in mice lacking CD81. *The EMBO journal* **16**, 4217-4225 (1997).

310. van Zelm, M.C. *et al.* CD81 gene defect in humans disrupts CD19 complex formation and leads to antibody deficiency. *The Journal of clinical investigation* **120**, 1265-1274 (2010).

311. Tai, X.G. *et al.* A role for CD9 molecules in T cell activation. *The Journal of experimental medicine* **184**, 753-758 (1996).

312. Yashiro-Ohtani, Y. *et al.* Non-CD28 costimulatory molecules present in T cell rafts induce T cell costimulation by enhancing the association of TCR with rafts. *Journal of immunology (Baltimore, Md. : 1950)* **164**, 1251-1259 (2000).

313. Kobayashi, H. *et al.* The tetraspanin CD9 is preferentially expressed on the human CD4(+)CD45RA+ naive T cell population and is involved in T cell activation. *Clinical and experimental immunology* **137**, 101-108 (2004).

314. Rocha-Perugini, V. *et al.* Tetraspanins CD9 and CD151 at the immune synapse support T-cell integrin signaling. *European journal of immunology* **44**, 1967-1975 (2014).

315. van Spriel, A.B. *et al.* A regulatory role for CD37 in T cell proliferation. *Journal of immunology (Baltimore, Md. : 1950)* **172**, 2953-2961 (2004).

316. Knobeloch, K.P. *et al.* Targeted inactivation of the tetraspanin CD37 impairs T-cell-dependent B-cell response under suboptimal costimulatory conditions. *Molecular and cellular biology* **20**, 5363-5369 (2000).

317. Sheng, K.C. *et al.* Tetraspanins CD37 and CD151 differentially regulate Ag presentation and T-cell co-stimulation by DC. *European journal of immunology* **39**, 50-55 (2009).

318. Nicholson, R.H. *et al.* Phemx, a Novel Mouse Gene Expressed in Hematopoietic Cells Maps to the Imprinted Cluster on Distal Chromosome 7. *Genomics* **68**, 13-21 (2000).

319. Robb, L. *et al.* Molecular characterisation of mouse and human TSSC6: evidence that TSSC6 is a genuine member of the tetraspanin superfamily and is expressed specifically in haematopoietic organs. *Biochim Biophys Acta* **1522**, 31-41 (2001).

320. Tarrant, J.M. *et al.* The absence of Tssc6, a member of the tetraspanin superfamily, does not affect lymphoid development but enhances in vitro T-cell proliferative responses. *Molecular and cellular biology* **22**, 5006-5018 (2002).

321. Gartlan, K.H. *et al.* A complementary role for the tetraspanins CD37 and Tssc6 in cellular immunity. *Journal of immunology (Baltimore, Md. : 1950)* **185**, 3158-3166 (2010).

322. Jiang, X., Zhang, J. & Huang, Y. Tetraspanins in cell migration. *Cell adhesion & migration* **9**, 406-415 (2015).

323. Hemler, M.E. Tetraspanin functions and associated microdomains. *Nature reviews. Molecular cell biology* **6**, 801-811 (2005).

324. Berditchevski, F. Complexes of tetraspanins with integrins: more than meets the eye. *Journal of cell science* **114**, 4143-4151 (2001).

325. Engering, A. & Pieters, J. Association of distinct tetraspanins with MHC class II molecules at different subcellular locations in human immature dendritic cells. *International immunology* **13**, 127-134 (2001).

326. Szöllósi, J., Horejsí, V., Bene, L., Angelisová, P. & Damjanovich, S. Supramolecular complexes of MHC class I, MHC class II, CD20, and tetraspan molecules (CD53, CD81, and CD82) at the surface of a B cell line JY. *Journal of immunology (Baltimore, Md. : 1950)* **157**, 2939-2946 (1996).

327. van Spriel, A.B. Tetraspanins in the humoral immune response. *Biochemical Society transactions* **39**, 512-517 (2011).

328. Rocha-Perugini, V. *et al.* CD9 Regulates Major Histocompatibility Complex Class II Trafficking in Monocyte-Derived Dendritic Cells. *Molecular and cellular biology* **37** (2017).

329. Segura, E. & Villadangos, J.A. A modular and combinatorial view of the antigen cross-presentation pathway in dendritic cells. *Traffic (Copenhagen, Denmark)* **12**, 1677-1685 (2011).

330. van Spriel, A.B. *et al.* The tetraspanin CD37 orchestrates the α(4)β(1) integrin-Akt signaling axis and supports long-lived plasma cell survival. *Science signaling* **5**, ra82 (2012).

331. Yeung, L., Hickey, M.J. & Wright, M.D. The Many and Varied Roles of Tetraspanins in Immune Cell Recruitment and Migration. *Frontiers in immunology* **9**, 1644 (2018).

332. van Spriel, A.B. *et al.* A Regulatory Role for CD37 in T Cell Proliferation. *The Journal of Immunology* **172**, 2953-2961 (2004).

333. Wright, M.D. *et al.* Characterization of mice lacking the tetraspanin superfamily member CD151. *Molecular and cellular biology* **24**, 5978-5988 (2004).

334. Levy, S. & Shoham, T. The tetraspanin web modulates immune-signalling complexes. *Nature reviews. Immunology* **5**, 136-148 (2005).

335. Lee, M.P. *et al.* Two novel genes in the center of the 11p15 imprinted domain escape genomic imprinting. *Human molecular genetics* **8**, 683-690 (1999).

336. Robb, L. *et al.* Molecular characterisation of mouse and human TSSC6: evidence that TSSC6 is a genuine member of the tetraspanin superfamily and is expressed specifically in haematopoietic organs. *Biochim Biophys Acta* **1522**, 31-41 (2001).

337. Protty, M.B. *et al.* Identification of Tspan9 as a novel platelet tetraspanin and the collagen receptor GPVI as a component of tetraspanin microdomains. *The Biochemical journal* **417**, 391-400 (2009).

338. Fofana, I. *et al.* A novel monoclonal anti-CD81 antibody produced by genetic immunization efficiently inhibits Hepatitis C virus cell-cell transmission. *PloS one* **8**, e64221 (2013).

339. Johansen, T. *et al.* NIH 3T3 cells stably transfected with the gene encoding phosphatidylcholine-hydrolyzing phospholipase C from Bacillus cereus acquire a transformed phenotype. *Molecular and cellular biology* **14**, 646-654 (1994).

340. Guo, Y.-Y. *et al.* A strategy for enhanced circular DNA construction efficiency based on DNA cyclization after microbial transformation. *Microbial Cell Factories* **14**, 18 (2015).

341. Lehner, R., Wang, X. & Hunziker, P. Plasmid linearization changes shape and efficiency of transfection complexes. *European Journal of Nanomedicine* **5**, 205-212 (2013).

342. Chalfie, M., Tu, Y., Euskirchen, G., Ward, W. & Prasher, D. Green fluorescent protein as a marker for gene expression. *Science* **263**, 802-805 (1994).

343. Li, L., Saade, F. & Petrovsky, N. The future of human DNA vaccines. *Journal of biotechnology* **162**, 171-182 (2012).

344. Liu, S., Wang, S. & Lu, S. DNA immunization as a technology platform for monoclonal antibody induction. *Emerging microbes & infections* **5**, e33 (2016).

345. Hansen, D.T., Craciunescu, F.M., Fromme, P., Johnston, S.A. & Sykes, K.F. Generation of High-Specificity Antibodies against Membrane Proteins Using DNA-Gold Micronanoplexes for Gene Gun Immunization. *Current protocols in protein science* **91**, 29.20.21-29.20.22 (2018).

346. Condon, C., Watkins, S.C., Celluzzi, C.M., Thompson, K. & Falo, L.D. DNA–based immunization by in vivo transfection of dendritic cells. *Nature medicine* **2**, 1122-1128 (1996).

347. Williams, R.S. *et al.* Introduction of foreign genes into tissues of living mice by DNA-coated microprojectiles. *Proc Natl Acad Sci U S A* **88**, 2726-2730 (1991).

348. Chua, J.X. *et al.* Monoclonal Antibodies Targeting Le^cLe^x-Related Glycans with Potent Antitumor Activity. *Clinical Cancer Research* **21**, 2963-2974 (2015).

349. Bendelac, A., Savage, P.B. & Teyton, L. The biology of NKT cells. *Annual review of immunology* **25**, 297-336 (2007).

350. Barral, P. *et al.* B cell receptor-mediated uptake of CD1d-restricted antigen augments antibody responses by recruiting invariant NKT cell help in vivo. *Proc Natl Acad Sci U S A* **105**, 8345-8350 (2008).

351. Hamakubo, T., Kusano-Arai, O. & Iwanari, H. Generation of antibodies against membrane proteins. *Biochim Biophys Acta* **1844**, 1920-1924 (2014).

352. Satofuka, H. *et al.* Immunization method for multi-pass membrane proteins using highly metastatic cell lines. *Biochemical and biophysical research communications* **450**, 99-104 (2014).

353. Durrant, L.G., Harding, S.J., Green, N.H., Buckberry, L.D. & Parsons, T. A New Anticancer Glycolipid Monoclonal Antibody, SC104, which Directly Induces Tumor Cell Apoptosis. *Cancer research* **66**, 5901-5909 (2006).

354. Hansen, D.T. *et al.* Polyclonal Antibody Production for Membrane Proteins via Genetic Immunization. *Scientific Reports* **6**, 21925 (2016).

355. Lombardo, S.D. *et al.* Modulation of Tetraspanin 32 (TSPAN32) Expression in T Cell-Mediated Immune Responses and in Multiple Sclerosis. *International journal of molecular sciences* **20** (2019).

356. Kirilovsky, A. *et al.* Rational bases for the use of the Immunoscore in routine clinical settings as a prognostic and predictive biomarker in cancer patients. *International immunology* **28**, 373-382 (2016).

357. Dieu-Nosjean, M.C. *et al.* Long-term survival for patients with non-small-cell lung cancer with intratumoral lymphoid structures. *Journal of clinical oncology : official journal of the American Society of Clinical Oncology* **26**, 4410-4417 (2008).

358. Fridman, W.H., Pagès, F., Sautès-Fridman, C. & Galon, J. The immune contexture in human tumours: impact on clinical outcome. *Nature Reviews Cancer* **12**, 298-306 (2012).

359. Clemente, C.G. *et al.* Prognostic value of tumor infiltrating lymphocytes in the vertical growth phase of primary cutaneous melanoma. *Cancer* **77**, 1303-1310 (1996).

360. Simpson, J.A. *et al.* Intratumoral T cell infiltration, MHC class I and STAT1 as biomarkers of good prognosis in colorectal cancer. *Gut* **59**, 926-933 (2010).

361. Mlecnik, B. *et al.* Histopathologic-based prognostic factors of colorectal cancers are associated with the state of the local immune reaction. *Journal of clinical oncology : official journal of the American Society of Clinical Oncology* **29**, 610-618 (2011).

362. Sun, C. *et al.* The predictive value of centre tumour $CD8^+$ T cells in patients with hepatocellular carcinoma: comparison with Immunoscore. *Oncotarget* **6**, 35602-35615 (2015).

363. Berghoff, A.S. *et al.* Density of tumor-infiltrating lymphocytes correlates with extent of brain edema and overall survival time in patients with brain metastases. *Oncoimmunology* **5**, e1057388 (2016).

364. Berthel, A. *et al.* Detailed resolution analysis reveals spatial T cell heterogeneity in the invasive margin of colorectal cancer liver metastases associated with improved survival. *Oncoimmunology* **6**, e1286436 (2017).

365. Angell, H.K., Bruni, D., Barrett, J.C., Herbst, R. & Galon, J. The Immunoscore: Colon Cancer and Beyond. *Clinical Cancer Research* **26**, 332-339 (2020).

366. Anitei, M.-G. *et al.* Prognostic and Predictive Values of the Immunoscore in Patients with Rectal Cancer. *Clinical Cancer Research* **20**, 1891-1899 (2014).

367. Kwak, Y. *et al.* Immunoscore encompassing CD3+ and CD8+ T cell densities in distant metastasis is a robust prognostic marker for advanced colorectal cancer. *Oncotarget* **7**, 81778-81790 (2016).

368. Dickinson, H.O. Cancer trends in England and Wales. Good data and analysis are vital to improving survival. *BMJ (Clinical research ed.)* **320**, 884-885 (2000).

369. Service, N.C.R.a.A. Routes to diagnosis of cancer by stage 2012-2013 workbook. London 2016.

370. Watson, N.F.S. *et al.* Immunosurveillance is active in colorectal cancer as downregulation but not complete loss of MHC class I expression correlates with a poor prognosis. *Int J Cancer* **118**, 6-10 (2006).

371. Freiburghaus, C. *et al.* Bortezomib prevents cytarabine resistance in MCL, which is characterized by down-regulation of dCK and up-regulation of SPIB resulting in high NF-κB activity. *BMC Cancer* **18**, 466 (2018).

372. Koelzer, V.H. *et al.* Digital image analysis improves precision of PD-L1 scoring in cutaneous melanoma. *Histopathology* **73**, 397-406 (2018).

373. Koopman, T., Buikema, H.J., Hollema, H., de Bock, G.H. & van der Vegt, B. Digital image analysis of Ki67 proliferation index in breast cancer using virtual dual staining on whole tissue sections: clinical validation and inter-platform agreement. *Breast cancer research and treatment* **169**, 33-42 (2018).

374. Pognan, F. *et al.* Induction of hemangiosarcoma in mice after chronic treatment with S1P-modulator siponimod and its lack of relevance to rat and human. *Archives of toxicology* **92**, 1877-1891 (2018).

375. Doane, D.P. & Seward, L.E. Measuring Skewness: A Forgotten Statistic? *Journal of Statistics Education* **19**, null-null (2011).

376. Gabrielson, A. *et al.* Intratumoral CD3 and CD8 T-cell Densities Associated with Relapse-Free Survival in HCC. *Cancer immunology research* **4**, 419-430 (2016).

377. Pagès, F. *et al.* International validation of the consensus Immunoscore for the classification of colon cancer: a prognostic and accuracy study. *The Lancet* **391** (2018).

378. Hood, L., Heath, J.R., Phelps, M.E. & Lin, B. Systems biology and new technologies enable predictive and preventative medicine. *Science* **306**, 640-643 (2004).

379. Klauschen, F. *et al.* Standardized Ki67 Diagnostics Using Automated Scoring—Clinical Validation in the GeparTrio Breast Cancer Study. *Clinical Cancer Research* **21**, 3651-3657 (2015).

380. Røge, R., Riber-Hansen, R., Nielsen, S. & Vyberg, M. Proliferation assessment in breast carcinomas using digital image analysis based on virtual Ki67/cytokeratin double staining. *Breast cancer research and treatment* **158**, 11-19 (2016).

381. Zhong, F. *et al.* A Comparison of Visual Assessment and Automated Digital Image Analysis of Ki67 Labeling Index in Breast Cancer. *PloS one* **11**, e0150505 (2016).

382. Naito, Y. *et al.* CD8+ T cells infiltrated within cancer cell nests as a prognostic factor in human colorectal cancer. *Cancer research* **58**, 3491-3494 (1998).

383. Yang, Y. Cancer immunotherapy: harnessing the immune system to battle cancer. *The Journal of clinical investigation* **125**, 3335-3337 (2015).

384. Gros, A. *et al.* PD-1 identifies the patient-specific CD8^{+} tumor-reactive repertoire infiltrating human tumors. *The Journal of clinical investigation* **124**, 2246-2259 (2014).

385. Mami-Chouaib, F. *et al.* Resident memory T cells, critical components in tumor immunology. *Journal for immunotherapy of cancer* **6**, 87 (2018).

386. Carbone, F.R. Tissue-Resident Memory T Cells and Fixed Immune Surveillance in Nonlymphoid Organs. *Journal of immunology (Baltimore, Md. : 1950)* **195**, 17-22 (2015).

387. Iijima, N. & Iwasaki, A. T cell memory. A local macrophage chemokine network sustains protective tissue-resident memory CD4 T cells. *Science* **346**, 93-98 (2014).

388. Hu, W., Sun, R., Chen, L., Zheng, X. & Jiang, J. Prognostic significance of resident CD103+CD8+T cells in human colorectal cancer tissues. *Acta Histochemica* **121** (2019).

389. Gryfe, R. *et al.* Tumor microsatellite instability and clinical outcome in young patients with colorectal cancer. *The New England journal of medicine* **342**, 69-77 (2000).

390. Le, D.T. *et al.* PD-1 Blockade in Tumors with Mismatch-Repair Deficiency. *The New England journal of medicine* **372**, 2509-2520 (2015).

391. Roosenboom, B. *et al.* Intestinal CD103+CD4+ and CD103+CD8+ T-Cell Subsets in the Gut of Inflammatory Bowel Disease Patients at Diagnosis and During Follow-up. *Inflammatory bowel diseases* **25**, 1497-1509 (2019).

392. Sathaliyawala, T. *et al.* Distribution and compartmentalization of human circulating and tissue-resident memory T cell subsets. *Immunity* **38**, 187-197 (2013).

393. Arnold, D. *et al.* Prognostic and predictive value of primary tumour side in patients with RAS wild-type metastatic colorectal cancer treated with chemotherapy and EGFR directed antibodies in six randomized trials. *Annals of oncology : official journal of the European Society for Medical Oncology* **28**, 1713-1729 (2017).

394. Holch, J.W., Ricard, I., Stintzing, S., Modest, D.P. & Heinemann, V. The relevance of primary tumour location in patients with metastatic colorectal cancer: A meta-analysis of first-line clinical trials. *European journal of cancer (Oxford, England : 1990)* **70**, 87-98 (2017).

395. Qiu, M.Z. *et al.* Comparison of survival between right-sided and left-sided colon cancer in different situations. *Cancer medicine* **7**, 1141-1150 (2018).

396. Weiss, J.M. *et al.* Mortality by stage for right- versus left-sided colon cancer: analysis of surveillance, epidemiology, and end results--Medicare data. *Journal of clinical oncology : official journal of the American Society of Clinical Oncology* **29**, 4401-4409 (2011).

397. Popat, S., Hubner, R. & Houlston, R.S. Systematic review of microsatellite instability and colorectal cancer prognosis. *Journal of clinical oncology : official journal of the American Society of Clinical Oncology* **23**, 609-618 (2005).

398. Chevrier, S. *et al.* An Immune Atlas of Clear Cell Renal Cell Carcinoma. *Cell* **169**, 736-749.e718 (2017).

399. Lavin, Y. *et al.* Innate Immune Landscape in Early Lung Adenocarcinoma by Paired Single-Cell Analyses. *Cell* **169**, 750-765.e717 (2017).

400. Sahin, U. *et al.* Personalized RNA mutanome vaccines mobilize poly-specific therapeutic immunity against cancer. *Nature* **547**, 222-226 (2017).

401. Schumacher, T.N. & Schreiber, R.D. Neoantigens in cancer immunotherapy. *Science* **348**, 69-74 (2015).

402. Camus, M. *et al.* Coordination of intratumoral immune reaction and human colorectal cancer recurrence. *Cancer research* **69**, 2685-2693 (2009).

403. Deschoolmeester, V. *et al.* Tumor infiltrating lymphocytes: an intriguing player in the survival of colorectal cancer patients. *BMC immunology* **11**, 19 (2010).

404. Funada, Y. *et al.* Prognostic significance of CD8+ T cell and macrophage peritumoral infiltration in colorectal cancer. *Oncology reports* **10**, 309-313 (2003).

405. Schumacher, K., Haensch, W., Röefzaad, C. & Schlag, P.M. Prognostic significance of activated CD8(+) T cell infiltrations within esophageal carcinomas. *Cancer research* **61**, 3932-3936 (2001).

406. Vihervuori, H. *et al.* Tumor-infiltrating lymphocytes and CD8(+) T cells predict survival of triple-negative breast cancer. *Journal of cancer research and clinical oncology* **145**, 3105-3114 (2019).

407. Baitsch, L. *et al.* Exhaustion of tumor-specific $CD8^+$ T cells in metastases from melanoma patients. *The Journal of clinical investigation* **121**, 2350-2360 (2011).

408. Soares, A. *et al.* Novel application of Ki67 to quantify antigen-specific in vitro lymphoproliferation. *Journal of immunological methods* **362**, 43-50 (2010).

409. Wherry, E.J. *et al.* Molecular signature of CD8+ T cell exhaustion during chronic viral infection. *Immunity* **27**, 670-684 (2007).

410. Canale, F.P. *et al.* CD39 Expression Defines Cell Exhaustion in Tumor-Infiltrating CD8(+) T Cells. *Cancer research* **78**, 115-128 (2018).

411. Pivetta, E. *et al.* Multiplex staining depicts the immune infiltrate in colitis-induced colon cancer model. *Scientific Reports* **9**, 12645 (2019).

412. Tóth, Z.E. & Mezey, E. Simultaneous visualization of multiple antigens with tyramide signal amplification using antibodies from the same species. *The journal of histochemistry and cytochemistry : official journal of the Histochemistry Society* **55**, 545-554 (2007).

413. Tan, W.C.C. *et al.* Overview of multiplex immunohistochemistry/immunofluorescence techniques in the era of cancer immunotherapy. *Cancer communications (London, England)* **40**, 135-153 (2020).

414. Schmoll, H.J. *et al.* ESMO Consensus Guidelines for management of patients with colon and rectal cancer. a personalized approach to clinical decision making. *Annals of oncology : official journal of the European Society for Medical Oncology* **23**, 2479-2516 (2012).

415. Van Cutsem, E. *et al.* ESMO consensus guidelines for the management of patients with metastatic colorectal cancer. *Annals of oncology : official journal of the European Society for Medical Oncology* **27**, 1386-1422 (2016).

416. Van Cutsem, E., Cervantes, A., Nordlinger, B. & Arnold, D. Metastatic colorectal cancer: ESMO Clinical Practice Guidelines for diagnosis, treatment and follow-up. *Annals of oncology : official journal of the European Society for Medical Oncology* **25 Suppl 3**, iii1-9 (2014).

417. Miller, K.D. *et al.* Cancer treatment and survivorship statistics, 2019. *CA: a cancer journal for clinicians* **69**, 363-385 (2019).

418. González-Perera, I. *et al.* 5-fluorouracil toxicity in the treatment of colon cancer associated with the genetic polymorphism 2846 A>G (rs67376798). *Journal of oncology pharmacy practice : official publication of the International Society of Oncology Pharmacy Practitioners* **23**, 396-398 (2017).

419. Ogura, A. *et al.* Neoadjuvant (Chemo)radiotherapy With Total Mesorectal Excision Only Is Not Sufficient to Prevent Lateral Local Recurrence in Enlarged Nodes: Results of the Multicenter Lateral Node Study of Patients With Low cT3/4 Rectal Cancer. *Journal of clinical oncology : official journal of the American Society of Clinical Oncology* **37**, 33-43 (2019).

420. Lal, N., Beggs, A.D., Willcox, B.E. & Middleton, G.W. An immunogenomic stratification of colorectal cancer: Implications for development of targeted immunotherapy. *Oncoimmunology* **4**, e976052 (2015).

421. Wei, S.C. *et al.* Distinct Cellular Mechanisms Underlie Anti-CTLA-4 and Anti-PD-1 Checkpoint Blockade. *Cell* **170**, 1120-1133.e1117 (2017).

422. Pauken, K.E. & Wherry, E.J. Overcoming T cell exhaustion in infection and cancer. *Trends in immunology* **36**, 265-276 (2015).

423. Tang, J., Shalabi, A. & Hubbard-Lucey, V.M. Comprehensive analysis of the clinical immuno-oncology landscape. *Annals of oncology : official journal of the European Society for Medical Oncology* **29**, 84-91 (2018).

424. Montes, M. *et al.* Optimum in vitro expansion of human antigen-specific CD8 T cells for adoptive transfer therapy. *Clinical and experimental immunology* **142**, 292-302 (2005).

425. Liao, W. *et al.* KRAS-IRF2 Axis Drives Immune Suppression and Immune Therapy Resistance in Colorectal Cancer. *Cancer cell* **35**, 559-572.e557 (2019).